Neuropeptide Signaling in Crustaceans Probed by Mass Spectrometry

By

Zhidan Liang

A dissertation submitted in partial fulfillment of

the requirements for the degree of

Doctor of Philosophy

(Pharmaceutical Sciences)

at the

UNIVERSITY OF WISCONSIN-MADISON

2016

Date of final oral examination: 5/5/2016

The dissertation is approved by the following members of the Final Oral Committee:

Lingjun Li, Professor, Pharmaceutical Sciences and Chemistry
Richard P. Hsung, Professor, Pharmaceutical Sciences
Richard E. Peterson, Professor, Pharmaceutical Sciences
Timothy S. Bugni, Associate Professor, Pharmaceutical Sciences
Antony O. Stretton, Professor, Zoology

Acknowledgement

I would first like to acknowledge my advisor Dr. Lingjun Li, without whom none of the work in this thesis would be achieved. I want to first thank her for having faith in me and letting me join her lab in 2010 although I did not have too much analytical background back then. Dr. Li has led a world-class research program that bridges advanced bioanalytical techniques with neuroscience studies. The dynamic and creative work in her lab has drawn me in. I was led to discover the world of mass spectrometry and the development of cutting edge analytical strategies to address biological questions. I appreciate her guidance, patience and encouragement which helped me overcome so many obstacles and challenges in my research. I also very much appreciate the freedom she gave me to navigate through projects to discover my true interest and her continuous support in seeking collaborations and different areas of expertise to better address my questions. Dr. Li is an outstanding scientist and mentor, which has a great impact on my PhD career and prepared me to become an independent scientist. I am also thankful for the emotional support and connection she provided outside the lab. The six years in the Li lab has been very pleasant and productive and I will forever cherish and be grateful for this opportunity to work in her lab.

I would also like to thank my committee members, Dr. Antony Stretton, Dr. Richard Peterson, Dr. Richard Hsung, and Dr. Tim Bugni for providing valuable support and insights throughout my Ph.D. process. Their constructive criticism helped to prepare me as a more mature and rigorous scientist and has raised the academic caliber of this thesis work.

I would like to thank my collaborators and colleagues who contributed to this work. I am very thankful to Dr. Claire Schmerberg for her mentorship and assistance when I first joined the lab and her collaboration on multiple neuropeptide-related projects after. I would like to thank the assistance from the Trout Lake Research Station from the Department of Limnology, UW-Madison and Lindsay Sargent of the University of Notre Dame Environmental Research Center in the rusty crayfish project. Shan Jiang collaborated on microdialysis coupled with capillary electrophoresis projects; Undergrad Catherine Pearce worked with me on feeding-related neuropeptide changes. Alexander Yarger and Dr. Wolfgang Stein from Illinois State University worked together with me on circadian rhythm studies in Jonah crab. I also want to thank Aaron Cook and Dr. Michael Nusbaum for their collaboration and helpful discussions and suggestions on feeding project. In addition, I want to thank Dr. Feng Xiang, Dr. Dustin Frost, Dr. Tyler Greer, Dr. Xiaoyue Jiang, Dr. Chenxi Jia and Dr. Zichuan Zhang for their guidance and criticism when I first started my graduate research. I have learned so much from day-to-day interactions with Erin Gemperline, Amanda Buchberger, Kellen Delaney, and Xiaofang Zhong. Also, I'd like to thank Dr. Cameron Scarlett, Molly Hahn and Gary Girdaukas from the Analytical Instrumentation Center at School of Pharmacy for instrument training, trouble shooting and maintaining.

I am also indebted to the people who first encouraged me to pursue my Ph. D. degree in the US. My first research advisors in college, Dr. Kang Zhao and Dr. Yunfei Du at Tianjin University, China. I am also very grateful to my TA instructors Bonnie Fingerhut and Dr. Melgardt de Villiers who made teaching so much fun and embraced me from the start.

I would like to thank my parents, Wenbin Liang and Jinyan Liu, and my brother, Zhiyuan Liang for their unconditional love and support throughout my graduate career. I am incredibly lucky to have great emotional support from many friends. Thanks to Dan Zhou and Fei Yang, who are always there for me when I needed a distraction from work. Thanks to Liuqing Shi, Zisheng Zheng, Wenquan Yu, Yongliang Zhang and Yan Chen from college and Hui (Vivian) Ye, Na Liu, Shan Jiang, Jingxin Wang, Qing Yu, Shiyu Chen and Xiaoxun Li among others in Madison. I would like to dedicate this work to my grandmother Jingpu Shen, who is a woman of outstanding courage and wisdom and I've always looked up to since I was a kid. She passed away in 2015 and it will be a lifelong regret for me as my last time with her was in 2012. But I know that she would be very proud of what I have achieved.

Table of Contents

Page

Acknowledgement i

Table of Contents iv

Abstract v

Chapter 1. Introduction and Research Summary 1

Chapter 2. Crustacean Neuropeptidome: Spatio-Temporal Analysis by Mass Spectrometry 10

Chapter 3. Mass Spectrometric Characterization of the Neuropeptidome of the Crayfish, *Orconectes rusticus* 67

Chapter 4. Mass Spectrometric Characterization of Circulating Neuropeptides in Jonah Crab, *Cancer borealis* 127

Chapter 5. Data-Independent MS/MS Quantification for Profiling of Temporal Dynamics of Neuropeptides in Microdialysate 160

Chapter 6. Capture of *In Vivo* Neuropeptide Degradation Using MALDI-Mass Spectrometry 184

Chapter 7. Coupling *In Vivo* Microdialysis with a Multifaceted Mass Spectrometric Platform to Investigate Signaling Molecules and Metabolites in Crustacean 220

Chapter 8. Protocols for Mass Spectrometric Studies of Neuropeptides and Neurotransmitters 248

Chapter 9. Conclusions and Future Directions 268

Appendix I. List of Publications and Presentations 280

Neuropeptide Signaling in Crustaceans Probed by Mass Spectrometry

Zhidan Liang

Under the supervision of Professor Lingjun Li

At the University of Wisconsin-Madison

Abstract

Neuropeptides are one of the most diverse classes of signaling molecules whose identities and functions are not yet fully understood. They have been implicated in the regulation of a wide range of physiological processes, including feeding-related and motivated behaviors, and also environmental adaptations. In this work, improved mass spectrometry-based analytical platforms were developed and applied to the crustacean systems to characterize signaling molecules.

This dissertation begins with a review of mass spectrometry-based neuropeptide studies from both temporal- and spatial-domains. This review is then followed by several chapters detailing a few research projects related to the crustacean neuropeptidomic characterization and comparative analysis. The neuropeptidome of crayfish, *Orconectes rusticus* is characterized for the first time using mass spectrometry-based tools. *In vivo* microdialysis sampling technique offers the capability of direct sampling from extracellular space in a time-resolved manner. It is used to investigate the secreted neuropeptide and neurotransmitter content in Jonah crab, *Cancer borealis,* in this work. A new quantitation strategy using alternative mass spectrometry data acquisition approach is developed and applied for the first time to quantify neuropeptides. Coupling

of this method with microdialysis enables the study of neuropeptide dynamics concurrent with different behaviors. Proof-of-principle experiments validating this approach have been carried out in Jonah crab, *Cancer borealis* to study feeding- and circadian rhythm-related neuropeptide changes using micoridialysis in a time-resolved manner. This permits a close correlation between behavioral and neurochemical changes, providing potential candidates for future validation of regulatory roles. In addition to providing spatial information, mass spectrometry imaging (MSI) technique enables the characterization of signaling molecules while preserving the temporal resolution. A novel MSI-based platform is developed by interfacing with microdialysis sample collection and is applied to the study of *in vivo* neuropeptide degradation profiles in an off-line 'real-time' fashion. This unique platform provides novel insights into neuropeptide inactivation/elimination process, which is an essential step to understand peptidegic signaling pathway. In addition to neuropeptides, this platform has been further modified to study secreted neurotransmitters, and small molecule metabolites that might interact with neuropeptides in crustacean for the first time.

This work not only reports improvements upon neuropeptides identification and quantitation by developing improved analytical strategies, but also provides important evidence for the potential roles of several neuropeptides in regulating food intake and circadian rhythm behaviors. Novel platform that integrates MALDI-MSI with microdialysis in exploring neurochemical changes in dynamic biological events is also presented, which could be potentially applied to many other systems in future research. Collectively this dissertation research develops new analytical methods and improves our fundamental understanding of neuropeptide signaling.

Chapter 1

Introduction and Research Summary

1.1 Introduction

The overall focus of this dissertation research is the development and implementation of mass spectrometry-based analytical tools for neuroscience research using invertebrate model nervous system. Several aspects of research, both in analytical platform development and application in the study of biological systems, are covered in this dissertation. Experimental strategies for analysis of neuropeptides, neurotransmitters, and small molecule metabolites are developed and applied to characterize the signaling molecules in crustacean nervous system. The performance of these new approaches have been evaluated using crustacean model organism and various physiological manipulation. This chapter provides a general introduction to neuropeptide analysis and includes a brief overview of the research described in each subsequent chapter.

1.2 Background Information

The main goal of this work is to develop analytical tools to study signaling molecules, including neuropeptides and small molecule neurotransmitters, with a special focus on the secreted signaling molecules, which could potentially advance our knowledge of their regulatory roles in biological systems. Neuropeptide is initially synthesized as an inactive precursor protein. A series of proteolytic cleavage and posttranslational modifications (PTMs) events occur to generate the final bioactive peptide(s) which could regulate numerous physiological processes [1, 2].

Due to the complexity of the mammalian nervous systems, simpler invertebrate preparations have been employed for method development and contributed significantly to advance our general knowledge of neuroscience. One of such systems is the crustacean nervous system, whose simplicity is well represented by the number and types of

compounds present and also the number and connectivity of the neurons present [3]. Mass spectrometry techniques have been developed and extensively used to study neuropeptides in crustaceans, providing identification and function-related information. Chapter 2 reviewed the investigation of neuropeptides in crustacean nervous system using mass spectrometry from temporal- and spatial-domains. In addition to tissue-based studies, this chapter highlights the study of secreted neuropeptides in the circulatory system, which travel to distant sites to exert hormonal functions. Several fluid-based sampling methods, such as microdialysis, allow analysis of signaling molecules secreted into the circulating fluids. Microdialysis offers the capability of sample collection concurrent with certain behavior in a time-resolved manner. Therefore, in conjunction with mass spectrometry-based quantitative methods, *in vivo* microdialysis sampling technique permits the high degree of correlation between changes in neurochemistry and changes in behavior [4, 5]. In addition to neuropeptide study within the temporal domain, mass spectrometry imaging for neuropeptide localization studies is also described. This chapter introduces mass spectrometry-based methods for neuropeptide identification and extracting biologically relevant information to better understand neuropeptide signaling.

1.3 Neuropeptidomics Study from Tissue-based Preparations: *Mass Spectrometric Characterization of the Neuropeptidome of the Crayfish* Orconectes rusticus

The decapod crustacean crayfish *Orconectes rusticus* is studied in this project. This species has been used extensively in behavioral neuroscience and ecology research. However, its neuropeptide content remains unknown for the most part, which makes it a good choice for our method development purpose. Due to lack of available genomic information, the identification of peptide sequences is largely relied on data quality of

peptide fragmentation. However, mass spectrometric analysis of neuropeptides in biological matrices is complicated by interfering molecules such as extracellular proteases, salts, lipids, etc. As a result, these complicating factors may lead to ionization suppression and /or dynamic range issues. Thus in Chapter 3, two-dimensional separation is employed prior to mass spectrometry detection and two semi-automated analysis methods of MS/MS data for neuropeptide identification are also compared. Characterizing the neuropeptidome of this species lays the groundwork for further biochemical and physiological studies using this useful model organism.

1.4 Characterization of Secreted Signaling Molecules in Crustacean

1.4.1 *Mass Spectrometric Characterization of Circulating Neuropeptides in Jonah Crab,* Cancer borealis

In this section, *in vivo* microdialysis was coupled with mass spectrometry detection to study circulating neuropeptides in *Cancer borealis* as described in Chapter 4. Microdialysis probe is surgically implanted into area of interest to collect samples directly from extracellular space, which is based upon gradient driven diffusion between perfusion solution and extracellular space. This sampling technique offers the capability to collect signaling molecules on a neurobiologically relevant time scale. With high-resolution and accurate mass (HRAM) measurements, temporal resolution of microdialysis collection is systematically evaluated for neuropeptide identification purpose. Two MS/MS data processing methods are used and compared to gain complementary identification results. In addition, results from microdialysis sampling and direct sampling from hemolymph (circulating fluid in crustacean) preparation are compared. In total, 52 neuropeptides from 8 different families are detected and identified

from microdialysate and 22 neuropeptides from hemolymph extracts, yielding the most comprehensive identification of secreted neuropeptides in crustacean.

1.4.2 *Coupling* In Vivo *Microdialysis with a Multifaceted Mass Spectrometric Platform to Investigate Signaling Molecules and Metabolites in Crustacean*

Another multifaceted mass spectrometry platform was developed to study circulating neurotransmitters and small molecule metabolites in crustacean in Chapter 7. *In vivo* neurochemical measurements pose tremendous challenges due to many factors. In biological systems, neurotransmitters usually are present at nM-pM range [6], but spanning wide dynamic range at the same time. Moreover, many active neurotransmitters have very short half-life after being secreted [7]. Our effort to characterize secreted neurotransmitters and metabolites were realized by coupling microdialysis sampling to a matrix-assisted laser desorption/ionization (MALDI) mass spectrometry platform. Capillary electrophoresis (CE) separation and ion mobility mass spectrometry are also utilized to aid separation and identification in this work. Detection is achieved primarily with MALDI mass spectrometric imaging (MSI). Performance of MALDI platform is also compared to electro-spray ionization (ESI) detection and a total of 208 small molecule metabolites are identified. Although the number of identified compounds is relatively small, this platform provides great potential as the inherent property of sub-microscale sample consumption from CE enables improved temporal resolution over LC-ESI-MS analysis.

1.5 Comparative Neuropeptidomics: *Data-Independent MS/MS Quantification for Profiling of Temporal Dynamics of Neuropeptides in Microdialysate*

The power of mass spectrometry has been well demonstrated in analyzing complex biological samples with high sensitivity. Quantitative analysis offers more bio-relevant information and has gained considerable interest in the field. In Chapter 5, an untargeted data analysis approach for simultaneous neuropeptide identification and quantitation is developed using data-independent acquisition (DIA) MS/MS technique. DIA MS/MS based quantitation technique has been applied to protein level analysis [8-10] by monitoring multiple peptides per protein. In our work, to perform quantitation on neuropeptides, an open-source, vendor-neutral software Skyline [11] is employed for data processing, which is typically used for multiple reaction monitoring (MRM) type of quantitation experiments. We use it to conduct pseudo-MRM analysis of neuropeptides by performing post-acquisition filtering. The entire known neuropeptidome of *Cancer borealis* is monitored using this method. The linearity of this approach is demonstrated with a set of crustacean and mammalian peptide standards.

This DIA MS/MS based quantitation has been proven to be highly useful for discovery studies by applying it to the study of behavior-related neuropeptide changes. It is applied to study feeding-related and circadian rhythm-related neuropeptide changes in *Cancer borealis*. In Chapter 5, microdialysis sampling from the hemolymph of Jonah crabs is used to monitor peptide changes during feeding behavior and daily light-dark cycle. It is known that neuropeptides play critical roles in feeding regulation in mammals [12]. The study of feeding-related neuropeptide changes in the crustacean system may reveal neural and biochemical pathways that overlap in mammals. Circadian rhythms commonly refer to the rhythmic and reproductive physical, mental and behavioral changes in a roughly 24-hour cycle, primarily in response to environmental light and dark

changes. Such rhythm is driven by master clock and no master clock has been identified in crustacean yet. Cellular systems involve neuroendocrine X-organ sinus gland system and some neuropeptides have been implicated [13] to play critical roles in circadian rhythm regulation. Monitoring neuropeptide dynamics in crustacean and performing comparative analysis to insect systems in the future may allow the identification of candidate clock neurons/peptides in crustacean.

1.6 Investigation of Post-release Fate of Neuropeptides: *Capture of* In Vivo *Neuropeptide Degradation Using MALDI-Mass Spectrometry*

To date, the study on neuropeptides has been focused on its synthesis, secretion, structure and function. However, to fully understand how neuropeptides function, it is important to understand how they are inactivated or removed from the extracellular space. Studies have shown that peptidase activity could tune motor pattern modulation [14]. However, the study on neuropeptide degradation has been very limited. In Chapter 6, we couple microdialysis sampling with MALDI-MSI platform to characterize *in vivo* degradation profile of neuropeptides from different families. This platform allows continuous collection of microdialysate and MALDI platform maintained such temporal resolution thus offering the capability to monitor the *in vivo* degradation process in an off-line 'real-time' fashion. Mammalian and different crustacean endogenous neuropeptides are administered to Jonah crab *via* retrodialysis to investigate the specificity of crustacean peptidases activities. An *in vitro* assay is also developed to rapidly determine the different degradation rates of each neuropeptide. The developed microdialysis-MALDI-MSI platform offers a novel analytical strategy to monitor highly

dynamic biological events. The study of neuropeptide degradation profiles provides a more comprehensive picture of peptide signaling pathway.

1.7 Conclusions and Supplemental Information

The final section of this dissertation presents an overall conclusion of the research projects described in various chapters and provides potential future directions that the related projects could take as described in chapter 9. Chapter 8 summarizes different protocols used for sample preparation, instrumental analysis and data processing which hopefully could aid future related studies in this area. In summary, this PhD thesis work developed numerous useful methods and new approaches for future neuropeptide studies. In the meantime, these new methods enabled several interesting findings in neuropeptide dynamic changes in response to physiological manipulations and neuropeptide degradation that laid the groundwork for more in-depth and targeted neuropeptide signaling pathway exploration.

1.8 References:

1. Christie, A.E., Stemmler, E.A., and Dickinson, P.S., *Crustacean neuropeptides.* Cell Mol Life Sci, 2010. **67**(24): p. 4135-69.
2. Schmerberg, C.M. and Li, L., *Function-driven discovery of neuropeptides with mass spectrometry-based tools.* Protein Pept Lett, 2013. **20**(6): p. 681-94.
3. Marder, E. and Bucher, D., *Understanding circuit dynamics using the stomatogastric nervous system of lobsters and crabs.* Annu Rev Physiol, 2007. **69**: p. 291-316.
4. Schmerberg, C.M. and Li, L., *Mass spectrometric detection of neuropeptides using affinity-enhanced microdialysis with antibody-coated magnetic nanoparticles.* Anal Chem, 2013. **85**(2): p. 915-22.
5. Schmerberg, C.M., Liang, Z., and Li, L., *Data-independent MS/MS quantification of neuropeptides for determination of putative feeding-related neurohormones in microdialysate.* ACS Chem Neurosci, 2015. **6**(1): p. 174-80.
6. Li, Q., Zubieta, J.K., and Kennedy, R.T., *Practical aspects of in vivo detection of neuropeptides by microdialysis coupled off-line to capillary LC with multistage MS.* Anal Chem, 2009. **81**(6): p. 2242-50.
7. Jennings, K.A., *A comparison of the subsecond dynamics of neurotransmission of dopamine and serotonin.* ACS Chem Neurosci, 2013. **4**(5): p. 704-14.
8. Liu, S., Chen, X., Yan, Z., Qin, S., Xu, J., Lin, J., Yang, C., and Shui, W., *Exploring skyline for both MS(E) -based label-free proteomics and HRMS quantitation of small molecules.* Proteomics, 2014. **14**(2-3): p. 169-80.
9. Levin, Y., Hradetzky, E., and Bahn, S., *Quantification of proteins using data-independent analysis (MSE) in simple andcomplex samples: a systematic evaluation.* Proteomics, 2011. **11**(16): p. 3273-87.
10. Silva, J.C., Gorenstein, M.V., Li, G.Z., Vissers, J.P., and Geromanos, S.J., *Absolute quantification of proteins by LCMSE: a virtue of parallel MS acquisition.* Mol Cell Proteomics, 2006. **5**(1): p. 144-56.
11. MacLean, B., Tomazela, D.M., Shulman, N., Chambers, M., Finney, G.L., Frewen, B., Kern, R., Tabb, D.L., Liebler, D.C., and MacCoss, M.J., *Skyline: an open source document editor for creating and analyzing targeted proteomics experiments.* Bioinformatics, 2010. **26**(7): p. 966-8.
12. Moran, T.H. and Dailey, M.J., *Intestinal feedback signaling and satiety.* Physiol Behav, 2011. **105**(1): p. 77-81.
13. Strauss, J. and Dircksen, H., *Circadian clocks in crustaceans: identified neuronal and cellular systems.* Front Biosci (Landmark Ed), 2010. **15**: p. 1040-74.
14. Wood, D.E. and Nusbaum, M.P., *Extracellular peptidase activity tunes motor pattern modulation.* J Neurosci, 2002. **22**(10): p. 4185-95.

Chapter 2

Crustacean Neuropeptidome: Spatio-Temporal Analysis by Mass Spectrometry

Adapted from

1. Mass spectrometric analysis of spatio-temporal dynamics of crustacean neuropeptides. **Zhidan Liang**, Chuanzi Ouyang, Lingjun Li. *Biochim Biophys Acta*. **2015**, *1854*, 798-811.
2. Biologically Active Peptides in Invertebrates: Discovery and Functional Studies. Qing Yu, Chuanzi Ouyang, **Zhidan Liang**, Lingjun Li. Monograph, Colloquium Series on Neuropeptides, Morgan & Claypool Publishers.
3. Mass Spectrometric Characterization of the Crustacean Neuropeptidome. Qing Yu, Chuanzi Ouyang, **Zhidan Liang**, Lingjun Li. *EuPA Open Proteomics*, **2014**, *3*, 152-170.

Abstract

Neuropeptides represent one of the largest classes of signaling molecules used by the nervous system to regulate a wide range of physiological processes. Invertebrates, such as decapod crustaceans, have made important contributions in the discovery and characterization of neuropeptides. Over the past decade, mass spectrometry (MS)-based strategies have accelerated the field of neuropeptide discovery in numerous model organisms, especially in decapod crustaceans. In this article, advances in MS-based analytical tools to study neuropeptides in invertebrate systems are discussed, and the use of these techniques to map neuropeptides in spatial domain and monitoring their dynamic changes in temporal domain are highlighted. Matrix-assisted laser desorption/ionization (MALDI) mass spectrometric imaging (MSI) technique allows for the mapping of neuropeptides localizations in tissue, whereas fluid-based analysis coupled with electrospray ionization (ESI) MS could chart the temporal dynamics of neuropeptides. These MS-enabled investigations provide valuable information about the distribution, secretion and potential function in addition to neuropeptide sequence identification. This review contains both methodology information and the current state of knowledge with regards to crustacean neuropeptides.

2.1 Introduction

Neuropeptides (NPs) are endogenous peptides synthesized in nerve cells or peripheral organs that are involved in cell-cell signaling. NPs are initially synthesized in the cell body as larger, inactive precursor proteins and undergo a series of post-translational modifications (PTMs) to finally render mature, bioactive NPs which have regulatory roles. Some of these precursors only generate a single mature NP, while others contain several sets of mature NPs. The number of known NPs far exceeds the number of classical neurotransmitters discovered with their wide range of physiological involvements [1]. The number of peptides being identified within the vertebrate and invertebrate nervous systems kept growing over the past few decades as a result of advancement in biological analytical techniques, especially mass spectrometry (MS).

NPs are present throughout the animal kingdom (as well as in plants), including the hydra, a member of coelenterates with a very simple nervous system. A nervous system can be considered as an organized collection of neurons. Neuronal cell bodies are grouped into clusters called ganglia. Vertebrates are characterized by dorsal spinal cords, brains, and chains of autonomic ganglia. The simplest type of nervous system is found in hydras and jellyfish, and is referred as a ‘nerve net’. Many invertebrate species are characterized by ventral nerve cords consisting of segmentally organized ganglia with relatively limited numbers of easily identifiable large neurons, and “brains” which are so termed largely because they are found in the head region of the animal and include the regions of the nervous system that process visual and olfactory inputs [2]. In segmented invertebrates, each neuron may express an identifiable phenotype and the layout of the nervous system to a large extent reflects the degree of body segmentation, which in turn

corresponds with functional localization. Each body segment possessing a corresponding segment of neurons responsible for a particular function in one or several linked ganglia makes it possible to conduct specific studies on those targeted ganglia and functions. Given the well-defined anatomy and function-specific circuits found in invertebrates, it is often possible to understand how changes in behavior arise from changes at specific sites or specific group of neurons within the nervous system. Most vertebrate systems do not permit this kind of detailed analysis. Meanwhile, the technical and ethical problems of directly studying functions of peptide-containing neurons buried deep in the vertebrate brain are more or less solved by exploiting advantages of these uniquely identifiable neurons in invertebrates. Questions related to the functions of peptidergic neurons can be studied more conveniently and more precisely in invertebrate models. The study of invertebrate preparations has advanced our general knowledge of neuroscience by providing the means to explore many key mechanisms of neuronal function [3].

2.2 The crustacean model system

Two major nervous systems are consisted in the crustacean nervous system, including the central nervous system (CNS) and the stomatogastric nervous system (STNS). The CNS includes the brain and the ventral nerve cord. The STNS consists of several linked motor pattern generating centers, and is one of the premier systems to understand how neural circuit generates behavior. The properties of its neurons and their connections makes the biochemical and molecular characterization accessible at the single-cell and neural circuit level, thus serves as an attractive model for neuromodulation and NP study [4].

In the STNS, the small number of easily identifiable neurons enabled complete

characterization of connectivity among the neurons of the stomatogastric ganglion (STG). A central pattern generating (CPG) circuit within the STNS in adult animal generates the gastric rhythm, which operates the gastric teeth, and the pyloric rhythm, which separates out food particles for further digestion. The STNS consists of the paired commissural ganglia (CoGs), the unpaired esophageal ganglion (OG), and the STG (**Figure 2-1**). Together the CoGs and OG contain many descending modulatory neurons that control STG activity [5]. The STNS is an ideal model for studying neuromodulation in a well-defined neural network because: (1) It contains relatively small number of neurons. The lobster STG only contains 31 neurons; (2) There is a high incidence of identified neurons which are neurons that can be found from animal to animal with the same physiological properties; (3) Electrophysiological properties of the system can be readily assessed; and (4) This system contains an array of NPs which can be categorized into multiple peptide families based on sequence similarities.

Compared to STNS, CNS is even more complex. Sensory input to the brain of decapod crustaceans, as in insects, is provided by compound eyes mediating vision or an array of specialized sensilla located at antennules mediating all other sensory modalities [6]. Also, the brain is connected with the STNS by projection through CoG/OG or directly into the STG to regulate the motor patterns in the stomach [7, 8]. Therefore, the brain is the connection between two nervous systems. In addition, other neurohemal structures such as the pericardial organs (PO) and the sinus glands (SG) contain a wide array of neurohormonal substances that can be released into circulating system and regulate the functions of distant organs (Figure 2c). A large number of NPs were identified by mass spectrometry despite the almost complete lack of genomic information

for the organism of interest [9-11].

Analogous to the blood in vertebrates, hemolymph is the circulatory fluid in crustaceans. Crustaceans have open circulatory systems, meaning hemolymph fills the interior (the hemocoel) of the animal's body and bathes all internal organ systems. Nutrients, oxygen, hormones and cells are distributed in the hemolymph [12]. As crustaceans lack complete venous system, after the hemolymph has bathed the organs and passed through the 3 capillary-like vessels, it will drain into a series of sinuses. The hemolymph eventually returns back to the pericardial sinus and then flows into the heart [13].

Many concepts first described in the crustaceans have since been found to be applicable to higher order systems. Research in the STNS model system led to the notion that different modulators produce completely different outputs for the same neural network [14] which subsequently was found to be true in mammals as well [15]. Furthermore, electrically coupled neurons were first described in crustacean and later found in the mammalian cortex [16]. In addition, many peptide families observed in the crustacean STNS have been shown to exhibit a high degree of sequence homology across different phyla, including mammals. For example, the family terminated by arginine-phenylalanine-amide (RFamide) is expressed in species ranging from nematodes to human [17-19].

2.3 Mass-spectrometry (MS) based techniques enabling NP discovery

2.3.1 *Introduction to non-MS based techniques*

Substance P, was discovered by potent depressor effects as noted by Euler and Gaddum in 1931 [20], unexpectedly, when they studied acetylcholine (ACh). The primary sequence of Substance P was not determined until 40 years later by Chang and colleagues [21]. Historically, NPs were identified during searches for endogenous molecules that produced a physiological effect and Edman degradation was used as a standard method to determine the primary sequences of newly discovered NPs. These investigational approaches are referred to as "function first" and require some type of bioassay or other related technique to screen crude tissue extracts [22]. Similarly, the first invertebrate NPs were discovered through bioassays. To name a few, it was suggested earlier that a myotropic substance extracted from the viscera of the cockroach, *Periplaneta americana*, might function as an excitatory transmitter substance in insect visceral muscle, while its identity was mysterious. The myotropic substance was purified and *confirmed to be proctolin* by multiple *orthogonal chromatographic methods and bioassays* [23]**.** Obviously, this was a slow and tedious process, requiring substantial amounts of precious peptide preparations. The pace of discovery increased when Victor Mutt and collaborators focused on the isolation of C-terminally amidated peptides. Their rationale was that the C-terminal α-amide structure was a characteristic feature of many biologically active peptides [24] and such molecules could survive proteolytic degradation. After exposing tissue homogenates to enzymatic degradation that release the characteristic COOH-terminal amides of these hormones followed by dansylating and isolating the dansyl derivatives of the amides from the mixture, several naturally occurring peptides (peptide HI (PHI), peptide YY (PYY)) from extracts of porcine intestine were identified and these peptide amides produced previously unknown biologically activities [25]. Not long after, NPY [26]

was discovered by using the same technique and it paved the way to further study of its biological relevance. David de Wied pioneered the study of the activity of NPs in rat behavior from the 1950s onward and discovered that adrenocorticotropic hormone (ACTH), melanocyte-stimulating hormone (MSH), and vasopressin acted on the brain and affected learning and memory processes [27, 28]. In the 1970s he coined the term “neuropeptides” to designate neuroactive peptide hormones and thereafter, the term “neuropeptide” has been widely adopted by the community [29, 30].

With technology development, multiple NP discovery and characterization strategies other than traditional bioassay has become available as reviewed by Lloyd D Fricker [22]. Multiple novel NP families have been discovered and hundreds of novel NPs have been characterized and confirmed to play key roles in various physiological conditions. This book will focus on an emerging and rapidly evolving technique – mass spectrometry – which has already revolutionized the way NPs are discovered.

2.3.2 *MS-based peptidomic techniques for invertebrate NP discoveries*

Before the 1970s, research had been focused mostly on vertebrate neuroendocrinology, even though in many cases, the invertebrate systems offer simpler models in helping us understand more complex vertebrate systems. It was not until 1972 that the first invertebrate NP red pigment concentrating hormone (RPCH) was isolated from *Pandalus borealis (caridean* shrimp). Even though its activities had been already recognized previously [31, 32], its identity remained obscure. After spending several years at Kristineberg's Zoological Station on the west coast of Sweden, Fernlund and coworkers were finally able to purify RPCH via a butanol extraction procedure followed by a series of chromatographic separation [33]. They processed 125 kg of *Periplaneta americana*

(American cockroach) to obtain 180 µg of pure peptide. It was found that RPCH did not contain free N- or C- terminus which made it unsusceptible to traditional Edman degradation to deduce its sequence. Due to the lack of proper methods, they were not able to report RPCH's primary sequence until five years later. The group embraced the newly developed mass spectrometric technique and spent approximately 20 µg of peptide preparation to derive the RPCH's primary sequence [34]. This was the first time that mass spectrometry (MS) was employed for invertebrate NP characterization, though the procedures for isolation and characterization of peptides were crude by today's standards. Another example in which MS was used in the early ages was the structural elucidation of adipokinetic hormone in *Locusta migratoria.* Adipokinetic hormone was suggested to be present in corpora cardiaca yet never fully characterized. Following a couple stages of chromatographic purification, a combinatorial strategy composed of enzymatic digestion, electrophoresis, and MS was employed to confidently derive the peptide's structure [35]. Since then, the number of NPs isolated and characterized has increased greatly and the advantage of MS has been highly exploited.

The combined use of precursor (MS) and product (MS/MS) scans enabled the discovery of novel members of established NP families and the identification of new peptide families, significantly expanding the neuropeptidome in multiple invertebrate species [36-38]. With their structural information available, it is easier to determine a peptide's function during various physiological processes compared to a shot-gun purification approach employed previously. Another aspect to consider in a comprehensive NP study is the peptide localization, which is highly related to function. The application of matrix-assisted laser desorption/ionization (MALDI) MS imaging

(MSI), first demonstrated by Caprioli and coworkers [39, 40], greatly facilitates the localization of NPs in tissue slices. Mass spectra are acquired according to a predefined grid across the sample while a coordinate system is superimposed on the tissue. After a series of spectra is collected, hundreds of ions can be assigned to different coordinates, therefore relating their identities and potential functions to locations. The advancement of MS-based tools and tandem MS capability, coupled with isotope labeling strategies and label-free approaches, have accelerated several large-scale comparative neuropeptidomic analyses, enabling a global view of coordinated changes of NPs related to a physiological process.

2.3.3 *Sample preparation*

Because of the biochemical complexity, high-salt contents, and endogenous proteases, sample preparation is often critical to produce the desired outcome of a peptidomic experiment. Depending on the goals and requirements of specific experiments, various sample preparation methods have been developed. Samples can be prepared by homogenization and extraction of tissues, analyzed by direct tissue experiments or collected by microdialysis techniques followed by liquid chromatography (LC) coupled to MS or MS/MS analysis.

Many neuropeptidomic analyses employ tissue homogenization followed by extraction method. Direct tissue analysis and fluid-based sampling will be covered in later sessions. In this approach, specific tissues from multiple animals are often pooled and homogenized, followed by extraction with acidic buffer and then further separated or fractionated. The resulting extract is then analyzed by MS, generally either online or offline with electrospray ionization (ESI) type of instruments, and sometimes matrix-

assisted laser desorption/ionization (MALDI) instruments. Advantages of this approach are the feasibility with any organism regardless of the tissue size. With pooling method, significant amounts of NPs can be extracted followed by LC-MS/MS for identifications, which is suitable for MS instruments with modest sensitivity.

Homogenization and extraction are performed in the presence of solvent buffers which can deactivate proteases from degrading proteins and peptides in the sample. Acidified methanol [41, 42] is most commonly used in studying crustacean NPs, with other examples being acidified acetone [43, 44], a combination of acidified methanol spiked with EDTA and protease inhibitors [45]. Following the homogenization and extraction, centrifugation is typically performed to eliminate cell debris. The supernatant was then concentrated and, if necessary, a C18 desalting protocol can be applied. In many cases, reversed-phase liquid chromatography (RPLC) is adapted to fractionate complex crustacean NP mixtures as to increase neuropeptidome coverage by enabling detections of low abundance NPs [46-48].

This strategy has been successfully used to characterize NPs in many crustacean species [42, 46, 47, 49-55]. In addition, two-dimensional reversed-phase liquid chromatography (2D RP-LC) has been used by Hui et al. to characterize the neuropeptidome of the pericardial organ in blue crab *Callinectes sapidus* [56]. Alternative multidimensional chromatographic separation, which employs strong cation-exchange (SCX) chromatography followed by reversed phase liquid chromatography (RPLC) has been developed and used in studying peptides and proteins in other organisms, such as *Caenorbabditis elegans* and *Rattus norvegicus* [57, 58]. Most recently, another integration of two chromatographic techniques, hydrophilic interaction

liquid chromatography (HILIC) and RPLC, was introduced as a promising addition [59, 60]. Another approach to enrich NP content in samples is immuno-based methodology. For example, specific antibodies that recognize consensus sequence in a peptide family can enrich the target NP family from complex sample background [55, 61].

2.4 Mass spectrometric imaging- the spatial probe of crustacean NPs

2.4.1 *Introduction to mass spectrometric imaging*

Immunohistochemical (IHC) staining has long been a powerful tool for visualizing the distribution of NPs *in situ* [62-66]. This antibody-based technique provides accurate spatial information of peptides when utilizing microscopy. In comparison to *in situ* hybridization, IHC staining does not require precise chemical information of the NPs of interest for the recognition interaction. However, the production of specific antibodies against each peptide family could be quite costly and time-consuming [67]. It is also difficult to produce and develop highly specific antibodies that can distinguish among multiple peptide isoforms in each family due to cross-reaction of similar NPs to the antibodies. Since the pioneering work by Caprioli and co-workers [68], MALDI MSI has emerged as an attractive technology for mapping the localization of various biomolecules including metabolites, lipids, NPs and proteins *etc* [67, 69-74]. In a typical MALDI-MSI study, tissue section is placed in a pre-defined 2-dimensional coordinate (x, y) system. To investigate the chemical contents over the entire tissue slice, the sample stage carrying the tissue section is rastered against a laser beam across each position to generate a mass spectrum with its on-tissue dimensional information co-registered in the data acquisition software. This approach enables comprehensive mapping of the distribution of thousands of biomolecules simultaneously with high

specificity and high throughput, which overcomes the aforementioned imperfections of IHC staining. When reconstructing MS imaging information from all consecutive tissue sections together, a global view of 3-dimensional localization pattern can be obtained. Confident identification of analytes could be achieved as well in MSI via *in situ* MS/MS fragmentation [75-77]. Thanks to recent developments of methodology and instrumentation, it is possible to hybridize both positive and negative mode acquisitions into one MS imaging acquisition to obtain more in-depth spatial characterization with shorter experimental time [78]. The MS/MS identification process has been incorporated into MS imaging runs utilizing multiplexed setup with either targeted mass list or data dependent acquisition for more convenient molecular identity validation [79, 80]. Thereupon, not only the known NPs could be unambiguously differentiated with their colocalization patterns, novel NPs could also be revealed via on tissue *de novo* sequencing. Moreover, semi-quantitative information of all the observed NPs could be obtained with appropriate experimental conditions and post-acquisition data normalization [81-85]. Overall, MS imaging is an advantageous tool to study the spatial distribution of biomolecules in tissue with high sensitivity, specificity and throughput.

2.4.2 *Sample preparation for MS imaging*

To accurately reflect the spatial distribution characteristics of a dynamic range of NPs with various abundances, it is vital to carefully handle every step of the sample preparation process.

2.4.2.1 Tissue harvest and preservation

To maintain the cell morphology, tissue dissection is usually performed in chilled artificial physiological saline. However, high concentration salt contents from

extracellular matrix and saline not only interfere with the signal from NPs, but also lower the detection sensitivity of MALDI MS by suppressing the ionization and masking the signal which is especially adverse for low abundance NPs. Rapid rinse of tissue in purified water immediately after isolating tissue from animal could efficiently remove the physiological saline [9, 67, 86]. It also has been reported that changing physiological saline to dilute DHB aqueous solution during dissection could help reducing the inherent salt context [87].

Endogenous degradation caused by protease activities often poses negative effect on peptide profiles even at 3 minutes post-mortem [88, 89]. Crucial PTMs in the brain tissue have been reported to significantly change within minutes post-mortem [90, 91]. In order to minimize and prevent the degradation of valuable biologically active molecules by proteases, tissue preservation is of great importance during and after tissue harvest. One of the most commonly adapted methods is to snap-freeze the tissue in dry ice, liquid nitrogen or cold bath using different organic solvents such as isopentane, ethanol and isopropanol to stop the enzymatic proteolysis [92]. The structural features of tissue are also well conserved at the same time (see more in tissue fixation). Generally, longer freezing time in cold-bath works better for preventing the tissue from cracking and keeping the tissue integrity [67]. Heat denaturation by Stabilizor T1 (Denator, Gothenburg, Sweden) has also been reported to efficiently eliminate post mortem degradation in various types of tissues [93, 94] including crustacean neuroendocrine organs [95]. Formaldehyde-fixed paraffin-embedding (FFPE) however, as a popular way to preserve tissue in biological and medical research, would cause severe crosslinking between peptides and proteins [96], which decreases its applicability in MS-based

studies. Attempts have been made to successfully image FFPE tissue with a paraffin removal step prior to matrix application [97-101]. Aspects such as oxidation and tissue degradation must be taken into consideration when processing data from such sample. Storage at -80°C is imperative if the tissue are not used immediately after dissection [102].

2.4.2.2 Tissue sectioning and fixation

For the purpose of sectioning specimens into thin slices to be analyzed in MS imaging experiments, tissue is usually embedded into scaffold materials at the time of snap-freezing to facilitate subsequent cutting. Among the various supporting materials that have been reported, most of them are polymer based, such as optimal cutting temperature (OCT) compound, 2% (wt/vol) carboxymethylcellulose (CMC), Tissue-tek and agar etc [103]. Although subsequent histological study could be conveniently carried out using these substrates [70], the strong background signals in MS from the polymer have limited their universal application to diverse biomolecules at a wide range of molecular weight [103, 104]. To eliminate the interference from embedding materials at the NP rich m/z region (typically from 500 to 3000 Da) in crustacean tissue, gelatin and water are recommended [76, 105]. The thickness of the tissue is typically 10 to 20 μm [106], which is around the diameter of a mammalian cell, for better exposing the intercellular and intracellular contents to be analyzed [103]. However, thinner sections (< 5 m) have been demonstrated to present better sensitivity on alternative LDI platform such as NIMS [107-109]. To fix the tissue slice for MS imaging experiment, thaw-mounting the -20 °C cold section onto a room temperature MALDI sample plate or glass slide is the most common method [103]. Double sided tape is another popular adhesive to

affix the tissue especially for samples with low water content [110]. When electrical conductive target is needed for instrumentation such as MALDI TOF MS, stainless steel target, gold-coated glass slide and indium-tin oxide coated glass slide are all excellent candidates [92]. Using transparent glass slides for tissue fixation also provide the opportunity for subsequent histological study [70]. Other than brain and thoracic ganglion (TG), most of the neural tissues in crustacean animals are too small to be sectioned, such as OG and STG. PO tissue is composed of fine interwoven nerve tubes that are difficult to section. To study the NP distribution in these organs, tissues are directly placed on the MALDI plate or glass slide followed by drying process in a dessicator at -20°C to fix the tissue [75, 111, 112].

2.4.2.3 Tissue washing

For the investigation of NPs in crustacean, tissue washing with organic solvents is typically avoided to prevent NP delocalization. Many crustacean NPs are relatively small and hydrophilic, making them readily extractable when using organic solvents such as methanol and ethanol. However, high abundance lipids ranging from 500 to 900 Da and from 1300 to 1600 Da in crustacean tissues often hinder the effective detection of NPs within the same mass range [113]. Chloroform and xylene have been reported to effectively eliminate lipid background as washing solvent to treat various tissues [113, 114]. When the target NPs are hydrophobic or have higher molecular weight such as the crustacean hyperglycemic hormone (CHH) peptides, it is more critical to carefully optimize tissue washing procedures to remove salts and small NPs while preserve the spatial localization of analytes of interest.

2.4.2.4 Matrix application

Since MALDI source is the most widely adopted MS imaging platform in crustacean NP study, the application of matrix onto the tissue prior to MS acquisition is one of the most important elements in sample preparation [115, 116]. The most common matrices in NP analysis by MALDI MS are DHB and CHCA, which are both benzene ring containing weak organic acids with the ability to absorb and transfer laser energy in the ultraviolet-wavelength range for the analyte desorption and ionization. Binary matrix mixture has been demonstrated to bring the advantages of both DHB and CHCA together and produce finer crystallization and enhanced signal intensity [105, 117]. To apply matrix, one could either spot the matrix solution onto discrete position on the tissue or continuously spray the matrix solution over the entire tissue area. In the case of manual matrix deposition, spraying with airbrush produces much smaller crystal resulting better lateral resolution than spotting while manual spotting would be more suitable for profiling prior to MS imaging acquisition. Robotic spotting utilizing focused acoustic dispenser has been developed to generate picoliter level droplet which greatly improve the lateral precision to around 3 m with better reproducibility [70]. Meanwhile, the crystal size and reproducibility could both be well controlled with automated spraying devices, such as TM sprayer (pneumatic sprayer, by HTX Imaging, NC, US) and ImagePrep (vibrational sprayer, by Bruker Daltonics, Bremen, Germany). It is important to note that the matrix solution must be optimized with both concentration and solvent composition for these spraying devices to achieve best results.

Low matrix concentration typically leads to slow crystallization and consequently results in more severe lateral diffusion as the tissue has been left to be wet for extended time. Furthermore, without sufficient matrix coating coverage, desorption and ionization

efficiency will dramatically decrease. If too much matrix is deposited on the tissue surface, fast evaporation would reduce the amount of NPs to be extracted into the matrix crystal layer, which lowers the signal intensity in MS as well. With similar principles, the optimal solvent composition should be adjusted to the sweet spot of best extraction efficiency, smallest crystal size and minimum lateral delocalization.

2.4.3 *Application of MS imaging to characterize the spatial distribution of NPs in crustacean*

A variety of decapod crustacean species have been extensively studied using multifaceted mass spectrometric platforms. MS imaging provides useful knowledge to correlate the spatial distribution of NPs in the nervous system to their specific biological functions as neuromodulators. The first MS imaging study of crustacean NPs was reported by DeKeyser et al [75] in *Cancer borealis* on a MALDI TOF/TOF MS platform. The MS imaging investigation in brain sections and intact PO has successfully revealed the spatial distribution of 38 NPs from 10 different families *via* mass matching. The identities of 16 of them were validated through on tissue MS/MS CID fragmentation. It is worth mentioning that the DHB matrix were applied differently on the tissue for MS imaging (airbrush manual spray) and the tissue for tandem MS acquisition (discrete manual spotting). In most of distribution density maps generated by MS imaging, NPs from the same family were similarly localized, in both brain and PO. However, exceptions did exist for NPs belonging to the RFamide and orcokinin families. Different localization of NPs in the nervous system suggested their potentially distinct functionalities despite their similar chemical structures. This differentiated spatial information about NP isoforms from the same family highlights the superior chemical

specificity of MS imaging over IHC staining. In the brain, most of RFamides showed high intensity in the caudal region while orcokinins were found in the rostral region. SIFamide and TRP 1a displayed similar distribution pattersn with those of RFamides. Although A-type and B-type AST were absent in the brain, they were detected in the PO with distinct spatial distribution patterns. Compared to conventional cellular mapping of immunoreactivity in the trunks of PO, MS imaging study enabled visualization of NPs of this organ to the extended areas such as anterior and posterior bar regions shown in **Figure 2-2**. Later studies by Chen et al [77] showed similar distribution patterns of RFamides and orcokinins being in contrast to each other in the brain of *C. borealis*.

In a study by Hui et al. [118] where a novel TRP CalsTRP was reported in the blue crab *Callinectes sapidus*, MSI study by MALDI TOF/TOF showed its consistent localization in the brain with previously identified CabTRP 1a in both fed and unfed animals. Through comparative feeding study, the relative amount of CalsTRP and CabTRP were suggested to be elevated in both brain and the CoGs when evaluating the MSI distribution density maps. This semi-quantitative result was reproducible across different biological replicates and was consistent with isotopic-labeling relative quantitation performed on a CE-MALDI MS platform. With aforementioned valuable spatial information from MS imaging, the colocalization of CabTRP 1a and CalsTRP in the brain suggested that both TRPs were encoded in the same preprotachykinin and functionalized in the gastric mill and pyloric rhythm.

In addition to brain and PO, the entire STNS also contains multiple NPs and neurotransmitters. The STG is the center of the STNS with only 26 neurons that are relatively large and well characterized with their cellular identities and

electrophysiological properties. This invertebrate neuronal network provides an excellent platform to investigate general principles of neuromodulation and the functional roles of NPs in circuit dynamics. Recently, Ye et al [112] were able to unambiguously map the spatial distribution of 55 NPs from 10 families in the 4 major ganglia in STNS of *C. sapidus* with high sensitivity, specificity and sub-neuron size spatial resolution of 25 m on autoflex III MALDI TOF/TOF instrument. Representative MS images are presented in **Figure 2-3**. Overall, distinct expression patterns of NPs at each ganglion and associated connecting nerves were revealed. For example, significantly higher abundance of two RYamides were detected in the CoGs compared to the STG, four orcokinins existed exclusively in the STG, B-type ASTs were widely distributed in the STG and *stn* with minimal signals in the CoGs. To further increase the confidence of identification of these highly complex NPs with similar masses, a high resolving power MALDI Fourier transform ion cyclotron resonance (FT-ICR) instrument was also employed. Two ions with mass difference of 0.09 Da were successfully distinguished with significantly different spatial expression patterns. Taking advantage of multifaceted platforms, a more complete coverage of the neuropeptidomes was achieved by combining instrumentation with complementary capabilities. For instance, a B-type AST GSNWSNLRGAWamide was detected by FT-ICR while absent by TOF/TOF detection, CabTRP 1a and CalsTRP on the other hand, were only seen with the TOF/TOF instrument.

Larger NPs from the CHH superfamily with molecular weight higher than 8 kDa were spatially characterized using MS imaging in the sinus gland (SG) of both *C. borealis* and *C. sapidus* for the first time by Jia et al. [119]. The distribution of the members from two different CHH subfamilies was reported to be in stark contrast, which

indicates their diverse signaling pathways in the physiological process. The MALDI TOF/TOF platform is excellent for studying large NPs and neurohormones due to its ability to detect biomolecules with wide mass range. In this study, both smaller CPRPs and large CHHs are simultaneously mapped in the SG. However, due to the structural complexity of these 72-mer NPs, such as various posttranslational modifications and post mortem degradation, the isolation window for plotting the spatial distribution was set to be ±10 Da to include variable isoforms of the same NP. To overcome the low specificity of MS imaging for large NPs and the poor on-tissue fragmentation of singly charged large molecules, multiply charged ions have been generated for MS imaging investigation using either novel matrix or electrospray based ionization platform [120, 121]. Because minimum sample tampering in MS imaging preparation tends to preserve more accurate PTM features, the production of multiply charged precursor ions *in situ* would be highly desirable for MS imaging and characterization of these large peptide hormones [122].

NPs of other species in decapod crustacean have also been spatially characterized using MS imaging, such as lobster *Homarus americanus* and giant tiger prawn *Penaeus monodon*. Chen et al [86] used both MALDI TOF/TOF and MALDI LTQ Orbitrap to map the distribution of NPs in the *H. americanus* neuropeptidomic study. Single isotope in an isotopic envelope was selected for high specificity mapping of the NPs with an isolation window of ±0.0025 Da from the data acquired on an Orbitrap platform. In addition to the high mass accuracy, confident and interference-free validation was granted by the ability to conduct selected reaction monitoring (SRM) MS/MS experiment in the LTQ ion trap. The abundant spatial distribution of CabTRP 1a and Val-SIFamide in the olfactory lobe (OL) and accessory lobe (AL) neuropils clearly suggested their

neuroregulatory functions in the olfactory system which significantly affects the chemosensory reception in crustacean. Moreover, the high concentration of orcokinin NFDEIDRSGFGFN in the antenna II neuropil (AnN) and lateral antennular neuropil (LAN) provided evidence of its inhibitory role in the tactile sensory. This work is an excellent example to demonstrate the great potential of MS imaging to reveal the physiological functions of NPs by correlating their spatial distribution information. Another work by Chansela et al [123] used the Ultraflex II MALDI TOF/TOF to investigate the NP distribution in *P. monodon*. These researchers examined paraffin-embedded tissue sections (PETs) of various neuroendocrine organs including eye stalk, brain lamina ganglionaris and TG. Among the 29 NPs detected in nanoLC-ESI-QTOF, eight NPs were visualized by MS imaging. PETs provide an opportunity to combine IHC staining with MS imaging results using minute size crustacean tissue for enhanced chemical information.

For a heterogeneous tissue like the brain of a crab, traditional MS imaging analyses only provide a small 2D fraction of the complexity of various neuropils and neuronal clusters, leading to incomplete description of NP distribution in the whole brain volume. However, when 2D ion density maps of one NP are stacked in consecutive orders, comprehensive 3D spatial distribution throughout the entire tissue could provide a more complete picture of NP localization in a complex neuronal structure such as brain. Detailed review of 3D MS imaging have been brought about by multiple research groups [71, 124, 125]. As an example, Chen et al [76] demonstrated the reconstruction of more than 20 NPs from 8 families in the 3D volume of the *C. borealis* brain by creating consecutive series of seven layers of brain sections with equal intervals. Moreover, a

comparison between the localization of NPs and phospholipids in the brain was made to highlight the distinct distribution patterns of these diverse classes of signaling molecules throughout the nervous system.

Although MALDI MSI has been the predominant technique to map the spatial distribution of biomolecules, limitations associated with the use of matrix such as background interference, possible diffusion during matrix application, and the reduced spatial resolution caused by matrix crystal size, have proven to be challenging to overcome. Efforts have been made by Sturm et al [109] to take advantage of the relatively new matrix-free NIMS imaging platform to study the NPs and lipids in the brain of *C. borealis*. Since NIMS has been demonstrated to be capable of detecting biomolecules below 1800 Da including metabolites, lipids and drugs, most of the NPs in crustacean were believed to be detectable as well since they fall in this mass range. However, only lipids from the brain were readily detected using NIMS while tissue from the same preparation studied with MALDI MS enabled the detection of NPs with decent signal intensities.

In **Table 2-1**, we summarize the NPs whose spatial distributions have been mapped in various crustacean species. We also categorize the types of MS instruments with which the imaging experiments were performed. It is important to point out that only the ones that were explicitly mentioned and/or plotted in the literature were included in the table. For instance, Chen et al [76] constructed 3D MS images of 20 NPs in the study of *C. borealis* brain, but only the seven NPs whose identities were revealed in the paper are listed here. In the column labeled as "*in situ* identification", either on-tissue

MS/MS fragmentation (labeled as MS^2) or matching by accurate mass (AM) was specified as the method for identification and/or validation.

2.4.4 *Challenges and outlook of MSI technique in the study of NPs in crustacean*

Hundreds of NPs have been characterized in different species of crustacean providing great opportunities for a better understanding of potential correlation between location and functionalities of NPs [92, 126]. Nonetheless, challenges still exist when it comes to the detection of the small NPs and neurotransmitters with m/z overlapping the matrix and lipids rich regions. With the prosperous development in nanoscience, we expect to see exciting new materials to replace conventional matrix with prospective properties such as minimum background interference, excellent desorption/ionization efficiency, low to no limit to the lateral resolution etc [127-129]. Most of the known NPs are *de novo* sequenced via an LC-MS platform. On tissue *de novo* sequencing associated with MS imaging has only limited success for high abundance NPs. To further expand the power of *in situ* NP discovery via *de novo* sequencing, such as high throughput data dependent MS/MS imaging acquisition, we need more sensitive MS instruments with better ion transmission efficiency and new matrices that enable robust production of multiply charged ions for better fragmentation efficiency. In addition, the ambient ionization enabled by the atmospheric pressure (AP)-MALDI platform [130, 131] can provide an alternative desorption/ionization mode that has the potential for detection of NPs with labile modifications, such as tyrosine sulfation in sulfakinin NP [132].

2.5 Microdialysis- the temporal probe of crustacean NPs

2.5.1 *Introduction*

Complementary to tissue imaging studies in which we can learn about the spatial location of molecules of interest, *in vivo* sampling techniques, such as microdialysis and push-pull perfusion, offer the unique advantages of monitoring signaling molecules involved in biological events with temporal resolution.

Microdialysis has been widely employed in the field of neuroscience, due to its ability to collect neurochemicals during a physiological behavior or stimulus of interest in a time-resolved fashion with minimal disturbance to the animals, providing useful insights into the action of molecules *in vivo*. In this sampling technique, a microdialysis probe is implanted into the tissue of interest allowing continuously sampling from the extracellular space. Since its first introduction by Bito et al. [133], studies employing the use of microdialysis have been expanded into a wide variety of tissues and organs in the body including liver, heart, skin, blood, placenta, stomach and ear, as summarized elsewhere [134, 135]. The types of analytes that microdialysis probe could sample have also been explored and proven to be rather diverse, from low molecular weight substances such as electrolytes [136], amines and amino acids [137], to higher molecular substances such as NPs [138, 139].

Like any analytical sampling technique, microdialysis has numerous advantages resulting in widespread applications, but it also suffers from several limitations. First, the small diameter of the microdialysis probe allows minimal damage to the tissue and disturbance to the animal. Consequently, long-term sampling can be achieved while the animal is awake and freely moving. Second, the microdialysis probe membrane, which has a pre-defined molecular weight cutoff can act as a physical barrier between the perfusion solution and tissue, this in turn not only protects tissue from the turbulent flow

of the perfusion solution, but also excludes high-molecular-weight substances which would yield a cleaner sample. Finally, a more precise quantitative comparison of analytes could be conducted from microdialysis samples as one animal serves as its own control thus could minimize individual variation.

Despite the advantages of microdialysis over other techniques, there are some disadvantages worth noting. First, microdialysis is most powerful for providing timely-resolved information. However, the temporal resolution is also limited, mostly by the sensitivity of detection method. Second, the relatively low recovery rate of analyte using microdialysis makes the detection technique more demanding especially for larger molecules like NPs or proteins.

Being considered as a prime method to sample from biofluid, microdialysis has been successfully applied to several crustacean species despite the obvious obstacle of the hard shell. Cebada *et al*. [137] used microdialysis method to study fluctuations of non-essential amino acids, GABA, and histamine in hemolymph of crayfish and quantified these molecules on hourly basis. Two studies from our lab [138, 139] reported on the use of MS-based techniques to study NP content in the hemolymph from Jonah crab, *Cancer borealis*, collected via microdialysis sampling method.

2.5.2 *Principle of microdialysis process*

Among the various types of microdialysis probes that are commercially available, a common key component is the dialysis membrane at the probe tip (**Figure 2-4**). The dialysis membrane is semipermeable, which is limited by the molecular weight cutoff of the membrane. When sampling from extracellular space, it is based on gradient driven diffusion across the dialysis membrane. As perfusion solution is pushed through inlet,

normally at a rate of 0.1-3.0 µl/min [140], molecules fall below the molecular weight cutoff of the membrane would diffuse across the membrane and get collected in the dialysate for analysis.

Interpretation of microdialysis data could prove to be challenging. When sampling with microdialysis, the concentration of analyte of interest in the dialysate (C_{out}) will be smaller than that in extracellular space (C_{ext}). The relative recovery (R) is defined as the ratio of C_{out}/C_{ext}, and could be affected by a number of factors, such as flow rate, pore size of membrane (molecular weight cutoff), etc. Extensive efforts have been made to increase R according to the analyte of interest. For instance, by using ultraslow flow rate, which gives enough time for interaction of analytes and the membrane, R has been significantly increased for amines and drugs [141, 142]. Knowing the relative recovery is essential for estimation of external concentration of substance of interest from that in dialysate. It is easier to determine the *in vitro R* in dialysis of known concentration of samples and measure C_{out}. However, it has long been recognized that *in vitro R* is not an accurate representation of *in vivo R* due to the fact that the extracellular environment is much more complicated and highly dynamic within the animal. Several methods to measure *in vivo R* have been developed including manipulating the flow rate and adding an internal standard. No net flux (NNF), the concept was first introduced by Lonroth *et al*. in 1987 [143], soon was applied to quantitative microdialysis by several researchers [144-146] and has become one of the most popular methods. This method, also known as zero flow rate method, determines extracellular concentration by correlating perfusate flow rate with transfer coefficient. Moreover, the dialysate concentration at zero flow rate is expected to equal the extracellular concentration. Another common method is adding

an internal standard, normally isotopically labeled, and then measuring the loss of the isotopically labeled internal standard from the perfusate [147, 148]. Due to the technical difficulties, most studies to date quantify relative dynamic changes. The absolute quantitation will require more sophisticated assays.

2.5.3 *Microdialysis in crustacean*

NPs in circulatory fluid, hemolymph, secreted from major neuroendocrine organs in decapod crustaceans, act as circulating hormones and regulate numerous physiological processes. However, characterization of NP content in crustacean hemolymph has always been challenging. These low-level NPs are difficult to detect due to high salt interference and suppression from the high abundance protein degradation products in crude hemolymph extracts. Chen et al. developed a simple and effective hemolymph preparation method suitable for MALDI MS analysis of NPs, and successfully identified 10 secreted NPs from several families, such as RFamide, AST, orcokinin, TRP and CCAP in Jonah crab *Cancer borealis* [76].

An alternative way to study hemolymph is the use of microdialysis. As described by Behrens [138] and Schmerberg [139], the microdialysis probe was implanted into the pericardial sinus of live crabs. Crustacean, unlike mammal, has an open circulatory system and the pericardial organ is a major hormonal release site. Thus, microdialysis is an ideal method to sample the circulating fluid in order to study NP release. For microdialysis sampling from crustaceans, the perfusion solution is crab saline to minimize the effect of sampling on the ionic strength of crustacean hemolymph. Members from 10 NP families including ASTs, TRP, orcokinin, RFamide, RYamide were identified from Jonah crab *Cancer borealis* hemolymph as reported in the first

application of *in vivo* microdialysis method for MS analysis of NPs from a freely moving crab [13]. Coupling microdialysis with MS has several advantages compared to direct hemolymph extraction method. Not only more NPs have been identified with microdialysis sampling due to removal of larger protein species and producing cleaner sample matrix, but also the *in vivo* sampling method allows monitoring dynamic changes of NPs in a timely-resolved fashion thus correlating chemistry with animal behaviors.

Comparing to small molecules, NPs have a lower *R* value due to their relatively larger size, which would hinder passing through the dialysis membrane. Efforts have been made to improve *R* for larger molecules, such as sampling with microdialysis probe with larger pore size [149] yielding better recovery for proteins. An alternative way to improve *R* for microdialysis sampling of NPs is affinity-enhanced microdialysis (AE-MD), where better recovery rate could be achieved by adding affinity agent into the perfusate. Numerous applications have employed this strategy for a wide range of analytes [150-152]. A recent study from our lab utilized RFamide antibody linked magnetic nanoparticles to increase recovery of RFamide-related peptides when sampling from Jonah crab, *Cancer borealis* by microdialysis [139]. *In vitro* R value has been increased up to 41-fold with NP standards tested, and more than 10 NPs were detected in a 30 min collection sample as compared to previous 4-hour collection time without the use of AE-MD. Due to the improvement of recovery rate and subsequent increase of NP identifications, more reliable quantitation of NPs during a dynamic process, such as feeding, has also been achieved.

2.5.3 *Temporal resolution*

Microdialysis has the advantage of providing temporal information over other sampling techniques. The shortest time duration over which a dynamic change event could be observed is how temporal resolution is measured. The course of such information is mostly relied on the detection sensitivity, where enough analytes need to be collected at certain flow rate per fraction to be able reach the detection limit. To monitor dynamic changes of chemicals during a specific behavior, it is critical to capture the content in a high temporal resolution fashion because concentration change of analyte could happen rather rapidly. Several highly sensitive methods are available for resolution as good as couple of seconds for fraction collection, and for online microdialysate analysis.

With common HPLC methods, the temporal resolution for NP detection could reach 10 to 30 min [140]. As results shown from several studies, capillary electrophoresis, which could handle much smaller sample volume compared to HPLC by using microcolumn, coupled with laser-induced fluorescence detection could resolve analytes of interest in the order of seconds via online coupling with microdialysis sampling [153-155]. However, the high temporal resolution is realized using anesthetized animal at high dialysis flow rates, which leads to lower recovery rate. Further improvement of *in vivo* microdialysis application has been achieved by using segment flow for freely moving animals at low flow rates via microfluidic segmented outflow [156, 157], with temporal resolution of seconds. Chip-based electrophoresis provided the capability of monitoring amino acids at high temporal resolution as fast as two seconds [9, 158]. Enzymatic assay to monitor glutamate dynamic changes [159] produced a

temporal resolution of 7s *in vivo* and 200 ms *in vitro*. Coupling segmented flow with electrochemical [160] and mass spectrometry [161] have been conducted.

2.5.4 *Mass spectrometric detection of NPs from microdialysis*

Circulating peptide hormones are present at extremely low concentrations in extracellular space [162], ranging from pM to nM. Moreover, low recovery rate of sampling NPs from the hemolymph makes the subsequent detection more difficult. Detection of microdialysis samples usually requires high sensitivity, and the capability of handling µL volumes. Traditional immunoassays, fluorometric or radioactive or enzyme, were extensively used to measure NP release collected via microdialysis [163, 164]. However, these methods lack specificity due to cross reaction, making them not suitable for complex mixture analysis and novel peptide discovery. Moreover, the number of assayable substances is also limited in each sample. The volume requirements for these assays need to be taken into consideration in regard to temporal resolution. Numerous assays have been developed for the characterization of different neurotransmitters [165].

Since first described by Emmett *et al*. [166], the coupling of MS detection with microdialysis sampling has become a common strategy for identification and quantitation of analytes of interest. One of the most common separation methods coupled with MS analysis is LC. The power of LC-MS has been showcased by several laboratories in the identification and quantitation of different neurotransmitters in microdialysates [167-170].

Trace level concentration and highly dynamic changes of NPs *in vivo* make it challenging to detect these low abundance signaling molecules in the microdialysates. Capillary LC-MS^n (CLC-MS^n) platform has been developed by several groups towards

the detection of NPs. Over the past several years, the field has seen significant progress. Using such platform, NP secretion has been explored in different organisms, from crustaceans [138] to mammalian [171, 172] to primates [173]. The on-going improvement in LC-MS methods has boosted the capability of microdialysis to provide unique insight into the role of NPs in behavior. The study by DiFeliceantonio *et al*. [174] described the first detection of opioid peptide, enkephalin, during feeding, which increased in the dorsal striatum of rats. This finding about opioid peptide acting as a signal to eat was further confirmed by microinjection of the opioid peptide into the same brain region evoking feeding behavior. Quantitative measurement of NPs during feeding behavior in Jonah crab, *Cancer borealis* by Schmerberg and Li [139] also revealed several candidates as signaling molecules involved in food intake in crustacean.

2.5.5 *Challenges and perspectives of probing temporal dynamics via microdialysis sampling technique*

To date, application of microdialysis is more restricted to mammalian nervous systems. There are only a few publications about microdialysis in crustaceans. Technical difficulties associated with microdialysis in crustacean are the main obstacles for its widespread use. The hard shell of the animal makes the surgery and implantation of the microdialysis probe more complicated, in addition to maintaining the microdialysis probe in working condition underwater. Other factors such as low concentration of circulating hormones in crustaceans and relatively poor recovery rate of the dialysis membrane make the detection of NPs in microdialysate very challenging. Despite significant challenges, nanoflow LC coupled to tandem MS enabled detection of NPs in the microdialysate collected from Jonah crab, *Cancer borealis* [138, 139]. AE-MD showed great potential

for further improving temporal resolution by increased recovery rate. Future work will focus on further improving peptidome coverage and quantitation as well as combining multi-pronged approach to enable correlation of neurochemical and circuit dynamics with behavior.

2.6 Conclusions and Future Perspectives

Decapod crustaceans have made significant contributions to the study of NPs and neuromodulation, both in analytical method development and in our molecular understanding of how NPs can modulate circuit dynamics. MS-based techniques are optimal for studying NPs, due to their high specificity when compared with other techniques. MSI is an emerging technique to map the distribution of NPs in a given tissue with greater specificity than antibody-based imaging techniques and the ability to characterize the distribution of thousands of analytes in a single experiment. Complementary to tissue expression and spatial distribution of NPs, *in vivo* microdialysis sampling on living crustacean coupled to MS detection enables correlation of NP temporal dynamics with activity.

Although recent advances in MS have significantly accelerated the pace of NP discovery and functional identification, further technological advances are under development and the full suite of crustacean NPs has not yet been described completely. Advances in MS technology will greatly improve the capabilities of this technique to provide tissue localization, identity, and quantity information. In the area of MSI, methods for tissue coating with matrix are being improved to create smaller, more uniform crystals, to decrease analyte diffusion, provide better spatial resolution, increase sensitivity, and reduce “hot spots” of signal on the tissue. Improvements to laser

technology will also improve the spatial resolution of this technique. For identification, faster scan rates, higher accuracy, and better resolution will improve the quality of identifications and allow less abundant compounds to be identified. Furthermore, NPs can be monitored continuously with the aid of the minimally invasive sampling technique of microdialysis coupled to LC-MS/MS approach. Combined with quantitative technique, this method will narrow down the list of hundreds of NPs to a few "interesting" NPs in an unbiased and systematic manner. The ongoing improvement of instrument sensitivity and strategies to reduce sampling intervals and enable on-line coupling will further improve temporal resolution for monitoring of neurochemical dynamics in behaving animal. Further improvements to the analysis methods with increased spatial and temporal information that enable the study of NP functions will greatly increase our understanding of this important class of signaling molecules, both in crustaceans and in other organisms, including mammals.

2.7 References

1. Burbach, J.P., *What are neuropeptides?* Methods Mol Biol, 2011. **789**: p. 1-36.
2. North G, G.R.J., *Invertebrate neurobiology*. 2007: Cold Spring Harbor Laboratory Press New York.
3. Clarac, F. and Pearlstein, E., *Invertebrate preparations and their contribution to neurobiology in the second half of the 20th century.* Brain Res Rev, 2007. **54**(1): p. 113-61.
4. Marder, E. and Bucher, D., *Understanding circuit dynamics using the stomatogastric nervous system of lobsters and crabs.* Annu Rev Physiol, 2007. **69**: p. 291-316.
5. Coleman, M.J., Nusbaum, M.P., Cournil, I., and Claiborne, B.J., *Distribution of modulatory inputs to the stomatogastric ganglion of the crab, Cancer borealis.* J Comp Neurol, 1992. **325**(4): p. 581-94.
6. Schmidt, M., *The olfactory pathway of decapod crustaceans--an invertebrate model for life-long neurogenesis.* Chem Senses, 2007. **32**(4): p. 365-84.
7. Kirby, M.S. and Nusbaum, M.P., *Central nervous system projections to and from the commissural ganglion of the crab Cancer borealis.* Cell Tissue Res, 2007. **328**(3): p. 625-37.
8. Li, L., Pulver, S.R., Kelley, W.P., Thirumalai, V., Sweedler, J.V., and Marder, E., *Orcokinin peptides in developing and adult crustacean stomatogastric nervous systems and pericardial organs.* J Comp Neurol, 2002. **444**(3): p. 227-44.
9. Ma, M., Wang, J., Chen, R., and Li, L., *Expanding the Crustacean neuropeptidome using a multifaceted mass spectrometric approach.* J Proteome Res, 2009. **8**(5): p. 2426-37.
10. Ma, M., Bors, E.K., Dickinson, E.S., Kwiatkowski, M.A., Sousa, G.L., Henry, R.P., Smith, C.M., Towle, D.W., Christie, A.E., and Li, L., *Characterization of the Carcinus maenas neuropeptidome by mass spectrometry and functional genomics.* Gen Comp Endocrinol, 2009. **161**(3): p. 320-34.
11. Ma, M., Chen, R., Sousa, G.L., Bors, E.K., Kwiatkowski, M.A., Goiney, C.C., Goy, M.F., Christie, A.E., and Li, L., *Mass spectral characterization of peptide transmitters/hormones in the nervous system and neuroendocrine organs of the American lobster Homarus americanus.* Gen Comp Endocrinol, 2008. **156**(2): p. 395-409.
12. Vazquez, L., Alpuche, J., Maldonado, G., Agundis, C., Pereyra-Morales, A., and Zenteno, E., *Review: Immunity mechanisms in crustaceans.* Innate Immun, 2009. **15**(3): p. 179-88.
13. McGaw, I.J., *The decapod crustacean circulatory system: a case that is neither open nor closed.* Microsc Microanal, 2005. **11**(1): p. 18-36.
14. Dickinson, P.S., Mecsas, C., and Marder, E., *Neuropeptide fusion of two motor-pattern generator circuits.* Nature, 1990. **344**(6262): p. 155-8.

15. Nusbaum, M.P. and Beenhakker, M.P., *A small-systems approach to motor pattern generation.* Nature, 2002. **417**(6886): p. 343-50.

16. Grillner, S., Markram, H., De Schutter, E., Silberberg, G., and LeBeau, F.E., *Microcircuits in action--from CPGs to neocortex.* Trends Neurosci, 2005. **28**(10): p. 525-33.

17. Lopez-Vera, E., Aguilar, M.B., and Heimer de la Cotera, E.P., *FMRFamide and related peptides in the phylum mollusca.* Peptides, 2008. **29**(2): p. 310-7.

18. Zajac, J.M. and Mollereau, C., *RFamide peptides. Introduction.* Peptides, 2006. **27**(5): p. 941-2.

19. Bruzzone, F., Lectez, B., Tollemer, H., Leprince, J., Dujardin, C., Rachidi, W., Chatenet, D., Baroncini, M., Beauvillain, J.C., Vallarino, M., Vaudry, H., and Chartrel, N., *Anatomical distribution and biochemical characterization of the novel RFamide peptide 26RFa in the human hypothalamus and spinal cord.* J Neurochem, 2006. **99**(2): p. 616-27.

20. US, V.E. and Gaddum, J.H., *An unidentified depressor substance in certain tissue extracts.* J Physiol, 1931. **72**(1): p. 74-87.

21. Chang, M.M., Leeman, S.E., and Niall, H.D., *Amino-Acid Sequence of Substance P.* Nature-New Biology, 1971. **232**(29): p. 86-&.

22. Fricker, L.D. *Neuropeptides and other bioactive peptides: from discovery to function*. in *Colloquium Series on Neuropeptides*. 2012. : Morgan & Claypool Life Sciences.

23. Brown, B.E. and Starratt, A.N., *Isolation of Proctolin, a Myotropic Peptide, from Periplaneta-Americana.* Journal of Insect Physiology, 1975. **21**(11): p. 1879-1881.

24. Tatemoto, K. and Mutt, V., *Chemical Determination of Polypeptide Hormones.* Proceedings of the National Academy of Sciences of the United States of America, 1978. **75**(9): p. 4115-4119.

25. Tatemoto, K. and Mutt, V., *Isolation and Characterization of the Intestinal Peptide Porcine Phi (Phi-27), a New Member of the Glucagon-Secretin Family.* Proceedings of the National Academy of Sciences of the United States of America-Biological Sciences, 1981. **78**(11): p. 6603-6607.

26. Tatemoto, K., Carlquist, M., and Mutt, V., *Neuropeptide-Y - a Novel Brain Peptide with Structural Similarities to Peptide-Yy and Pancreatic-Polypeptide.* Nature, 1982. **296**(5858): p. 659-660.

27. Bohus, B. and De Wied, D., *Inhibitory and facilitatory effect of two related peptides on extinction of avoidance behavior.* Science, 1966. **153**(3733): p. 318-20.

28. De Wied, D., *Long term effect of vasopressin on the maintenance of a conditioned avoidance response in rats.* Nature, 1971. **232**(5305): p. 58-60.

29. Wied, D., *Peptides and Behavior*, in *Memory and Transfer of Information*, H. Zippel, Editor. 1973, Springer US. p. 373-389.

30. Gispen, W.H., *David de Wied Eminent scientist and academic leader: A personal note.* European Journal of Pharmacology, 2010. **626**(1): p. 4-8.

31. Perkins, E.B., *Color changes in crustaceans, especially in Palaemonetes.* Journal of Experimental Zoology, 1928. **50**(1): p. 71-105.

32. Josefsson, L., *Invertebrate neuropeptide hormones.* Int J Pept Protein Res, 1983. **21**(5): p. 459-70.

33. Fernlund, P. and Josefsson, L., *Chromactivating hormones of Pandalus Borealis. Isolation and purification of the 'red-pigment-concentrating hormone'.* Biochim Biophys Acta, 1968. **158**(2): p. 262-73.

34. Fernlund, P. and Josefsso.L, *Crustacean Color-Change Hormone - Amino-Acid Sequence and Chemical Synthesis.* Science, 1972. **177**(4044): p. 173-&.

35. Stone, J.V., Mordue, W., Batley, K.E., and Morris, H.R., *Structure of locust adipokinetic hormone, a neurohormone that regulates lipid utilisation during flight.* Nature, 1976. **263**(5574): p. 207-11.

36. Christie, A.E., Stemmler, E.A., and Dickinson, P.S., *Crustacean neuropeptides.* Cell Mol Life Sci, 2010. **67**(24): p. 4135-69.

37. Keller, R., *Crustacean neuropeptides: structures, functions and comparative aspects.* Experientia, 1992. **48**(5): p. 439-48.

38. Baggerman, G., Boonen, K., Verleyen, P., De Loof, A., and Schoofs, L., *Peptidomic analysis of the larval Drosophila melanogaster central nervous system by two-dimensional capillary liquid chromatography quadrupole time-of-flight mass spectrometry.* J Mass Spectrom, 2005. **40**(2): p. 250-60.

39. Caprioli, R.M., Farmer, T.B., and Gile, J., *Molecular imaging of biological samples: Localization of peptides and proteins using MALDI-TOF MS.* Analytical Chemistry, 1997. **69**(23): p. 4751-4760.

40. Garsin, D.A., Villanueva, J.M., Begun, J., Kim, D.H., Sifri, C.D., Calderwood, S.B., Ruvkun, G., and Ausubel, F.M., *Long-lived C-elegans daf-2 mutants are resistant to bacterial pathogens.* Science, 2003. **300**(5627): p. 1921-1921.

41. Jia, C., Lietz, C.B., Ye, H., Hui, L., Yu, Q., Yoo, S., and Li, L., *A Multi-scale Strategy for Discovery of Novel Endogenous Neuropeptides in the Crustacean Nervous System.* J Proteomics, 2013.

42. Dua, K., Sheshala, R., Ling, T.Y., Hui Ling, S., and Gorajana, A., *Anti-inflammatory, antibacterial and analgesic potential of cocos nucifera linn.: a review.* Antiinflamm Antiallergy Agents Med Chem, 2013. **12**(2): p. 158-64.

43. Li, L.J., Pulver, S.R., Kelley, W.P., Thirumalai, V., Sweedler, J.V., and Marder, E., *Orcokinin peptides in developing and adult crustacean stomatogastric nervous systems and pericardial organs.* Journal of Comparative Neurology, 2002. **444**(3): p. 227-244.

44. Yin, P., Hou, X.W., Romanova, E.V., and Sweedler, J.V., *Neuropeptidomics: Mass Spectrometry-Based Qualitative and Quantitative Analysis.* Neuropeptides: Methods and Protocols, 2011. **789**: p. 223-236.

45. Chen, R.B., Ma, M.M., Hui, L.M., Zhang, J., and Li, L.J., *Measurement of Neuropeptides in Crustacean Hemolymph via MALDI Mass Spectrometry.* Journal of the American Society for Mass Spectrometry, 2009. **20**(4): p. 708-718.

46. Cape, S.S., Rehm, K.J., Ma, M., Marder, E., and Li, L.J., *Mass spectral comparison of the neuropeptide complement of the stomatogastric ganglion and brain in the adult and embryonic lobster, Homarus americanus.* Journal of Neurochemistry, 2008. **105**(3): p. 690-702.

47. Ma, M.M., Chen, R.B., Sousa, G.L., Bors, E.K., Kwiatkowski, M.A., Goiney, C.C., Goy, M.F., Christie, A.E., and Li, L.J., *Mass spectral characterization of peptide transmitters/hormones in the nervous system and neuroendocrine organs of the American lobster Homarus americanus.* General and Comparative Endocrinology, 2008. **156**(2): p. 395-409.

48. Bulau, P., Meisen, I., Schmitz, T., Keller, R., and Peter-Katalinic, J., *Identification of neuropeptides from the sinus gland of the crayfish Orconectes limosus using nanoscale on-line liquid chromatography tandem mass spectrometry.* Molecular & Cellular Proteomics, 2004. **3**(6): p. 558-564.

49. Behrens, H.L., Chen, R.B., and Li, L.J., *Combining microdialysis, nanoLC-MS, and MALDI-TOF/TOF to detect neuropeptides secreted in the crab, Cancer borealis.* Analytical Chemistry, 2008. **80**(18): p. 6949-6958.

50. Chen, R.B., Jiang, X.Y., Conaway, M.C.P., Mohtashemi, I., Hui, L.M., Viner, R., and Li, L.J., *Mass Spectral Analysis of Neuropeptide Expression and Distribution in the Nervous System of the Lobster Homarus americanus.* Journal of Proteome Research, 2010. **9**(2): p. 818-832.

51. DeKeyser, S.S. and Li, L.J., *Mass spectrometric charting of neuropeptides in arthropod neurons.* Analytical and Bioanalytical Chemistry, 2007. **387**(1): p. 29-35.

52. Hui, L.M., Cunningham, R., Zhang, Z.C., Cao, W.F., Jia, C.X., and Li, L.J., *Discovery and Characterization of the Crustacean Hyperglycemic Hormone Precursor Related Peptides (CPRP) and Orcokinin Neuropeptides in the Sinus Glands of the Blue Crab Callinectes sapidus Using Multiple Tandem Mass Spectrometry Techniques.* Journal of Proteome Research, 2011. **10**(9): p. 4219-4229.

53. Ma, M.M., Chen, R.B., Ge, Y., He, H., Marshall, A.G., and Li, L.J., *Combining Bottom-Up and Top-Down Mass Spectrometric Strategies for De Novo Sequencing of the Crustacean Hyperglycemic Hormone from Cancer borealis.* Analytical Chemistry, 2009. **81**(1): p. 240-247.

54. Ma, M.M., Gard, A.L., Xiang, F., Wang, J.H., Davoodian, N., Lenz, P.H., Malecha, S.R., Christie, A.E., and Li, L.J., *Combining in silico transcriptome*

mining and biological mass spectrometry for neuropeptide discovery in the Pacific white shrimp Litopenaeus vannamei. Peptides, 2010. **31**(1): p. 27-43.

55. Ma, M.M., Sturm, R.M., Kutz-Naber, K.K., Fu, Q., and Li, L.J., *Immunoaffinity-based mass spectrometric characterization of the FMRFamide-related peptide family in the pericardial organ of Cancer borealis.* Biochemical and Biophysical Research Communications, 2009. **390**(2): p. 325-330.

56. Hui, L.M., Xiang, F., Zhang, Y.Z., and Li, L.J., *Mass spectrometric elucidation of the neuropeptidome of a crustacean neuroendocrine organ.* Peptides, 2012. **36**(2): p. 230-239.

57. Husson, S.J., Clynen, E., Baggerman, G., De Loof, A., and Schoofs, L., *Discovering neuropeptides in Caenorhabditis elegans by two dimensional liquid chromatography and mass spectrometry.* Biochemical and Biophysical Research Communications, 2005. **335**(1): p. 76-86.

58. Mihailova, A., Karaszewski, B., Hauser, R., Lundanes, E., and Greibrokk, T., *Identification of neuropeptides in rat brain rhinencephalon.* Journal of Separation Science, 2007. **30**(2): p. 249-256.

59. Lam, M.P.Y., Siu, S.O., Lau, E., Mao, X.L., Sun, H.Z., Chiu, P.C.N., Yeung, W.S.B., Cox, D.M., and Chu, I.K., *Online coupling of reverse-phase and hydrophilic interaction liquid chromatography for protein and glycoprotein characterization.* Analytical and Bioanalytical Chemistry, 2010. **398**(2): p. 791-804.

60. Zhao, Y., Kong, R.P.W., Li, G.H., Lam, M.P.Y., Law, C.H., Lee, S.M.Y., Lam, H.C., and Chu, I.K., *Fully automatable two-dimensional hydrophilic interaction liquid chromatography-reversed phase liquid chromatography with online tandem mass spectrometry for shotgun proteomics.* Journal of Separation Science, 2012. **35**(14): p. 1755-1763.

61. Olsson, N., James, P., Borrebaeck, C.A.K., and Wingren, C., *Quantitative Proteomics Targeting Classes of Motif-containing Peptides Using Immunoaffinity-based Mass Spectrometry.* Molecular & Cellular Proteomics, 2012. **11**(8): p. 342-354.

62. Higuchi, H., *Molecular analysis of central feeding regulation by neuropeptide Y (NPY) neurons with NPY receptor small interfering RNAs (siRNAs).* Neurochem Int, 2012. **61**(6): p. 936-41.

63. Kanai, A., Zabbarova, I., Oefelein, M., Radziszewski, P., Ikeda, Y., and Andersson, K.E., *Mechanisms of action of botulinum neurotoxins, beta3-adrenergic receptor agonists, and PDE5 inhibitors in modulating detrusor function in overactive bladders: ICI-RS 2011.* Neurourol Urodyn, 2012. **31**(3): p. 300-8.

64. Do Rego, J.L., Seong, J.Y., Burel, D., Luu-The, V., Larhammar, D., Tsutsui, K., Pelletier, G., Tonon, M.C., and Vaudry, H., *Steroid biosynthesis within the frog brain: a model of neuroendocrine regulation.* Ann N Y Acad Sci, 2009. **1163**: p. 83-92.

65. Verleyen, P., Huybrechts, J., and Schoofs, L., *SIFamide illustrates the rapid evolution in Arthropod neuropeptide research.* Gen Comp Endocrinol, 2009. **162**(1): p. 27-35.

66. Szabo, T.M., Chen, R., Goeritz, M.L., Maloney, R.T., Tang, L.S., Li, L., and Marder, E., *Distribution and physiological effects of B-type allatostatins (myoinhibitory peptides, MIPs) in the stomatogastric nervous system of the crab Cancer borealis.* J Comp Neurol, 2011. **519**(13): p. 2658-76.

67. Ye, H., Greer, T., and Li, L., *Probing neuropeptide signaling at the organ and cellular domains via imaging mass spectrometry.* Journal of proteomics, 2012. **75**(16): p. 5014-5026.

68. Caprioli, R.M., Farmer, T.B., and Gile, J., *Molecular imaging of biological samples: localization of peptides and proteins using MALDI-TOF MS.* Anal Chem, 1997. **69**(23): p. 4751-60.

69. Chen, R. and Li, L., *Mass spectral imaging and profiling of neuropeptides at the organ and cellular domains.* Analytical and bioanalytical chemistry, 2010. **397**(8): p. 3185-3193.

70. Chughtai, K. and Heeren, R.M., *Mass spectrometric imaging for biomedical tissue analysis.* Chemical reviews, 2010. **110**(5): p. 3237-3277.

71. Ye, H., Greer, T., and Li, L., *From pixel to voxel: a deeper view of biological tissue by 3D mass spectral imaging.* Bioanalysis, 2011. **3**(3): p. 313332.

72. Lietz, C.B., Gemperline, E., and Li, L., *Qualitative and quantitative mass spectrometry imaging of drugs and metabolites.* Advanced drug delivery reviews, 2013. **65**(8): p. 1074-1085.

73. Ye, H., Gemperline, E., and Li, L., *A vision for better health: mass spectrometry imaging for clinical diagnostics.* Clinica chimica acta; international journal of clinical chemistry, 2013. **420**: p. 11-22.

74. Erin, G., Bingming, C., and Lingjun, L., *Challenges and recent advances in mass spectrometric imaging of neurotransmitters.* Bioanalysis, 2014.

75. DeKeyser, S.S., Kutz-Naber, K.K., Schmidt, J.J., Barrett-Wilt, G.A., and Li, L., *Imaging Mass Spectrometry of Neuropeptides in Decapod Crustacean Neuronal Tissues.* Journal of Proteome Research, 2007. **6**(5): p. 17821791.

76. Chen, R., Ma, M., Hui, L., Zhang, J., and Li, L., *Measurement of neuropeptides in crustacean hemolymph via MALDI mass spectrometry.* J Am Soc Mass Spectrom, 2009. **20**(4): p. 708-18.

77. Chen, R., Hui, L., Cape, S.S., Wang, J., and Li, L., *Comparative Neuropeptidomic Analysis of Food Intake via a Multifaceted Mass Spectrometric Approach.* ACS Chemical Neuroscience, 2010. **1**(3): p. 204214.

78. Korte, A.R. and Lee, Y.J., *Multiplex mass spectrometric imaging with polarity switching for concurrent acquisition of positive and negative ion images.* Journal of the American Society for Mass Spectrometry, 2013. **24**(6): p. 949-955.

79. Perdian, D.C. and Lee, Y.J., *Imaging MS methodology for more chemical information in less data acquisition time utilizing a hybrid linear ion trap-orbitrap mass spectrometer.* Analytical chemistry, 2010. **82**(22): p. 9393-9400.

80. Yagnik, G.B., Korte, A.R., and Lee, Y.J., *Multiplex mass spectrometry imaging for latent fingerprints.* Journal of mass spectrometry : JMS, 2013. **48**(1): p. 100-104.

81. Jimenez, C.R., Li, K.W., Dreisewerd, K., Spijker, S., Kingston, R., Bateman, R.H., Burlingame, A.L., Smit, A.B., van Minnen, J., and Geraerts, W.P., *Direct mass spectrometric peptide profiling and sequencing of single neurons reveals differential peptide patterns in a small neuronal network.* Biochemistry, 1998. **37**(7): p. 2070-6.

82. Jimenez, C.R., Li, K.W., Dreisewerd, K., Mansvelder, H.D., Brussaard, A.B., Reinhold, B.B., Van der Schors, R.C., Karas, M., Hillenkamp, F., Burbach, J.P., Costello, C.E., and Geraerts, W.P., *Pattern changes of pituitary peptides in rat after salt-loading as detected by means of direct, semiquantitative mass spectrometric profiling.* Proc Natl Acad Sci U S A, 1997. **94**(17): p. 9481-6.

83. Jimenez, C.R., ter Maat, A., Pieneman, A., Burlingame, A.L., Smit, A.B., and Li, K.W., *Spatio-temporal dynamics of the egg-laying-inducing peptides during an egg-laying cycle: a semiquantitative matrix-assisted laser desorption/ionization mass spectrometry approach.* J Neurochem, 2004. **89**(4): p. 865-75.

84. Jimenez, C.R., Li, K.W., Smit, A.B., and Janse, C., *Auto-inhibitory control of peptidergic molluscan neurons and reproductive senescence.* Neurobiol Aging, 2006. **27**(5): p. 763-9.

85. Ellis, S.R., Bruinen, A.L., and Heeren, R.M., *A critical evaluation of the current state-of-the-art in quantitative imaging mass spectrometry.* Anal Bioanal Chem, 2014. **406**(5): p. 1275-89.

86. Chen, R., Jiang, X., Conaway, M.C., Mohtashemi, I., Hui, L., Viner, R., and Li, L., *Mass spectral analysis of neuropeptide expression and distribution in the nervous system of the lobster Homarus americanus.* Journal of proteome research, 2010. **9**(2): p. 818-832.

87. Kutz, K.K., Schmidt, J.J., and Li, L., *In situ tissue analysis of neuropeptides by MALDI FTMS in-cell accumulation.* Anal Chem, 2004. **76**(19): p. 5630-40.

88. Jia, X., Hollung, K., Therkildsen, M., Hildrum, K.I., and Bendixen, E., *Proteome analysis of early post-mortem changes in two bovine muscle types: M. longissimus dorsi and M. semitendinosis.* Proteomics, 2006. **6**(3): p. 936-44.

89. Svensson, M., Skold, K., Nilsson, A., Falth, M., Nydahl, K., Svenningsson, P., and Andren, P.E., *Neuropeptidomics: MS applied to the discovery of novel peptides from the brain.* Anal Chem, 2007. **79**(1): p. 15-6, 18-21.

90. Svensson, M., Skold, K., Svenningsson, P., and Andren, P.E., *Peptidomics-based discovery of novel neuropeptides.* J Proteome Res, 2003. **2**(2): p. 213-9.

91. O'Callaghan, J.P. and Sriram, K., *Focused microwave irradiation of the brain preserves in vivo protein phosphorylation: comparison with other methods of sacrifice and analysis of multiple phosphoproteins.* Journal of Neuroscience Methods, 2004. **135**(1–2): p. 159-168.

92. Yu, Q., OuYang, C., Liang, Z., and Li, L., *Mass spectrometric characterization of the crustacean neuropeptidome.* EuPA Open Proteomics, 2014. **3**(0): p. 152-170.

93. Svensson, M., Boren, M., Skold, K., Falth, M., Sjogren, B., Andersson, M., Svenningsson, P., and Andren, P.E., *Heat stabilization of the tissue proteome: a new technology for improved proteomics.* J Proteome Res, 2009. **8**(2): p. 974-81.

94. Skold, K., Svensson, M., Norrman, M., Sjogren, B., Svenningsson, P., and Andren, P.E., *The significance of biochemical and molecular sample integrity in brain proteomics and peptidomics: stathmin 2-20 and peptides as sample quality indicators.* Proteomics, 2007. **7**(24): p. 4445-56.

95. Sturm, R.M., Greer, T., Woodards, N., Gemperline, E., and Li, L., *Mass spectrometric evaluation of neuropeptidomic profiles upon heat stabilization treatment of neuroendocrine tissues in crustaceans.* J Proteome Res, 2013. **12**(2): p. 743-52.

96. Lemaire, R., Desmons, A., Tabet, J.C., Day, R., Salzet, M., and Fournier, I., *Direct analysis and MALDI imaging of formalin-fixed, paraffin-embedded tissue sections.* J Proteome Res, 2007. **6**(4): p. 1295-305.

97. Lemaire, R., Desmons, A., Tabet, J.C., Day, R., Salzet, M., and Fournier, I., *Direct analysis and MALDI imaging of formalin-fixed, paraffin-embedded tissue sections.* Journal of proteome research, 2007. **6**(4): p. 1295-1305.

98. Groseclose, M.R., Massion, P.P., Chaurand, P., and Caprioli, R.M., *High-throughput proteomic analysis of formalin-fixed paraffin-embedded tissue microarrays using MALDI imaging mass spectrometry.* Proteomics, 2008. **8**(18): p. 3715-3724.

99. Ronci, M., Bonanno, E., Colantoni, A., Pieroni, L., Di Ilio, C., Spagnoli, L.G., Federici, G., and Urbani, A., *Protein unlocking procedures of formalin-fixed paraffin-embedded tissues: application to MALDI-TOF imaging MS investigations.* Proteomics, 2008. **8**(18): p. 3702-3714.

100. Stauber, J., Lemaire, R., Franck, J., Bonnel, D., Croix, D., Day, R., Wisztorski, M., Fournier, I., and Salzet, M., *MALDI imaging of formalin-fixed paraffin-embedded tissues: application to model animals of Parkinson disease for biomarker hunting.* Journal of proteome research, 2008. **7**(3): p. 969-978.

101. Djidja, M.-C.C., Francese, S., Loadman, P.M., Sutton, C.W., Scriven, P., Claude, E., Snel, M.F., Franck, J., Salzet, M., and Clench, M.R., *Detergent addition to tryptic digests and ion mobility separation prior to MS/MS improves peptide yield and protein identification for in situ proteomic investigation of frozen and formalin-fixed paraffin-embedded adenocarcinoma tissue sections.* Proteomics, 2009. **9**(10): p. 2750-2763.

102. Crecelius, A., Gotz, A., Arzberger, T., Frohlich, T., Arnold, G.J., Ferrer, I., and Kretzschmar, H.A., *Assessing quantitative post-mortem changes in the gray matter of the human frontal cortex proteome by 2-D DIGE.* Proteomics, 2008. **8**(6): p. 1276-91.

103. Schwartz, S.A., Reyzer, M.L., and Caprioli, R.M., *Direct tissue analysis using matrix-assisted laser desorption/ionization mass spectrometry: practical aspects of sample preparation.* J Mass Spectrom, 2003. **38**(7): p. 699-708.

104. Crecelius, A.C., Cornett, D.S., Caprioli, R.M., Williams, B., Dawant, B.M., and Bodenheimer, B., *Three-Dimensional Visualization of Protein Expression in Mouse Brain Structures Using Imaging Mass Spectrometry.* Journal of the American Society for Mass Spectrometry, 2005. **16**(7): p. 1093-1099.

105. Khatib-Shahidi, S., Andersson, M., Herman, J.L., Gillespie, T.A., and Caprioli, R.M., *Direct molecular analysis of whole-body animal tissue sections by imaging MALDI mass spectrometry.* Anal Chem, 2006. **78**(18): p. 6448-56.

106. Crossman, L., McHugh, N.A., Hsieh, Y., Korfmacher, W.A., and Chen, J., *Investigation of the profiling depth in matrix-assisted laser desorption/ionization imaging mass spectrometry.* Rapid Commun Mass Spectrom, 2006. **20**(2): p. 284-90.

107. Woo, H.K., Northen, T.R., Yanes, O., and Siuzdak, G., *Nanostructure-initiator mass spectrometry: a protocol for preparing and applying NIMS surfaces for high-sensitivity mass analysis.* Nat Protoc, 2008. **3**(8): p. 1341-9.

108. Greving, M.P., Patti, G.J., and Siuzdak, G., *Nanostructure-initiator mass spectrometry metabolite analysis and imaging.* Anal Chem, 2011. **83**(1): p. 2-7.

109. Sturm, R.M., Greer, T., Chen, R., Hensen, B., and Li, L., *Comparison of NIMS and MALDI platforms for neuropeptide and lipid mass spectrometric imaging in C. borealis brain tissue.* Analytical Methods, 2013. **5**(6): p. 1623.

110. Kawamoto, T., *Use of a new adhesive film for the preparation of multi-purpose fresh-frozen sections from hard tissues, whole-animals, insects and plants.* Arch Histol Cytol, 2003. **66**(2): p. 123-43.

111. Hui, L., Xiang, F., Zhang, Y., and Li, L., *Mass spectrometric elucidation of the neuropeptidome of a crustacean neuroendocrine organ.* Peptides, 2012. **36**(2): p. 230-9.

112. Ye, H., Hui, L., Kellersberger, K., and Li, L., *Mapping of neuropeptides in the crustacean stomatogastric nervous system by imaging mass spectrometry.* Journal of the American Society for Mass Spectrometry, 2013. **24**(1): p. 134-147.

113. Lemaire, R., Wisztorski, M., Desmons, A., Tabet, J.C., Day, R., Salzet, M., and Fournier, I., *MALDI-MS Direct Tissue Analysis of Proteins: Improving Signal Sensitivity Using Organic Treatments.* Analytical Chemistry, 2006. **78**(20): p. 7145-7153.

114. Goodwin, R.J., Pennington, S.R., and Pitt, A.R., *Protein and peptides in pictures: imaging with MALDI mass spectrometry.* Proteomics, 2008. **8**(18): p. 3785-800.

115. Kaletas, B.K., van der Wiel, I.M., Stauber, J., Guzel, C., Kros, J.M., Luider, T.M., and Heeren, R.M., *Sample preparation issues for tissue imaging by imaging MS.* Proteomics, 2009. **9**(10): p. 2622-33.

116. MacAleese, L., Stauber, J., and Heeren, R.M., *Perspectives for imaging mass spectrometry in the proteomics landscape.* Proteomics, 2009. **9**(4): p. 819-34.

117. Shanta, S.R., Zhou, L.-H., Park, Y.S., Kim, Y.H., Kim, Y., and Kim, K.P., *Binary Matrix for MALDI Imaging Mass Spectrometry of Phospholipids in Both Ion Modes.* Analytical Chemistry, 2011. **83**(4): p. 1252-1259.

118. Hui, L., Zhang, Y., Wang, J., Cook, A., Ye, H., Nusbaum, M.P., and Li, L., *Discovery and Functional Study of a Novel Crustacean Tachykinin Neuropeptide.* ACS Chemical Neuroscience, 2011. **2**(12): p. 711722.

119. Jia, C., Hui, L., Cao, W., Lietz, C.B., Jiang, X., Chen, R., Catherman, A.D., Thomas, P.M., Ge, Y., Kelleher, N.L., and Li, L., *High-definition de novo sequencing of crustacean hyperglycemic hormone (CHH)-family neuropeptides.* Molecular & cellular proteomics : MCP, 2012. **11**(12): p. 1951-1964.

120. Takáts, Z., Wiseman, J.M., Gologan, B., and Cooks, R.G., *Mass spectrometry sampling under ambient conditions with desorption electrospray ionization.* Science (New York, N.Y.), 2004. **306**(5695): p. 471-473.

121. Demian, R.I., Justin, M.W., Qingyu, S., and Cooks, R.G., *Development of capabilities for imaging mass spectrometry under ambient conditions with desorption electrospray ionization (DESI).* International Journal of Mass Spectrometry, 2007. **259**.

122. Trimpin, S., Ren, Y., Wang, B., Lietz, C.B., Richards, A.L., Marshall, D.D., and Inutan, E.D., *Extending the laserspray ionization concept to produce highly charged ions at high vacuum on a time-of-flight mass analyzer.* Anal Chem, 2011. **83**(14): p. 5469-75.

123. Chansela, P., Goto-Inoue, N., Zaima, N., Sroyraya, M., Sobhon, P., and Setou, M., *Visualization of neuropeptides in paraffin-embedded tissue sections of the central nervous system in the decapod crustacean, Penaeus monodon, by imaging mass spectrometry.* Peptides, 2012. **34**(1): p. 10-18.

124. Seeley, E.H. and Caprioli, R.M., *3D imaging by mass spectrometry: a new frontier.* Analytical chemistry, 2012. **84**(5): p. 2105-2110.

125. Xiong, X., Xu, W., Eberlin, L.S., Wiseman, J.M., Fang, X., Jiang, Y., Huang, Z., Zhang, Y., Cooks, R.G., and Ouyang, Z., *Data processing for 3D mass spectrometry imaging.* Journal of the American Society for Mass Spectrometry, 2012. **23**(6): p. 1147-1156.

126. Hummon, A.B., Amare, A., and Sweedler, J.V., *Discovering new invertebrate neuropeptides using mass spectrometry.* Mass Spectrometry Reviews, 2006. **25**(1): p. 77-98.

127. Zhu, Z.J., Rotello, V.M., and Vachet, R.W., *Engineered nanoparticle surfaces for improved mass spectrometric analyses.* Analyst, 2009. **134**(11): p. 2183-8.

128. Peterson, D.S., *Matrix-free methods for laser desorption/ionization mass spectrometry.* Mass Spectrom Rev, 2007. **26**(1): p. 19-34.

129. Chiang, C.K., Chen, W.T., and Chang, H.T., *Nanoparticle-based mass spectrometry for the analysis of biomolecules.* Chem Soc Rev, 2011. **40**(3): p. 1269-81.

130. Sudhir, P.-R., Wu, H.-F., and Zhou, Z.-C., *Identification of Peptides Using Gold Nanoparticle-Assisted Single-Drop Microextraction Coupled with AP-MALDI Mass Spectrometry.* Analytical Chemistry, 2005. **77**(22): p. 7380-7385.

131. Moyer, S.C. and Cotter, R.J., *Peer Reviewed: Atmospheric Pressure MALDI.* Analytical Chemistry, 2002. **74**(17): p. 468 A-476 A.

132. Dickinson, P.S., Stevens, J.S., Rus, S., Brennan, H.R., Goiney, C.C., Smith, C.M., Li, L., Towle, D.W., and Christie, A.E., *Identification and cardiotropic actions of sulfakinin peptides in the American lobster Homarus americanus.* J Exp Biol, 2007. **210**(Pt 13): p. 2278-89.

133. Bito, L., Davson, H., Levin, E., Murray, M., and Snider, N., *The concentrations of free amino acids and other electrolytes in cerebrospinal fluid, in vivo dialysate of brain, and blood plasma of the dog.* J Neurochem, 1966. **13**(11): p. 1057-67.

134. Nandi, P. and Lunte, S.M., *Recent trends in microdialysis sampling integrated with conventional and microanalytical systems for monitoring biological events: a review.* Anal Chim Acta, 2009. **651**(1): p. 1-14.

135. Shippenberg, T.S. and Thompson, A.C., *Overview of microdialysis.* Curr Protoc Neurosci, 2001. **Chapter 7**: p. Unit7 1.

136. Chung, Y.T., Ling, Y.C., Yang, C.S., Sun, Y.C., Lee, P.L., Lin, C.Y., Hong, C.C., and Yang, M.H., *In vivo monitoring of multiple trace metals in the brain extracellular fluid of anesthetized rats by microdialysis-membrane desalter-ICPMS.* Anal Chem, 2007. **79**(23): p. 8900-10.

137. Cebada, J., Alvarado-Alvarez, R., Becerra, E., Neri-Bazan, L., Rocha, L., and Garcia, U., *An improved method for long-term measuring of hemolymph fluctuations of non-essential amino acids, GABA and histamine from freely moving crayfish.* J Neurosci Methods, 2006. **153**(1): p. 1-7.

138. Behrens, H.L., Chen, R., and Li, L., *Combining microdialysis, NanoLC-MS, and MALDI-TOF/TOF to detect neuropeptides secreted in the crab, Cancer borealis.* Anal Chem, 2008. **80**(18): p. 6949-58.

139. Schmerberg, C.M. and Li, L., *Mass spectrometric detection of neuropeptides using affinity-enhanced microdialysis with antibody-coated magnetic nanoparticles.* Anal Chem, 2013. **85**(2): p. 915-22.

140. Watson, C.J., Venton, B.J., and Kennedy, R.T., *In vivo measurements of neurotransmitters by microdialysis sampling.* Anal Chem, 2006. **78**(5): p. 1391-9.

141. Lada, M.W. and Kennedy, R.T., *Quantitative in vivo monitoring of primary amines in rat caudate nucleus using microdialysis coupled by a flow-gated*

interface to capillary electrophoresis with laser-induced fluorescence detection. Anal Chem, 1996. **68**(17): p. 2790-7.

142. Cremers, T.I., de Vries, M.G., Huinink, K.D., van Loon, J.P., v d Hart, M., Ebert, B., Westerink, B.H., and De Lange, E.C., *Quantitative microdialysis using modified ultraslow microdialysis: direct rapid and reliable determination of free brain concentrations with the MetaQuant technique.* J Neurosci Methods, 2009. **178**(2): p. 249-54.

143. Lonnroth, P., Jansson, P.A., and Smith, U., *A microdialysis method allowing characterization of intercellular water space in humans.* Am J Physiol, 1987. **253**(2 Pt 1): p. E228-31.

144. Hooks, M.S., Colvin, A.C., Juncos, J.L., and Justice, J.B., Jr., *Individual differences in basal and cocaine-stimulated extracellular dopamine in the nucleus accumbens using quantitative microdialysis.* Brain Res, 1992. **587**(2): p. 306-12.

145. Martin-Fardon, R., Sandillon, F., Thibault, J., Privat, A., and Vignon, J., *Long-term monitoring of extracellular dopamine concentration in the rat striatum by a repeated microdialysis procedure.* J Neurosci Methods, 1997. **72**(2): p. 123-35.

146. Krebs-Kraft, D.L., Rauw, G., Baker, G.B., and Parent, M.B., *Zero net flux estimates of septal extracellular glucose levels and the effects of glucose on septal extracellular GABA levels.* Eur J Pharmacol, 2009. **611**(1-3): p. 44-52.

147. Larsson, C.I., *The use of an "internal standard" for control of the recovery in microdialysis.* Life Sci, 1991. **49**(13): p. PL73-8.

148. Scheller, D. and Kolb, J., *The internal reference technique in microdialysis: a practical approach to monitoring dialysis efficiency and to calculating tissue concentration from dialysate samples.* J Neurosci Methods, 1991. **40**(1): p. 31-8.

149. Roy, M.C., Ikimura, K., Nishino, H., and Naito, T., *A high recovery microsampling device based on a microdialysis probe for peptide sampling.* Anal Biochem, 2010. **399**(2): p. 305-7.

150. Duo, J., Fletcher, H., and Stenken, J.A., *Natural and synthetic affinity agents as microdialysis sampling mass transport enhancers: current progress and future perspectives.* Biosens Bioelectron, 2006. **22**(3): p. 449-57.

151. Herbaugh, A.W. and Stenken, J.A., *Antibody-enhanced microdialysis collection of CCL2 from rat brain.* J Neurosci Methods, 2011. **202**(2): p. 124-7.

152. Pettersson, A., Markides, K., and Bergquist, J., *Enhanced microdialysis of neuropeptides.* Acta Biochim Pol, 2001. **48**(4): p. 1117-20.

153. Lada, M.W., Vickroy, T.W., and Kennedy, R.T., *High temporal resolution monitoring of glutamate and aspartate in vivo using microdialysis on-line with capillary electrophoresis with laser-induced fluorescence detection.* Anal Chem, 1997. **69**(22): p. 4560-5.

154. Bert, L., Robert, F., Denoroy, L., Stoppini, L., and Renaud, B., *Enhanced temporal resolution for the microdialysis monitoring of catecholamines and excitatory amino acids using capillary electrophoresis with laser-induced*

fluorescence detection. Analytical developments and in vitro validations. J Chromatogr A, 1996. **755**(1): p. 99-111.

155. Hogan, B.L., Lunte, S.M., Stobaugh, J.F., and Lunte, C.E., *On-line coupling of in vivo microdialysis sampling with capillary electrophoresis.* Anal Chem, 1994. **66**(5): p. 596-602.

156. Wang, M., Roman, G.T., Schultz, K., Jennings, C., and Kennedy, R.T., *Improved temporal resolution for in vivo microdialysis by using segmented flow.* Anal Chem, 2008. **80**(14): p. 5607-15.

157. Deeba, S., Corcoles, E.P., Hanna, G.B., Pareskevas, P., Aziz, O., Boutelle, M.G., and Darzi, A., *Use of rapid sampling microdialysis for intraoperative monitoring of bowel ischemia.* Dis Colon Rectum, 2008. **51**(9): p. 1408-13.

158. Wang, M., Slaney, T., Mabrouk, O., and Kennedy, R.T., *Collection of nanoliter microdialysate fractions in plugs for off-line in vivo chemical monitoring with up to 2 s temporal resolution.* J Neurosci Methods, 2010. **190**(1): p. 39-48.

159. Slaney, T.R., Nie, J., Hershey, N.D., Thwar, P.K., Linderman, J., Burns, M.A., and Kennedy, R.T., *Push-pull perfusion sampling with segmented flow for high temporal and spatial resolution in vivo chemical monitoring.* Anal Chem, 2011. **83**(13): p. 5207-13.

160. Rogers, M., Leong, C., Niu, X., de Mello, A., Parker, K.H., and Boutelle, M.G., *Optimisation of a microfluidic analysis chamber for the placement of microelectrodes.* Phys Chem Chem Phys, 2011. **13**(12): p. 5298-303.

161. Song, P., Hershey, N.D., Mabrouk, O.S., Slaney, T.R., and Kennedy, R.T., *Mass spectrometry "sensor" for in vivo acetylcholine monitoring.* Anal Chem, 2012. **84**(11): p. 4659-64.

162. Fastner, S., Predel, R., Kahnt, J., Schachtner, J., and Wegener, C., *A simple purification protocol for the detection of peptide hormones in the hemolymph of individual insects by matrix-assisted laser desorption/ionization time-of-flight mass spectrometry.* Rapid Commun Mass Spectrom, 2007. **21**(1): p. 23-8.

163. Ebner, K., Rjabokon, A., Pape, H.C., and Singewald, N., *Increased in vivo release of neuropeptide S in the amygdala of freely moving rats after local depolarisation and emotional stress.* Amino Acids, 2011. **41**(4): p. 991-6.

164. Frost, S.I., Keen, K.L., Levine, J.E., and Terasawa, E., *Microdialysis methods for in vivo neuropeptide measurement in the stalk-median eminence in the Rhesus monkey.* J Neurosci Methods, 2008. **168**(1): p. 26-34.

165. Perry, M., Li, Q., and Kennedy, R.T., *Review of recent advances in analytical techniques for the determination of neurotransmitters.* Anal Chim Acta, 2009. **653**(1): p. 1-22.

166. Emmett, M.R., Andren, P.E., and Caprioli, R.M., *Specific molecular mass detection of endogenously released neuropeptides using in vivo microdialysis/mass spectrometry.* J Neurosci Methods, 1995. **62**(1-2): p. 141-7.

167. Buck, K., Voehringer, P., and Ferger, B., *Rapid analysis of GABA and glutamate in microdialysis samples using high performance liquid chromatography and tandem mass spectrometry.* J Neurosci Methods, 2009. **182**(1): p. 78-84.

168. Carrozzo, M.M., Cannazza, G., Pinetti, D., Di Viesti, V., Battisti, U., Braghiroli, D., Parenti, C., and Baraldi, M., *Quantitative analysis of acetylcholine in rat brain microdialysates by liquid chromatography coupled with electrospray ionization tandem mass spectrometry.* J Neurosci Methods, 2010. **194**(1): p. 87-93.

169. Uutela, P., Ketola, R.A., Piepponen, P., and Kostiainen, R., *Comparison of different amino acid derivatives and analysis of rat brain microdialysates by liquid chromatography tandem mass spectrometry.* Anal Chim Acta, 2009. **633**(2): p. 223-31.

170. Song, P., Mabrouk, O.S., Hershey, N.D., and Kennedy, R.T., *In vivo neurochemical monitoring using benzoyl chloride derivatization and liquid chromatography-mass spectrometry.* Anal Chem, 2012. **84**(1): p. 412-9.

171. Reed, B., Bidlack, J.M., Chait, B.T., and Kreek, M.J., *Extracellular biotransformation of beta-endorphin in rat striatum and cerebrospinal fluid.* J Neuroendocrinol, 2008. **20**(5): p. 606-16.

172. Bernay, B., Gaillard, M.C., Guryca, V., Emadali, A., Kuhn, L., Bertrand, A., Detraz, I., Carcenac, C., Savasta, M., Brouillet, E., Garin, J., and Elalouf, J.M., *Discovering new bioactive neuropeptides in the striatum secretome using in vivo microdialysis and versatile proteomics.* Mol Cell Proteomics, 2009. **8**(5): p. 946-58.

173. Zhang, X., Rauch, A., Xiao, H., Rainer, G., and Logothetis, N.K., *Mass spectrometry-based neurochemical analysis: perspectives for primate research.* Expert Rev Proteomics, 2008. **5**(5): p. 641-52.

174. DiFeliceantonio, A.G., Mabrouk, O.S., Kennedy, R.T., and Berridge, K.C., *Enkephalin surges in dorsal neostriatum as a signal to eat.* Curr Biol, 2012. **22**(20): p. 1918-24.

2.8 Figures and Tables

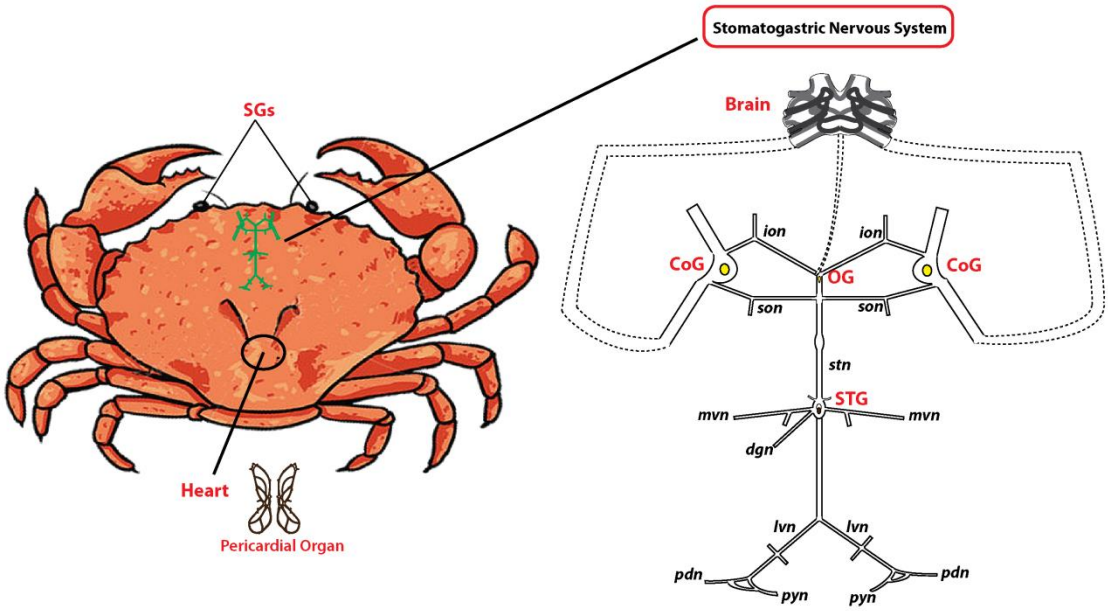

Figure 2-1. Schematic drawing of the stomatogastric nervous system (STNS) of the Jonah crab, *Cancer borealis*. The SGs (sinus glands: located in the eyestalks of the crab) and the POs (pericardial organs: located in the chamber surrounding the heart) release hormones into the hemolymph. The brain is connected to the STNS *via* a tiny nerve called the inferior ventricular nerve (*ivn*), and the STNS consists of the stomatogastric ganglion (STG), oesophageal ganglion (OG), paired commissural ganglia (CoG), which are connected by motor nerves.

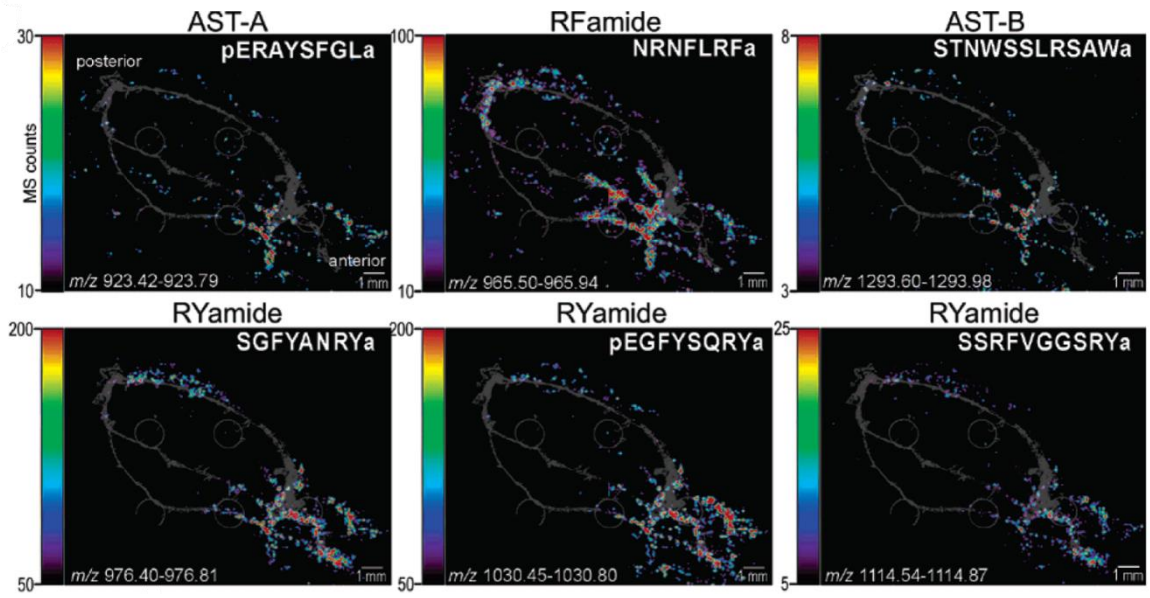

Figure 2-2. Differential localization of neuropeptide families in the pericardial organs (PO). The MS images, colored according to associated color-intensity scale, are shown as an overlay on top of an optical image of the PO. Members of different neuropeptide families are differentially located. The most apparent contrast is observed between the RYamide family and the RFamide family.

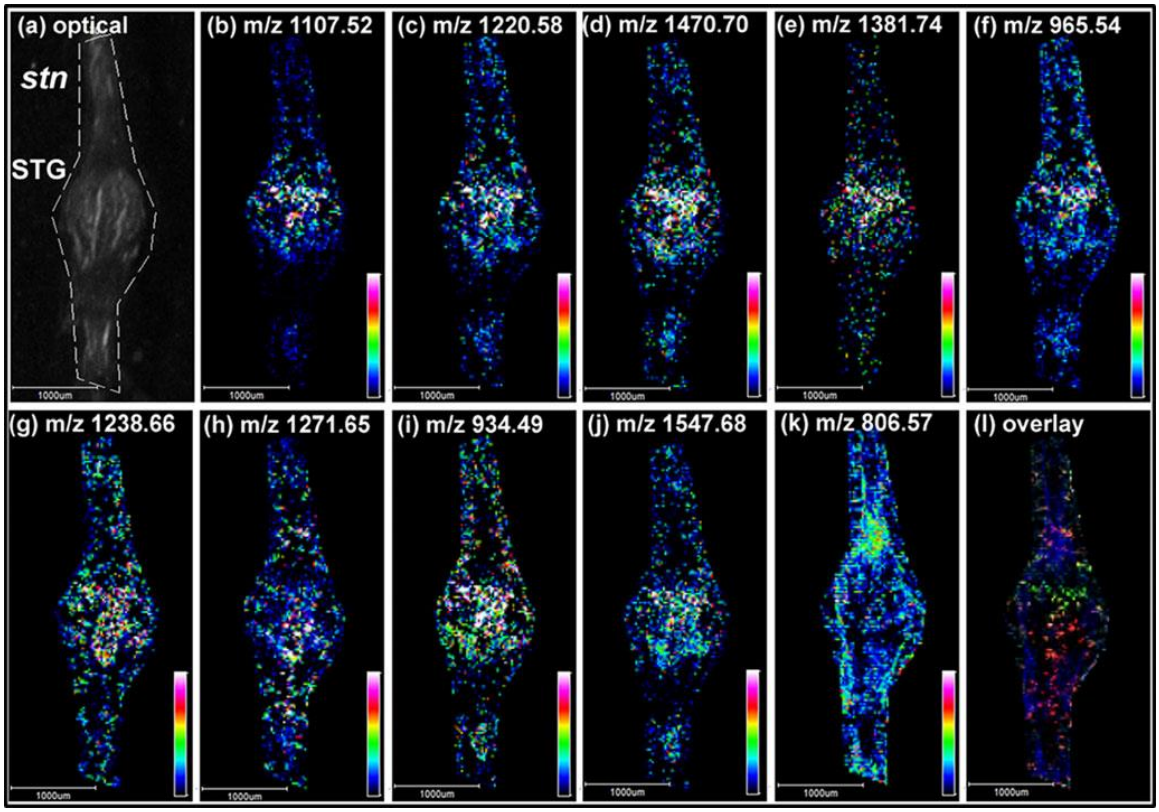

Figure 2-3. Representative MSI results of the neuropeptide distributions in *Callinectes sapidus* STG by MALDI TOF/TOF. (a) An optical image of the STG subjected to subsequent MSI acquisiton. Nine neuropeptides from five different families were shown above. B-type ASTs: (b) AGWSSMRGAWa (*m/z* 1107.52), (c) SGDWSSLRGAWa (*m/z* 1220.58), and (d) VPNDWAHFRGSWa (*m/z* 1470.70). SIFamide: (e) GYRKPPFNGSIFa (*m/z* 1381.74). RFamides: (f) NRNFLRFa (*m/z* 965.54), (g) SQPSKNYLRFa (*m/z* 1238.66), and (h) pQDLDHVFLRFa (*m/z* 1271.64). CabTRP 1a: APSGFLGMRa (*m/z* 934.49). Orcokinin: NFDEIDRSSFGFN (*m/z* 1547.68). For comparison, the distribution of a lipid PC (38:6) (*m/z* 806.57) is shown in (k). (l) is an overlaid image of (c), (h), and (k), displayed in green, red, and blue, respectively.

Table 2-1. Neuropeptides spatially characterized via MS imaging in crustacean nervous system

Neuropeptide Family	**Sequence**	**Tissue and Species**	**MS instrumentation**	***In situ* Identification**	**Reference**
FMRFamides	NRNFLRFa	*C. borealis* PO and brain *C. sapidus* STG	MALDI-TOF/TOF	MS^2 ([75, 76, 112])	[75-77, 112]
	GNRNFLRFa	*C. borealis* PO and brain	MALDI-TOF/TOF	MS^2 ([75])	[75]
	SDRNFLRFa	*C. borealis* PO	MALDI-TOF/TOF	AM ([75])	[75]
	SQPSKNYLRFa	*C. sapidus* STG	MALDI-TOF/TOF	AM ([112])	[112]
	GAHKNYLRFa	*C. borealis* PO and brain	MALDI-TOF/TOF	AM ([75, 77])	[75, 77]
	GYSKNYLRFa	*C. borealis* PO and brain	MALDI-TOF/TOF	AM ([75])	[75]
	AYNRSFLRFa	*C. borealis* PO and brain	MALDI-TOF/TOF	MS^2 ([75])	[75]
	SENRNFLRFa	*C. borealis* PO and brain	MALDI-TOF/TOF	MS^2 ([75])	[75]
	SMPSLRLRFa	*C. borealis* brain	MALDI-TOF/TOF	AM ([75])	[75, 76]
	APQRNFLRFa	*C. borealis* brain	MALDI-TOF/TOF	MS^2 ([75])	[75]
	pQDLDHVFLRFa	*C. sapidus* STG	MALDI-TOF/TOF	AM ([112])	[112]

	DVRTPALRLRFa	*C. borealis* brain	MALDI-TOF/TOF	AM ([75] [77])	[75-77]
	GDRNFLRFa	*P. monodon* brain and TG	MALDI-TOF/TOF	AM ([123])	[123]
SIFamide	GYRKPPFNGSIFa	*C. borealis* brain *C. sapidus* STG *P. monodon* brain and TG	MALDI-TOF/TOF	MS^2 ([75, 123]) AM ([112])	[75, 76, 112, 123]
	VYRKPPFNGSIFa	*H. americanus* brain	MALDI-LTQ-Orbitrap MALDI-TOF/TOF	AM ([86])	[86]
AST-A	pERAYSFGLa	*C. borealis* PO	MALDI-TOF/TOF	AM [75])	[75]
	PRDYAFGLa	*C. borealis* PO	MALDI-TOF/TOF	AM [75])	[75]
	ANEDEDAASLFAFGLa	*P. monodon brain and TG*	MALDI-TOF/TOF	MS^2 [123])	[123]
AST-B	NWNKFQGSWa	*C. borealis* PO	MALDI-TOF/TOF	MS^2 ([75])	[75]
	GNWNKFQGSWa	*C. borealis* PO	MALDI-TOF/TOF	MS^2 ([75])	[75]
	AGWSSMRGAWa	*C. sapidus* STG	MALDI-TOF/TOF	AM ([112])	[112]
	NNWSKFQGSWa	*C. borealis* PO	MALDI-TOF/TOF	MS^2 ([75])	[75]

	STNWSSLRSAWa	*C. borealis* PO	MALDI-TOF/TOF	MS^2 ([75])	[75]
	NNNWSKFQGSWa	*C. borealis* PO	MALDI-TOF/TOF	MS^2 ([75])	[75]
	SGDWSSLRGAWa	*C. sapidus* STG	MALDI-TOF/TOF	AM ([112])	[112]
	VPNDWAHFRGSWa	*C. borealis* PO *C. sapidus* STG	MALDI-TOF/TOF	MS^2 ([75]) AM ([112])	[75] [112]
CCAP	PFCNAFTGCa	*C. borealis* PO	MALDI-TOF/TOF	MS^2 [75])	[75]
Orcokinins	NFDEIDRSGFG	*C. borealis* brain	MALDI-TOF/TOF	AM ([75])	[75]
	NFDEIDRSGFDG	*P. monodon* brain and TG	MALDI-TOF/TOF	AM ([123])	[123]
	NFDEIDRSGFGFA	*C. borealis* brain	MALDI-TOF/TOF	MS^2 ([75-77])	[75-77]
	NFDEIDRSGFGFV	*C. borealis* brain *P. monodon* brain and TG	MALDI-TOF/TOF	AM ([75], [123])	[75, 123]
	NFDEIDRSSFGFV	*C. borealis* brain	MALDI-TOF/TOF	AM ([75])	[75]
	NFDEIDRSSFGFN	*C. borealis* brain *C. sapidus* STG	MALDI-TOF/TOF	AM ([75, 112])	[75, 112]
	NFDEIDRSGFGFN	*H. americanus* brain	MALDI-LTQ-Orbitrap	AM ([86])	[86]

			MALDI-TOF/TOF		
	NFDEIDRTGFGFH	*C. borealis* brain	MALDI-TOF/TOF	AM ([77])	[76, 77]
Orcomyotropin-related	FDAFTTGFGHS	*C. borealis* brain	MALDI-TOF/TOF	AM ([75])	[75]
RYamides	FYSQRYa	*C. borealis* PO	MALDI-TOF/TOF	AM ([75])	[75]
	SGFYANRYa	*C. borealis* PO	MALDI-TOF/TOF	MS^2 ([75])	[75]
	SSRFVGGSRYa	*C. borealis* PO	MALDI-TOF/TOF	AM ([75])	[75]
	pEGFYSQRYa	*C. borealis* PO	MALDI-TOF/TOF	MS^2 ([75])	[75]
TRPs	APSGFLGMRa	*C. borealis* brain *H. americanus* brain *C. sapidus* STG	MALDI-LTQ-Orbitrap MALDI-TOF/TOF	AM ([75-77, 86, 112])	[75-77, 86, 112]
	YRSGFLGMRa	*C. sapidus* brain	MALDI-TOF/TOF	AM ([118])	[118]
	PSGFLGMRamide	*P. monodon* brain and TG	MALDI-TOF/TOF	AM ([123])	[123]
YRamide	HIGSLYRa	*C. borealis* PO	MALDI-TOF/TOF	AM ([75])	[75]
CHH superfamily	$^{Cab\text{-}SG\text{-}}$CHH-I	*C. borealis* SG	MALDI-TOF/TOF	AM ([119])	[119]

	$^{Cab\text{-}SG\text{-}}$CHH-II	*C. borealis* SG	MALDI-TOF/TOF	AM ([119])	[119]
	$^{Cab\text{-}SG\text{-}}$MIH	*C. borealis* SG	MALDI-TOF/TOF	AM ([119])	[119]
	$^{Cab\text{-}SG\text{-}}$MOIH	*C. borealis* SG	MALDI-TOF/TOF	AM ([119])	[119]
	HEEYQAHVQTV	*P. monodon* brain, SG and TG	MALDI-TOF/TOF	MS^2 ([123])	[123]
PDH	NSELINSLLGIPK	*P. monodon* retina, brain and TG	MALDI-TOF/TOF	MS^2 ([123])	[123]
Others	HI/LASLYKPR	*H. americanus* brain	MALDI-LTQ-Orbitrap	AM ([86])	[86]

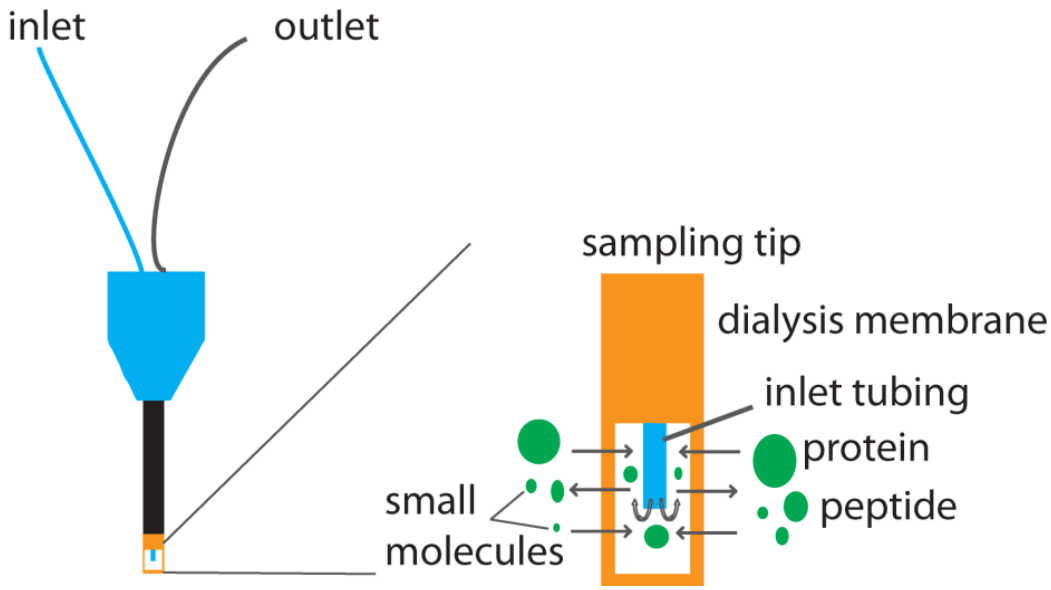

Figure 2-4. An illustration of microdialysis probe with an expanded view of the membrane tip. Analytes with a mass below the molecular weight cutoff of the membrane diffuse into the probe and get collected at the outlet.

Chapter 3

Mass Spectrometric Characterization of the Neuropeptidome of the Crayfish *Orconectes rusticus*

Adapted from **Zhidan Liang**, Claire M. Schmerberg, and Lingjun Li. *J. Proteome. To be submitted*.

Abstract

The rusty crayfish, *Orconectes rusticus*, is an important species in behavioral neuroscience and invasive species ecology. It presents several well-defined behaviors, permitting it to be a successful invasive species in the upper Midwest United States and an ideal model species for studying social dominance and aggression. Monoamine neurotransmitters (NTs), human drugs of abuse, and spatial learning have also been studied in *O. rusticus*. Despite its significance, the neuropeptides (NPs) of *O. rusticus* have not yet been cataloged, although NPs have been implicated in aggression, addiction, and adaptation to environmental change in other species. NP studies in other crayfish species have been limited in the techniques or organs used. In this work, *O. rusticus* was used as a model organism for the development of mass spectrometry-based analytical methodology for NP identification. For a relatively comprehensive coverage of NP content, the sinus gland (SG) and brain in *O. rusticus* were used. Fractions from high performance liquid chromatography (HPLC) were enzymatically digested, if necessary, and injected into ultra-high performance liquid chromatography (UPLC) coupled on-line with an electrospray ionization (ESI) quadrupole time-of-flight (QTOF) mass spectrometer operating in data-dependent acquisition (DDA) mode. MS/MS interpretation was conducted by two different strategies: database search software (Mascot), and *de novo* sequencing software (PEAKS). These approaches were aided by the construction of a home-built crustacean NP database. Highly confident identifications were made with 215 high quality peptide-spectrum-matches (PSMs) mapped to previously identified NP sequences from 10 families. Fourty-seven additional putative NPs were also identified from 12 families, including sequences from families already

observed in *Orconectes* species (CPRPs, PDHs), and peptides not previously identified in crustaceans using mass spectrometry. These represent potentially novel NPs in crustacean species. Due to overlap in NP sequences, the minimum number of unique peptides that could generate the observed PSMs is 57. This catalogue of NPs will be vital for further research into the roles of NPs in behavior, environmental adaptation, and addiction in *O. rusticus*.

3.1 Introduction

The rusty crayfish *Orconectes rusticus* is an important model organism in two major areas of biology. It has been widely used for studies in behavioral neuroscience research, including applications ranging from aggression to the effects of human drugs of abuse. Due to its invasive nature, *O. rusticus* is also of vital importance in the field of invasive species ecology. Its invasion of several bodies of water in Northern Wisconsin has been documented in detail (http://dnr.wi.gov/topic/invasives/fact/rustycrayfish2012.html).

3.1.1 *Significance of Orconectes rusticus to the Field of Neurobiology*

As reviewed elsewhere, the rusty crayfish expresses several well-described and stereotyped behaviors in the field of behavioral neuroscience [1, 2] and thus had been widely used as a model organism for such purposes. *O. rusticus* and other crayfish typically lead solitary lives without alliances or pair-bonds. Interaction is mostly antagonistic, resulting from competition over resources such as food, shelter, and mates, but exists even when there is no contested resource. This is likely due to the high density at which they live in the wild. Social dominance is based mostly on size, and fighting determines hierarchies when the animals' sizes are similar. Fights have a set progression from one stereotyped behavior to another; they start with ritualized visual displays, followed by a progression to antennal whipping, claw locking, wrestling, and finally claw use [1, 2]. The ethology of aggression in *O. rusticus* is thus very well defined. Attempts have been made to understand the neurochemical basis of this behavior in the context of monoamine neurotransmitters (NTs), as reviewed in several papers [1, 2]. Studies in

decapods including *O.rusticus* are equivocal in the roles of amine NTs in antagonistic posture and behavior. Thus, it appears that no single NT is a whole-body signal for aggression, but that state- and dose-specific effects are important [1, 2]. The potential of *O. rusticus* to serve as a model species in the fields of addiction [3-7], learning, and memory [8-13] has also recently been demonstrated. However, the neurochemistry of these behaviors has not been studied in as much detail. Although *O. rusticus* is a useful model animal in a number of behavioral neuroscience applications and a large amount of progress has been made in understanding the neurochemical basis of this aggression in this species, much remains to be studied.

3.1.2 *Significance of Orconectes rusticus to the Field of Ecology*

O. rusticus is also an important species in the field of invasive species ecology. Its invasion of the area in northern Wisconsin near the Michigan border—far from its native range in the Ohio River drainage—has been studied in detail, with numerous research and review articles having been written. A 2006 meta-review of data on crayfish collected since 1932 illustrates the displacement of several native crayfish species by *O. rusticus*, which was introduced starting in the 1960's [14]. A recent review enumerated the factors that enable it to be a successful invader and the negative ecological impacts it can have [15]. The aggressiveness of *O. rusticus* is a major factor in their ability to kill or evict native crayfish. They decrease the diversity and amount of macrophytes, large aquatic plants that provide both food and shelter for fish and other invertebrates. Snails and other mollusks, fish eggs, and various types of litter are food sources for rusty crayfish, and these are reduced in number when *O. rusticus* are present [15]. The potential for *O. rusticus* to further invade lakes and rivers and displace native crayfish was modeled in

2011, and a 25% chance of this was determined for 115 lakes and 5,000 km of streams in Wisconsin [16]. From this and many other studies, it is clear that the rusty crayfish presents a significant threat to freshwater ecosystems. Its survival appears to be dependent on a threshold dissolved calcium content and lake water pH of 2.5 mg/L and 5.5, respectively, as reviewed by Olden et al. [14]. Predation levels also influence the population of *O. rusticus* [17-19].

3.2 Current Stage of Neuropeptide Identification in *Orconectes species* and Significance of This Work

It has been previously demonstrated that neuropeptides (NPs) are an important class of signaling molecules in the regulation of adaptation to environmental stresses, and aggression along with many other physiological events. Especially in crustaceans, the role of NPs under different environmental manipulations has been explored using various analytical techniques. For instance, in the crab *Carcinus maenas* NPs from RFamides, RYamide, B-type allatostatin and orcokinin families were reported to exhibit changes in their relative abundances in response to salinity stress [20] which indicated their function. In crab *Cancer borealis,* abundance of members from RFamide, RYamide and orcokinin families were observed to be significantly changed under thermal perturbation [21].

The neuropeptidomes of several decapod crustacean species that have been characterized especially benefitted from the advancement of mass spectrometry (MS) techniques, including the NP content in the eyestalk of the crayfish *Orconectes limosus* [22]. However, the neuropeptidome of *O. rusticus* has not yet been systematically described. In this work, multifaceted MS-based approaches were used to characterize the NP contents of both the brain and eyestalk of *O. rusticus*. Tandem MS (MS/MS) is used

to confidently identify the sequence of a peptide from the ions it produced upon gas-phase fragmentation. This technique has become the gold standard for NP identification due to its high sensitivity, high throughput, high accuracy and potential for novel NP discovery.

The application of MS has revolutionized the field of NP identification, especially in decapod crustacean where most genome information is unavailable due to the large degree of post-translational processing. The NP contents of several ganglia in the related species *Orconectes limosus* have been reported in a number of different studies, using MS-based techniques and/or Edman degradation for identification, but these reports have only yielded a total of 14 unique peptides from the following families: pigment dispersing hormones (PDH), molt-inhibiting hormones (MIH), crustacean hyperglycemic hormones (CHH), CHH precursor-related peptides (CPRPs), orcokinins, orcomyotropin, and A-type allatostatins (A-AST) [22-27]. The most comprehensive one of the previously mentioned studies employed nanoscale liquid chromatography (nano-LC) coupled to tandem mass spectrometry (MS/MS) for *de novo* sequencing of NPs obtained from an extract of the X-organ-sinus gland (XO-SG) complex [22], one of the main neurosecretory structures in crustacean species. This study identified a total of six peptides, with three additional truncated versions of the CPRP peptides also identified. Compared with more recent studies in which 122 NPs could be identified from tissues of the green crab *Carcinus maenas* [28], it is fair to assume that many *Orconectes* NPs remain undiscovered. This was further supported by a recent study by Veenstra [29], where 58 NP precursors were predicted to be present in the crayfish *Procambarus clarkii*. Advances in MS and MS/MS instrumentation, combined with multistage separation

techniques, permit such a study to provide a more comprehensive picture of the neuropeptidome of a given species.

In this work, the neuropeptidome of the *O. rusticus* XO-SG (supraoesophageal ganglion) and brain was characterized. A two-dimensional reversed phase liquid chromatography (RPLC) strategy was employed, with neutral and acidic mobile phases to provide orthogonality. The second dimension nano-LC was coupled directly to a highly sensitive quadrupole time-of-flight (QTOF) mass spectrometer for MS/MS analysis. Software programs for database search interpretation of MS/MS spectra (Mascot, Matrix Science) and *de novo* sequencing-based MS/MS interpretation (PEAKS, Bioinformatics Solutions, Inc.) were employed and the results were compared. In all, 262 unique peptide-spectrum matches (PSMs) were obtained, with 215 of which could mapped to previously identified crustacean NPs from 10 families and 47 putative NP PSMs from 12 families. This is the first investigation of NPs in *O. rusticus* and greatly increases the number of known NPs in *Orconectes* and other crustacean species.

3.3 Experimental Section

3.3.1 *Animals*

Male and female *O. rusticus* were kindly provided by Alex Laztka, a graduate student in the laboratory of Jake Vander Zanden, in the Department of Limnology at the University of Wisconsin-Madison, and co-workers. They were obtained from fresh water lakes in Northern Wisconsin centered around the Limnology Department's Trout Lake Research Station, on Trout Lake in Boulder Junction, WI. The animals were sampled as part of a National Science Foundation (NSF)-funded Long-Term Ecological Research (LTER) study, and were obtained and transported with the permission of the Wisconsin

Department of Natural Resources. Permission for transport must be obtained due to the status of *O. rusticus* as an invasive species in Wisconsin.

O. rusticus were obtained in modified minnow traps placed in lakes at a depth of approximately 1 m in an area where the lake substrate is "cobble," or rocks approximately 6-8 cm in diameter. The traps were modified by increasing the entrance hole to 5cm to accommodate mature male crayfish. Traps were baited with beef or chicken liver. This method has been shown to preferentially collect male crayfish, and although both genders were observed, around 75% of the animals were male. Traps were emptied at an interval of 20-24 hrs. *O. rusticus* were then separated from other catch by hand and kept in buckets in a refrigerator at 4ºC for approximately 12 hrs. The crayfish should not be stored in water, as the water will quickly become foul and deoxygenated. Storing animals in water in the refrigerator and/or during transport led to approximately 95% mortality in a batch of around 350 crayfish. Stored dry and cold, they enter a state similar to hibernation and can survive longer. They were then transferred to a carrying container that contains an ice pack and transported to Madison, WI by personal vehicle (a trip of approximately 3.5 hrs). Species identity was verified prior to housing in Madison in freshwater aquaria.

Aquaria contained fresh, dechlorinated water, and crushed gravel substrate. They also were equipped with Aquaclear 30 (Hagen) filtration units and conventional air bubbler. No more than 45 individuals were housed per 20-gallon tank. Care was taken to ensure a tight fit for the lid of the aquarium as the crayfish can escape through very small holes. Animals were not stored more than a day at a density of 45 animals/20-gallon tank, and at lower densities, of about 20 per 20-gallon tank, could be housed indefinitely.

If kept for longer periods of time, *O. rusticus* were fed and monitored for molting, and regular water changes were conducted. Crayfish will cannibalize if they are not fed every 2-3 days, and fighting often occurs over food. They were fed white fish, as it does not foul the water and pelleted food designed for bottom-feeding fish from a pet store. If *O. rusticus* molted, they were isolated with the old shell until their new shell hardens. These newly molted individuals could consume the old shell for essential nutritional purposes. Shell hardening takes 1-2 days. Due to waste accumulation in the substrate and water, the tanks were cleaned weekly with a 20% water change, or more often if housed in high density.

3.3.2 *Dissection*

Brains and eyestalks were dissected from *O. rusticus* without the aid of a microscope. Whole eyestalk extracts were prepared instead of dissecting the sinus gland out of the eyestalk due to its miniscule size, which is difficult to locate even under a dissecting microscope. *O. rusticus* was put on ice until movement ceased (approximately 15-20 min). Appendages were removed and the tail nerve cut with dissecting scissors to prevent tail flipping. The carapace was cut along a line starting below one eyestalk, continuing up toward the rostrum, and then down toward the other eyestalk (indicated in figures in Chapter 8). The distal part of the body was then discarded and the brain was located inside the shell immediately behind the rostrum. It was removed with fine forceps and placed in a 1.5 mL tube containing 0.5 mL acidified methanol (90:9:1 methanol: water: acetic acid by volume) on ice. 25-30 brains were placed in a single tube. They were stored at -20°C or -80°C if storage occurred for more than a month until extraction. Entire eyestalks were removed by cutting the soft tissue where they were connected to the

head with fine scissors. These were placed in a similar tube, with about 20-25 pairs per tube.

3.3.3 *Tissue Extraction and Sample Preparation*

Tissues were homogenized in acidified methanol using plastic pestles for soft tissues and a glass vial and pestle for whole eyestalks. Vigorous homogenization followed by sonication (5 min) was required for all tissues, in particular the eyestalks. Centrifugation was used to separate liquid and solid portions (5 min x 16,100 g), and the solids were re-extracted 3 times with the initial volume of acidified methanol, saving the liquid fraction each time. It was later determined via MALDI-TOF/TOF that the third extraction from *O. rusticus* brain tissue yielded mostly lipids and few peptides, so only the first two were combined for that tissue. For other tissues, all liquid portions were combined. The solvent was then evaporated. Two brain and two eyestalk samples were prepared and analyzed, each containing tissues pooled from 25-30 individual crayfish.

O. rusticus brain samples were subjected to a delipidation step. They were reconstituted in water and combined with an equal volume of a solution of chloroform: methanol (3:1) and a liquid-liquid extraction was conducted. The aqueous layer was saved, and the lipid layer was re-extracted 3 times. All samples were reconstituted in 0.1% formic acid (FA) in water.

3.3.4 *Liquid Chromatography-Mass Spectrometry*

Samples were subjected to a first dimension of LC as a pre-purification step. A neutral pH solvent system (7.4, solvent A: 25mM NH_4HCO_3, solvent B: 9:1 ACN: 25mM NH_4HCO_3) and reversed-phase column (Inertsil ODS-4 column, 3µm, 2.1 x 150 mm, GL

Sciences, Tokyo, Japan) were used with an Alliance HPLC (Waters, Milford, MA) system. Fractions were collected every 3 min with a Rainin Dynamax Model FC-4 fraction collector. Early eluting fractions were combined with late eluting fractions to reduce the total number of samples while maintaining separation.

Samples were injected onto a C18 reversed-phase column (BEH130 C18, 1.7 µm, 75 µm x 100 mm, Waters, Milford, MA) using a Waters nanoAcquity UPLC system (Waters, Milford, MA). The outlet of this column was connected to a fused silica capillary with a pulled tip of 5 µm internal diameter (Sutter Instrument Company, Novato, CA). This was used as the ESI inlet on a Waters Synapt G2 QTOF (Waters, Milford, MA). A 120 min reversed-phase run with solvent A as 0.1% FA in water and B as 0.1% FA in ACN was used. The instrument was operated in data-dependent MS/MS mode and Glu-fibrinopeptide was infused for lockspray calibration.

3.3.5 *Databases*

As there is no available genome for any decapod crustacean, various databases were assembled using a combination of in-house compiled information and publicly available data. The in-house component contained all known crab and lobster NPs, compiled from published papers from the Li lab and others. This database portion is referred to as LiDB. The National Center for Biotechnology Information (NCBI) protein database (www.ncbi.nlm.nih.gov/protein) was also searched to obtain sets of relevant known protein sequences. One such list was created by bioinformatics mining by a previous lab member. This contained all NCBI crustacean NP sequences, several crustacean protein sequences, and numerous other NP sequences from a variety of multicellular organisms. This list of sequences is referred to as WF, for the name of the

previous lab member. The entire list of decapod sequences was also downloaded from NCBI (“decapod”), as was the entire list of crustacean sequences (“crustacean”). Finally, a database was acquired from NCBI by restricting the taxonomy to crustacea and searching for the keywords “peptide” or “hormone” (NCBI query: (peptide [All Fields] OR hormone [All Fields]) AND "Crustacea"[Organism]). This is referred to as crustaceanNP. Databases were compiled in FASTA format and edited for redundancy. Only results from LiDB are shown, as this small database contains only crustacean NPs and thus promised more confident identification. All PSMs were manually checked for matches quality.

3.3.6 *Data Analysis*

Protein Lynx Global Server (PLGS, Waters, Milford, MA) was used to search a variety of home-built databases, containing all known crustacean neuropeptides against the data obtained and to convert the data from .raw files into .pkl files for Mascot search. This software also conducted an internal mass calibration with the lock mass compound. Several databases and combinations of databases were used, as detailed in the results and discussion. For each search, the C-terminal amidation, pyroglutamation, and methionine oxidation modifications were always added. In all searches, a no enzyme search was conducted, a minimum of 3 fragment ion matches per peptide were required. The software’s built-in *de novo* sequencing tool was also employed with default mass tolerances and the same modifications. No results were obtained with either the database search or *de novo* functions.

The .pkl files created by PLGS were searched *via* an in-house Mascot server (Matrix Science, London, UK) using the Daemon batch uploader tool. For each search,

C-terminal amidation, pyroglutamation, and methionine oxidation were selected. In all searches, a no-enzyme search was conducted and mass tolerance was set to 0.5 Da for precursors and 0.25 Da for fragments. Peptide charges were set to 2+, 3+, and 4+. Files from all fractions were combined by Mascot into a single file for searching.

These same .pkl files were also analyzed using PEAKS studio 5.3 (Bioinformatics Solutions Inc., Waterloo, ON). Data was preprocessed to select only high-quality spectra. *De novo* was conducted with no enzyme and the modifications were set to C-terminal amidation, pyroglutamation, and methionine oxidation. Mass tolerance was 0.5 Da for precursors and 0.25 Da for fragments. Following the *de novo* search, a comparison to database sequences was conducted.

Peptide spectrum matches (PSMs) obtained with PEAKS and Mascot were output in comma separated values (.csv) format for further analysis in Microsoft Excel. Mascot reports a "Mascot score," which is their version of a -10logP value, which is also what PEAKS reports. All PSMs scoring less than 15 were removed from the results. The two brain and two eyestalk samples were analyzed in parallel, and the best score obtained was saved. False-discovery rates (FDRs) were not generated by PEAKS due to the small database size, and the FDRs generated by Mascot were for a score threshold of 40, not useful for our score cutoff of 15. Occasionally, PSMs with large numbers of repeating residues were disregarded as likely false positives. PSMs for peptides or hormones were subjected to meta-analysis to compare the performance of Mascot and PEAKS. Venn diagrams were generated using software created at the Pacific Northwest National Laboratory. For final reporting of the NPs identified, some overlapping PSMs were

manually aligned and parsimony was used to determine the minimal number of precursors that could lead to those PSMs. Peptides are reported in **Table 3-1**.

Several sequences determined by PEAKS *de novo* interpretation of MS/MS spectra were not found in databases, and these were subjected to further analysis. Those that appeared in more than one extract, or had sequence motifs common to NPs, were searched against the NCBI protein database using *t*blastn and restricting to Crustacea (taxon id 6657). Matches with the lowest E-value were reported. Where multiple proteins had the same E-value, either all are listed or they are described generally. This data is also reported in **Table 3-5.**

3.4 Results and Discussion

In total, 262 high-quality PSMs were made from MS/MS spectra, with 215 PSMs could be mapped to NPs previously observed in decapod crustaceans using MS, from 10 different families. The additional spectra mapped to 47 putative NPs from 12 families. These either represent peptides observed in non-decapod crustaceans, or peptides whose presence had previously only been identified by genetic techniques. Additional matches were made to non-NP entries in the database, including hemocyanin, actin, and currently unidentified products of the *Daphnia* genome. Although other databases were used, only data from database containing known crustacean NPs is presented for more confident identification. A smaller database is desired when searching for NPs, as searches must be done without using specific enzyme cleavage sites to capture the full complexity of NPs and potential novel proteolytic processing products. This smaller database, although it permitted such searches to be carried out in a reasonable period of time (hours instead of days), led to a number of issues, mostly with determining the quality of a match.

Reproducibility between samples of the same tissue type was moderate. Around half of PSMs from Mascot and one fourth from PEAKS were observed in pooled brain tissue samples (**Figure 3-1**) and about half of PSMs from PEAKS and two thirds from Mascot were observed to be overlapping in eyestalk. This illustrates the necessity of analyzing multiple replicates. It is likely that this is due to the somewhat random nature of precursor selection for MS/MS, and that technical replicates might be sufficient. It is unlikely that the samples contained substantially different NP contents, since they were pooled tissues from 25+ animals, all collected from the same geographical region around the same season. It is nevertheless possible that slight differences in the locations and days of collection led to NP variation between the samples. Another possible source of this variation between samples could be the inclusion of a number of random matches, which are not likely to occur the same way in two different samples. This concern, however, cannot be addressed in NP studies with the current statistical methods of assigning FDRs and the probabilities (P) of matches being correct.

FDRs and match probability were determined based on statistical methods that take into account a number of factors, and should presumably return a good estimate of the accuracy of assigning a MS/MS spectrum to a given peptide sequence. All current methods to calculate this value take into account the number of fragment ion matches observed versus the number of possible matches. These formulas will provide a good estimation of the quality of a match when the peptide is large, but may not do so for smaller peptides with fewer possible matching ions. The gold standard for acceptability of a PSM remains visual verification, and in our experience, PSMs with lower Mascot scores still passed this test, while PSMs with similar scores from PEAKS did not.

Although both software programs report a -10logP value, the exact scoring mechanisms to calculate that probability differ. Therefore, it may be appropriate to use different thresholds for score cutoff when interpreting results from each program. For comparison of the programs in this study, a score cutoff of 15 was chosen for PEAKS and 10 was chosen for Mascot before subjected to manual validation. These values were chosen by observations of multiple replications, and a desire not to dismiss visually good matches that may have a low score. The use of crustacean NP+LiDB for the database also led to complications because the LiDB sequences are short, representing just the active NP. Sequences in the crustaceanNP database are long preprohormones. Thus, matches to these longer proteins were scored better than similar matches to the shorter active NP sequences. It is clear from these results that the methods for assigning scores to PSMs used by both programs may not be very accurate in describing the quality of matches to NPs, and additional by-hand analysis of low-scoring matches will still be necessary.

An alternative approach that may be successful is appending decoy proteins to the database, and choosing a score threshold based on the acceptable FDR using matches to the decoy proteins. Mascot and PEAKS are both capable of estimating a FDR in this manner, but with small databases that contain both NP and prepropeptide sequences, this approach may not lead to an accurate determination of the FDR. Indeed, when searching what was determined to be the "best" database, LiDB+crustaceanNP, PEAKS did not return FDR values, and Mascot only estimated FDR at a score of 40. The score cutoff for which Mascot returns a FDR is based on the quality of the database, and one cannot ask the program to return a FDR for any given score, such as the score empirically observed to produce acceptable matches. Therefore, another approach to determining the number

of random positive identifications of PSMs should be employed, although no appropriate statistical method currently exists.

3.4.1 *Mapping of Neuropeptides in O. rusticus by MS/MS to Previously Known Crustacean Neuropeptides*

Many PSMs from this study mapped to NPs previously observed in other decapod crustacean species using MS/MS. These included A- and B-type allatostatin (AST), FMRFamide-like peptides (FLPs), myosuppressin, orcokinins, orcomyotropin, and SIFamide (**Table 3-1**). PDH and CPRPs will be discussed separately, as both previously observed NPs and novel gene products were observed. PSMs may represent 1) fragments of mature peptides that are produced as a result of degradation or fragmentation that occurs before or after sample collection, 2) unique mature peptides created by different processing pathways, or 3) incompletely processed peptides. Therefore, the multitude of orcokinin sequences, most of which contain homologous sequences, could all represent unique molecules present in the animal with unique activities. Alternatively, they could all represent fragments of 8 individual orcokinin peptides. For this reason, all PSMs were reported. Most NPs are present in both tissues at equal abundance. This is in agreement with previous findings in other crustacean species [22, 28, 30-33].

Many of the identified sequences match those previously observed by MS/MS or Edman degradation sequencing in the closely related crayfish *Orconectes limosus*. Two of the orcokinins (NFDEIDRSGFGFN and NFDEIDRSGFGFV) were previously identified in *Orconectes limosus* [24, 27]. A different form of orcomyotropin (**Figure 3-2a**), FDAFTTGFamide, was previously found in the hindgut of *O. limosus* [24]. Two

AST-A family members were also detected in this work, although they were different from reported sequences found in *O. limosus* [25].

B-type allatostatins (AST-Bs), FMRFamide-like peptides (FLPs), SIFamides, myosuppressin, and several of the orcokinins observed have not been previously identified in the studies of *Orconectes limosus*, but have been observed in many other decapod crustacean species, including other crayfish [34-39], lobsters [40], and crabs [41-45]. Although not every species has the same set of NPs, members of each of these families have been found in species across the order *Decapoda*, and some have been found in more distantly related species as well. Of particular note is the orcokinin DFDEIDRSGFA. This has previously been identified in one other species, *Callinectes sapidus*, and may represent the product of deamidation of the typical N-terminal N residue, either *in vivo* or during sample preparation and analysis [32]. One possible explanation is that deamidation of this residue is a modification that occurs *in vivo* to change this orcokinin's signaling properties. This method of signaling modulation is not without precedent [46]. However, the binding efficiencies of NFDEIDRSGFA vs. DFDEIDRSGFA at their receptor have not been established; in fact the orcokinin receptor has yet to be identified. In this study, the presence of PSMs mapping to AST-B, FLPs, SIFamide, myosuppressin, and orcokinins with sequences similar to those previously found in other crustacean species expands our understanding of the conservation of these NPs across species, and the high degree of homology may indicate that these NP families are critical to neurotransmission and neuroendocrine regulation in many organisms.

Several other studies have used MS/MS or Edman sequencing techniques to map NPs in *O. limosus*, including molt-inhibiting hormone (MIH) [23], and CHH [26]. These peptides were not identified in this study. It would be unlikely to identify CHH or MIH using these techniques, as they are large peptides (8-9 kDa) that require multi-scale MS approaches for complete sequencing [47]. A typical approach would be digestion with a protease such as trypsin, followed by MS/MS analysis of the fragments and assembly of the fragments into the full peptide, called bottom-up sequencing. Such method was not employed in this study.

Software programs for DDA acquisition and peptide sequencing preferentially pick multiply charged precursors, as singly charged molecules present in a LC-ESI analysis of tissue extracts are typically lipids or small molecules as opposed to peptides. Scoring functions for both Mascot and PEAKS are biased to produce low scores for short peptides even with good matches. These low-scoring matches may have been discarded by the software. Manual *de novo* sequencing of MS/MS spectra that did not yield hits according to the software programs may be able to identify some of these smaller peptides. It is not surprising that studies of the related crayfish *O. limosus* have yielded some of the same NPs, as many sequences can be expected to be similar. The NPs that have been seen in *O. limosus* but not in this study are likely missing due to different experimental or data processing approaches.

Other NPs observed in some of these species but not identified in *Orconectes rusticus* may still be present. In addition to CHH and MIH mentioned previously, C-type ASTs, allatotropins, crustacean cardioactive peptide (CCAP), corazonin, kinins, YRamide, RYamides, proctolin, pyrokinin, red pigment concentrating hormone (RPCH),

and tachykinin-related peptides have also been observed in decapod crustacean species. Some PSMs mapped to the known sequences of these peptides or their preprohormones, but these matches represented portions of the sequence not previously identified by MS/MS in these species, and they will be discussed in a separate section. It is probable that the peptides not identified in this study but expected to be present in this species are 1) found in neural organs other than the brain and eyestalk, 2) small peptides not well studied with MS/MS interpretation software, 3) large peptides that must be processed enzymatically prior to MS/MS analysis for identification, 4) present in very low quantities, and/or 5) subject to extensive post-mortem degradation. Other ganglia typically analyzed by MS/MS for NP quantitation include the thoracic and abdominal ganglia, the commissural organs, the stomatogastric ganglion, the pericardial organ, and several large nerves. These were not analyzed in this study due to more extensive dissection requirements. In addition, a multi-faceted mass spectrometric approach has been demonstrated to provide more complete coverage of a species' neuropeptidome [32, 34, 40, 41, 44, 47-52]. Although several neuropeptide families were not found in this study, it is possible that they do exist in *O. rusticus*; other experimental approaches may be able to identify them. Variation in NP expression profiles among species is also a possible explanation, and the absence of some NPs in *Orconectes rusticus* may be important to its physiology or behavior. For instance, it is possible that other less aggressive species may have NPs involved in social bonding, similar to oxytocin in mammals. Not having an NP with this function may be one reason for increased aggressiveness in *O. rusticus*.

3.4.2. *Identification of PDH and CPRP Isoforms in Orconectes rusticus*

Five isoforms of CPRP and 3 of PDH have been previously identified in the related crayfish species *Orconectes limosus* [22], and the sequences of these peptides are compared to the PSMs obtained in this study in **Table 3-2** and **Table 3-3**. Two groups of NPs that have high sequence homology across many crustacean species are the CPRPs and PDHs. Due to the high degree of sequence similarity and overlap between known crustacean CPRPs and PDHs, it is difficult to determine exactly how many mature peptides could be generated from the obtained PSMs in this study. PSMs for previously known NPs and novel products of the genes for these peptides were observed in this study. The CPRPs observed could be assigned to previously described *Orconectes limosus* CPRPs A, A*, and B (**Figure 3-3**). In addition, some other PSMs could be aligned to CPRPs previously identified from other crustacean species including Hoa_CPRP_A from American lobster *Homarus americanus*, Cabo_CPRP_I from Jonah crab *Cancer borealis*, and Capa_CPRP* from crab *Cancer pagurus*. Extensive coverage of the CPRPs was achieved, and most sequences came from eyestalk extracts (**Table 3-2**). This is expected, due to the localization of CHH primarily in the sinus gland of the eyestalk. The absence of any mutated residues indicates that CPRPs are highly conserved between these two *Orconectes* species. Comparison to known CPRP sequences from other crustaceans [22, 28, 32, 44, 50, 53-64] also suggests a great deal of homology. Sequence conservation throughout evolutionary time may indicate that this peptide family has an important biological function, instead of being simply a byproduct of CHH synthesis. This study of *O. rusticus* identified 72 PSMs, primarily from the sinus glands, that map to 10 distinct CPRPs that were previously identified in *O. limosus* and

other crustacean species. The results indicated a high degree of homology across multiple crustacean CPRPs.

Sequences for the pigment dispersing hormone (PDH) sequences are longer and more varied between species, although they are also more commonly found in the eyestalk. Several PSMs were made to peptides of the PDH family, as indicated in **Table 3-3**. In **Figure 3-4** A, alignments are made to the N-terminal portion of the peptide, which contains a precursor-related peptide only seen by MS in a single previous study (*Callinectes sapidus*, pQELHVPEREA [32]). This portion of the sequence has been characterized primarily by genetic techniques until now. The presence of these PDH-precursor related peptides may indicate analysis of incompletely processed PDH, or may suggest that these compounds are signaling molecules in their own right. The pyroglutamic acid residue at the N-terminus and amidated C-termini are common PTMs seen in authentic NPs. Currently, only one full PDH gene in *Orconectes limosus* has been sequenced, and several PSMs identified in this study do not match with portions of this gene. Indeed, several PSMs matched to the PDH gene found in the other crustacean species. By parsimony, a minimum of 10 unique sequences would be needed to cover PSMs that map to the N-terminal portions of PDHs. As indicated in **Figure 3-4** B, although only one PDH gene has been identified in *Orconectes*, multiple active PDH peptides have been identified. These peptides may thus be products of an additional PDH gene or genes. Also shown in **Figure 3-4** B, such PDH sequences included the one must come from a non-*Orconectes* PDH sequence, PDH-I of *Marsupenaeus japonicus* and α-PDH from *Pandalus borealis/jordani*. This study mapped 31 PSMs to the N-terminus of PDH, but the currently described *Orconectes* PDH gene is insufficient to describe the

variety of sequences observed here. In addition, several PSMs mapped to the PDH gene from related crustacean species. Finally, a PDH sequence corresponding to the previously known *O. limosus* PDH-A plus PDH-I from *M. japonicus* and α-PDH from *P. borealis/jordani* were observed with a total of 18 PSMs. This study has greatly increased the number of known PDH sequences and further suggests that the C-terminal portion of the prepro-PDH gene may constitute a unique NP.

3.4.3. *Neuropeptides Not Previously Identified by MS/MS in Crustaceans*

An additional 47 PSMs were made to 43 unique identified neuropeptide sequences (some PSMs mapped to the same identified peptide) (**Table 3-5**). These matches were made to compounds previously only identified by genetic means, and often in the portions of the sequence not typically associated with an active peptide. PSMs were found in the non-peptide regions of crustacean cardioactive peptide (CCAP), FMRFamide-like peptides, red pigment concentrating hormone (RPCH), orcokinin, SIFamide, and tachykinin. These may indicate new precursor-related peptide products of the same genes responsible for producing those well-known neuropeptides. An alternative explanation is that these fragments are left over after production of the genuine NP. Several PSMs mapped to crustacean hyperglycemic hormone (CHH) fragments, although too few were obtained to determine a partial sequence for this peptide in *O. rusticus*. Additional CPRP isoforms could be suggested by several matches to CPRPs other than those previously found in *O. limosus*. Matches to bursicon-α were found for the first time using MS/MS. The presence of this peptide in crustacean genomes has previously been noted, but had not been found using MS/MS techniques [28, 50]. Four of these matches appear in the signal peptide region, which would

presumably be cleaved post-translationally. Although the coverage of the bursicon-α gene is not high, these results are encouraging for further analysis, particularly targeted bottom-up proteomics approaches. Two overlapping PSMs were found for a calcitonin-like diuretic hormone (CLDH) from *Homarus americanus* [65]. They map to a region of the gene immediately preceding the putative mature peptide, which could create a precursor-related peptide. Other matches include crustacean female hormone, eclosion hormone, eyestalk peptide, an insulin-like peptide, and an oxytocin-neurophysin-like peptide. Many of these peptides have multiple PSMs from multiple organs and/or analysis techniques, thus increasing the confidence of their assignments. These matches are not sufficient to positively state the presence of these peptides in *O. rusticus*¸ mostly because they do not provide full coverage of sequences of the hormones in question. Many of these are large hormones that would need additional treatment prior to MS/MS analysis to map their sequences. These additional PSMs are intriguing and suggest that additional precursor-related peptides may be encoded by the same genes that encode known NPs, and that several NPs not previously detected with MS/MS may be present in *O. rusticus.*

3.4.4. *Comparison of Data Sets*

Results for PSMs mapping to proteins or unidentified transcripts of the *Daphnia pulex* genome are presented in **Table 3-5**. The *D. pulex* genome has already been subjected to genome mining for neuropeptide sequences [66, 67], but it is possible that some of these still unidentified proteins produce NPs that were missed in the previous studies. A number of spectra were assigned sequences by *de novo* sequencing only with PEAKS. The identities of these were interrogated by BLAST, and it was determined that

no neuropeptides or hormones were found in this data set, although several PSMs mapped to unidentified *D. pulex* proteins, which may yet contain undiscovered NP sequences.

PEAKS performed slightly better than Mascot in terms of numbers of identifications in both the brain and eyestalk (**Figure 3-1**), which suggested it might be more suitable for smaller peptide identification. The PSMs made in eyestalk had very few overlap with those in the brain. This is likely due to the presence of large NPs in the eyestalk, such as CPRPs and PDHs. Smaller NPs typically found in the brain, such as ASTs and FLPs, were not identified well due to problems mentioned earlier. Many NPs have a tissue-specific pattern of distribution. Interestingly, only CPRPs and PDHs had a clear family trend in tissue distribution—most were present in the eyestalk. It is likely that the addition of these two groups to the eyestalk tally led to the overall identification of more NP sequences in this tissue, as CPRPs and PDHs had many PSMs. The distribution of PSMs to neuropeptide families is indicated in **Figure 3-5**.

As mentioned previously, each PSM may indicate a unique NP with biological activity, or they may map to fragments of authentic NPs. For this reason, the PSMs were assembled into the lowest number of possible NPs that could produce the observed peptides. The least possible number of NP precursors that could explain the NPs observed to match the 10 NP families for which identifications were made to previously observed compounds was determined by parsimony and the resulting peptides are indicated in **Table 3-4**. Fifty-seven NPs are sufficient to explain these PSMs, although it is expected that this number is a very low estimation.

3.5. Conclusions and Future Work

In this work, the NPs present in the crayfish *Orconectes rusticus* were catalogued using MS/MS. This species is of particular interest to neuroscience, for the behavioral studies conducted in it, and ecology, for its impact on the environment as an invasive species. This list of NPs will be of aid for further studies into this organism, which will be useful in understanding how an organism responds to changing environmental conditions via neuroendocrine regulation, among other things. Two MS/MS interpretation approaches were used: database searching using the program Mascot and *de novo* sequencing using the program PEAKS. Determining a score cutoff was difficult, as the algorithms that these programs use to score the probability of a match are not optimal for small peptides, as many NPs are, and small databases, such as the ones employed in this study. The mixture of large preprohormones and small active NPs in the combination database used may also have contributed to difficulties obtaining scores that accurately represent the quality of a PSM. It is suggested that a different set of criteria be used for databases containing only short sequences of active NPs than for protein/preprohormone databases. A lower score threshold, or even a different scoring mechanism could be used to ensure that all NPs present are fairly assigned. Lowering the score threshold will increase the manual work, as spectra will have to be verified by hand, but development of a new algorithm to score short peptide matches to spectra requires expertise in statistical methods.

This study identified NPs belonging to allatostatin (both A- and B-type), CPRP, FMRFamide-like peptide, myosuppressin, orcokinin, orcomyotropin, PDH, and SIFamide families from previously identified NPs in the extracts of brain and eyestalk. Potentially novel PDHs were discovered, which may represent new PDH-precursor related signaling

molecules, which were first suggested by Hui and colleagues [32]. A total of 215 PSMs were made to NPs previously observed in other decapod crustacean species. PSMs for signaling molecules not previously identified in decapod crustaceans were also made. Other PSMs map to previously unobserved (by MS) sequence regions of CHHs, bursicon, FMRFamides, a crustacean female hormone, insulin-like hormones, calcitonin-like diuretic hormones (CLDHs), eclosion hormone, eyestalk peptides, an oxytocin-neurophysin-like hormone, red pigment concentrating hormone (RPCH), and tachykinins. These peptides warrant further study, as many have homology to mammalian NPs involved in critical physiology.

3.6 References

1. Kravitz, E.A. and Huber, R., *Aggression in invertebrates.* Current Opinion in Neurobiology, 2003. **13**(6): p. 736-743.
2. Panksepp, J.B., Yue, Z., Drerup, C., and Huber, R., *Amine neurochemistry and aggression in crayfish.* Microscopy Research and Technique, 2003. **60**(3): p. 360-368.
3. Dziopa, L., Imeh-Nathaniel, A., Baier, D., Kiel, M., Sameera, S., Brager, A., Beatriz, V., and Nathaniel, T.I., *Morphine-conditioned cue alters c-Fos protein expression in the brain of crayfish.* Brain Research Bulletin, 2011. **85**(6): p. 385-395.
4. Huber, R., *Amines and motivated behaviors: a simpler systems approach to complex behavioral phenomena.* Journal of Comparative Physiology a-Neuroethology Sensory Neural and Behavioral Physiology, 2005. **191**(3): p. 231-239.
5. Nathaniel, T.I., Huber, R., and Panksepp, J., *Repeated cocaine treatments induce distinct locomotor effects in Crayfish.* Brain Research Bulletin, 2012. **87**(2-3): p. 328-333.
6. Nathaniel, T.I., Panksepp, J., and Huber, R., *Drug-seeking behavior in an invertebrate system: Evidence of morphine-induced reward, extinction and reinstatement in crayfish.* Behavioural Brain Research, 2009. **197**(2): p. 331-338.
7. Panksepp, J.B. and Huber, R., *Ethological analyses of crayfish behavior: a new invertebrate system for measuring the rewarding properties of psychostimulants.* Behavioural Brain Research, 2004. **153**(1): p. 171-180.
8. Acquistapace, P., Hazlett, B.A., and Gherardi, F., *Unsuccessful predation and learning of predator cues by crayfish.* Journal of Crustacean Biology, 2003. **23**(2): p. 364-370.
9. Tierney, A.J. and Lee, J., *Spatial Learning in a T-Maze by the Crayfish Orconectes rusticus.* Journal of Comparative Psychology, 2011. **125**(1): p. 31-39.
10. Weisbord, C.D., Callaghan, D.T., and Pyle, G.G., *Associative learning in male rusty crayfish (Orconectes rusticus): conditioned behavioural response to an egg cue from walleye (Sander vitreus).* Canadian Journal of Zoology-Revue Canadienne De Zoologie, 2012. **90**(1): p. 85-92.
11. Hazlett, B.A., *Conditioned reinforcement in the crayfish Orconectes rusticus.* Behaviour, 2007. **144**: p. 847-859.
12. Hazlett, B.A., Acquistapace, P., and Gherardi, F., *Differences in memory capabilities in invasive and native crayfish.* Journal of Crustacean Biology, 2002. **22**(2): p. 439-448.
13. Guo, K., Ji, C., and Li, L., *Stable-isotope dimethylation labeling combined with LC-ESI MS for quantification of amine-containing metabolites in biological samples.* Anal Chem, 2007. **79**(22): p. 8631-8.

14. Olden, J., McCarthy, J., Maxted, J., Fetzer, W., and Vander Zanden, M., *The rapid spread of rusty crayfish (Orconectes rusticus) with observations on native crayfish declines in Wisconsin (U.S.A.) over the past 130 years.* Biological Invasions, 2006. **8**(8): p. 1621-1628.

15. Strayer, D.L., *Alien species in fresh waters: ecological effects, interactions with other stressors, and prospects for the future.* Freshwater Biology, 2010. **55**: p. 152-174.

16. Olden, J.D., Vander Zanden, M.J., and Johnson, P.T.J., *Assessing ecosystem vulnerability to invasive rusty crayfish (Orconectes rusticus).* Ecological Applications, 2011. **21**(7): p. 2587-2599.

17. Hein, C.L., Roth, B.M., Ives, A.R., and Vander Zanden, M.J., *Fish predation and trapping for rusty crayfish (Orconectes rusticus) control: a whole-lake experiment.* Canadian Journal of Fisheries and Aquatic Sciences, 2006. **63**(2): p. 383-393.

18. Tetzlaff, J.C., Roth, B.M., Weidel, B.C., and Kitchell, J.F., *Predation by native sunfishes (Centrarchidae) on the invasive crayfish Orconectes rusticus in four northern Wisconsin lakes.* Ecology of Freshwater Fish, 2011. **20**(1): p. 133-143.

19. Hein, C.L., Vander Zanden, M.J., and Magnuson, J.J., *Intensive trapping and increased fish predation cause massive population decline of an invasive crayfish.* Freshwater Biology, 2007. **52**(6): p. 1134-1146.

20. Zhang, Y., Buchberger, A., Muthuvel, G., and Li, L., *Expression and distribution of neuropeptides in the nervous system of the crab Carcinus maenas and their roles in environmental stress.* Proteomics, 2015.

21. Chen, R., Xiao, M., Buchberger, A., and Li, L., *Quantitative neuropeptidomics study of the effects of temperature change in the crab Cancer borealis.* J Proteome Res, 2014. **13**(12): p. 5767-76.

22. Bulau, P., Meisen, I., Schmitz, T., Keller, R., and Peter-Katalinic, J., *Identification of neuropeptides from the sinus gland of the crayfish Orconectes limosus using nanoscale on-line liquid chromatography tandem mass spectrometry.* Mol Cell Proteomics, 2004. **3**(6): p. 558-64.

23. Bulau, P., Okuno, A., Thome, E., Schmitz, T., Peter-Katalinic, J., and Keller, R., *Characterization of a molt-inhibiting hormone (MIH) of the crayfish, Orconectes limosus, by cDNA cloning and mass spectrometric analysis.* Peptides, 2005. **26**(11): p. 2129-36.

24. Dircksen, H., Burdzik, S., Sauter, A., and Keller, R., *Two orcokinins and the novel octapeptide orcomyotropin in the hindgut of the crayfish Orconectes limosus: identified myostimulatory neuropeptides originating together in neurones of the terminal abdominal ganglion.* J Exp Biol, 2000. **203**(Pt 18): p. 2807-18.

25. Dircksen, H., Skiebe, P., Abel, B., Agricola, H., Buchner, K., Muren, J.E., and Nassel, D.R., *Structure, distribution, and biological activity of novel members of*

the allatostatin family in the crayfish Orconectes limosus. Peptides, 1999. **20**(6): p. 695-712.

26. Kegel, G., Reichwein, B., Tensen, C.P., and Keller, R., *Amino acid sequence of crustacean hyperglycemic hormone (CHH) from the crayfish, Orconectes limosus: emergence of a novel neuropeptide family.* Peptides, 1991. **12**(5): p. 909-13.
27. Stangier, J., Hilbich, C., Burdzik, S., and Keller, R., *Orcokinin: a novel myotropic peptide from the nervous system of the crayfish, Orconectes limosus.* Peptides, 1992. **13**(5): p. 859-64.
28. Ma, M., Bors, E.K., Dickinson, E.S., Kwiatkowski, M.A., Sousa, G.L., Henry, R.P., Smith, C.M., Towle, D.W., Christie, A.E., and Li, L., *Characterization of the Carcinus maenas neuropeptidome by mass spectrometry and functional genomics.* General and Comparative Endocrinology, 2009. **161**(3): p. 320-334.
29. Veenstra, J.A., *The power of next-generation sequencing as illustrated by the neuropeptidome of the crayfish Procambarus clarkii.* Gen Comp Endocrinol, 2015. **224**: p. 84-95.
30. Fu, Q., Goy, M.F., and Li, L., *Identification of neuropeptides from the decapod crustacean sinus glands using nanoscale liquid chromatography tandem mass spectrometry.* Biochem Biophys Res Commun, 2005. **337**(3): p. 765-78.
31. Hsu, Y.W.A., Messinger, D.I., Chung, J.S., Webster, S.G., de la Iglesia, H.O., and Christie, A.E., *Members of the crustacean hyperglycemic hormone (CHH) peptide family are differentially distributed both between and within the neuroendocrine organs of Cancer crabs: implications for differential release and pleiotropic function.* Journal of Experimental Biology, 2006. **209**(16): p. 3241-3256.
32. Hui, L., Cunningham, R., Zhang, Z., Cao, W., Jia, C., and Li, L., *Discovery and characterization of the Crustacean hyperglycemic hormone precursor related peptides (CPRP) and orcokinin neuropeptides in the sinus glands of the blue crab Callinectes sapidus using multiple tandem mass spectrometry techniques.* J Proteome Res, 2011. **10**(9): p. 4219-29.
33. Fu, Q., Kutz, K.K., Schmidt, J.J., Hsu, Y.W., Messinger, D.I., Cain, S.D., de la Iglesia, H.O., Christie, A.E., and Li, L., *Hormone complement of the Cancer productus sinus gland and pericardial organ: an anatomical and mass spectrometric investigation.* J Comp Neurol, 2005. **493**(4): p. 607-26.
34. Dickinson, P.S., Stemmler, E.A., Barton, E.E., Cashman, C.R., Gardner, N.P., Rus, S., Brennan, H.R., McClintock, T.S., and Christie, A.E., *Molecular, mass spectral, and physiological analyses of orcokinins and orcokinin precursor-related peptides in the lobster Homarus americanus and the crayfish Procambarus clarkii.* Peptides, 2009. **30**(2): p. 297-317.
35. Skiebe, P., *Neuropeptides in the crayfish stomatogastric nervous system.* Microsc Res Tech, 2003. **60**(3): p. 302-12.
36. Skiebe, P., Dreger, M., Borner, J., Meseke, M., and Weckwerth, W., *Immunocytochemical and molecular data guide peptide identification by mass*

spectrometry: orcokinin and orcomyotropin-related peptides in the stomatogastric nervous system of several crustacean species. Cell Mol Biol (Noisy-le-grand), 2003. **49**(5): p. 851-71.

37. Skiebe, P., Dreger, M., Meseke, M., Evers, J.F., and Hucho, F., *Identification of orcokinins in single neurons in the stomatogastric nervous system of the crayfish, Cherax destructor.* J Comp Neurol, 2002. **444**(3): p. 245-59.

38. Yasuda, A., Yasuda-Kamatani, Y., Nozaki, M., and Nakajima, T., *Identification of GYRKPPFNGSIFamide (crustacean-SIFamide) in the crayfish Procambarus clarkii by topological mass spectrometry analysis.* Gen Comp Endocrinol, 2004. **135**(3): p. 391-400.

39. Yasuda-Kamatani, Y. and Yasuda, A., *Identification of orcokinin gene-related peptides in the brain of the crayfish Procambarus clarkii by the combination of MALDI-TOF and on-line capillary HPLC/Q-Tof mass spectrometries and molecular cloning.* Gen Comp Endocrinol, 2000. **118**(1): p. 161-72.

40. Ma, M., Chen, R., Sousa, G.L., Bors, E.K., Kwiatkowski, M.A., Goiney, C.C., Goy, M.F., Christie, A.E., and Li, L., *Mass spectral characterization of peptide transmitters/hormones in the nervous system and neuroendocrine organs of the American lobster Homarus americanus.* Gen Comp Endocrinol, 2008. **156**(2): p. 395-409.

41. Hui, L., Xiang, F., Zhang, Y., and Li, L., *Mass spectrometric elucidation of the neuropeptidome of a crustacean neuroendocrine organ.* Peptides, 2012. **36**(2): p. 230-9.

42. Ma, M., Bors, E.K., Dickinson, E.S., Kwiatkowski, M.A., Sousa, G.L., Henry, R.P., Smith, C.M., Towle, D.W., Christie, A.E., and Li, L., *Characterization of the Carcinus maenas neuropeptidome by mass spectrometry and functional genomics.* Gen Comp Endocrinol, 2009. **161**(3): p. 320-34.

43. Ma, M., Sturm, R.M., Kutz-Naber, K.K., Fu, Q., and Li, L., *Immunoaffinity-based mass spectrometric characterization of the FMRFamide-related peptide family in the pericardial organ of Cancer borealis.* Biochem Biophys Res Commun, 2009. **390**(2): p. 325-30.

44. Ma, M., Wang, J., Chen, R., and Li, L., *Expanding the Crustacean neuropeptidome using a multifaceted mass spectrometric approach.* J Proteome Res, 2009. **8**(5): p. 2426-37.

45. Szabo, T.M., Chen, R., Goeritz, M.L., Maloney, R.T., Tang, L.S., Li, L., and Marder, E., *Distribution and physiological effects of B-type allatostatins (myoinhibitory peptides, MIPs) in the stomatogastric nervous system of the crab Cancer borealis.* J Comp Neurol, 2011. **519**(13): p. 2658-76.

46. Lorand, L. and Graham, R.M., *Transglutaminases: crosslinking enzymes with pleiotropic functions.* Nat Rev Mol Cell Biol, 2003. **4**(2): p. 140-156.

47. Jia, C., Hui, L., Cao, W., Lietz, C.B., Jiang, X., Chen, R., Catherman, A.D., Thomas, P.M., Ge, Y., Kelleher, N.L., and Li, L., *High-definition De Novo*

Sequencing of Crustacean Hyperglycemic Hormone (CHH)-family Neuropeptides. Mol Cell Proteomics, 2012.

48. Chen, R., Hui, L., Cape, S.S., Wang, J., and Li, L., *Comparative Neuropeptidomic Analysis of Food Intake via a Multi-faceted Mass Spectrometric Approach.* ACS Chem Neurosci, 2010. **1**(3): p. 204-214.

49. Chen, R., Jiang, X., Conaway, M.C., Mohtashemi, I., Hui, L., Viner, R., and Li, L., *Mass spectral analysis of neuropeptide expression and distribution in the nervous system of the lobster Homarus americanus.* J Proteome Res, 2010. **9**(2): p. 818-32.

50. Ma, M., Gard, A.L., Xiang, F., Wang, J., Davoodian, N., Lenz, P.H., Malecha, S.R., Christie, A.E., and Li, L., *Combining in silico transcriptome mining and biological mass spectrometry for neuropeptide discovery in the Pacific white shrimp Litopenaeus vannamei.* Peptides, 2010. **31**(1): p. 27-43.

51. Wang, J., Jiang, X., Sturm, R.M., and Li, L., *Combining tissue extraction and off-line capillary electrophoresis matrix-assisted laser desorption/ionization Fourier transform mass spectrometry for neuropeptide analysis in individual neuronal organs using 2,5-dihydroxybenzoic acid as a multi-functional agent.* J Chromatogr A, 2009. **1216**(47): p. 8283-8.

52. Wang, J., Zhang, Y., Xiang, F., Zhang, Z., and Li, L., *Combining capillary electrophoresis matrix-assisted laser desorption/ionization mass spectrometry and stable isotopic labeling techniques for comparative crustacean peptidomics.* J Chromatogr A, 2010. **1217**(26): p. 4463-70.

53. Choi, C.Y., Zheng, J., and Watson, R.D., *Molecular cloning of a cDNA encoding a crustacean hyperglycemic hormone from eyestalk ganglia of the blue crab, Callinectes sapidus.* Gen Comp Endocrinol, 2006. **148**(3): p. 383-7.

54. Davey, M.L., Hall, M.R., Willis, R.H., Oliver, R.W., Thurn, M.J., and Wilson, K.J., *Five Crustacean Hyperglycemic Family Hormones of Penaeus monodon: Complementary DNA Sequence and Identification in Single Sinus Glands by Electrospray Ionization-Fourier Transform Mass Spectrometry.* Mar Biotechnol (NY), 2000. **2**(1): p. 80-91.

55. Dircksen, H., Bocking, D., Heyn, U., Mandel, C., Chung, J.S., Baggerman, G., Verhaert, P., Daufeldt, S., Plosch, T., Jaros, P.P., Waelkens, E., Keller, R., and Webster, S.G., *Crustacean hyperglycaemic hormone (CHH)-like peptides and CHH-precursor-related peptides from pericardial organ neurosecretory cells in the shore crab, Carcinus maenas, are putatively spliced and modified products of multiple genes.* Biochem J, 2001. **356**(Pt 1): p. 159-70.

56. Fu, Q., Christie, A.E., and Li, L., *Mass spectrometric characterization of crustacean hyperglycemic hormone precursor-related peptides (CPRPs) from the sinus gland of the crab, Cancer productus.* Peptides, 2005. **26**(11): p. 2137-50.

57. Hsu, Y.W., Messinger, D.I., Chung, J.S., Webster, S.G., de la Iglesia, H.O., and Christie, A.E., *Members of the crustacean hyperglycemic hormone (CHH) peptide family are differentially distributed both between and within the neuroendocrine*

organs of Cancer crabs: implications for differential release and pleiotropic function. J Exp Biol, 2006. **209**(Pt 16): p. 3241-56.

58. Hsu, Y.W., Weller, J.R., Christie, A.E., and de la Iglesia, H.O., *Molecular cloning of four cDNAs encoding prepro-crustacean hyperglycemic hormone (CHH) from the eyestalk of the red rock crab Cancer productus: identification of two genetically encoded CHH isoforms and two putative post-translationally derived CHH variants.* Gen Comp Endocrinol, 2008. **155**(3): p. 517-25.

59. Ma, M., Chen, R., Ge, Y., He, H., Marshall, A.G., and Li, L., *Combining bottom-up and top-down mass spectrometric strategies for de novo sequencing of the crustacean hyperglycemic hormone from Cancer borealis.* Anal Chem, 2009. **81**(1): p. 240-7.

60. Marco, H.G., Hansen, I.A., Scheller, K., and Gade, G., *Molecular cloning and localization of a cDNA encoding a crustacean hyperglycemic hormone from the South African spiny lobster, Jasus lalandii.* Peptides, 2003. **24**(6): p. 845-51.

61. Stemmler, E.A., Hsu, Y.W., Cashman, C.R., Messinger, D.I., de la Iglesia, H.O., Dickinson, P.S., and Christie, A.E., *Direct tissue MALDI-FTMS profiling of individual Cancer productus sinus glands reveals that one of three distinct combinations of crustacean hyperglycemic hormone precursor-related peptide (CPRP) isoforms are present in individual crabs.* Gen Comp Endocrinol, 2007. **154**(1-3): p. 184-92.

62. Toullec, J.Y., Serrano, L., Lopez, P., Soyez, D., and Spanings-Pierrot, C., *The crustacean hyperglycemic hormones from an euryhaline crab Pachygrapsus marmoratus and a fresh water crab Potamon ibericum: eyestalk and pericardial isoforms.* Peptides, 2006. **27**(6): p. 1269-80.

63. Tsai, K.W., Chang, S.J., Wu, H.J., Shih, H.Y., Chen, C.H., and Lee, C.Y., *Molecular cloning and differential expression pattern of two structural variants of the crustacean hyperglycemic hormone family from the mud crab Scylla olivacea.* Gen Comp Endocrinol, 2008. **159**(1): p. 16-25.

64. Wilcockson, D.C., Chung, S.J., and Webster, S.G., *Is crustacean hyperglycaemic hormone precursor-related peptide a circulating neurohormone in crabs?* Cell Tissue Res, 2002. **307**(1): p. 129-38.

65. Christie, A.E., Stevens, J.S., Bowers, M.R., Chapline, M.C., Jensen, D.A., Schegg, K.M., Goldwaser, J., Kwiatkowski, M.A., Pleasant, T.K., Shoenfeld, L., Tempest, L.K., Williams, C.R., Wiwatpanit, T., Smith, C.M., Beale, K.M., Towle, D.W., Schooley, D.A., and Dickinson, P.S., *Identification of a calcitonin-like diuretic hormone that functions as an intrinsic modulator of the American lobster, Homarus americanus, cardiac neuromuscular system.* The Journal of Experimental Biology, 2010. **213**(1): p. 118-127.

66. Christie, A.E., McCoole, M.D., Harmon, S.M., Baer, K.N., and Lenz, P.H., *Genomic analyses of the Daphnia pulex peptidome.* Gen Comp Endocrinol, 2011. **171**(2): p. 131-50.

67. Dircksen, H., Neupert, S., Predel, R., Verleyen, P., Huybrechts, J., Strauss, J., Hauser, F., Stafflinger, E., Schneider, M., Pauwels, K., Schoofs, L., and Grimmelikhuijzen, C.J., *Genomics, transcriptomics, and peptidomics of Daphnia pulex neuropeptides and protein hormones.* J Proteome Res, 2011. **10**(10): p. 4478-504.

3.7 Figures and Tables

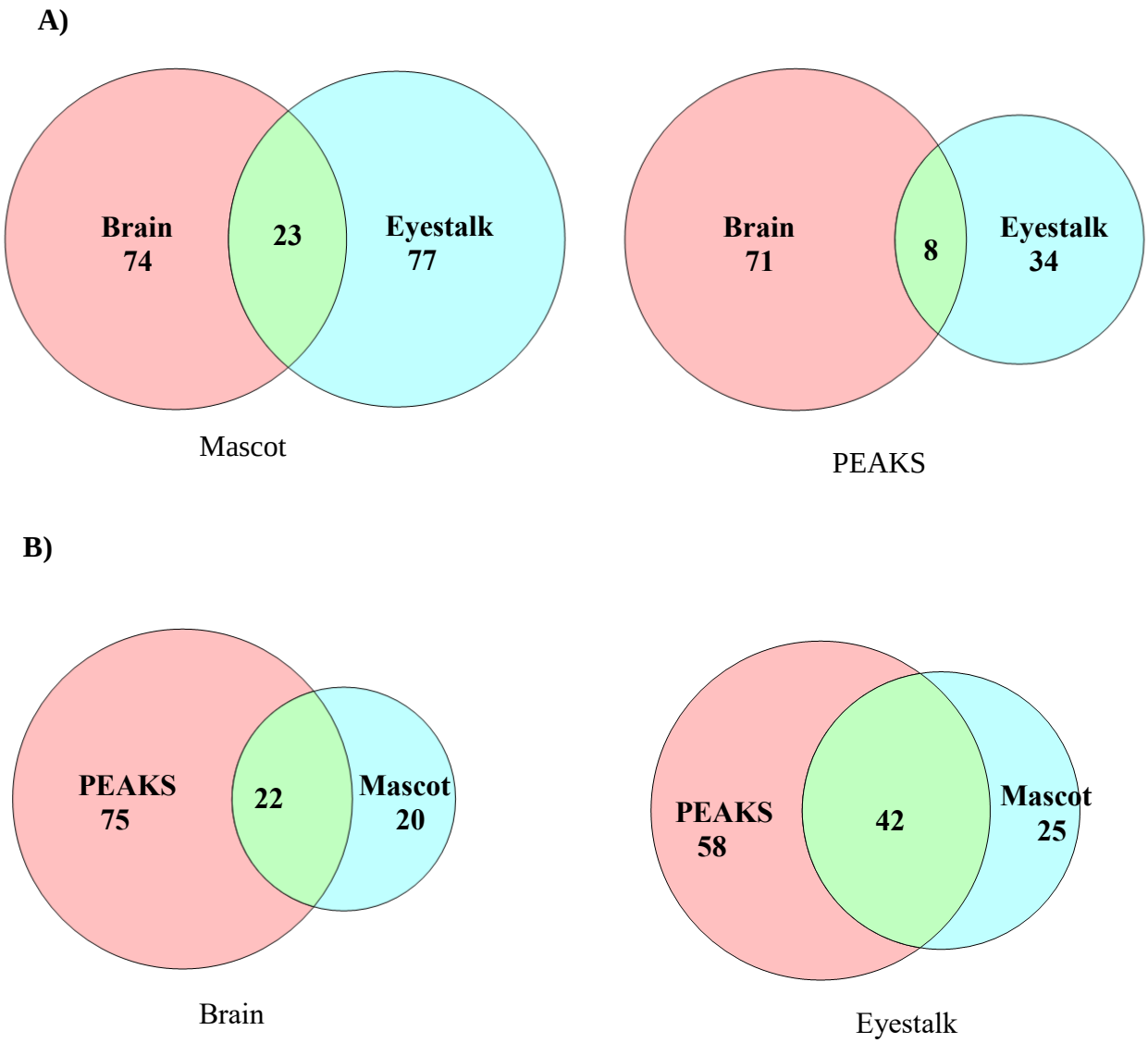

Figure 3-1. Comparison of peptide spectrum matches (PSMs) from Mascot and PEAKS using crustacean database. A) overlap between tissues; B) overlap of the two data interpreting programs in PSMs identification.

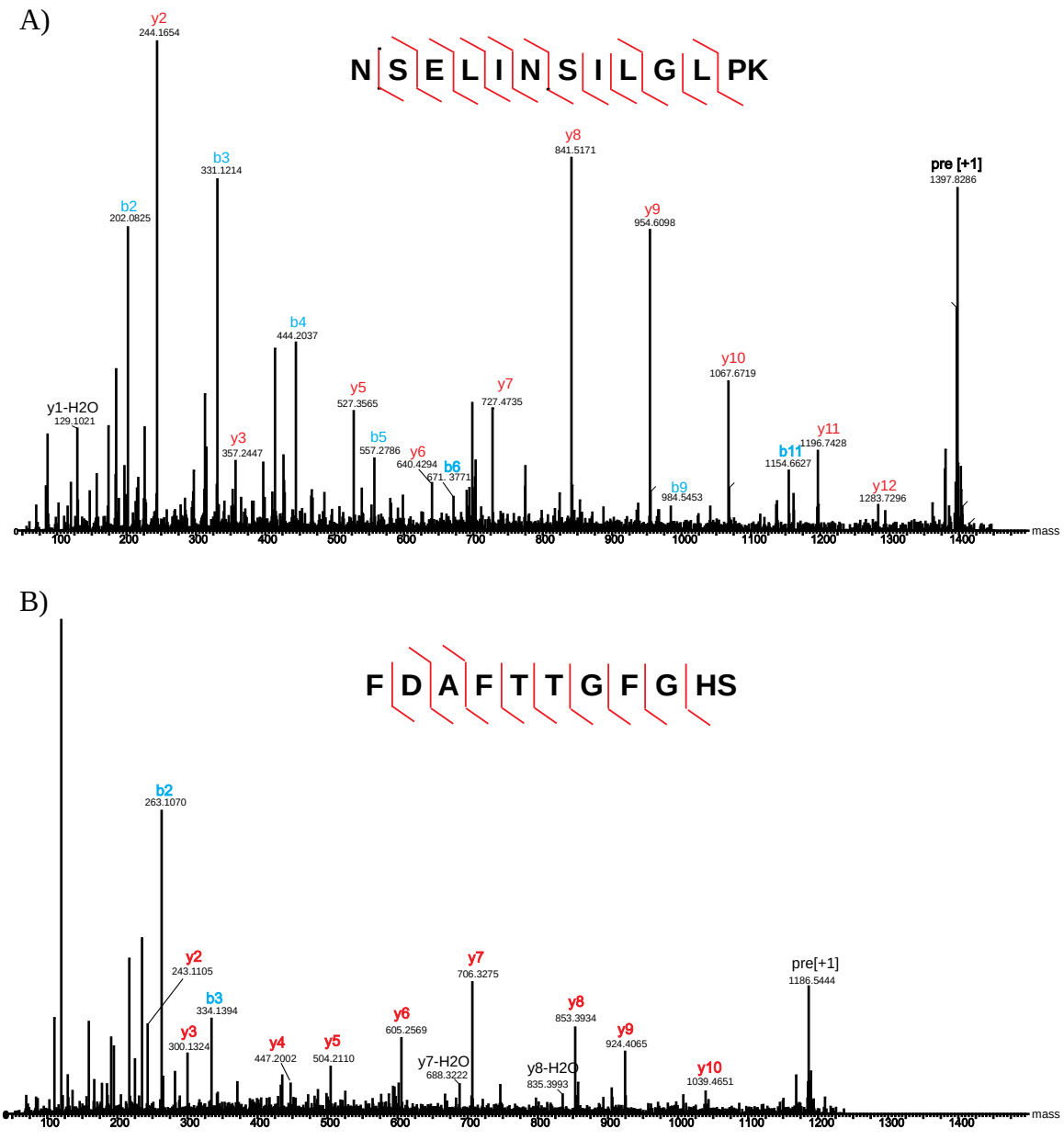

Figure 3-2. MS/MS fragmentation of neuropeptide. A) A PDH peptide; B) NP orcomyotropin.

Olim CPRP A RSVEGSSRMERLLSSGSSSSEPLSFLSQDHSVS
Olim CPRP A* RSVEGSSRMERLLSSGSSSSEPLSFLSQDQSVS
Olim CPRP B RSVEGSSRMERLLSSGSSSSEPLSFLSQDQSVN

RSVEGSSRmERLLSSGSSSSEPLSFLSQDQSVS CPRP A*
RSVEGSSRMERLLSSGSSSSEPLSFLSQDQSVN CPRP B
RSVEGSSRMERLLSSGSSSSEPLSFLSQDQSVNamide CPRP B
RSVEGS
RSVEGSSR
RSVEGSSRm
RSVEGSSRMERL
RSVEGSSRMERLL
SVEGSSRmER
GSSRMERLL
MERLLSSGSSSSEPLSFLSQDQSVS CPRP A*
RLLSSGSSSSEPLSFLSQDQSVS CPRP A*
RLLSSGSSSSEPLSFL
RLLSSGSSSSEPLSF
RLLSSGSSSSEPLS
RLLSSGSSSSEPL
LLSSGSSSSEPLS
LLSSGSSSSEPLSF
LLSSGSSSSEPLSFL
LLSSGSSSSEPLSFLSQ
LLSSGSSSSEPLSFLSQDQSVS CPRP A*
LLSSGSSSSEPLSFLSQDQSVN CPRP B
LSSGSSSSEPLSFL
LSSGSSSSEPLSFLSQDQSVS CPRP A*
SSGSSSSEPLSFLSQDHSV CPRP A
SSGSSSSEPLSFLSQDQSVS CPRP A*
SGSSSSEPLSFL
SGSSSSEPLSF
SGSSSSEPLSFLSQDQSVS CPRP A*
SGSSSSEPLSFLSQDQSVN CPRP B
SGSSSSEPLSFLSQDHSV CPRP A
SSSSEPLSFLSQDQSVS CPRP A*
SSSEPLSFLSQDQSVS CPRP A*
SSEPLSFLSQDQSVS CPRP A*
SEPLSFLSQDQSVS CPRP A*
PLSFLSQDQSVS CPRP A*
LSFLSQD
FLSQDHSVN CPRP B
FLSQDHS CPRP A
LSQDQSVNa CPRP B
LSQDHSa CPRP A

Figure 3-3. Alignment of CPRP PSMs. A lowercase m indicates an oxidized methionine. *Orconectes limosus* CPRP sequences are taken from a reference and compared to sequences obtained in this study. Red indicates the residue that distinguishes CPRP A* from A, and green indicates the residue that distinguishes B from the others. The column to the far right shows which CPRP each fragment maps to. For those fragments that occur in multiple CPRPs, it is left blank.

A. N-Terminus

Orconectes limosus PDH precursor (S59496.1) 1-56

MRSAMVVLVLVAMVAVFTRAQE LKYPEREVVAELAAQIYGWPGSLGTMAGGPHKRN
SELINSILGLPKVMNEAGRR

pQElKYPEREVVA
pQElKYPEREVVAEl
pQElKYPEREVVAElA
pQElKYPEREVVAElAA
pQElKYPEREVVAElAAQ
QElKYPEREVVA
QElKYPEREVVAEl
QElKYPEREVVAElA
QElKYPEREVVAElAA
QElKYPEREVVAElAAQ
SSlKYFEa
SSlKYFEREa
SSlKYFEREVVSElAAQll
SSlKYFEREVVSElAAQllR
SSlKYFEREVVSElAAQllRV
KYPEREVV
KYQEREmV
pEREVVSEamide
SElAAQllRVa
AAQllRVAQGPSAFVAGPHK
QllRVAQGP
QAVKGAHTGVAAGPH
QAVKGAHTGVAAGPHamide
pQAPWAGAVGPH
VAQGPSAFVAGPHK
AQGPSAFVAGPHK
QAPAAGAVGP
QAPWAAAVGP
WAAAVGPHKRN
AGGlPHKRNamide
DlNPTEKamide

B. C-Terminus

Olim PDH-A NSELINSILGLPKVMNEAamide
Marj PDH-I NSELINSLLGIPKVMTDAamide
Panbo α-PDH NSGMINSILGIPRVMTEAamide
NSElINSllGlPKVMNEAamide
NSElINSl
NSElINSll
NSElINSllGl
NSElINSllGlP
NSElINSllGlPK
SElINSllGlPamide
NSllGlPKVMT
SllGlPKVM
SllGlPKVm
SllGlPKVmNEA
SllGlPKVMNEA
SllGlPKVMNEAa
llGlPKVMNEAa
llGlPKVmT

lPRVmTEa
PKVMND
MlNSllGlPRVMT

Figure 3-4. Alignment of PDH sequences. A lowercase m indicates an oxidized methionine. A lowercase l in a PSM sequence indicates a L or I residue, since they cannot be distinguished using MS. A lowercase p in front of a Q indicates the pyroglutamic acid form of Q. A) Alignment of sequences to the N-terminal portion of the precursor. Active peptides formed from this portion are sometimes called PDH precursor-related peptides. Reference sequences are given first, followed by several rows of PSMs from the data. Underlined sequences differ from the literature sequence for *O. limosus.* B) Alignment to the C-terminal portion. This is the active PDH peptide. Sequences for PDH A, B, and C from *O. limosus* are indicated as Olim PDH-A. Sequence for *Marsupenaeus japonicu*s PDH I is indicated as Marj PDH-I. Sequence for *Pandalus borealis* α-PDH is indicated as Panbo α-PDH. Blue indicates the residues that differ between Olim PDH-A and Marj PDH-I. Red indicates the residues that differ between Olim PDH-A and Panbo α-PDH. PSMs follow the reference sequences, with modified residues indicated by colors, and the precursor that PSM requires indicated in the righthand column. For PSMs where multiple precursors are suggested, this column is left blank.

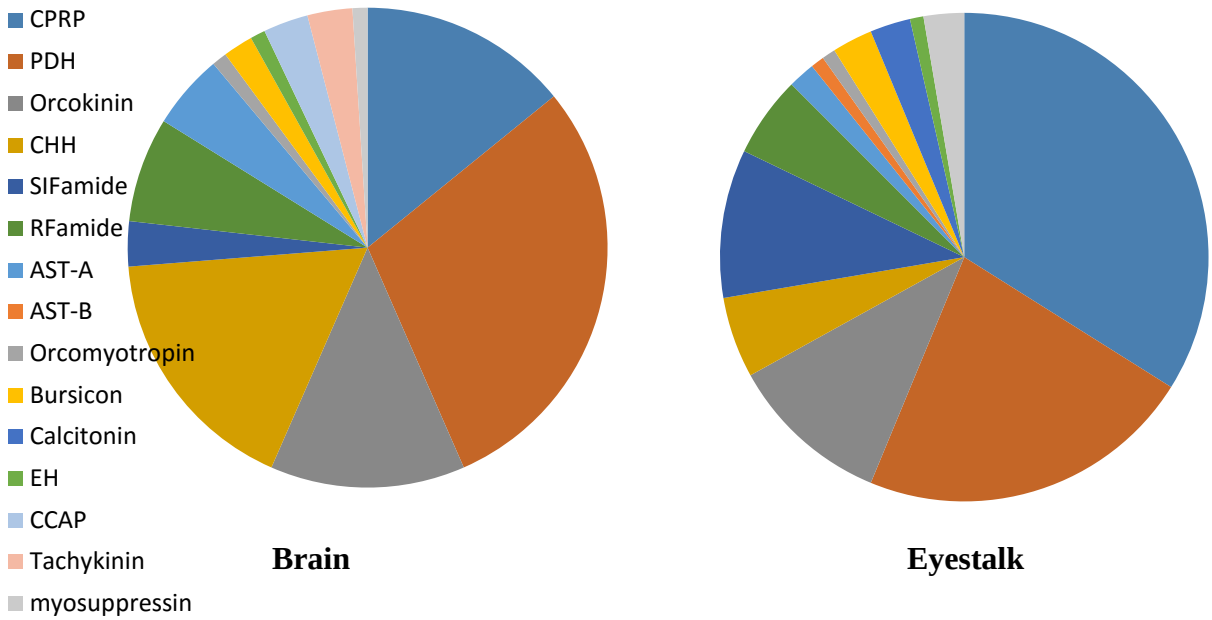

Figure 3-5. PSMs mapped to each NP family in brain and eyestalk tissues. In total, 155 PSMs in brain and 145 in eyestalk.

Table 3-1. PSMs that map to putative neuropeptides previously identified in decapod crustaceans. Abbreviations in text. PEAKS and Mascot scores are both -10logP.

NP Family	NP Matching Sequence	Sequence of PSM	Eyestalk		Brain	
			PEAKS Score	Mascot Score	PEAKS Score	Mascot Score
AST	DPYAFGLGKRPADLYEFGLamide	KRPADLYEa			31.82	
AST-A	PDAEESNKRDRLYAFGLamide	KRDRLYa	17.91			
	TARGALDLDQSPAYASDLGKRIGSAYSFGLamide	KRIGSAY			30.06	
		PAYASDLGKa	44.16		22.37	
		LDQSPAYASDL			17.59	
		pQSPAYASDLGKRIGSAYa	18.52		17.81	14.87
AST-B	TNWNKFQGSWamide	TNWNKFQGSWa	43.03			
		TNWNKFQ			19.22	
FMRFamide-like peptides	EPLDHVFLRFamide YAIAGRPRFamide YSLRARPRFamide DRTPALRLRFamide SQGLNSDLRFamide EFVDPNLRFamide KPDPSQLANMAEALKYLEQELDKYYSQVSRPRFamide	EPLDHVFLR		35.40		
		EPLDHVFLRFa		51.93		29
		YAIAGRPR			51.73	
		YSLRAR	35.93			
		DRTPAL	32.69			
		GLNSDLa			26.01	
		pEFVDPNa			20.14	
		LKYLEQEL			30.44	
		PSQLANM(O)AEALa			16.91	
		YSQVSRPRFa			41.96	
		QLANMAEAL			24.85	

		MAEALKYLEQELD				14.14
		LEQELDKYYSQVSa				18.04
Myosuppressin	pQDLDHVFLRFamide	pQDLDHVFLR	33.24	35.44		
		pQDLDHVFLRF	29.98	16.55		
		pQDLDHVFLRFa	53.35	48.09	29.92	
Orcokinin	DFDEIDRSGFA DFDEIDRSGFG NFDEIDRSGFA NFDEIDRSSFG NFDEIDRSGFGFN NFDEIDRSGFGFA NFDEIDRSGFGFV NFDEIDRTGFGFH EIDRSSFGFN TPRDIANLYamide NFDEIDRTGFa	DFDEIDRSGFA			60.31	47.46
		EIDRSGFGFN	42.51		74.36	20.69
		EIDRSGFGFV			35.43	
		DEIDRSGFGFN	38.29			
		DFDEIDRSGFG			36.09	
		NFDEIDR	59.94	14.45	42.43	33.62
		NFDEIDRS	32.51	22.09		
		NFDEIDRSGFA	49.34	30.17	79.98	46.19
		NFDEIDRSGFG	61.35		97.05	55.37
		NFDEIDRSGFGF			35.2	46.50
		NFDEIDRSGFGFA	96.01	41.64	64.67	45.62
		NFDEIDRSGFGFN	25.26		100.69	101.41
		NFDEIDRSGFGFV	95.47	64.80	123.37	72.59
		NFDEIDRSSFG			46.81	
		NFDEIDRTGFa	20.54			
		NFDEIDRTGFG		28.28		36.02
		NFDEIDRTGFGF	39.49	34.47		
		NFDEIDRTGFGFH				32.27
		DRSSFGFa			15.31	
		TPRDIANLYa	22.32			

Orcomyotropin	FDAFTTGFGHS	FDAFTTGF			25.85	
		FDAFTTGFGHS		63.09	90.79	44.71
SIFamide	GYRKPPFNGSIFa	FNGSIFa	36.26			
		GYRKPPFN	62.60	19.93		
		GYRKPPFNG	71.74	14.72		
		GYRKPPFNGS(OI	75.24			
		GYRKPPFNGSIF	83.26	49.05		
		GYRKPPFNGSIFa	96.28	17.21		
		KPPFNGSIF	52.28	36.10		
		KPPFNGSIFa	43.03			
		RKPPF				24.33
		RKPPFN			57.21	13
		RKPPFNG				17.20
		RKPPFNGSI		27.40		
		RKPPFNGSIF	76.69	21.18		
		RKPPFNGSIFa	67.15	23.38		
		YRKPPFNGSIF	27.30			
Others	DLPKVDTALK	DLPKVDTALK	78.45	34.42	69.79	45.83
		DLPKVDTAL	43.95		20.30	
		DLPKVDTA	42.11			
		PKVDTALK	62.13	32.08	19.23	
	AVLLPKKTEKK	AVLLPK			59.04	30.49
		AVLLPK				10.74
		AVLLPKKTEKK			58.46	46.20
		VLLPKKTEKK			54.75	
		VLLPKKTEK			22.22	50.66
		LLPKKTEKK			38.42	23.06

		LPKKTEKK			63.63	30.25
		PKKTEKK				40.51
	KPKTEKK	KPKTEKK			45.05	42.12
	GPSGGFNGALAR	PSGGFNGALA			31.08	

Table 3-2. PSMs for CPRP. Abbreviations in text. M(O) indicates an oxidized methionine. pQ indicates pyroglutamate. Lowercase l indicates either a I or L residue, as these are isobaric. PEAKS and Mascot scores are both -10logP.

NP Family	Sequence of PSM	Eyestalk		Brain	
		PEAKS Score	Mascot Score	PEAKS Score	Mascot Score
CPRP	GSSRMERLL	31.71			
	LLSSGSSSSEPLS		33.58		
	LLSSGSSSSEPLSF	66.65	24.51		
	LLSSGSSSSEPLSFL	87.41	34.23		
	LLSSGSSSSEPLSFLSQ	90.29	58.59		
	LLSSGSSSSEPLSFLSQDQSVN	107.15	51.34		
	LLSSGSSSSEPLSFLSQDQSVS	135.41	110.12		
	LSSGSSSSEPLSFL	29.79			
	LSSGSSSSEPLSFLSQDQSVS	41.93	33.76		
	MERLLSSGSSSSEPLSFLSQDQSVS	99.63	151.55		
	PLSFLSQDQSVS	94.98	82.14		
	RLLSSGSSSSEPL		46.47		
	RLLSSGSSSSEPLS		94.86		
	RLLSSGSSSSEPLSF	90.35	92.68		
	RLLSSGSSSSEPLSFL	98.35	59.08		
	RLLSSGSSSSEPLSFLSQDQSVS	118.62	100.77		
	RSVEGS			16.10	
	RSVEGSSR	30.78			
	RSVEGSSRM(O)			15.27	
	RSVEGSSRMERL		28.92		
	RSVEGSSRMERLL		15.38		

	RSVEGSSRMERLLSSGSSSSEPLSFLSQDQSVN		81.28		
	RSVEGSSRMERLLSSGSSSSEPLSFLSQDQSVNamide		71.45		
	RSVEGSSRMERLLSSGSSSSEPLSFLSQDQSVS		129.71		
	SVEGASRMEKLLSSSNSPSSTPLGFLSQDHSVN		30.79		
	SVEGSSRM(O)ER			18.08	
	GSSRMERLL	31.71			
	SEPLSFLSQDQSVS	49.35	16.31		
	SSGSSSSEPLSFL	18.35			
	SSGSSSSEPLSF	32.81			
	SGSSSSEPLSFLSQDQSVN		14.25	33.21	
	SGSSSSEPLSFLSQDQSVS	73.77	73.4		
	SFLSQDQSVNa			44.26	
	SSEPLSFLSQDQSVS	40.92	20.03		
	SGSSSSEPLSFLSQDHSV	21.91			
	SSGSSSSEPLSFLSQDHSV	42.54	36.59		
	SSGSSSSEPLSFLSQDQSVS	98.35	69.08		
	SSSEPLSFLSQDQSVS	50.38	11.1		
	SSSSEPLSFLSQDQSVS	34.39	48.58		
	LSQDQSVNa	34.41		21.76	
	LSFLSQD	29.85			
	LSQDHSa	15.15			
	FLSQDHSVN	52.54	11.81		
	FLSQDHS	41.58			
	LSSISPSSTP	20.27		32.64	
	SSISPSSTPa			28.78	
	ISPSSTPL	21.73		32.15	
	TPLGFLSQDa			16	
	TPLGDLSGSVGH			15.05	

	PLGDLSGSLGHa			21.57	
	DTVTPLR			38.61	
	EPLSFLSQDHa	32.69			
	LASLKSDT			32.08	
	LDGLAR			28.71	
	TPLGDLSGSLa			26.78	
	KLLSTSSSASAA			26.21	
	LASYRGALEPSTa			25.73	
	LAALKTSPM(O)Ea			23.42	
	LAALKTSPM(O)	23.9			
	GALEPS			21.26	
	LAVEHGTT	17.78			
	SISPSSMPLGFa	17.26			
	ALEPNTPL	16.92		16.74	
	LASYRGALESNa	16.88			
	PSTPLGDLSGSLGH	16.05			
	SLDGLARIE			15.32	
	LLASLKADSLGa			31.47	
	pEKLLSTSSSASa			38.38	18.38
	M(O)GHLGELT	24.53			
	LGPVQDF				14.14
	MGKMERLLAS		20.45		
	QGLGKMERLLVSY		17.55		

Table 3-3. PSMs for PDH. Abbreviations in text. M(O) indicates an oxidized methionine. pQ indicates pyroglutamate. Lowercase l indicates either a I or L residue, as these are isobaric. PEAKS and Mascot scores are both -10logP.

NP Family	Sequence of PSM	Eyestalk		Brain	
		PEAKS Score	Mascot Score	PEAKS Score	Mascot Score
PDH	QllRVAQGP			27.43	
	AAQllRVAQGPSAFVAGPHK				41.91
	AGGlPHKRNamide			52.58	
	AQGPSAFVAGPHK	28.74	19.75		
	DlNPTEKamide			48.37	
	llGlPKVMNEAamide	62.4			
	NSEllNSl		13.9		
	NSEllNSll	32.06			
	NSEllNSllGl		41.4		
	NSEllNSllGlP	75.94	65.83		
	NSEllNSllGlPK	126.88	76.4		
	NSEllNSllGlPKVMNEAamide	74.91	102.18		
	PKVMND			15.78	
	pQElKYPEREVVA			28.75	
	pQElKYPEREVVAEl	17.85		107.9	
	pQElKYPEREVVAElA	21.98		59.92	
	pQElKYPEREVVAElAA	34.83			
	pQElKYPEREVVAElAAQ			30.23	
	QElKYPEREVVA				13.11
	QElKYPEREVVAEl				36.41
	QElKYPEREVVAElA				33.28
	QElKYPEREVVAElAA		27.99		
	QElKYPEREVVAElAAQ				31.19

	QElHVPEREA			31.56	
	SElINSllGlPamide			53.89	17.02
	SllGlPKVM(O)NEA	43.34			
	SllGlPKVMNEA	34.49			
	SllGlPKVMNEAamide	66.48	30.9		
	SSlKYFEa			32.75	
	SSlKYFEREa	17.05		25.06	
	KYPEREVV			36.31	
	pEREVVSEa			25.87	
	SSlKYFEREVVSElAAQll		25.25		
	SSlKYFEREVVSElAAQllR		31.27		
	SSlKYFEREVVSElAAQllRV		27.69		
	VAQGPSAFVAGPHK			38.37	27.48
	AATELAIQIL				15.05
	QAVKGAHTGVAAGPH				16.6
	QAVKGAHTGVAAGPHa				55.02
	MlNSllGlPRVMT		10.7		
	SElAAQllRVAa				12.75
	QAPQAGAVGP			32.62	
	QAPWAAAVGP	24.33			
	WAAAVGPHKRN			15.51	
	QDLKYQAR	21.98			
	QAREM(O)VAELAQ			15.57	
	pQAPWAGAVGPH	17.92		32.91	
	QllQAVKGA			17.37	
	EGAGGlP	27.36			
	APlEGAGGlPHa	22.23			
	KYQEREM(O)V	19.75		18.65	
	QlYRVAQAP			18.4	

	RTTYMFP			15.41	
	RTTYM(O)FPL			37.11	
	lSESKRN			33.79	
	MFPllSESKR			17.86	
	EKEVlSNM(O)l			33.56	
	pEVlSNM(O)			30.58	
	lSAlMNEa	18.59			
	lGlSAlM(O)Na	30.45		45.63	
	SllGlSAlM(O)NE	25.4			
	lPRVM(O)TEa			16.26	
	KRNAElla			15.34	
	LLGIPKVM(O)T	30.42			
	SLLGIPKVM		18.8		
	SLLGIPKVM(O)	53.65			
	NSLLGIPKVMT				14.17
	SLLGVPR			31.91	

Table 3-4. NPs required to explain all observed PSMs, and sequences of unique PSMs. There are more unique sequences than NPs are required due to sequence variations being present at different parts of the overall sequence. A lowercase m indicates an oxidized methionine. Lowercase l's indicate either I or L residues. Pyroglutamic acid is indicated as pQ or pE.

NP Family	Least PossibleLowest Number of Identified NPs that Can Explain Observed PSMs	Sequences
AST	1	DPYAFGLGKRPADLYEFGLamide
AST-A	2	PDAEESNKRDRLYAFGLamide
		TARGALDLDQSPAYASDLGKRIGSAYSFGLamide
AST-B	1	TNWNKFQGSWamide
CPRP	10	WSLDGLARIEKLLSTSSSASAASPTRGQALNL
		RSVEGSSRMERLLSSGSSSSEPLSFLSQDHSVS
		RSVEGSSRMERLLSSGSSSSEPLSFLSQDQSVS
		RSVEGSSRMERLLSSGSSSSEPLSFLSQDQSVN
		RSVEGASRMEKLLSSSNSPSSTPLGFLSQDHSVN
		RSAEGLGRMGRLLASLKSDTVTPLRGFEGETGHPLE
		RSAQGLGKMERLLASYRGALEPNTPLGDLSGSVGHPVE
		RSAQGMGKMERLLASYRGALEPSTPLGDLSGSLGHPVE
		RSAEGFGRMGRLLASLKADSLGPVQDFGVEGAAHPVE

		RSAEGFGRMERLLASIRGGADSMGHLGELTGAG EGAGHPLE
FMRFamide-like peptides	7	EPLDHVFLRFamide
		YAIAGRPRFamide
		YSLRARPRFamide
		DRTPALRLRFamide
		SQGLNSDLRFamide
		EFVDPNLRFamide
		KPDPSQLANMAEALKYLEQELDKYYSQVSRPRF amide
Myosuppressin	1	pQDLDHVFLRFamide
Orcokinin	11	DFDEIDRSGFA
		DFDEIDRSGFG
		NFDEIDRSGFA
		NFDEIDRSGFGFA
		NFDEIDRSGFGFN
		NFDEIDRSGFGFV
		NFDEIDRSSFG
		NFDEIDRTGFamide
		NFDEIDRTGFGFH
		EIDRSSFGFN
		TPRDIANLYamide
Orcomyotropin	1	FDAFTTGFGHS
PDH	18	pQElKYPEREVVAElAAQ
		pQELHVPEREA
		SSlKYFEREVVSElAAQllRV

		EAVATlAAHllKVVCAPlEGAGGlPHKamide
		AAQllRVAQGPSAFVAGPHK
		lGTmAGGPHKamide
		AGGlPHKRNamide
		EYllKFamide
		DlNPTEKamide
		NSELINSILGLPKVMNEAamide
		NSELINSLLGIPKVMTDAamide
		NSGMINSILGIPRVMTEAamide
		QELHVPEREAVANLAARILKIVHAPHDAAGVPH KRNSELINSLLGISALMNEA
		DSSLKYFEREVVSELAAQILRVAQGPSAFVAGP HKRNSELINSLLGIPKVMTDA
		QSRDFSISEREIVASLAKQLLRVARMGYVPEGDL PRKRNAELINSLLGVPRVMSDAamide
		QDLKYQAREMVAELAQQIYRVAQAPQAGAVGP HKRNSELINSILGLPKVMNDAamide
		QELKYQEREMVAELAQQIYRVAQAPWAAAVGP HKRNSELINSILGLPKVMNDAamide
		QREPTASKCQAATELAIQILQAVKGAHTGVAAG PHKRNSELINSLLGLPKFMIDAamide
		QDLNPTEKEVLSNMLDFLQRHSRTTYMFPLLSE SKRNSELINSLLGAPRVLNNAamide
SIFamide	1	GYRKPPFNGSIFamide
Others	3	KPKTEKK
		AVLLPKKTEKK
		GPSGGFNGALAR

Table 3-5. PSMs for NPs and hormones not previously identified with MS/MS in decapods. Some map to precursor regions of known NP genes. M(O) indicates an oxidized methionine. Pyroglutamate residues are indicated as pE or pQ. Accession numbers starting with LL are from the in-house database LiDB.

Accession Number	Peptide Family	Description	PSM Sequence	Eyestalk		Brain	
				PEAKS	Mascot	PEAKS	Mascot
ABX55995.1	Bursicon	Bursicon alpha [Carcinus maenas]	VTVLVVIG		37.72		
ACG50067.1	Bursicon	Bursicon hormone alpha subunit [Callinectes sapidus]	AM(O)VGAAVT		19.38		
ACG50067.1	Bursicon	Bursicon hormone alpha subunit [Callinectes sapidus]	M(O)VGAAVTV	15.02			
ACG50067.1	Bursicon	Bursicon hormone alpha subunit [Callinectes sapidus]	VLTRAPIDCMCRPCT	17.91			
ADI86242.1	Bursicon	Bursicon alpha subunit [Homarus gammarus]	TVVWSDECSLT			18.99	
ACX46386.1	Calcitonin	Prepro-calcitonin-like diuretic hormone [Homarus americanus]	LTRLGHSIIRANELEKFVRSSGSA				28.86
ACX46386.1	Calcitonin	Prepro-calcitonin-like diuretic hormone [Homarus americanus]	TRLGHSIIRANELEKF				58.81
ABB46292.1	CCAP	Crustacean cardioactive peptide [Homarus gammarus]	TPHTQPR			15.38	

BAF34909.1	CCAP	Crustacean cardioactive peptide [Procambarus clarkii]	AGPLAKRDIG				18.3
BAF34909.1	CCAP	Crustacean cardioactive peptide [Procambarus clarkii]	KLWEQLQ				18.17
AAD45236.1	CHH	Hyperglycemic hormone-like [Metapenaeus ensis]	pEAASPGASSPWVEHR	22.2			
ACN65120.1	CHH	Crustacean hyperglycemic hormone [Panulirus homarus]	SPPPAGRTATVIGCSVNVSTTYamide		19.46		
ACS35346.1	CHH	Crustacean hyperglycemic hormone isoform 1 [Rimicaris kairei]	HPSGLAALTASH			21.51	
AER27833.1	CHH	Crustacean hyperglycaemic hormone [Ptychognathus pusillus]	PAGHPLEKRQamide	15.04			
AFD28272.1	CHH	CHH protein [Scylla paramamosain]	LVACIAMATLPQTQamide	21.37			
AFD28272.1	CHH	CHH protein [Scylla paramamosain]	pEGAAHPLEKRamide	19.2			
AFG16934.1	CHH	Hyperglycemic hormone [Pandalopsis japonica]	EEHVDIR			22.81	
AFM29133.1	CHH	Crustacean hyperglycmic hormone [Portunus pelagicus]	APM(O)QGYGTEamide		28.32		
LL206	CHH	Crustacean hyperglycemic hormone Hoa-CHH-A (pCHH-A[pQ61-V132amide]) [Homarus amerianus]	LDDLLLSDV	15.63			

O15981.1	CHH	Crustacean hyperglycemic hormone 5; Pej-SGP-V [Marsupenaeus japonicus]	LVAGASSAGT	21.73			
O97384.1	CHH	Crustacean hyperglycemic hormone 2; Pm-SGP-II [Penaeus monodon]	SSPVASLIRG	15.07			
AAM21927.1	CPRP	Crustacean hyperglycemic hormone precursor [Pachygrapsus marmoratus]	DRSLFGKL		30.15		
AAS46643.1	CPRP	Crustacean hyperglycemic hormone precursor [Macrobrachium rosenbergii]	RIEKLLST			18.05	
ABS01332.1	CPRP	Prepro-crustacean hyperglycemic hormone [Galathea strigosa]	LSFMPEHP			16.15	
LL343	CPRP	CHH precursor-related peptide Capr CPRP II [13-38] [Cancer productus]	GDLPGGLVHamide			19.29	
ADO00266.1	Crustacean female hormone	Crustacean female hormone [Callinectes sapidus]	DGGYIDLSENamide	17.36			
ADO00266.1	Crustacean female hormone	Crustacean female hormone [Callinectes sapidus]	ERQIQGP			18.19	
ADO00266.1	Crustacean female hormone	Crustacean female hormone [Callinectes sapidus]	QGPLPIQPVamide			19.84	

AFK81936.1	EH	Eclosion hormone [Amphibalanus amphitrite]	PGLASLGGSTST			15.44	
AF112986_1	Eyestalk peptide	Eyestalk peptide [Jasus edwardsii]	DVRQDGQTNamide			17.93	
AF112986_1	Eyestalk peptide	Eyestalk peptide [Jasus edwardsii]	TPARQR			18.55	
BAE06263.1	FMRFamide	FLRFamide precursor protein B [Procambarus clarkii]	PAEYSRNVR			16.77	
EFX80896.1	FMRFamide	Putative sulfakinin-like peptide [Daphnia pulex]	PVELGSSNPamide	20.84			
ADA67878.1	Insulin-like	Insulin-like androgenic gland hormone precursor [Penaeus monodon]	VGMLMVLSLT	20.02			
EFX70023.1	Insulin-like	Insulin/IGF/relaxin-like peptide 2 [Daphnia pulex]	SLGLTTTAATPNamide			18.11	
EFX76240.1	Insulin-like	Insulin/IGF/relaxin-like peptide 1 [Daphnia pulex]	M(O)IIPSTVGRCWM(O)			18.54	
EFX76240.1	Insulin-like	Insulin/IGF/relaxin-like peptide 1 [Daphnia pulex]	VTPAEP			18.49	
Q9NL83.1	Orcokinin	Orcomyotropin/orcokinin precursor-like peptide [Procambarus clarkii]	MTAQM(O)FTIALLLSLS				22.03
Q9NL83.1	Orcokinin	Orcomyotropin/orcokinin precursor-like peptide [Procambarus clarkii]	VYVPRYIAN	51.8	17.89	22.85	

Q9NL83.2	Orcokinin	Orcomyotropin/orcokinin precursor-like peptide [Procambarus clarkii]	VYVPRYIANLY			45.72	22.28
ADD24046.1	Oxytocin-neurophysin	Oxytocin-neurophysin 1 [Lepeophtheirus salmonis]	QYKQCSSCGP			21.23	
ADN95181.1	RPCH	Red pigment concentrating hormone precursor [Scylla paramamosain]	SVGGAPGGVVPSSPGSSSGDSamide				29.9
ADQ73633.1	RPCH	Red pigment concentrating hormone precursor [Scylla olivacea]	PPGSSSGDSCGP			18.39	
Q867W1.1	SIFamide-related peptide	GYRKPPFNGSIF-amide; FRP1_PROCL [Procambarus clarkii]	AGGDSLYEPGK			38.23	45.89
BAC82426.1	Tachykinin	Preprotachykinin [Procambarus clarkii]	AGMDSELETLL				16.8
BAC82426.1	Tachykinin	Preprotachykinin [Procambarus clarkii]	HFDDESEIDAY			38.47	37.25
BAC82426.1	Tachykinin	Preprotachykinin [Procambarus clarkii]	HFDDESEIDAYIQAL			77.24	87.4

Chapter 4

Mass Spectrometric Characterization of Circulating Neuropeptides in Jonah Crab, *Cancer borealis*

Adapted from **Zhidan Liang**, Claire M. Schmerberg, Lingjun Li. 'Mass spectrometric measurement of neuropeptide secretion in the crab, *Cancer borealis*, by *in vivo* microdialysis'. *Analyst*. 2015, *140*, 3803-3813.

Abstract

Neuropeptides (NPs), a unique and highly important class of signaling molecules across the animal kingdom, have been extensively characterized in the neuronal tissues of various crustaceans. Because many NPs are released into circulating fluid (hemolymph) and travel to distant sites in order to exhibit physiological effects, it is important to measure the secretion of these NPs from living animals. In this study, we report on extensive characterization of NPs released in the crab *Cancer borealis* by utilizing *in vivo* microdialysis to sample NPs from the hemolymph. We determined the necessary duration for collection of microdialysis samples, enabling more comprehensive identification of NP content while maintaining the temporal resolution of sampling. Analysis of *in vivo* microdialysates using a hybrid quadrupole-Orbitrap^{TM} Q-Exactive mass spectrometer revealed that more than 50 neuropeptides from 9 peptide families—including the allatostatin, RFamide, orcokinin, tachykinin-related peptide and RYamide families–were released into the circulatory system. The presence of these peptides both in neuronal tissues as well as in hemolymph indicates their putative hormonal roles, a finding that merits further investigation.

4.1 Introduction

Neuropeptides (NPs) are one of the most diverse classes of signaling molecules, and they are present in a wide variety of organisms. They are known to have regulatory roles in many physiological processes, including food intake, reproduction, pain and stress [1]. To exert their hormonal effects on different organs, NPs are often secreted into circulating fluids to travel to different parts of the body [2, 3]. Characterization of these released NPs is essential towards understanding their actions.

Both tissue-based and fluid-based methods are commonly used in NP analysis. In tissue-based methods, the animal is sacrificed to permit dissection of the tissue of interest for analysis. However, there are several limitations to tissue-based techniques [4], including an inability to obtain repeated samples from a single animal throughout the time course of a dynamic experiment. In addition, sampling NPs from tissue lacks the ability to distinguish inactive NPs from active forms of NPs, due to the nature of tissue homogenization and NP synthesis.

Due to the need to study secreted NPs, fluid-based methods have been developed as an alternative to tissue-based methods. These methods include sampling NPs from stimulated neuronal releasate [5, 6], blood or hemolymph [7]. Direct analysis of signaling neuromodulators without sacrificing the animal via fluid-based methods also allows the study of biologically active molecules under different physiological conditions in a single animal. Because baseline values for NP content can vary greatly between animals, especially in wild-caught (as opposed to laboratory-raised) animals such as crabs, being able to compare NP concentrations in a single animal across an experimental manipulation will allow us to identify fold-changes in NP content that may otherwise be

difficult to observe. Thus, hemolymph NP profiling from appropriate fluid-based samples would offer great insight into NP release in response to different stimuli or under different states in the same animal.

NPs can be sampled directly from hemolymph, obtained from the animal with the use of a needle and a syringe [7]. However, the presence of extracellular peptidases and a wide variety of molecules in addition to NPs, such as lipids, albumins, clotting factors and enzymes would make for an extremely complex sample. As a result, special treatment and several cleanup steps are often required for effective detection of NPs. Moreover, the stress caused by using a needle and a syringe may induce the release of stress-related NPs.

As an alternative, *in vivo* microdialysis allows for collection of extracellularly released molecules and enables real-time monitoring of substance release. Microdialysis shows great utility in the field of neuroscience, as it offers the ability to monitor dynamic changes of neurochemical content during different internal states of a single animal in a time-resolved fashion with minimal disturbance to the animal [8]. As a result, this technique could provide unique insight into our understanding of the effects of neuromodulator release on different behavior. The tip of the microdialysis probe consists of a semi-permeable dialysis membrane, which has a defined molecular weight cutoff (MWCO). The microdialysis probe is implanted into the tissue of interest and dialysate is collected at the outlet while perfusion fluid is pushed through the inlet, normally at a low flow rate [9]. Diffusion can occur between the perfusion fluid and the extracellular space as the perfusion fluid passes through the probe tip, and molecules such as NPs will diffuse into the perfusion fluid, driven down their concentration gradient. Microdialysis

has been widely used to monitor a wide range of molecules including electrolytes [10], amines and amino acids [11, 12], NPs [13, 14] and proteins [12, 15].

As a complement to different methods of sampling secreted NPs, highly sensitive and effective detection methods to analyze peptide hormones present in circulating hemolymph are currently unavailable but highly important. Liquid chromatography (LC) –MS is well-suited to this purpose. Over the last two decades, biological MS has shown powerful capabilities in the discovery of NPs in crustacean neuronal tissues [5, 7, 16-18]. However, compared with tissue-based NP studies, fluid-based sampling methods coupled with MS for detection of NP release in crustaceans are still poorly developed. Chen *et al*. [7] explored different NP extraction protocols from *Cancer borealis* hemolymph and subsequently detected 10 secreted NPs from five families, including RFamides, allatostatins, orcokinins, tachykinin-related peptides (TRPs), and crustacean cardioactive peptide (CCAP). Compared with the large number of NPs detected in tissues, the reduced number of NPs detected in the hemolymph suggested a need to develop methods with improved sample preparation and higher sensitivity.

By providing a cleaner sample due to collection through a dialysis membrane, microdialysis should provide a less complex sample and thus improve upon NP detection rates from hemolymph. So far, only a handful of reports have used *in vivo* microdialysis to investigate the NPs present in circulating fluid in the crustacean, although this sampling technique is more commonly used in NP analysis in the mammalian nervous system [19, 20]. Behrens *et al.* [13] reported the identification of NPs from 10 families in microdialysates collected from the pericardial space (a hemolymph-filled cavity) of *Cancer borealis* using LC-ESI-QTOF and MALDI-TOF/TOF mass spectrometry.

Moreover, a recent study by Schmerberg and Li[1] reported improved relative recovery of NPs by utilizing affinity agents, antibody-coated magnetic nanoparticles, and suggested an increased potential for improved detection of NPs released into hemolymph with this method.

To provide a more complete picture of neurosecretion and information complementary to tissue-based NP analyses of the crustacean system, herein we employ an advanced high-resolution, accurate-mass (HRAM) MS platform to study NP secretion in hemolymph using fluid-based sampling methods. Comparison for NP identification is made between crude hemolymph NP extraction and an *in vivo* microdialysis sampling strategy in the Jonah crab, *Cancer borealis*. Appropriate sample preparation steps are performed for both types of samples, which are then analyzed by a hybrid quadrupole-Orbitrap™ Q-Exactive MS instrument. This new platform has greatly increased the confidence of NP identification by offering high resolution and high mass accuracy measurement and employing two complementary MS/MS spectral interpreting strategies (Mascot and PEAKS). Two *in vivo* sampling methods were also compared to aid in identification of secreted NPs. Microdialysate collection time was evaluated to achieve the best NPs coverage.

4.2 Materials and methods

4.2.1 *Chemicals*

Formic acid (FA) was purchased from Sigma-Aldrich (St. Louis, MO, USA). All other chemicals were purchased from Fisher Scientific (Pittsburgh, PA, USA). ACS reagent-grade solvents and Mill-Q water were used for sample preparation. Optima grade solvents were used for sample analysis on the MS instrument.

4.2.2 *Animals*

Jonah crabs, *Cancer borealis*, were purchased from Ocean Resources, Inc. (Sedgwick, ME, USA) and The Fresh Lobster Company (Gloucester, MA, USA). Crabs were maintained in an artificial seawater tank at 10-13 ºC with a 12 h/12 h light/dark cycle. The crabs were allowed to adjust to the tanks for at least one week after shipment before performing hemolymph extraction or microdialysis. Details of animal housing procedures were described elsewhere [1]. Animals were housed, treated and sacrificed following the animal care protocol in accordance with the University of Wisconsin-Madison's animal care guidelines.

4.2.3 *Hemolymph Extraction*

Details of the procedure were previously described by Chen *et al*. [7]. Briefly, crabs were removed from the tank and cold-anesthetized on ice for 5 min. Hemolymph was withdrawn by inserting a 25 gauge needle attached to a 1 mL or 3 mL BD plastic syringe through the junction of the thorax and abdomen into the pericardial chamber. An aliquot of 750 microliters of freshly obtained hemolymph was spiked with an equal amount of acidified MeOH (90% MeOH, 9% glacial acetic acid, 1% water) immediately and mixed well to extract peptides and precipitate large proteins. Samples were subsequently purified by a 10 kDa molecular weight cutoff (MWCO) step and C_{18} spin column desalting step (Argos, Elgin, IL, USA). Eluates from the C_{18} spin columns were dried down and resuspended in 10 µL of 0.1% FA in water before MS injection.

4.2.4 *Microdialysis Supplies*

CMA/20 Elite probes with 4 mm membranes of polyarylether sulfone (PAES) were purchased from CMA Microdialysis (Harvard Apparatus, Holliston, MA, USA). A

KD Harvard 22 (Harvard Apparatus, Holliston, MA, USA), and a Pump 11 Elite Nanomite Syringe Pump (Harvard Apparatus, Holliston, MA, USA) were used to drive perfusate through MD probes and tubing. Additional FEP (CMA) and PEEK (Upchurch-Scientific, Index Health and Science, Oak Harbor, WA, USA) tubing was used to lengthen the tubing of the microdialysis probe as needed. This was connected by flanged connectors from CMA and BASi (West Lafayette, IN, USA). Probes were rinsed with crab saline prior to implantation.

4.2.5 *In Vivo* Microdialysis Experiments

The procedure for *in vivo* microdialysis surgery on Jonah crabs was adapted from previous publications [1, 13]. After the probe was surgically implanted in the crab, the animal was allowed to recover for at least 24 hr before dialysate was collected for MS analysis. Physiological crab saline (440 mM NaCl; 11 mM KCl; 13 mM $CaCl_2$; 26 mM $MgCl_2$; 10 mM HEPES acid; pH 7.4, adjusted with NaOH) was used as perfusion solution. The flow rate was set at 0.5 µL / min by a programmable syringe pump. For circadian NP analysis, dialysate samples were collected every 2 hr with a refrigerated fraction collector (BASi Honeycomb, Bioanalytical Systems, Inc. Indianapolis, IN, USA). Upon collection, 3 µL of FA was added to each sample, which was then stored at -20 ^{o}C immediately to improve NP stability [21]. The dialysates were concentrated ~6-fold in a SpeedVac (Thermo Fisher Scientific, Waltham, MA, USA). The concentrated dialysate was desalted using C_{18} ZipTips (EMD Millipore, Billerica, MA, USA), and eluted in 10 µL 0.1% FA in 50% acetonitrile (v/v). Similarly, for analysis of the optimal temporal resolution of *in vivo* microdialysis, samples were collected every 2, 4, 6, and 8 h with the same setup. They were immediately acidified to a final acid concentration of 5%

and stored at -20 ^{o}C. They were later concentrated 6-, 12-, 18, and 24-fold, respectively. The concentrated dialysate was desalted using C_{18} ZipTips and eluted in 0.1% FA in 50% acetonitrile (v/v). C_{18} Ziptip desalting was performed for an aliquot of concentrated dialysate that was correlated to every 2 h microdialysis fraction. The desalted dialysates were then all concentrated to a final volume of 10 µL prior to UPLC MS/MS analysis.

4.2.6 *Instrumentation*

The nanoLC-MS/MS experiment was performed using a Waters nanoAcquity UPLC system (Waters Corp, Milford, MA, USA) coupled to a quadrupole-Orbitrap^{TM} Q-Exactive mass spectrometer (Thermo Scientific, Bremen, Germany). Chromatographic separations were performed on a home-packed C_{18} reversed phase capillary column (360 µm OD, 75 µm ID × 15 cm length, 1.7 µm particle size, 150 Å pore size, (BEH C18 material obtained from Waters UPLC column, part no. 186004661)). The mobile phases used were: 0.1% FA in water (A) and 0.1% FA in acetonitrile (B). An aliquot of 3.5 µL of desalted hemolymph/microdialysis sample dissolved in 0.1% FA in water was injected and loaded onto the column without trapping. A 108 min gradient was employed with 0-0.5 min, 0-10% B; 0.5-70 min, 10-35% B; 70-80 min, 35-75% B; 80-82 min, 75-95% B; 82-92 min, 95% B; 92-93 min, 95-0% B; 93-108 min, 100% A. Data was collected under positive electrospray ionization data dependent acquisition (DDA) mode with the top 10 most abundant precursor ions selected for HCD fragmentation. The MS scan range was from *m/z* 300 to 2000 at 70,000 resolution, and the MS/MS scan was at 17,500 resolution from *m/z* 120 to 6000 with an isolation width of 2 Da, collision energy 30.

4.2.7 *Data Processing*

MS raw data files were processed and analyzed by PEAKS Studio7 (Bioinformatics Solutions Inc., Waterloo, ON, CAN) and Mascot (Matrix Science Inc., Boston, MA, USA). C-terminal amidation, pyroglutamation, and methionine oxidation were specified as variable post-translational modifications (PTMs). Precursor ion mass tolerance was 20 ppm, and fragment ion mass tolerance was 0.01 Da. *De novo* sequencing and database search were conducted with no enzyme cleavage specified. The database used was constructed in-house with known crustacean neuropeptides and is available upon request. Peptide spectrum matches (PSMs) with a -10logP value cutoff of 15 in PEAKS and 10 in Mascot were considered for further manual validation.

4.3 Results and Discussion

4.3.1 *Hemolymph Extraction*

In total, 22 NPs were identified from a direct hemolymph preparation (**Table 4-1**) analyzed with ultrahigh performance liquid chromatography (UPLC)-tandem mass spectrometry (MS/MS). It is worth noticing that only 7 out of the 22 NPs also have decent matches with Mascot database searching, which may indicate that PEAKS is more suitable for identification of smaller NPs. As a result of improved instrumentation, more NPs were identified compared to a previous study using a similar sample preparation procedure with a modest resolution MALDI TOF/TOF instrument [7]. Out of these identified NPs, only CCAP and I/LNFTHKFa were detected in both studies. Besides the use of different instruments and different ionization methods in these two studies, the highly dynamic circulatory system in crustaceans could also be responsible for the poor reproducibility of NPs found in hemolymph samples.

The presence of a wide variety of molecules in addition to NPs, such as lipids, peptidases, and clotting factors, makes the analysis of NPs from hemolymph very difficult. Although more NPs were identified in this study than were previously found in hemolymph, compared with tissue-based studies, the number is still relatively small. There are also many peaks in the MS spectra of hemolymph samples that could not be assigned to any known NPs or high probability *de novo* matches, which may lead to discovery of novel peptides or other hemolymph components in the future. The complex composition of crude hemolymph extract may suppress the signal of NPs on the MS instrument.

4.3.2 *In Vivo Microdialysis*

Performing microdialysis surgery on crabs has proven to be challenging mainly due to the crab shell. Since it was first introduced in 2008 [13], a rather sophisticated procedure has been developed in our group. Beyond technical challenges related to probe implantation, however, the low concentration of circulating hormones has continued to make the detection of NP content in dialysate difficult. Compared with the number of NPs identified from neuronal tissues, much less is known about the circulating peptides. In previous work employing microdialysis and earlier iterations of MS-based techniques, over 30 NPs were determined to be present in the circulating hemolymph of *Cancer borealis* with samples collected over more than 10 hours. However, most of these NPs were identified based on accurate mass matching, with only 3 that have been confirmed by tandem MS due to their low abundances.

One of the most powerful advantages of microdialysis sampling is that the collection is concurrent with different internal states or activity in the animal. As a result,

it allows correlation of neurochemical content with physiology or behavior to provide important function-related information. Temporal resolution, which is defined by the shortest time period over which a fluctuation can be observed, is an important parameter associated with microdialysis. In order to optimize temporal resolution and increase NP identification numbers, we first evaluated the collection time required to provide a more comprehensive identification of secreted NPs in *Cancer borealis*.

Microdialysates collected for 2, 4, 6, and 8 h at a flow rate of 0.5 µL/min would produce samples with volumes of 60, 120, 180, and 240 µL respectively, followed by desalting using C18 Ziptips and resuspension in 10 µL of 0.1% FA in water. An aliquot (3.5 µL) of each resulting sample was injected onto UPLC-MS/MS. Data was then processed as described above. The number of NPs identified from these dialysates increased as the collection duration increased, as expected (**Figure 4-1**), since increasing collection time increased the concentration of the final sample submitted for analysis. Twenty-two previously known crustacean NPs were identified from a 2 h collection; similarly 36 were observed in a 4 h sample, 39 in a 6 h collection, and only 3 RFamide peptides in an 8 h collection. The NPs identified from these samples overlapped quite well, and yielded overall 52 peptides from 9 NP families as shown in **Table 4-2**. This represents the most comprehensive characterization of the secreted crustacean neuropeptidome.

Two MS/MS interpretation platforms, Mascot and PEAKS, were used. It was proven to be difficult to choose a score cutoff for NPs, as the algorithms for these programs are designed for larger molecules, such as proteins. Therefore, most scores do not accurately represent the quality of a peptide-spectrum match (PSM). The results were

further manually examined for accurate matches of b- and y-ions. The overlap of NP identifications between Mascot and PEAKS was moderate, with 22 out of the 52 listed peptides being identified using both algorithms. The peptides identified from this study represent the largest number of circulating peptides characterized via mass spectrometry using *in vivo* microdialysis sampling from any crustacean.

However, when the collection time was increased to 8 h or longer, the number of identifiable NPs decreased dramatically, with fewer than 10 NPs identified. With the same sample handling process, one possible explanation would be the tolerance of MS instruments to compounds like salt and other interfering compounds, including small organics, present in the hemolymph (**Figure 4-2**). As the collection time increases, the total amount of dialysate collected also increases. Desalting was performed for an aliquot of concentrated dialysate which corresponded to 2 h microdialysis fraction; thus, dialysate with longer collection duration yielded larger volume of desalting elution solution. All desalted dialysate samples for 2 h, 4 h, 6 h and 8 h were then further concentrated and resuspended into the same volume prior to UPLC MS/MS analysis. Increasing the volume of the sample prior to concentration and analysis has the clear advantage of increasing NP concentration, and thus improving detection sensitivity, but it also leads to increased concentrations of other components, including salts. Concentrating the sample from an 8 h or longer collection time may have led to accumulation of various compounds including salts that could interfere with NP detection on the MS instrument. Similarly, the concentration of NPs and other components may reach a good balance by MS detection in the 6 h sample. With the addition of more salts and other components of hemolymph in more concentrated samples, the NP signal is likely to be suppressed or

masked by other interfering signals. Based on our study, 180 µL of microdialysate obtained at 0.5 µL/min seems to be a good volume to obtain for the purpose of identification of secreted NPs in the crustacean.

The low endogenous concentration of NPs, usually present *in vivo* at the nM-pM range [21], accounts for some of the challenges associated with detection of these compounds. In microdialysis, the concentration collected is even lower as it is governed by passive diffusion. NPs have a lower relative recovery rate (20%-40%)[1] in comparison to small molecules due to their larger sizes, which increase the hindrance of passing through the dialysis membrane. Flow rate is closely related to recovery rate, and the temporal resolution of microdialysis collection is directly affected by the sensitivity of detection technique.

Allatostatin (AST)

As demonstrated by a number of studies [16, 17, 22, 23], ASTs are widely distributed across many neuronal tissues in various crustacean species. In *Cancer borealis*, ASTs were identified from the pericardial organ (PO) [24], brain [22], and the stomatogastric ganglion (STG) [25]. A-type ASTs share C-terminal motif –YXFGLa, and B-type ASTs have a WX_6Wa motif on the C-terminus. Three ASTs sequenced from microdialysate in our study had sequence similarity to LMFAPLAWPKGGARWa (*m/z* 1699.93) isolated from crab PO, with all of three sequenced from microdialysates possessing an oxidized methionine. This particular modification may be critical for functional reasons, or may be an artifact of sample processing. Interestingly, only B-type ASTs were observed in microdialysate, whereas no B-type ASTs were found in hemolymph extracts. This may result from quick degradation of B-type ASTs due to the

presence of related peptidases in crude hemolymph. ASTs are known to inhibit the pyloric motor pattern and stomatogastric neurotransmission [26, 27], and the presence of these potentially novel ASTs in the hemolymph further supports the functional roles of these circulating peptides.

The FMRFamide –like peptides

Since the discovery of FMRFamide [28] from the clam, *Macorocallista nimbosa* [28], a large group of FMRFamide-like peptides (FLPs) have been found in both vertebrates and invertebrates. A C-terminal RFamide motif is shared by crustacean FLPs, which can be further categorized into several subfamilies [25]. These subfamilies include myosuppressins, characterized by a C-terminal HVFLRFamide; the neuropeptide Fs, which share sequence homology with the vertebrate neuropeptide Y and have the C-terminal motif RXRFamide; and sulfakinins, known as invertebrate homologs of vertebrate gastrin and cholecystokinin (CCK). In addition to these subfamilies, a large number of FLPs identified from decapod crustaceans possess the C-terminal motif –FLRFamide [29].

In our study, 23 FLPs all sharing a C-terminal -FLRFamide were identified in hemolymph microdialysate. Similar with hemolymph extraction, more members of the FLP family were identified than members of any other family. Moreover, FLPs identified from hemolymph extraction and microdialysis overlap with each other quite well. The occurrence of a wide array of FLPs in circulating hemolymph may indicate that these NPs play diverse functional roles and might be involved in many different neuroendocrine processes.

Mass spectral investigation of neuronal tissues, especially mass spectrometric imaging techniques, has provided important evidence about the wide distribution of –FLRFamides in the nervous systems of crustaceans [22, 30, 31]. Physiological assessment of the identified –FLRFamides has revealed a broad array of possible neuromodulatory roles including cardioexcitation, modulation of muscle contraction and regulation of feeding behavior[32, 33]. Ten of the secreted FLRFamides identified in this work have been previously found in the POs [22].The fact that these NPs are present in both hemolymph and POs may suggest that they were released from the POs into the circulatory system to have hormonal effects on the crustacean heart or more distant organs. Studies have shown that SDRNFLRFamide (*m/z* 1053.5588) and TNRNFLRFamide (*m/z* 1066.5905) (**Figure 4-3**) exhibited excitatory effects on different muscles in the stomach and heart [32, 33]. The co-release of these neuropeptides may suggest that they belong to related pathways to coordinate various muscle contractions involved in behavior or a physiological process. The identification of FLPs in hemolymph microdialysate that were previously identified in the crab's main neurosecretory organ, the PO, provides more specific information on which NPs may be important neuromodulators.

Orcokinins and orcomyotropin

NFDEIDRSGFGFN was the first identified orcokinin and was first found in the crayfish, *Orconectes limosus* [34]. The orcokinins occur widely across different crustacean species. Seven neuropeptides from the orcokinin family and two from the orcomyotropin family were found to be secreted into hemolymph in our study. These findings are in good correlation with previous MS and immunohistochemical studies

conducted on the neuronal tissues of *Cancer borealis [22]*. Hoa-Orcokinin, SSEDMPSSLGFGFN (*m/z* 1474.51) and VYGPRDIANLY (*m/z* 1280.44) were previously sequenced in the brain, the stomatogastric nervous system (STNS), and the sinus gland (SG) of the lobster *Homarus americanus* [35] by investigating orcokinin precursors. However, these two neuropeptides were confirmed to be present in *Cancer borealis* for the first time in this study.

Crustacean hyperglycemic hormone precursor-related peptides

The crustacean hyperglycemic hormone precursor-related peptides (CPRPs) found in hemolymph in this study are apparently truncated, which seems to be common in CPRP sequences [17]. The detection of 5 truncated CPRPs derived from the same full-length CPRP in the circulating fluid suggest that they may be co-released with crustacean hyperglycemic hormone (CHH), likely secreted from another important neurosecretory organ, the SG, in *Cancer borealis* [22]. The CHH is a well-known regulator of hemolymph glucose levels in crustaceans; however, the functions of CPRPs are unknown. The detection of these truncated forms of CPRP, which is encoded by the CHH prohormone, in hemolymph microdialysate provides potential functional clues about these novel forms of CPRPs in energy homeostasis and feeding regulation. Further investigation will be needed to determine the precise roles of these secreted NPs.

The CHH superfamily, well known for its multifunctional roles in the X-organ and SG system [36], however, was not detected in our study. CHHs are relatively large compared to other NPs, ranging from 70 to 80 amino acids in length. When sampling with microdialysis, as molecular weight increases, so does the hindrance for analyte diffusion into the microdialysis probe [37, 38]. As a result, it is very likely that the level

of CHHs collected via microdialysis with the particular probe employed is too low to be efficiently detected with MS.

RYamide

Almost all the known RYamides have been characterized by MS-based strategies. The first RYamide was observed in the releasate of the POs of *Cancer borealis* in 2003 [5], and since then there have been numerous reports documenting the identification of an array of RYamides from various decapod crustacean species [17, 30, 39, 40]. However, much less is known about the bioactivity of RYamides in crustaceans. The presence of RYamides in neuroendocrine organs in conjunction with this evidence of their existence in the circulatory system (representative ones shown in **Figure 4-4**) provides additional insight for investigation of their potential bioactivities.

Tachykinin-related peptides (TRP)

TRPs in crustaceans have sequence similarity to vertebrate tachykinins, and possess the C-terminal motif –FXGXRamide. The secreted neuropeptides identified here appear to be related to the mature APSGFLGMRamide (CabTRP-I) and TPSGFLGMRamide. These two peptides have been well described previously including the oxidized version [22]. As the invertebrate homologs of mammalian substance P, TRPs have been reported to be involved in various physiological processes [41]. Studies in Jonah crabs [42] have shown that TRP containing neurons in the STG form networks that could generate rhythms to modulate chewing and filtering behaviors. Co-transmission of TRP with proctolin and GABA could stimulate a distinct pyloric motor pattern in the STG [42].

4.4 Conclusions

It is important to study NP secretion to increase our understanding of neuromodulation in a well-defined nervous system. In this work, we were able to identify over 50 circulating NPs from several main neuropeptide families, including ASTs, FLPs, orcokinins, TRPs, PDH, CPRPs, RYamides, and CCAP. These results agree with studies determining the neuropeptidomes of various neuronal tissues. The fact that these NPs are present in both neuronal tissues and the circulatory system suggests that they have roles as neuromodulators and hormones. *In vivo* microdialysis provides the advantage of sampling while the animal is alert and allows for the correlation of neurochemical content dynamics with different behaviors or other changes.

4.5 References

1. Schmerberg, C.M. and Li, L., *Function-driven discovery of neuropeptides with mass spectrometry-based tools.* Protein Pept Lett, 2013. **20**(6): p. 681-94.
2. Mykles, D.L., Adams, M.E., Gade, G., Lange, A.B., Marco, H.G., and Orchard, I., *Neuropeptide action in insects and crustaceans.* Physiol Biochem Zool, 2010. **83**(5): p. 836-46.
3. Marder, E. and Bucher, D., *Understanding circuit dynamics using the stomatogastric nervous system of lobsters and crabs.* Annu Rev Physiol, 2007. **69**: p. 291-316.
4. Li, L. and Sweedler, J.V., *Peptides in the brain: mass spectrometry-based measurement approaches and challenges.* Annu Rev Anal Chem (Palo Alto Calif), 2008. **1**: p. 451-83.
5. Li, L., Kelley, W.P., Billimoria, C.P., Christie, A.E., Pulver, S.R., Sweedler, J.V., and Marder, E., *Mass spectrometric investigation of the neuropeptide complement and release in the pericardial organs of the crab, Cancer borealis.* J Neurochem, 2003. **87**(3): p. 642-56.
6. Billimoria, C.P., Li, L., and Marder, E., *Profiling of neuropeptides released at the stomatogastric ganglion of the crab, Cancer borealis with mass spectrometry.* J Neurochem, 2005. **95**(1): p. 191-9.
7. Chen, R., Ma, M., Hui, L., Zhang, J., and Li, L., *Measurement of neuropeptides in crustacean hemolymph via MALDI mass spectrometry.* J Am Soc Mass Spectrom, 2009. **20**(4): p. 708-18.
8. Kennedy, R.T., *Emerging trends in in vivo neurochemical monitoring by microdialysis.* Curr Opin Chem Biol, 2013. **17**(5): p. 860-7.
9. Watson, C.J., Venton, B.J., and Kennedy, R.T., *In vivo measurements of neurotransmitters by microdialysis sampling.* Anal Chem, 2006. **78**(5): p. 1391-9.
10. Chung, Y.T., Ling, Y.C., Yang, C.S., Sun, Y.C., Lee, P.L., Lin, C.Y., Hong, C.C., and Yang, M.H., *In vivo monitoring of multiple trace metals in the brain extracellular fluid of anesthetized rats by microdialysis-membrane desalter-ICPMS.* Anal Chem, 2007. **79**(23): p. 8900-10.
11. Timmerman, W. and Westerink, B.H., *Brain microdialysis of GABA and glutamate: what does it signify?* Synapse, 1997. **27**(3): p. 242-61.
12. Vasicek, T.W., Jackson, M.R., Poseno, T.M., and Stenken, J.A., *In vivo microdialysis sampling of cytokines from rat hippocampus: comparison of cannula implantation procedures.* ACS Chem Neurosci, 2013. **4**(5): p. 737-46.
13. Behrens, H.L., Chen, R., and Li, L., *Combining microdialysis, NanoLC-MS, and MALDI-TOF/TOF to detect neuropeptides secreted in the crab, Cancer borealis.* Anal Chem, 2008. **80**(18): p. 6949-58.

14. Schmerberg, C.M. and Li, L., *Mass spectrometric detection of neuropeptides using affinity-enhanced microdialysis with antibody-coated magnetic nanoparticles.* Anal Chem, 2013. **85**(2): p. 915-22.

15. Bajpai, G., Simmen, R.C., and Stenken, J.A., *In vivo microdialysis sampling of adipokines CCL2, IL-6, and leptin in the mammary fat pad of adult female rats.* Mol Biosyst, 2014. **10**(4): p. 806-12.

16. Ye, H., Hui, L., Kellersberger, K., and Li, L., *Mapping of neuropeptides in the crustacean stomatogastric nervous system by imaging mass spectrometry.* J Am Soc Mass Spectrom, 2013. **24**(1): p. 134-47.

17. Hui, L., D'Andrea, B.T., Jia, C., Liang, Z., Christie, A.E., and Li, L., *Mass spectrometric characterization of the neuropeptidome of the ghost crab Ocypode ceratophthalma (Brachyura, Ocypodidae).* Gen Comp Endocrinol, 2013. **184**: p. 22-34.

18. Jia, C., Lietz, C.B., Ye, H., Hui, L., Yu, Q., Yoo, S., and Li, L., *A multi-scale strategy for discovery of novel endogenous neuropeptides in the crustacean nervous system.* J Proteomics, 2013. **91**: p. 1-12.

19. Sundstrom, I., Arts, J., Westerlund, D., and Andren, P.E., *In vivo investigation of brain and systemic ketobemidone metabolism.* Analyst, 2010. **135**(2): p. 405-13.

20. Sun, L., Stenken, J.A., Brunner, J.E., Michel, K.B., Adelsberger, J.K., Yang, A.Y., Zhao, J.J., and Musson, D.G., *An in vivo microdialysis coupled with liquid chromatography/tandem mass spectrometry study of cortisol metabolism in monkey adipose tissue.* Anal Biochem, 2008. **381**(2): p. 214-23.

21. Li, Q., Zubieta, J.K., and Kennedy, R.T., *Practical aspects of in vivo detection of neuropeptides by microdialysis coupled off-line to capillary LC with multistage MS.* Anal Chem, 2009. **81**(6): p. 2242-50.

22. Ma, M., Wang, J., Chen, R., and Li, L., *Expanding the Crustacean neuropeptidome using a multifaceted mass spectrometric approach.* J Proteome Res, 2009. **8**(5): p. 2426-37.

23. Cape, S.S., Rehm, K.J., Ma, M., Marder, E., and Li, L., *Mass spectral comparison of the neuropeptide complement of the stomatogastric ganglion and brain in the adult and embryonic lobster, Homarus americanus.* J Neurochem, 2008. **105**(3): p. 690-702.

24. Ma, M., Szabo, T.M., Jia, C., Marder, E., and Li, L., *Mass spectrometric characterization and physiological actions of novel crustacean C-type allatostatins.* Peptides, 2009. **30**(9): p. 1660-8.

25. Szabo, T.M., Chen, R., Goeritz, M.L., Maloney, R.T., Tang, L.S., Li, L., and Marder, E., *Distribution and physiological effects of B-type allatostatins (myoinhibitory peptides, MIPs) in the stomatogastric nervous system of the crab Cancer borealis.* J Comp Neurol, 2011. **519**(13): p. 2658-76.

26. Skiebe, P. and Schneider, H., *Allatostatin peptides in the crab stomatogastric nervous system: inhibition of the pyloric motor pattern and distribution of allatostatin-like immunoreactivity.* J Exp Biol, 1994. **194**: p. 195-208.

27. Jorge-Rivera, J. and Marder, Y.E., *Allatostatin decreases stomatogastric neuromuscular transmission in the crab Cancer borealis.* J Exp Biol, 1997. **200**(Pt 23): p. 2937-46.

28. Price, D.A. and Greenberg, M.J., *Structure of a molluscan cardioexcitatory neuropeptide.* Science, 1977. **197**(4304): p. 670-1.

29. Christie, A.E., Stemmler, E.A., and Dickinson, P.S., *Crustacean neuropeptides.* Cell Mol Life Sci, 2010. **67**(24): p. 4135-69.

30. Ma, M., Gard, A.L., Xiang, F., Wang, J., Davoodian, N., Lenz, P.H., Malecha, S.R., Christie, A.E., and Li, L., *Combining in silico transcriptome mining and biological mass spectrometry for neuropeptide discovery in the Pacific white shrimp Litopenaeus vannamei.* Peptides, 2010. **31**(1): p. 27-43.

31. Ma, M., Sturm, R.M., Kutz-Naber, K.K., Fu, Q., and Li, L., *Immunoaffinity-based mass spectrometric characterization of the FMRFamide-related peptide family in the pericardial organ of Cancer borealis.* Biochem Biophys Res Commun, 2009. **390**(2): p. 325-30.

32. Wilkens, J.L., Shinozaki, T., Yazawa, T., and ter Keurs, H.E., *Sites and modes of action of proctolin and the FLP F2 on lobster cardiac muscle.* J Exp Biol, 2005. **208**(Pt 4): p. 737-47.

33. Jorge-Rivera, J.C. and Marder, E., *TNRNFLRFamide and SDRNFLRFamide modulate muscles of the stomatogastric system of the crab Cancer borealis.* J Comp Physiol A, 1996. **179**(6): p. 741-51.

34. Stangier, J., Hilbich, C., Burdzik, S., and Keller, R., *Orcokinin: a novel myotropic peptide from the nervous system of the crayfish, Orconectes limosus.* Peptides, 1992. **13**(5): p. 859-64.

35. Dickinson, P.S., Stemmler, E.A., Barton, E.E., Cashman, C.R., Gardner, N.P., Rus, S., Brennan, H.R., McClintock, T.S., and Christie, A.E., *Molecular, mass spectral, and physiological analyses of orcokinins and orcokinin precursor-related peptides in the lobster Homarus americanus and the crayfish Procambarus clarkii.* Peptides, 2009. **30**(2): p. 297-317.

36. Webster, S.G., Keller, R., and Dircksen, H., *The CHH-superfamily of multifunctional peptide hormones controlling crustacean metabolism, osmoregulation, moulting, and reproduction.* Gen Comp Endocrinol, 2012. **175**(2): p. 217-33.

37. Kendrick, K.M., *Microdialysis measurement of in vivo neuropeptide release.* J Neurosci Methods, 1990. **34**(1-3): p. 35-46.

38. Kendrick, K.M., *Use of microdialysis in neuroendocrinology.* Methods Enzymol, 1989. **168**: p. 182-205.

39. Ma, M., Bors, E.K., Dickinson, E.S., Kwiatkowski, M.A., Sousa, G.L., Henry, R.P., Smith, C.M., Towle, D.W., Christie, A.E., and Li, L., *Characterization of the Carcinus maenas neuropeptidome by mass spectrometry and functional genomics.* Gen Comp Endocrinol, 2009. **161**(3): p. 320-34.

40. Fu, Q., Kutz, K.K., Schmidt, J.J., Hsu, Y.W., Messinger, D.I., Cain, S.D., de la Iglesia, H.O., Christie, A.E., and Li, L., *Hormone complement of the Cancer productus sinus gland and pericardial organ: an anatomical and mass spectrometric investigation.* J Comp Neurol, 2005. **493**(4): p. 607-26.

41. Qing Yu, Z.L., Chuanzi Ouyang, Lingjun Li, *Biologically Active Peptides in Invertebrates: Discovery and Functional Studies.* Colloquium Series on Neuropeptides. Submitted. Morgan&Claypool Life Sciences, 2014: p. 88-92.

42. Nusbaum, M.P., Blitz, D.M., Swensen, A.M., Wood, D., and Marder, E., *The roles of co-transmission in neural network modulation.* Trends Neurosci, 2001. **24**(3): p. 146-54.

4.6 Figures and Tables

Table 4-1. Neuropeptides identified in *Cancer borealis* hemolymph extract

Neuropeptide Family	Neuropeptide Seqeunce	M+H	Mascot Score	PEAKS Score
AST (Allatostatin)	SYWKQCAFNAVSCFa (C-type AST)	1650.7192		30.08
	DPYAFGLGKRPDMYAFGLa (A-type AST)	2017.0000	26.30	31.93
CCAP (Crustacean cardioactive Peptide)	PFCNAFTGCa	956.3753	22.13	45.12
CPRP (CHH precursor-related peptide)	RASQGLGKMEa	1075.5677	22.00	65.68
	TPLGDLSGSVGHPV	1335.6903		21.30
FLP (FMRFamide-like peptide)	I/LNFTHKFa	905.4992		30.64
	NRNFLRFa	965.5428	31.77	59.99
	DRNFLRFa	966.5268		78.28
	SPRNFLRFa	1035.5847		65.59
	SDRNFLRFa	1053.5588	26.88	91.08
	TNRNFLRFa	1066.5905	27.85	92.93
	ENRNFLRFa	1094.5854		17.10
	LNPSNFLRFa	1106.6105		69.08

	EMPSLRLRFa	1147.6405		23.79
Orcokinin	VYGPRDIANLY	1280.6634		24.69
PDH (Pigment dispersing hormone)	NSILGIPR	869.5203		54.52
	NSI/LLGAPRVa	925.5578		77.68
	NSILGAPRV	926.5418		33.41
	NSILGIPKVM(O)N	1201.6609		26.68
RPCH (Red pigment concentrating hormone)	pQLNFSPGWa	930.4468		46.14
Others	AVLLPKKTEKK	1254.8144	33.65	60.92
	EEPEAPa	670.3042		55.35

Legend: “a” at the end of a peptide indicates C-terminal amidation. “(O)” indicates an oxidized methionine. “pQ” or “pE” indicates pyroglutamic acid.

Table 4-2. Neuropeptides identified in *Cancer borealis* hemolymph via *in vivo* microdialysis

Family	Sequence	M+H	Mascot Score	PEAKS Score
AST (Allatostatin)	MFAPLAWPKGGARWa	1586.8413	28.63	
	M(O)FAPLAWPKGGARWa	1602.8362		42.7
	M(O)FAPLAWPKGGARW	1603.8202	23.34	34.25
	LMFAPLAWPKGGARWa	1699.9253	19.27	
	LM(O)FAPLAWPKGGARW	1716.9043	25.93	
CPRP (CHH precursor-related peptide)	LSGSLGHPVE	995.5156	39.56	52.95
	DLSGSLGHPVE	1110.5426		21.55
	TPLGDLSGSLGHPVE	1478.7485		42.90
	RGALEPNTPLGDLSGSLGHPVE	2216.1306	14.97	48.27
FLPs (FMRFamide-like peptide)	pQRNFLRFa	962.5319		21.47
	NRNFLRFa	965.5428	14.99	
	DRNFLRFa	966.5268	23.69	49.13
	NPSDFLRFa	994.5105	24.00	42.21
	GNRNFLRFa	1022.5643	17.07	
	LETNFLRFa	1038.5731		33.81

	SDRNFLRFa	1053.5588	29.60	68.30
	LDRNFLRFa	1079.6109	25.92	46.37
	DGGRNFLRFa	1080.5697		41.13
	QNRNFLRFa	1093.6014		24.87
	ENRNFLRFa	1094.5854	23.05	28.94
	GSDRNFLRFa	1110.5803	28.79	46.41
	TGNRNFLRFa	1123.6119		50.59
	LGDRNFLRFa	1136.6323		35.31
	DGNRNFLRFa	1137.5912		32.06
	GYSKNYLRFa	1146.6054	23.45	25.44
	ALDRNFLRFa	1150.6480	19.26	
	SENRNFLRFa	1181.6174	19.49	33.25
	DENRNFLRFa	1209.6123		48.08
	LTGNRNFLRFa	1236.6960	24.05	
	LDGPLAPFLRFa	1244.7150	9.80	
	YGSDRNFLRFa	1273.6436	26.14	
Orcokinin	NFDEIDRSGFG	1256.5542	35.07	18.22
	DFDEIDRSGFG	1257.5382	25.86	27.4
	NFDEIDRSGFGF	1403.6226	32.22	

	SSEDMPSSLGFGFN	1474.6155	10.17	
	NFDEIDRSGFGFA	1474.6597	20.16	46.77
	DFDEIDRSGFGFA	1475.6437	18.00	21.50
	DFDEIDRSGFGFV	1503.6750		22.31
Orcomyotropin	FPAFTTGFGHS	1168.5422	26.69	34.47
	FDAFTTGFGHS	1186.5164	51.3	50.03
PDH (Pigment dispersing hormone)	NSELINSILGLPKVM(O)NEAa	1957.0423	15.25	37.74
RPCH (Red pigment concentrating hormone)	pQLNFSPGWa	930.4468	21.68	
RYamide	SGFYANRYa	976.4635	33.77	52.83
	SGFYADRYa	977.4476		37.64
	pQGFYSQRYa	1030.4741	22.37	36.60
	LSGFYANRYa	1089.5476	14.24	
	LEWYSQRYa	1143.5582	23.53	
TRP (Tachykinin-related peptide)	TPSGFLGMRa	964.5033	35.2	36.74
	APSGFLGMRa	934.4927	38.64	42.92
	APSGFLGM(O)RGa	1007.5091		34.29

Legend: “a” at the end of a peptide indicates C-terminal amidation. “(O)” indicates an oxidized methionine. “pQ” or “pE” indicates pyroglutamic acid.

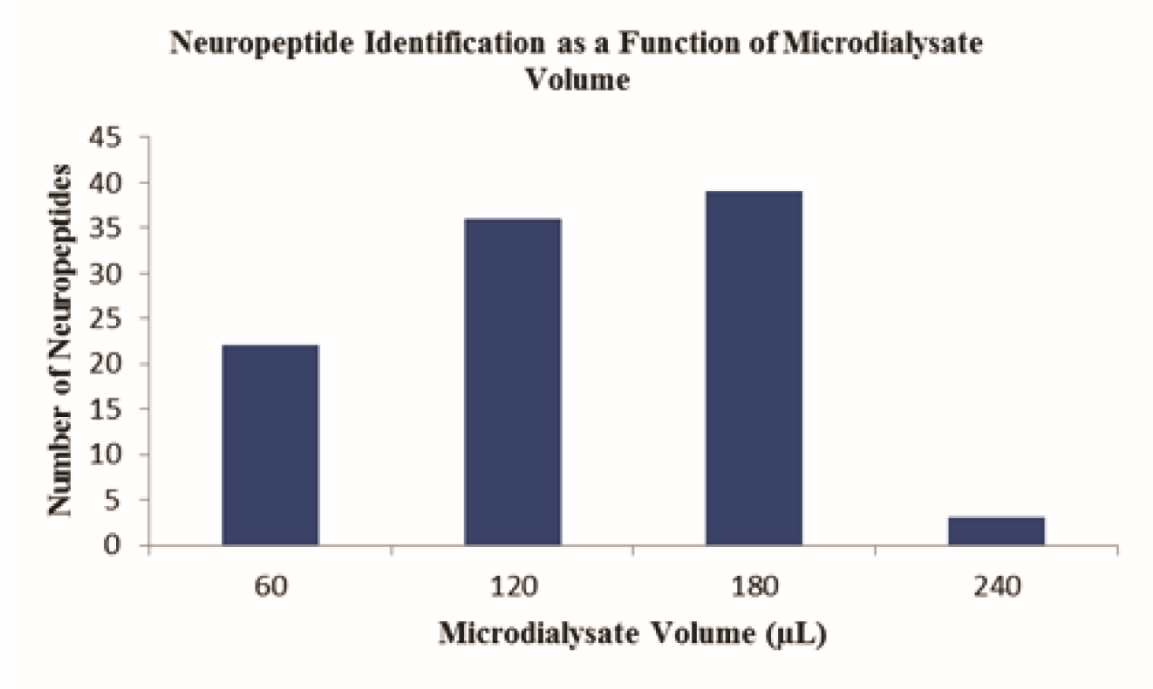

Figure 4-1. Number of neuropeptides identified from 60, 120, 180, and 240 µL dialysates from *Cancer borealis* hemolymph.

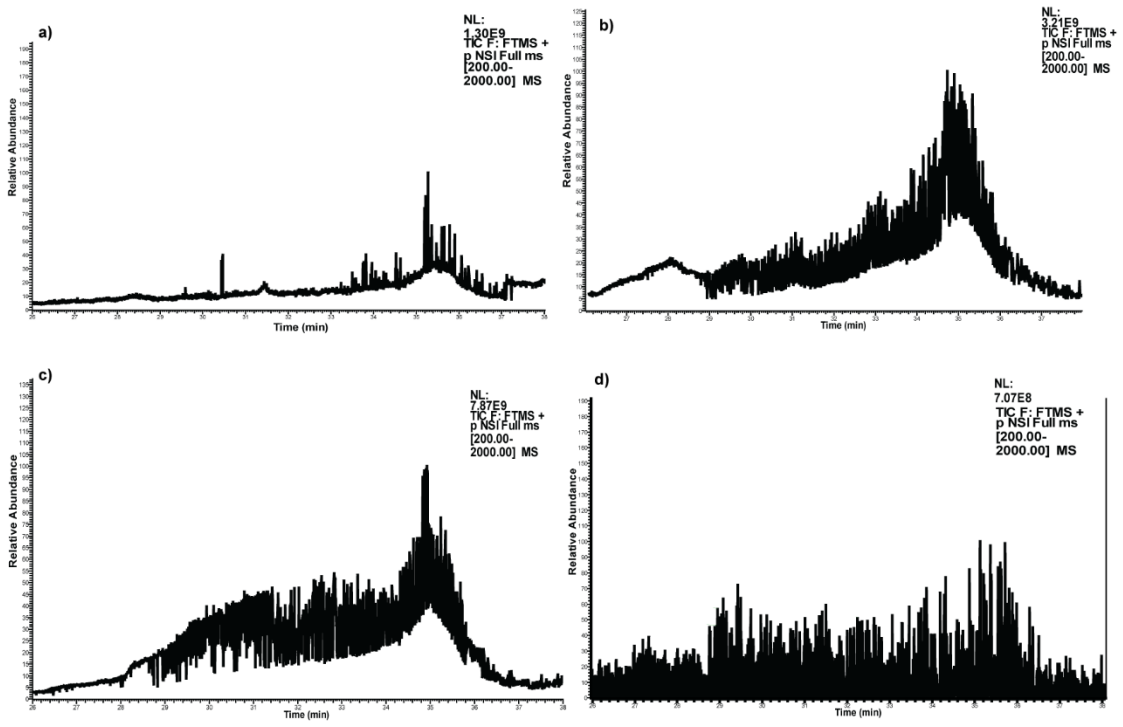

Figure 4-2. Chromatographs of 2 h, 4 h, 6 h and 8 h dialysate upon MS/MS analysis within retention time period between 26 min to 38 min where most peptides were eluted, x-axis is the relative intensity and y-axis is the retention time. **a**) 2 h dialysate; **b**) 4 h dialysate; **c**) 6 h dialysate; **d**) 8 h dialysate. As the collection time gets longer, the overall intensity increases.

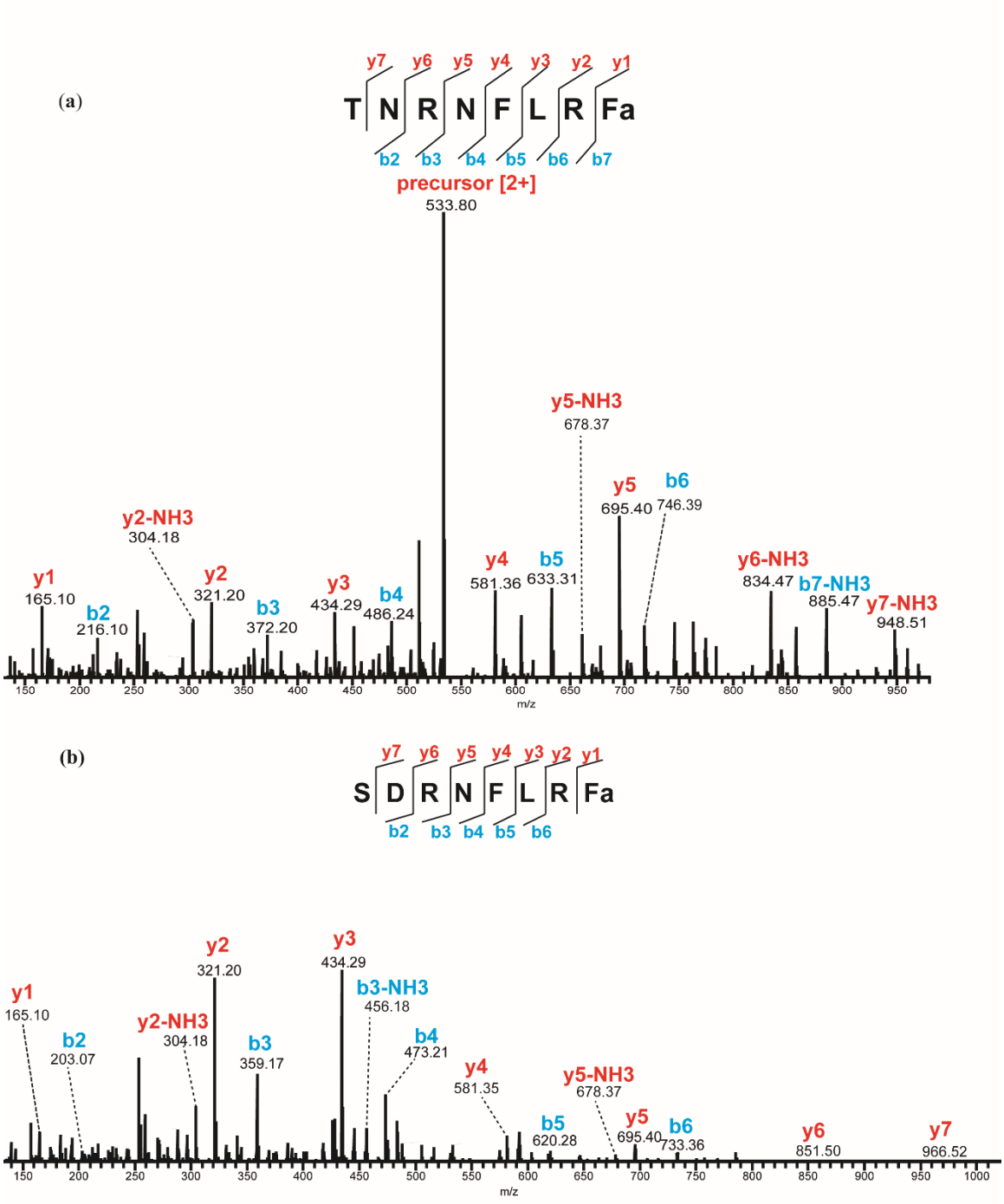

Figure 4-3. MS/MS spectra of (a) TNRNFLRFamide in hemolymph extract and (b) SDRNFLRFamide in microdialysate by HCD fragmentation. The presence of b- and y-ions is indicated by lines above (y-ions) or below (b-ions) the corresponding amino acid residues in the peptide sequence.

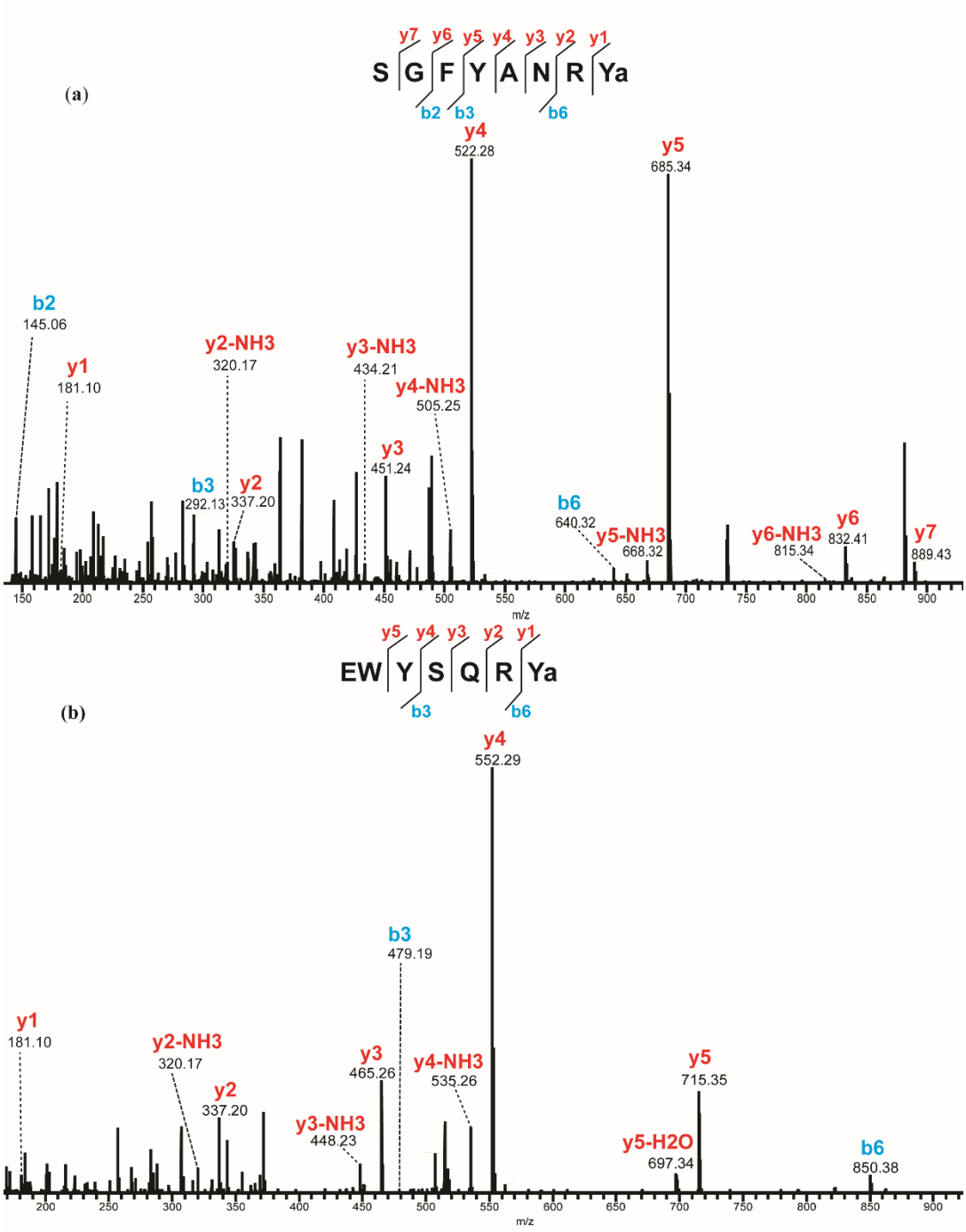

Figure 4-4. MS/MS spectra of identified RYamide from microdialysate under HCD fragmentation. (a) SGFYANRYamide and (b) EWYSQRYamide. The presence of b- and y-ions is indicated by lines above (y-ions) or below (b-ions) the corresponding amino acid residues in the peptide sequence.

Chapter 5

Data-Independent MS/MS Quantification for Temporal Profiling of Neuropeptides in Microdialysate

Adapted from:

1. Claire Schmerberg, **Zhidan Liang**, Lingjun Li. 'Data-Independent MS/MS Quantification of Neuropeptides for Determination of Putative Feeding-Related Neurohormones in Microdialysate'. *ACS Chem Neurosci*. **2015**, *6*, 174-180.
2. **Zhidan Liang**, Claire Schmerberg, Lingjun Li. 'Mass spectrometric measurement of neuropeptide secretion in the crab, *Cancer borealis*, by *in vivo* microdialysis'. *Analyst*. **2015**, *140*, 3803-3813.

Abstract

Advanced analytical strategies work in complement in assessing the functions of neuropeptides (NPs) with other tools by providing their quantitative information in response to physiological alterations. Most mass spectrometry-based quantitation approaches are for protein level analysis, quantitative studies on neuropeptides especially on crustacean neuropeptides, on the other hand, still need to be further explored. In this work, we take advantage of the advancement data-independent acquisition (DIA) MS/MS and the open-source software program Skyline and perform post-acquisition filtering, we developed an untargeted label-free quantitation method for neuropeptide analysis. This method opened up the possibility to identify and quantify hundreds of compounds from a single DIA MS/MS run. By using this method, preliminary quantification of the entire *Cancer borealis* neuropeptidome (137 peptides from 18 families) was possible and was applied to monitor the dynamic changes of NPs during feeding behavior and throughout daily light-dark changes. The results showed great potential for the use of this method in the future to aid in correlation of NP changes with behavior by coupling *in vivo* microdialysis. This work presents an unbiased approach to winnowing candidate neuropeptides related to a behavior of interest in a functionally-relevant manner, thus demonstrated the success of such a DIA MS/MS quantitation method using the open source software Skyline.

5.1 Introduction

Neuropeptides (NPs) are known to regulate a wide range of physiological processes. For a better understanding of the regulatory roles of NPs, various techniques were developed to measure NPs and provide sensitive and specific chemical, dynamic, and spatial information. Mass spectrometry (MS), in particular, provides selectivity through accurate mass measurement and MS/MS sequence confirmation with high sensitivity and high throughput. In addition to characterize the sequence information of NPs, neuropeptidome, another aspect in determining NP functions is to assess their quantitative regulation in response to a physiological change or manipulation.

Tandem mass spectrometry (MS/MS) is a highly useful analytical tool both for identification of many molecules, especially neuropeptides, and their quantification. However, it typically cannot conduct both identification and quantification simultaneously, because different parameters are typically required for each type of experiment. There are several reasons different parameters would be required for identification and quantification, but the unifying feature is that mass filters are typically used for both approaches, albeit in different ways. These mass filters prevent monitoring multiple fragments in multiple-reaction monitoring (MRM)-type experiments, and thus preclude identification, or cause too few data points to be obtained for each peak, and thus preclude quantitation. Notable exceptions exist, such as spectral counting and tandem mass tags, but those methods have disadvantages for this study. For MS/MS experiments with high scan rates, the number of times an ion is selected for MS/MS analysis can be used as a measure of its abundance, called its spectral count [1]. This method is most robust for quantification at the protein level based on multiple peptides

identified, and is not applicable for endogenous neuropeptide (NP) study. A NP-compatible approach incorporates isobaric labeling tags at the MS^1 level which could produce specific reporter ions upon MS^2 fragmentation to offer quantitative information. One example of this approach is DiLeu labeling tags developed by the Li laboratory [2]. These tags use isotopes to generate characteristic fragment ions of given masses, and the relative intensities of these ions can be used for quantification. However, high intensity precursor ions must be generated, and this is often not possible with NPs study due to their extremely low endogenous concentrations. Finally, several transitions can be monitored with full fragment scans in some high-speed instruments, allowing for simultaneous identification and quantification of those predefined transitions with Skyline SRM software [3]. This method will be expanded upon in the current study using data-independent (DIA) MS analysis, with truly unbiased collection of MS^E data. *A priori* knowledge about the analytes of interest will not be used until post-acquisition data processing, in order to maximize the potential future utility of acquired data. As novel NPs are discovered with the advent of new analytical technologies, this approach is preferred for analysis in this emerging area of chemical neuroscience.

Data-independent acquisition (DIA) MS analysis employs no mass filter but produces both precursor and fragment ions. This increases the complexity of data interpretation, but it is possible to quantitate the product ions of specific precursors in a pseudo-multiple reaction monitoring (pMRM), or all-reactions monitoring (ARM), manner, as well as to determine identity in a single run. By eliminating mass filtering at the MS^1 level (or using large isolation windows), multiple precursors are fragmented simultaneously and their resulting fragments enter the second mass analyzer

simultaneously. This results in a highly complex MS/MS spectrum as the fragments cannot initially be assigned to precursors for sequence identification. However, precursors and fragments can be aligned by software using their retention times and mass to charge ratios (*m/z*). By eliminating filtering at the MS^2 level, the intensities of all of these fragments over time can be determined for quantification. By matching precursors and fragments, then quantifying the fragments of a given precursor, all fragmentation reactions are monitored (all reactions monitoring, ARM). Every peptide with several transitions observed can thus be quantified. Several instrument vendors have incorporated this technique into new instruments with slight variations, and the one described and used here is Waters MS^E.

This powerful acquisition technique has been employed for simultaneous identification and quantification in a variety of samples at the protein level [4-8], with each protein having multiple peptides detected. However, quantification has not previously been done with analytes at the peptide level. In addition, the SRM software Skyline has not previously been demonstrated in quantitation of DIA MS/MS data. In this work, the MS^E strategy for DIA MS/MS is employed to collect data for quantitation and identification of (neuro) peptides, using a protein digest as internal standard and Skyline software for data analysis. This technique is found to be linear for quantification of several model NP standards. Proof-of-principle experiments were conducted by using this method to analyze NP concentration baseline dynamics throughout daily light-dark cycle and during feeding in microdialysates obtained from Jonah crab *Cancer borealis*. The entire *C. borealis* < 2 kDa neuropeptidome (137 NPs from 18 families) was quantified in each experiment. It would be impractical or impossible to obtain information about this

many NPs using antibody-based techniques, and some of the slight changes in NP sequence that were able to be differentiated by MS-based techniques would not be detectable by non-molecular means. This method represents an early-stage function-driven discovery method to winnow bioactive peptides related to an experimental perturbation (feeding) or potential biomarkers for a physiological event (circadian rhythm) from a large list (here, the < 2 kDa neuropeptidome of *C. borealis*). This novel approach shows great potential in the investigation of dynamic NP changes in different physiological processes.

5.2 Materials and Methods

5.2.1 *Linearity Experiment Sample Preparation*

A set of standards to test the linearity of the method was prepared using myoglobin digest and peptide standards. Equine skeletal myoglobin (ERA, Colden, CO) was digested with trypsin (from bovine pancreas, Sigma-Aldrich, St. Louis, MO) following a published procedure [9]. Myoglobin was dissolved in 100 mM NH_4HCO_3 at 0.5 mg/mL. Trypsin was dissolved in the same solution at 1 µg/mL and added to the myoglobin solution at an enzyme: substrate ratio of 1:10. This was then diluted 1:1 with methanol and placed in a water bath at 37°C for 45 min. The reaction was stopped by adding ice-cold acetic acid to a final concentration of 5%. The sample was then spun at 15,100 x g for 5 min. The neuropeptide standards, crustacean cardioactive peptide (CCAP), *Homarus americanus* FMRFamide-like peptide I (FLP I), *H. americanus* FMRFamide-like peptide II (FLP II), alpha-melanocyte stimulating hormone (α-MSH), bradykinin, and substance P, were obtained from American Peptide Company (Sunnyvale, CA). These were spiked into a solution of 1x diluted crab saline (220 mM

NaCl; 5.5 mM KCl; 6.5 mM $CaCl_2$; 13 mM $MgCl_2$; 5 mM HEPES, pH 7.4) with 0.05% formic acid and 1.88 µM myoglobin digest at the following concentrations: 10, 5, 3.75, 2.5, 1.25, 0.63, and 0.25 nM. Samples were mixed in a 96-well plate and kept at 4 °C until analysis.

5.2.2 *In Vivo Microdialysis*

PAES (20 kDa MWCO, 4 mm membrane length) probes (CMA Microdialysis, Harvard Apparatus, Holliston, MA) were implanted in three separate *Cancer borealis* as described in previous work [10, 11]. Briefly, crabs were anesthetized with ice, the shell in the pericardial region was abraded, a hole was drilled in the shell, and the MD probe was inserted. Several layers of adhesive were employed to obtain a watertight seal. Following implantation, crabs with probes were kept separate from other animals with the aid of plexiglass dividers that the water could flow through and around. The outlet of the probe was connected to an automated refrigerated fraction collector (BASi Automated Refrigerated Fraction Collector, Bioanalytical Systems Inc, West Lafayette, IN). Animals were allowed to recover a minimum of 24 hrs prior to collecting samples that were used for analysis.

In feeding experiments, crabs typically would not eat until a minimum of 48 hrs had elapsed after surgery, so feeding experiments were conducted beginning the 2^{nd} day after surgery. Crab saline was infused through the system at a flow rate of 0.5 µL/min, and the probe was equilibrated at this rate for a minimum of 30 min before any samples were collected. In many cases, the experiment was started after the perfusate had been running at that rate for several hours and equilibration was already complete. If the rate had to be changed or the syringe refilled, 30 min of equilibration time immediately

preceded collection of samples for the feeding experiment. The dead volume of the probe system from the tip of the probe to the collection tube was calculated based on information from the manufacturers of the probe, tubing, and fraction collector, and this was taken into account for timing collections correctly with feeding. Crabs were fed white-fleshed raw fish (cod, tilapia, etc.), thawed and cut into small pieces (1/2''-1'') immediately prior to use. Most crabs took and started eating the food immediately. If it took more than 2-3 min for the crab to start eating, the experiment was abandoned for that day. For crabs that did eat, excess food was always present so that the animal could feed until satiety was reached. Crabs typically stopped eating (as judged by reduced movement of mouth parts) after 45-60 min. At t = 180 min, any remaining food was removed from the tank, even if the crab had to be moved to retrieve it. A second feeding experiment was conducted with most of the crabs a minimum of 24 hrs after the start of the first one. Crabs were not otherwise disturbed at any point during this process, and the room was maintained on a 12 hr on/12 hr off (red lights on) light cycle, with feeding experiments taking place during the dark period.

For feeding experiment, one baseline sample was obtained from t = -30 min to t = 0 min. The first baseline sample was collected approximately 2.5 hours after the lights turned off. Collection tubes were changed every 30 min during the experiment by the refrigerated fraction collector until 7 samples were obtained, for a final time of 180 min post-feeding. For circadian NP analysis, dialysate samples were collected every 2 hr continuously throughout the light-dark cycle. Samples were graphed according to the time midway through their collection time. The resulting samples were immediately acidified by adding 5% pure formic acid (FA) to them, as this has been shown to reduce

NP degradation [12]. The collected microdialysates were then kept at -20°C until they could be analyzed.

Samples were placed in LC vials and an internal standard (1 µL of 56.4 µM myoglobin digest solution) was added. Immediately prior to analysis on UPLC-MS/MS, 1 µL of a 0.91 M NH_4HCO_3 solution was added to increase the sample's pH so as not to damage the UPLC column.

5.2.3 *Instrumental Analysis*

Ultrahigh performance liquid chromatography (UPLC)-MS^E analysis was conducted on a Waters nanoAcquity UPLC coupled to a Waters Synapt G2 mass spectrometer (Waters, Milford, MA). Samples (2 µL) were trapped on a preconcentration column and desalted on-line. This column was then put in line with a C18 reversed-phase column (BEH130 C18, 1.7 µm, 75 µm x 100 mm, Waters, Milford, MA). The outlet of this column was connected to a fused silica capillary with a pulled tip of internal diameter ~5 µm (Sutter Instrument Company, Novato, CA). This was used as the ESI inlet. A 75 min reversed-phase run with solvent A as 0.1% FA in water and B as 0.1% FA in ACN was used. The instrument was operated in data-independent MS/MS mode with the high energy scan having a voltage ramp from 25 to 65 V and Glu-fibrinopeptide was infused for lockspray calibration.

5.3 Data Analysis

5.3.1 *Linearity Samples Analysis*

The sequences of the neuropeptide standards (CCAP: PFC(-H)NAFTGC(-H)amide, FLP I: SDRNFLRFamide, FLP II: TNRNFLRFamide, α-MSH: acetyl-

SYSMEHFRWGKPVamide, bradykinin: RPPGFSPFR, and substance P: RPKPQQFGGLMamide, with (-H) indicating a C in a disulfide bond that loses a hydrogen) and 9 myoglobin internal standard (ITSD) tryptic peptides (FDKFK, FKHLK, TEAEMK, TEAEM(Ox)K, TEAEMKASEDLK, ALEFLR, ALEFRNDIAAK, NDIAAK, and ELGFQG, with M(O) indicating an oxidized methionine) were input into the Skyline SRM software (version 2.6.0.6851). Modifications were added to peptides manually. A non-specific enzyme type was used, with cleavage at every amino acid, and 9 missed cleavages permitted, the most allowed, as a "no enzyme" setting is not present in Skyline. Most NPs are shorter than 9 amino acids, so this should be acceptable. In addition, Skyline will quantify peptides that do not meet its filter criteria if they are input manually and the exception to the filters is noted by the user. The iRT function with retention time predictor was used, calibrated off of results from Mascot (Matrix Science, London, UK) identifications of equine myoglobin tryptic peptides in a previous LC run of the myoglobin digest alone under the same UPLC conditions. The 2^+ and 3^+ precursors were monitored to the 4 most abundant 1^+ and 2^+ b and y ions. MS/MS filtering parameters were set to DIA with MSe isolation, and 10,000 resolving power. Peak integration was checked manually for a good match to the most abundant transitions and agreement with the predicted retention times. Between runs, which were all conducted sequentially on the same day, variation of less than 0.2 min was observed in retention time. Peak areas were exported to Microsoft Excel. All transitions for each peptide were summed, and the 9 myoglobin peptides were summed together. Peptide peak areas were normalized to the total myoglobin internal standard peak area. In SigmaPlot 10 (Systat Software, Inc. San

Jose, CA), data was plotted and linear regressions to the equation $f = y_0+ax$ using a least-squares method were conducted.

5.3.2 *Microdialysis Sample Data Analysis*

A list of all NPs previously identified in *C. borealis* and the 9 myoglobin tryptic peptides mentioned above was selected for data extraction and integration (database available upon request). The iRT function with retention time predictor was used, calibrated off of results from Mascot (Matrix Science) identifications of equine myoglobin tryptic peptides in a previous LC run of the myoglobin digest alone under the same UPLC conditions. Other parameters were identical to those used in the linearity experiment. Peak picking and integration was conducted with the aid of the mProphet integration refinement feature, using second-best peaks to train the model. Peak areas were exported to Microsoft Excel. All transitions for each peptide were summed, and the 9 myoglobin peptides were summed together. Peptide peak areas were divided by the total myoglobin internal standard peak area. This data was explored using RMANOVA in SPSS 21 (IBM, Armonk, NY) software (data not shown). This software also used to calculate the means and standard errors in the percent changes from baseline that are depicted in **Figure 5-2**, generated with SigmaPlot 10 (Systat Software, Inc.).

5.4 Results and Discussion

5.4.1 *Linearity for Quantification of Neuropeptide Standards*

Plotting the peak areas for the NP standards, normalized to the sum of the areas for the myoglobin tryptic peptides, versus the concentrations and performing linear regressions yielded fits with a high degree of linearity over the range of 0.25 to 10 nM

(**Figure 5-1**, **Table 5-1**). Values for the goodness of fit for these regressions range from 0.9144 to 0.9870. These results indicate that accurate measurement of individual peptide is possible by making enough measurements of its intensity through analyzing several transitions for each of two charge states per peptide. The inclusion of an internal standard (ITSD) with multiple peptides that can be monitored allows for even more measurements of its intensity to be made, and thus this value is more reproducible. For instance, if interference, signal loss, or artificial enhancement occurs with one of the multiple peptides in some samples, the impact of one irregular measurement is reduced by having other unchanged measurements also possible with the same ITSD. It could also be possible to use several peptide standards spiked in to the sample as an ITSD in a similar manner. Slopes of linear fits were positive and non-zero intercepts were obtained. The method is very sensitive, generated over the range 0.25-10 nM (0.5-20 fmol on column), enabling analysis of NPs in microdialysates obtained from crab hemolymph.

5.4.2 *Microdialysis Feeding Experiment*

The method was successful at generating reproducible measurements of NPs in multiple samples from 8 experimental replicates from a total of 4 crabs. A list of the 137 known *C. borealis* neuropeptides of mass < 2 kDa was input into the Skyline software package using DIA quantitation mode. Transitions for the 2+ and 3+ precursors to the parent, b_{n-3}, b_{n-2}, b_{n-1}, y_{n-3}, y_{n-2}, and y_{n-1} ions were considered. An automatic peak scoring function of Skyline that employs mProphet was used to pick peaks for integration [13]. Peak areas for each peptide were summed and divided by the total myoglobin area in each sample. Although absolute concentrations cannot be determined without generating calibration equations like those above for every NP, which would require the use of

authentic standards of known concentration for all 137 appropriate compounds, the general concentration ranges for these NPs are estimated to be 1 - 100 nM. Fifty-five of the NPs were quantified with less than 10 ppm error across all samples. Although this method was successful at providing information on the NP content of the microdialysates, variability was high between animals. This could be due to high background from the protein digest ITSD, or slight differences in the feeding experiment itself. For instance, crabs did not reliably eat during the same time periods of the test. A crab would be given food after having none for at least 24 hours, and it had to start eating (as evidenced by mouth part movement) for the experiment to be initiated. However, the duration of eating, number of eating bouts, and timing of those bouts were not consistent across animals. Typically, the initial feeding bout would last 30 min, followed by a 15 min period without eating. The crab then usually started another feeding bout, of a slightly shorter duration. Rarely, the crab would eat a third time. This heterogenaeity of behavioral patterns is likely to also result in heterogeneous neurochemical changes. A better understanding of crab feeding behavioral patterns, better time resolution for microdialysis, and/or concurrent video recording of feeding followed by scoring of feeding vs. quiescent behavior--to be later correlated with MD sample contents--would improve the quality of information that can be obtained from such a study. The NP content (represented as % change from baseline) versus time graphs for several selected peptides are shown in Fig. 2. It should be noted, that although several of these NPs share sequence motifs and thus some y-ions, their profiles appear different. It would be highly unlikely that techniques that do not employ MS-based detection could differentiate between these compounds. Although statistical tests did not reveal clear associations

between NP content and feeding (data not shown), this might be observed following further refinement of the behavioral protocol (perhaps by adding video analysis) and analysis methods (especially increasing NP detection sensitivity and decreasing background signal by using a less complex peptide mixture as ITSD). The natural fluctuation of NPs in the circulatory system at different time points of the day may also affect the results.

5.4.3 Circadian Rhythm Related Neuropeptide Changes in Microdialysate

A second application of this quantitation method was a proof-of-principle experiment to examine the baseline changes of NPs throughout the day. As the animals were subject to environmental settings of daily 12 h: 12 h light and dark cycle, such study might lead to the discovery of possible neuromodulatory candidates for circadian rhythm-associated NP changes that may occur with daily light period changes in Jonah crabs. Circadian rhythm refers to the endogenous rhythmic processes within about 24 hours that has been widely observed in many different living organisms [14], which prepares organisms to adapt to environmental changes. It is linked to the daily light-dark cycle and controlled by circadian clock. Studies in crustaceans have identified neuronal and cellular systems that are involved in circadian rhythmic regulation [15], but no master clock has been identified.

The dynamic changes of NPs in microdialysate using our DIA MS/MS quantitation method, throughout 12 h: 12 h light/dark cycle. Samples were collected continuously with a temporal resolution of 2 hr. Due to the preliminary nature of these studies, statistical analysis was not possible with the current number of animals available. But nonetheless, as summarized in **Figure 5-3**, the preliminary result showed the

capability of this non-targeted quantitative method of measuring the changes of a wide variety of NPs across multiple samples simultaneously. By tracking the retention time and multiple transitions, NPs from different NP families including allatastatin (A-, B-, and C-type AST), orcokinin, RFamide, RYamide, pigment dispersing hormone (PDH), crustacean cardioactive peptide (CCAP) and crustacean hyperglycemic hormone precursor-related peptide (CPRP) were identified and quantified.

From **Figure 5-3**, no clear changing patterns could be observed as NPs were grouped into families. **Figure 5-4** showed a few representative NPs with dynamic changes in response to light/dark cycle alternation. As the light went on, dramatic changes were observed for secreted PDH, CCAP and red pigment concentrating hormone (RPCH) (**Figure 5-4**). CCAP and PDH both exhibited decreases in their relative hemolymph levels. While CCAP exhibited a slower decrease (**Figure 5-4a**), occurring over a period of ~6 hrs, PDH decreased more rapidly (**Figure 5-4b**). RPCH, however, was observed to exhibit a unique oscillating pattern (**Figure 5-4c**) during the light period. Throughout the daily light/dark transition, not only do the eyes need to be adapted to light changes--which could correlate with the changes of PDH and RPCH, but the whole body also needs to have a coordinated response. In other words, the circadian rhythm must integrate information about light levels, obtained primarily from the eyes, with whole body changes. For instance, the crab tends to be less active when the light is on, and thus may need a lower level of cardiac activity. The observed decrease in hemolymph CCAP thus may prepare the body to adapt to such environmental changes by decreasing cardiac excitability. The observed changes in these secreted peptides provide strong evidence that locally released peptides travel to different organs via the hemolymph to have hormonal

effects. The results are preliminary but these findings lay the groundwork for further investigation of the potential circadian effects of these NPs at the organism level.

5.5 Conclusions

In this work, a method for quantitation of DIA MS/MS data in a pseudo-MRM manner was developed. It used an open-source, vendor-neutral software Skyline for accurate identification of precursors and fragments and integration of the resulting peaks. This quantitation method shows linearity for mixtures of peptide standards over the range 0.25-10 nM using a myoglobin digest as an internal standard. Proof-of-principle experiments were also conducted to determine baseline NP concentration fluctuation and NPs associated with feeding *via* an unbiased approach, looking at all *Cancer borealis* NPs of less than 2 kDa. Samples were collected using microdialysis from *C. borealis* during daily light-dark cycle and during feeding. For each time points in all experiments, all 137 known *C. borealis* NPs and the ITSD peptides were quantified. Potential candidates responsible for the adaptation to light and dark changes were found. Moreover, fifty-five NPs were quantified with an average mass error of less than 10 ppm in feeding experiment. This dataset can further be reassessed for quantity changes of other NPs of interest (for instance, if new NPs are discovered), due to the nature of MS^E acquisition and Skyline quantification methods. Time-resolved profiles of concentration changes in the 3 hours after feeding can also be generated from this data. Additional biological replicates may further illuminate interesting roles for other NPs in feeding behavior. Further refinement of the experiment to better define feeding behavior may permit a better correlation between NP concentration changes and important aspects of feeding behavior. We also suggest additional technical improvements, such as the use of

a mixture of reference peptides instead of a messy protein digest as the ITSD and the addition of a DDA-experimental step (run on pooled MD samples following their analysis by DIA) to improve identification confidence. However, in this paper we demonstrate that it is possible to take samples from a species for which a database of the proteins or peptides of interest exists and quantify compounds at the peptide level using this method. This method will be of great use in targeted and untargeted functional analysis studies of NPs.

5.6 Reference

1. Bantscheff, M., Lemeer, S., Savitski, M.M., and Kuster, B., *Quantitative mass spectrometry in proteomics: critical review update from 2007 to the present.* Analytical and Bioanalytical Chemistry, 2012. **404**(4): p. 939-965.
2. Xiang, F., Ye, H., Chen, R., Fu, Q., and Li, L., *N,N-dimethyl leucines as novel isobaric tandem mass tags for quantitative proteomics and peptidomics.* Anal Chem, 2010. **82**(7): p. 2817-25.
3. Sherrod, S.D., Myers, M.V., Li, M., Myers, J.S., Carpenter, K.L., MacLean, B., MacCoss, M.J., Liebler, D.C., and Ham, A.-J.L., *Label-Free Quantitation of Protein Modifications by Pseudo Selected Reaction Monitoring with Internal Reference Peptides.* Journal of Proteome Research, 2012. **11**(6): p. 3467-3479.
4. Geromanos, S.J., Vissers, J.P.C., Silva, J.C., Dorschel, C.A., Li, G.-Z., Gorenstein, M.V., Bateman, R.H., and Langridge, J.I., *The detection, correlation, and comparison of peptide precursor and product ions from data independent LC-MS with data dependant LC-MS/MS.* Proteomics, 2009. **9**(6): p. 1683-1695.
5. Gillet, L.C., Navarro, P., Tate, S., Rost, H., Selevsek, N., Reiter, L., Bonner, R., and Aebersold, R., *Targeted Data Extraction of the MS/MS Spectra Generated by Data-independent Acquisition: A New Concept for Consistent and Accurate Proteome Analysis.* Molecular & Cellular Proteomics, 2012. **11**(6).
6. Levin, Y., Hradetzky, E., and Bahn, S., *Quantification of proteins using data-independent analysis (MSE) in simple andcomplex samples: a systematic evaluation.* Proteomics, 2011. **11**(16): p. 3273-87.
7. Martins-de-Souza, D., Guest, P.C., Guest, F.L., Bauder, C., Rahmoune, H., Pietsch, S., Roeber, S., Kretzschmar, H., Mann, D., Baborie, A., and Bahn, S., *Characterization of the human primary visual cortex and cerebellum proteomes using shotgun mass spectrometry-data-independent analyses.* Proteomics, 2012. **12**(3): p. 500-504.
8. Mbeunkui, F. and Goshe, M.B., *Investigation of solubilization and digestion methods for microsomal membrane proteome analysis using data-independent LC-MSE.* Proteomics, 2011. **11**(5): p. 898-911.
9. Li, F., Schmerberg, C.M., and Ji, Q.C., *Accelerated tryptic digestion of proteins in plasma for absolute quantitation using a protein internal standard by liquid chromatography/tandem mass spectrometry.* Rapid Commun Mass Spectrom, 2009. **23**(5): p. 729-32.
10. Schmerberg, C.M. and Li, L., *Mass spectrometric detection of neuropeptides using affinity-enhanced microdialysis with antibody-coated magnetic nanoparticles.* Anal Chem, 2013. **85**(2): p. 915-22.
11. Behrens, H.L., Chen, R., and Li, L., *Combining microdialysis, NanoLC-MS, and MALDI-TOF/TOF to detect neuropeptides secreted in the crab, Cancer borealis.* Anal Chem, 2008. **80**(18): p. 6949-58.

12. Li, Q., Zubieta, J.K., and Kennedy, R.T., *Practical aspects of in vivo detection of neuropeptides by microdialysis coupled off-line to capillary LC with multistage MS.* Anal Chem, 2009. **81**(6): p. 2242-50.

13. Reiter, L., Rinner, O., Picotti, P., Huttenhain, R., Beck, M., Brusniak, M.Y., Hengartner, M.O., and Aebersold, R., *mProphet: automated data processing and statistical validation for large-scale SRM experiments.* Nat Methods, 2011. **8**(5): p. 430-5.

14. Edgar, R.S., Green, E.W., Zhao, Y., van Ooijen, G., Olmedo, M., Qin, X., Xu, Y., Pan, M., Valekunja, U.K., Feeney, K.A., Maywood, E.S., Hastings, M.H., Baliga, N.S., Merrow, M., Millar, A.J., Johnson, C.H., Kyriacou, C.P., O'Neill, J.S., and Reddy, A.B., *Peroxiredoxins are conserved markers of circadian rhythms.* Nature, 2012. **485**(7399): p. 459-64.

15. Strauss, J. and Dircksen, H., *Circadian clocks in crustaceans: identified neuronal and cellular systems.* Front Biosci (Landmark Ed), 2010. **15**: p. 1040-74.

5.7 Figures and Tables

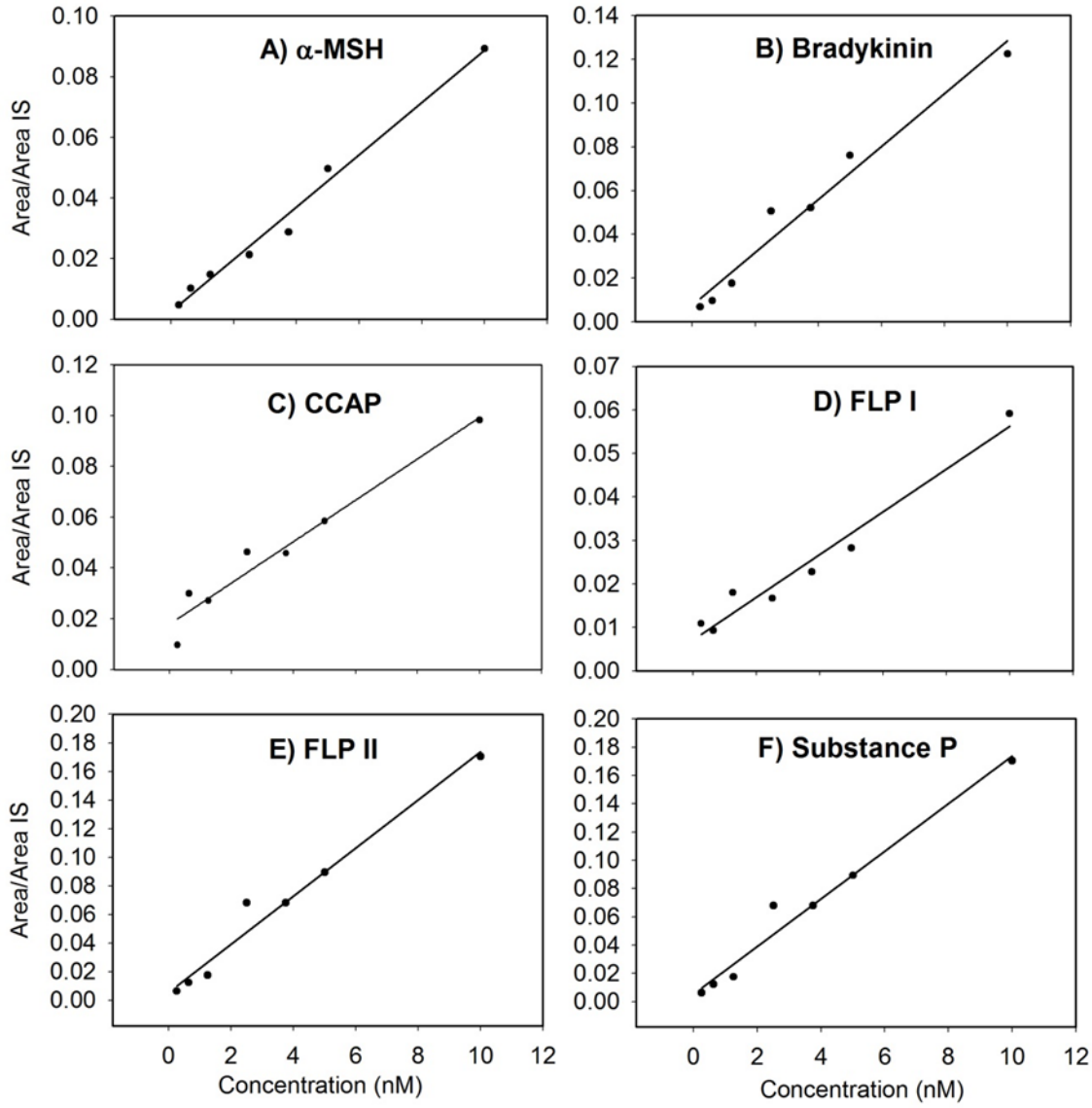

Figure 5-1. Linear calibration curves for A) α-melanocyte stimulating hormone (α-MSH), B) bradykinin, C) crustacean cardioactive peptide (CCAP), D) *Homarus americanus* FMRFamide-like peptide I (FLP I), E) *H. americanus* FMRFamide-like peptide II (FLP II), and F) substance P over the concentration range 0.25-10 nM (0.5-20 fmol on column).

Table 5-1. Parameters for linear fits of calibration curves for α-melanocyte stimulating hormone (α-MSH), bradykinin (BK), crustacean cardioactive peptide (CCAP), *Homarus americanus* FMRFamide-like peptide I (FLP I), *H. americanus* FMRFamide-like peptide II (FLP II) and substance P (SP).

Peptide	Slope		Intercept		R^2
	Value	SE	Value	SE	
α-MSH	0.0086	0.0004	0.0024	0.0200	0.9870
BK	0.0121	0.0010	0.0076	0.0045	0.9679
CCAP	0.0081	0.0008	0.0178	0.0037	0.9533
FLP I	0.0049	0.0004	0.0072	0.0020	0.9626
FLP II	0.0168	0.0012	0.0056	0.0057	0.9733

Figure 5-2. Changes in the concentrations of 6 selected NPs during the feeding experiment. Samples were collected via microdialysis on a total of 4 crabs during 8 separate experiments. Values shown are means ± SEMs.

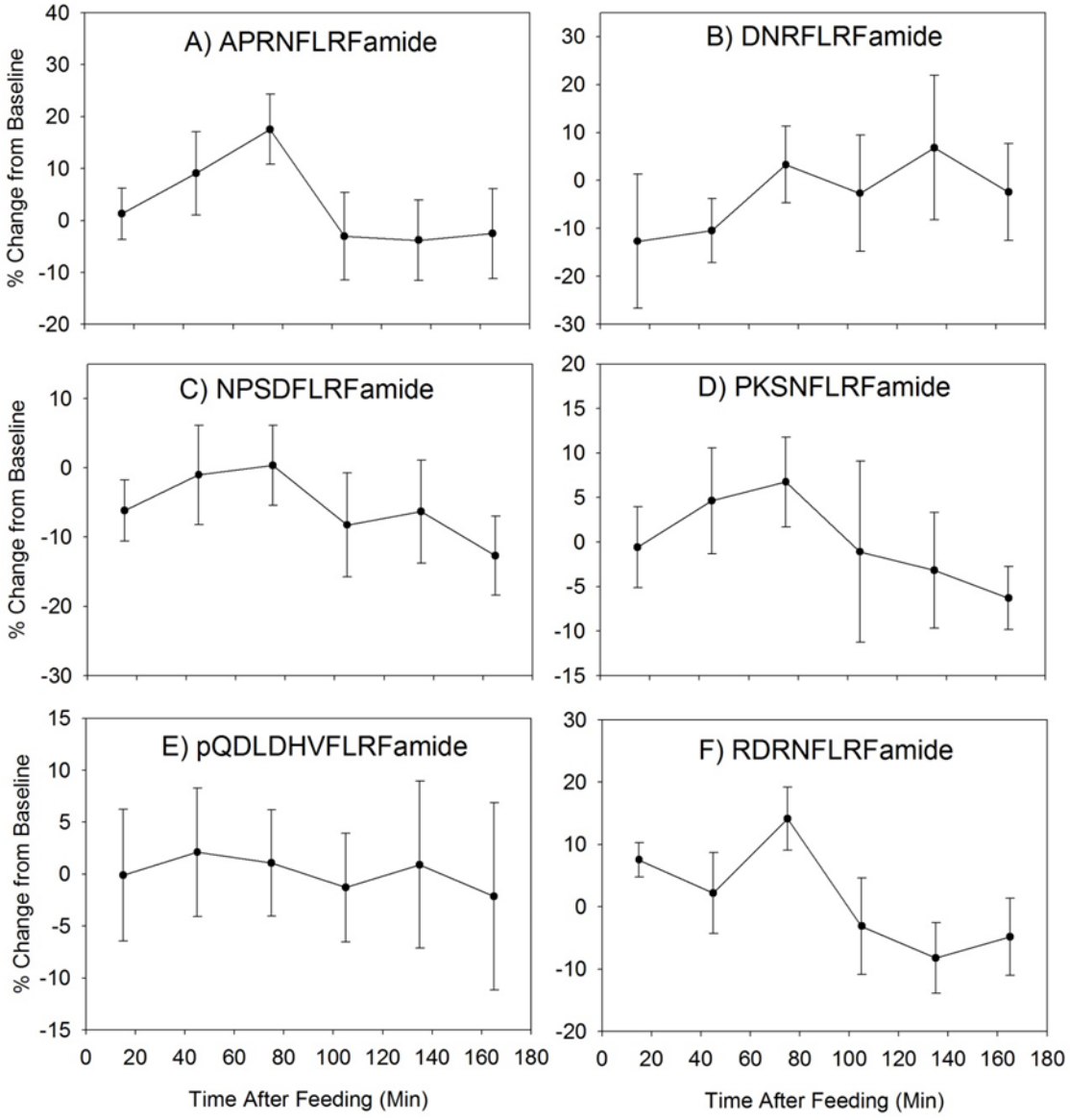

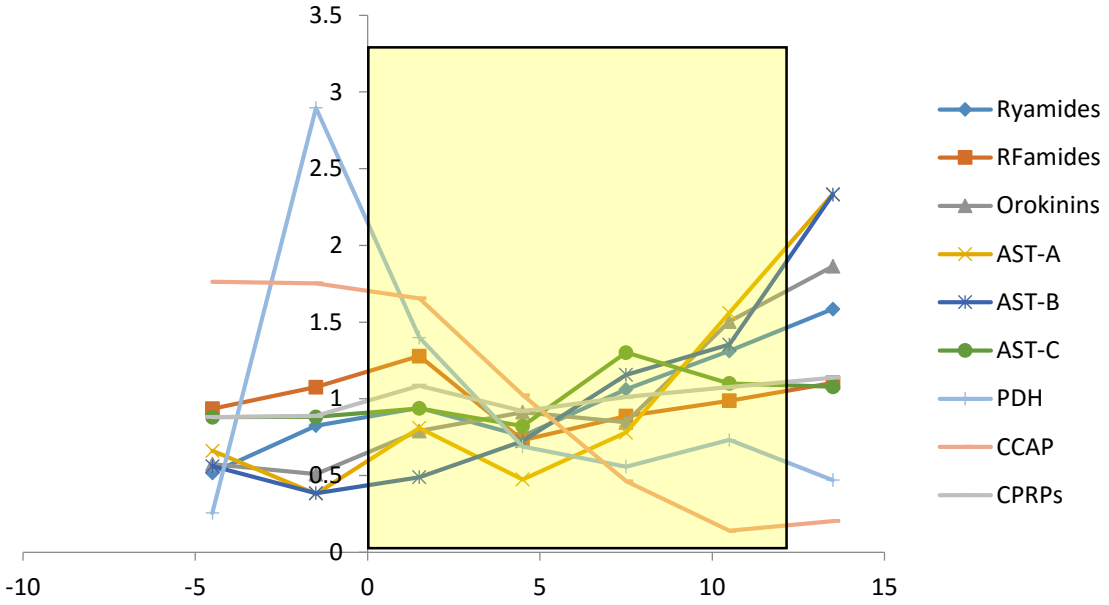

Figure 5-3. Summary of dynamic changes of neuropeptides from different families throughout daily light-dark cycle measured by *in vivo* microdialysis coupled with MS. Light went on at time zero and last for 12 h as indicated by the yellow box. Changes of peptides from the same familiy were summarized together.

a)

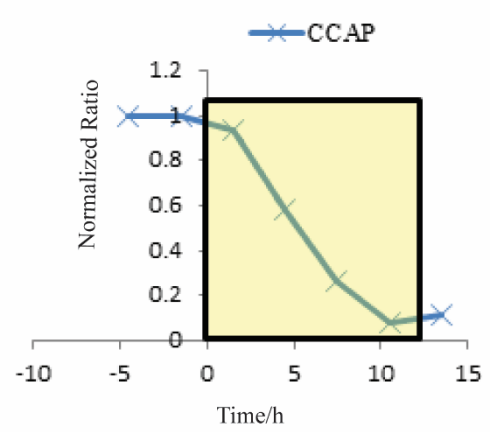

b)

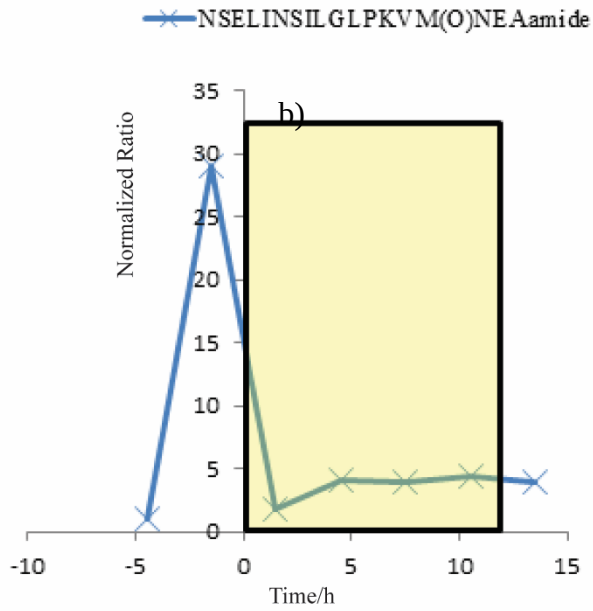

c)

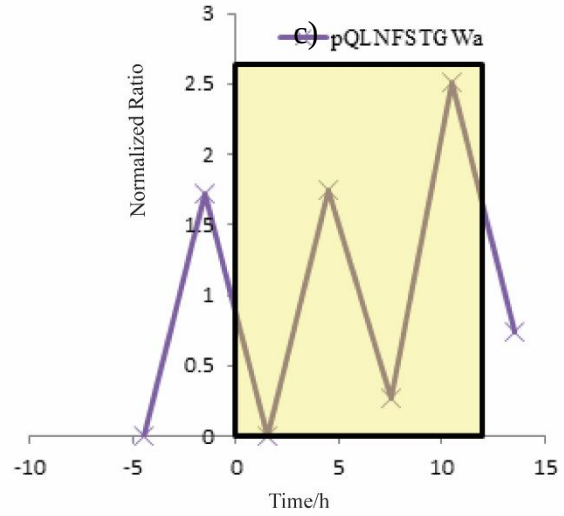

Figure 5-4. Dynamic changes of CCAP, PDH, and RPCH in 12 h: 12 h light/dark cycle. Light went on at time zero as indicated by the yellow box. Peptide intensity was normalized to an internal peptide standard. (a) CCAP decreased slowly as the light went on; (b) changes for PDH, which displayed a rather dramatic decrease as light period started; (c) RPCH exhibited an oscillating change pattern throughout the light period.

Chapter 6

Capture of *In Vivo* Neuropeptide Degradation Using MALDI-Mass Spectrometry

Adapted from **Zhidan Liang**, Shan Jiang, and Lingjun Li. 'Enzymatic Degradation of Neuropeptides Probed by *in vivo* microdialysis coupled with MALDI-Mass Spectrometry', Analyst invited manuscript, *to be submitted*.

Abstract

The term neuropeptide refers to a very large and diverse class of signaling molecules, such as peptide neurotransmitters and peptide hormones. Neuropeptides are used by the neurons to mediate neurotransmission. The diversity of neuropeptides is reflected not only by the fact that they are present even in the simplest nervous system, but also the large number of isoforms even within the same family of neuropeptides. The reason for the large peptide diversity is, however, not well understood. A proposed mechanism is that different peptide isoforms have different degradation rates, which are regulated by extracellular peptidase. As a result, the extracellular concentrations of neuropeptides are affected and influence the distance the peptides can travel/diffuse to exert actions and the length of those actions. Thus the regulation of neuropeptide degradation has important functional consequences. In this work, *in vivo* microdialysis was coupled to a mass spectrometry-based platform using matrix-assisted laser desorption/ionization-linear ion trap-Orbitrap mass spectrometer (MALDI-LTQ-Orbitrap) to capture the *in vivo* degradation processes of different known neuropeptides in Jonah crab, *Cancer borealis*. To determine if different degradation rates occur, neuropeptides from the orcokinin, RFamide, tachykinin-related peptide, and allatostatin families were evaluated. Microdialysis was coupled with MALDI-imaging for a direct characterization of the generation of different degradation products over time in an off-line 'real-time' manner. Mass spectrometry can provide sequence information for degradation products thus helping to determine the enzyme cleavage sites, which could offer insight into the potential peptidases involved in peptide degradation. Semi-quantitative changes of neuropeptide abundances across multiple time points were acquired by incorporating an internal standard,

and were used to explore the degradation rate for a mixture of different neuropeptides by incubating them *in vitro* in crude hemolymph. The results proved that different neuropeptides showed differential degradation rates, which may offer interesting insights and perspectives into our fundamental understanding of how neuropeptides function. Moreover, this novel approach of coupling microdialysis with mass spectrometry imaging shows great potential for its future application in neurochemical studies.

6.1 Introduction

Neuropeptides (NPs) are endogenous peptides synthesized in nerve cells or peripheral organs. The production of NPs begins in a similar manner as most secreted proteins. NPs are first synthesized as larger protein precursors known as proneuropeptides or prohormones. A series of proteolytic cleavage events and post-translational modifications (PTMs) steps then occur, giving rise to biologically active NPs [1-3]. Proteolytic processing can occur at dibasic residue sites, monobasic Arg sites, and even multibasic residue sites [4]. If a prohormone is cleaved by the endopeptidase at the COOH-terminal side, then the peptide intermediate contains a basic C-terminal extension and a carboxypeptidase is involved to remove these residues to generate the active NP. Alternatively, if such cleavage occurred at the NH_2-terminal, an aminopeptidase acts to remove the basic residue extension at the N-terminal. In cases where protelytic processing occurs between dibasic residues, both aminopeptidases and carboxypeptidases are required to produce the final NP.

NPs could be grouped into different families based on their sequence conservation at either the C-terminal or N-terminal. The diversity of NPs is represented not only by the numerous peptide families being discovered, but also in the fact that multiple isoforms exist even within the same peptide family [5, 6]. The reason for the large peptide diversity is not clear, but it could potentially be because of the various functional needs in complex nervous systems. Mature NPs, upon release, interact with receptors to mediate neurotransmission [7, 8]. Moreover, studies have shown that NPs appeared to be able to travel a relatively long distance from their release sites to reach their targets [9]. Previous studies have indicated that peptides from one family often showed comparable

eletrophysiological responses [10]; however the action of NPs could be affected by extracellular peptidases controlling NP concentrations thus limiting activity intensity and the length of the action period.

Much effort has been exerted to study the biosynthesis, modification, secretion and function of NPs across different organisms. However, much less is known regarding the post-release fate of these molecules and how it influences NP signaling. It is important to understand how NPs are removed or inactivated from the extracellular space to fully understand NP signaling. One proposed mechanism for NP removal is enzymatic degradation by extracellular peptidases, which would limit the actions of NPs [11, 12]. Peptidase activity has been implicated to tune motor pattern modulation in crustaceans possibly by limiting NP diffusion and terminating its actions [12, 13]. So the differential degradation of peptides could potentially serve as a mechanism for the differential peptidergic actions in the neural circuits.

In previous studies on NP degradation, *in vitro* assays using tissue/fluid incubation was often used to gain information about specific peptides or enzymes [13-17]. The degradation process is highly dynamic and environment dependent. Although *in vitro* assays are performed under a controlled environment to mimic *in vivo* conditions, *in vitro* assays cannot precisely replicate the cellular conditions in a living organism. Thus results from *in vitro* incubation of NPs with tissue or fluid suffer from the possibility of poor correlation with circumstances in living organism. The detection and quantification of specific NP degradation products can be achieved using high-performance liquid chromatography (HPLC) [13, 16] or immunochemical techniques, such as radioimmunoassay (RIA) [17, 18]. In these methods, prior knowledge about a specific

peptide and its potential degradation product is required, and thus such methods can be time consuming and labor intensive.

Mass spectrometry (MS)-based methods enables the comprehensive identification of NPs and their degradation products simultaneously without requiring prior knowledge of these compounds. To investigate NP degradation and determine the length of action in extracellular space, we employ matrix-assisted laser desorption/ionization (MALDI)-mass spectrometry imaging (MSI) coupled with *in vivo* microdialysis to trace the *in vivo* degradation profile of selected NPs. An *in vitro* assay was used to study the degradation rate of NPs by incubating NPs with freshly extracted hemolymph. A MS-based detection platform using MALDI-MS was developed to enable semi-quantitative measurements of changes in peptide abundance during degradation at multiple time points. This platform allows for high-throughput analysis of samples with µL or sub-µL volume. Among available MS-based quantitation methods, stable isotope labeling has been widely used in protein and peptide quantitation [19, 20]. However, the extra labeling step and time needed for data processing of samples from multiple time points make label-free methods a more suitable choice in this experiment. Adding an internal standard in label-free quantitation experiments [21, 22] has been proven to be a reliable alternative method. Peak intensity is often used to represent the relative concentration in label-free quantitation methods. However, due to the nature of sample preparation for MALDI-MS analysis, with potential differences in matrix crystallization and ionization, signal intensity is not always an accurate reflection of the relative concentration; therefore, the comparison of absolute signal intensities between samples may lead to inaccurate quantitative results. To compensate for this limitation, a peptide with a known concentration was used as an

internal standard and spiked into the MALDI matrix and the standard peak intensity was used to normalize the signal intensities of NPs and degradation products in the sample before relative quantitation comparison. This approach was demonstrated to be a rapid and relatively accurate way to determine the degradation rate.

Moreover, MALDI-MSI is coupled with microdialysate collection which offers the capability to trace the dynamic degradation process in an off-line, 'real-time' manner. As a prime *in vivo* sampling technique, microdialysis has long been used in neuroscience studies to sample a wide range of molecules, including NPs [23, 24] and neurotransmitters [25, 26], directly from extracellular space with minimal perturbation to the animal. Among the wide variety of applications of this microdialysis technique, it has an important role in the field of pharmacokinectics and pharmacodynamics studies [27]. It has been extensively used to monitor drug metabolism [28], which inspired us to see its potential in studying NP degradation in crustaceans. After NPs were delivered to live animals, the microdialysate was collected directly from circulating hemolymph thus allowing direct analysis of degradation occurring in an actual biological system. Despite the various advantages of microdialysis, one of the main challenges is the detection of the acquired sample. Microdialysis employs a semi-permeable probe at the tip, which has a defined molecular weight cutoff (MWCO) where only molecules below the cutoff can pass into the probe. The collection of molecules through the microdialysis probe is a concentration gradient driven diffusion. The low extracellular concentration of signaling molecules in extracellular space together with a low recovery rate [24] (the amount of molecules passing through dialysis probe compared with the amount present in extracellular space) require the detection technique to be highly sensitive and effective. Various detection methods

were developed to couple with microdialysis detection, including electrophoresis, HPLC and MS, as well summarized elsewhere [29, 30]. In particular, the use of MS to detect circulating NPs [23] and neurotransmitters [26] in crustaceans has proved to be a highly sensitive and effective.

In this work, microdialysate from Jonah crabs, *Cancer borealis*, was continuously collected onto a custom MALDI target plate. MALDI-MSI was used for NP and NP degradation product analysis. MALDI-MSI was selected for its higher tolerance to impurities, in comparison to electrospray ionization (ESI)-MS, thus no sample cleanup or separation step was needed after collection. The coupling of MSI detection with microdialysis collection allows us to identify the degradation products and while simultaneously providing relative intensity information from the imaging results. More importantly, we can take full advantage of microdialysis collection as the temporal resolution was maintained on the MALDI platform, thus allow us to monitor the 'real-time', *in vivo* changes. This novel platform promises great potential in correlating *in vivo* neurochemical dynamics with physiological processes in a highly time-resolved manner. In addition, this study presents one of the most in depth extracellular NP degradation investigations in the crustacean nervous system.

6.2 Materials and Methods

6.2.1 *Materials*

ACS reagent-grade solvents and Mill-Q water were used for sample preparation. Optima grade solvents were used for sample analysis on MS instruments. Formic acid (FA) and α-cyano-4-hydroxy-cinnamic acid (CHCA) were purchased from Sigma-Aldrich (St. Louis, MO, USA). Methanol, acetonitrile, and acetic acid were purchased from Fisher

Scientific (Pittsburgh, PA, USA). Peptide standards, bradykinin (RPPGFSPFR), substance P (RPKPQQFFGLM), FMRFamide, and FMRFamide-like peptide (SDRNFLRFamide FLP I) were purchased from the American Peptide Company (Sunnyvale, CA, USA). Crab tachykinin-related peptide (APSGFLGMRamide, CabTRP Ia) was synthesized at the UW-Madison Biotechnology Center.

6.2.2 *Animals*

Jonah crabs, *Cancer borealis*, were acquired from the Fresh Lobster Company (Gloucester, MA, USA). Crabs were maintained in an artificial seawater tank (Aquaneeing Inc. CA, USA) at 10-13 ^{o}C with a 12 h/12 h light/dark cycle. All animals were allowed to adjust to the tanks for at least one week after shipment before performing hemolymph extraction or microdialysis. Details of animal housing procedures were described elsewhere [31]. Animals were housed, treated and sacrificed following the animal care protocol in accordance with the University of Wisconsin-Madison's animal care guidelines.

6.2.3 *Hemolymph Collection and Neuropeptide Incubation*

Crabs were removed from the tank and cold-anesthetized on ice for 5 min. Two mL of hemolymph was withdrawn from each animal by inserting a 25-gauge needle attached to a 3 mL BD plastic syringe through the junction of the thorax and abdomen into the pericardial chamber. A mixture of peptide standards with equal concentrations (10 μM) of FMRFamide, mammalian peptide, bradykinin (RPPGFSPFR) and endogenous crustacean peptides SDRNFLRFamide (FLP I), SGKWSNLRGAWamide (AST-B), APSGFLGMRamide (CabTRP Ia) were incubated in freshly collected hemolymph at 12 ^{o}C water bath for 8 hours. At desired time points (every 30 mins for the first 3 hours and every hour for the remaining 5 hours), 100 μL aliquots of hemolymph were collected from

the animal and thoroughly mixed with 100 µL of acidified methanol (90% MeOH, 9% glacial acetic acid and 1% water) immediately to quench peptidase action and extract NP content. The hemolymph/acidified methanol mixture was then centrifuged for 10 min at 16,100 xg using an Eppendorf 5415D tabletop centrifuge. After centrifugation, the resulting supernatant was harvested and desalted using C_{18} ZipTips (EMD Millipore, Billerica, MA, USA), and eluted in 10 µL 0.1% FA in 50% acetonitrile (v/v). The resulting sample elution was concentrated ~3 fold in a SpeedVac (Thermo Fisher Scientific, Waltham, MA, USA). One microliter of the final extract was mixed 1:1 with CHCA matrix, which was spiked with substance P as internal standard, spotted onto a MALDI plate and allowed to crystallize at room temperature, followed by MALDI-LTQ-Orbitrap XL (Thermo Scientific, Bremen, Germany) analysis.

6.2.4 *Microdialysis Supplies*

CMA/20 Elite probes with 4 mm membranes of polyarylether sulfone (PEAS) were purchased from CMA Microdialysis (Harvard Apparatus, Holliston, MA, USA). A KD Harvard 22 (Harvard Apparatus, Holliston, MA, USA), and an 11 Elite Nanomite Syringe Pump (Harvard Apparatus, Holliston, MA, USA) were used to drive perfusion fluid through microdialysis probes and tubing. Additional FEP (CMA) and PEEK (Upchurch-Scientific, Index Health and Science, Oak Harbor, WA, USA) tubing was used to lengthen the tubing of the microdialysis probe as needed. Flanged connectors from CMA and BASi (West Lafayette, IN, USA) were used to connect the tubing. Probes were rinsed with crab saline prior to implantation.

6.2.5 *In vivo Microdialysis*

The procedure for *in vivo* microdialysis surgery on Jonah crabs was adapted from previous publications [23, 24]. Briefly, after the microdialysis probe was surgically implanted into the crab, the animal was allowed to recover for at least 24 h with crab saline (440 mM NaCl; 11 mM KCl; 13 mM $CaCl_2$; 26 mM $MgCl_2$; 10 mM HEPES acid; pH 7.4, adjusted with NaOH) as perfusion fluid before dialysate was collected for MS analysis. For the peptide degradation study, different NP standards and the mammalian peptide, bradykinin, were added into the perfusion crab saline. The flow rate was set to 0.5 μL/min by a programmable syringe pump. The outlet microdialysate was deposited directly onto a MALDI plate pre-coated with matrix whose movement was mechanically controlled by a syringe pump at a speed of 3.7 mm/min. Matrix pre-coating was performed by an automated TM-sprayer to improve extraction efficiency of target molecules from dialysate [26]. CHCA matrix (10 mg/mL in 0.1% FA and 50% ACN) was applied simultaneously as collection went on driven by syringe pump at a flow rate of 0.5 μL/min.

6.3 Instrumentation and Data Processing

All data was acquired on an MALDI-LTQ-Orbitrap XL mass spectrometer (Thermo Scientific, Bremen, Germany) equipped with 60 Hz 337 nm N_2 laser in positive ion mode. Three technical replicates of three biological replicates were analyzed for hemolymph incubation samples using a mass range of *m/z* 500-2000, a mass resolution of 60,000 (at *m/z* 400), and a mass error of ≤ 5 ppm. MS/MS was performed in HCD mode with normalized collision energies of 45 and isolation window of 3 *m/z*. Continuous measurement of microdialysate traces were achieved by MALDI imaging acquisition on the same instrument. A full MS scan was set up for selected traces from *m/z* 100-2000 at a

raster step size of 150 μm and 8μJ laser energy. The acquired imaging data was further processed using MSiReader [32] and all images were normalized by internal standard.

The abundance of each NP across different time points was normalized to that of spiked-in peptide standard, and three normalized abundances were averaged for each time point. As indicated in early studies, when substrates were presented at high concentrations many enzyme-catalyzed reactions exhibit first order kinetics [33, 34]. The equation for first order enzyme-catalyzed reaction is $Ln[NP]=constant-k_{cat}*C_E/K_m*t$, where k_{cat} represents the rate constant of enzymes, C_E is the enzyme concentration, K_m is the Michaelis constant, and *t* is time. To obtain the rate constant k, linear regression analysis is performed for the logarithmic abundance versus time to get the slope.

6.4 Results and Discussion

Three endogenous crustacean NPs, including peptides from B-type allatostatin (AST-B), crab tachykinin-related peptide (CabTRP Ia), FMRFamide-like peptide (FLP I), and FMRFamide, as well as one mammalian peptide, bradykinin, were chosen to study their *in vivo* and *in vitro* degradation profiles. The aim was to investigate the difference in degradation dynamics among different NP families which are known exist the in crustacean circulatory system. The mammalian peptide was also used to examine the specificity of activities of crustacean proteases. In the *in vitro* hemolymph incubation assay, all NPs were mixed together to obtain their degradation rate. In the *in vivo* microdialysis study, each peptide was infused individually or mixed with bradykinin which will be discussed in detailed in following sections.

6.4.1 *Determination of Degradation Rate*

Here, a MALDI-MS-based platform was used to quantify the changes in NPs across multiple time points in the degradation process. The detection needed to be high throughput to handle the large number of samples in a timely fashion. MALDI-MS fulfilled this demand with the additional benefit of maintaining the collection temporal resolution. However, MALDI is not widely applied to quantitative studies in comparison to liquid chromatography (LC)-MS, mostly due to the differences resulting from matrix crystallization and ionization during detection. To compensate for this limitation, equal amounts of peptide standards were spiked into each sample and its signal intensity was used to normalize variations. Three technical and three biological replicates were performed to ensure data quality.

NPs were incubated with circulating hemolymph at equal concentrations (10 µM) and thus were exposed to the same set of peptidases. Of the five studied NPs, the CabTRP Ia peptide with a sequence of APSGFLGMRamide had a unique degradation profile that did not obey first order kinetics. Unlike the other peptides, almost 90% of the CabTRP Ia peptide was degraded within the first 30 min to 1 hr of the experiment, as observed from quantitative analysis, and then maintained at a similar level until the end of the experiment (~ 8 hr). This could be due to the specificity of peptidases involved in degrading different peptide families and the concentration-related activity of different peptidases. It is reasonable to postulate that there is a functional need for this fast degradation process such as to give rise to other bioactive compounds or to serve as a trigger to activate signaling pathways. It is also possible that more peptidases, in addition to those present in hemolymph, are involved in CabTRP Ia peptide processing, or its *in vivo* physiological concentration is at a different level compared to the other peptides, thus leading to different

degradation profiles. Tachykinin-related peptides have been found in many different organisms including various crustacean species [35], such as *Cancer borealis* [36]. However, the function of this family of peptides remains unknown. It was suggested that CabTRP Ia might be involved in feeding-related behavior and this study has provided a different angle for functional investigation purposes.

The other four NPs, as shown in **Figure 6-1** and **6-2**, exhibited first order kinetics. As shown in **Figure 6-1**, to determine the degradation rate of NPs, Ln of normalized abundances of NPs were plotted as a function of time. Performing linear regression yields the slope of the trend line, which correlates to the degradation rate constant. As seen from the equation above, several factors including k_{cat} (rate constant of the catalyst), C_E (enzyme concentration) and K_m (Michaelis constant) determine the degradation rate. The approach presented here allows rapid and relatively accurate estimation of degradation rate constants. An averaged degradation rate constant was obtained from biological triplicates and the SEM (standard error of the mean) is indicated as error bars in **Figure 6-2**. The impact of temperature and protease inhibitors on degradation has been described in detail in a previous study [26] and will not be discussed here. Bradykinin had the fastest degradation rate and the AST-B peptide, SGKWSNLRGAWamide, degraded much slower. Previous studies had also found that terminal modifications, such as C-terminal amidation and N-terminal acetylation, could improve peptide stability [37, 38]. FLP I, FMRFamide and AST-B peptides all displayed amidated C-terminals.

FMRFamide and FLP I are both categorized into the RFamide family. These two RFamide peptides exhibited similar degradation rates, where FMRFa had a k value of 0.43 (SEM 0.03) and FLP I had a k value of 0.53 (SEM 0.01). FLP I has been found in *Cancer*

borealis [23] but FMRFamide, first discovered in mollusks [39], was not observed in *Cancer borealis* and was considered as non-endogenous RFamide peptide here. FMRFamide degraded slightly slower than SDRNFLRFamide in hemolymph incubation. This result may suggest that both peptides and/or their degradation products act as circulating hormones in the *Cancer borealis* nervous system and have functional roles by interacting with neurons in distance. In the study by Cruz-Bermúdez *et al*. [40], different members of the FMRFamide-like peptide family were found to have different degradation profiles, which was further confirmed to have different impacts on the pyloric rhythm. FMRFamide was also degraded in the crustacean circulatory system, which may result due to the fact that its peptide sequence is extremely similar to some degradation products. It could also be due to the presence of this peptide in the *Cancer borealis* system at such low concentrations that it could not be detected with current analytical methods.

An AST-B-family peptide, SGKWSNLRGAWamide (AST-B), was determined to have a degradation rate constant of 0.14 (SEM 0.08). AST peptides are well known to have myoinhibitory effects. There were extensive studies on the inhibition of AST peptides on the biosynthesis of juvenile hormones in insects [41] and the wide distribution of this family of NPs throughout crustacean nervous systems [5] indicates its functional importance. Studies in insects have demonstrated that ASTs were fast-acting peptides, and the slow degradation rate of AST-B in this study resulted in the continuous presence of this peptide in the system, leading to prolonged action. The findings suggested that there must be more pathways involved in the *in vivo* inactivation process with target tissues involved in addition to circulating hemolymph. The physical concentration of AST-B in *Cancer borealis* is unknown and the degradation rate is concentration-related, thus an *in vivo* assay

was essential for more in-depth investigation. Different crustacean AST-B peptide family members share sequence homology and have similar physiological actions in inhibiting the pyloric rhythm of the STG [32]. The regulation of different peptide isoform degradation and inactivation could potentially be one important mechanism determining the differential actions of AST-B family peptides. The study of cockroach AST peptide degradation led to the design of a series of this peptide's analogues which have proven to be resistant to hemolymph peptidase degradation [42].

6.4.2 *Degradation Products*

In this work, peptide members from several major *Cancer borealis* peptide families were chosen to study their representative degradation rates, thus offering an excellent opportunity to investigate the related functional consequences. MS detection enables the simultaneous detection of both parent peptides and their corresponding degradation products. The background was subtracted by comparing the hemolymph incubated sample with crude hemolymph extract. As summarized in **Table 6-1,** a wide variety of degradation products from all five NPs were observed in the time course of this study. The resulting degradation products were further confirmed by tandem MS as shown in **Figure 6-3**. After incubation at 12 ^{o}C for 5 hr, parent peptides and various degradation products were detected and tandem mass spectra confirmed the amino acids sequence of degradation products from AST-B and CabTRP Ia peptides.

All peptides were incubated with freshly withdrawn hemolymph from *Cancer borealis* to correlate with the *in vivo* microdialysis studies. All five peptides including, mammalian peptide bradykinin, were cleaved successively at almost every peptide bond from either the C- or N-termini by various peptidases. Exopeptidases, such as

carboxypeptidases, target the peptide bond on C-terminus, whereas aminopeptidases cleave amino acids on the N-terminus. The detailed characterization of the amino acid sequences of these degradation products revealed the cleavage sites of the studied NPs, suggesting the presence of both carboxypeptidases and aminopeptidases in the circulatory system of *Cancer borealis*. In addition, the detection of degradation products such as SDRNFLR (*m/z* 889.4639) and SGKWSNLR (*m/z* 929.4952) suggested the presence of trypsin-like serine proteases which target the carboxyl group of arginine (R) peptide residues [43]. Neural endopeptidase (NEP), which cleaves substrates on the amino side of hydrophobic amino acids, has been described both in invertebrates and vertebrates [44]. The cleavage between GF in bradykinin and AST-B, and NF in FLP I could potentially serve as a piece of evidence for NEP-like activity in *Cancer borealis*. A certain degree specificity of peptidase activity is observed which may account for the rapid degradation of CabTRP Ia APSGFLGMRamide. As discussed in the above section, CabTRP Ia was the only one of the five studied NPs that did not exhibit first-order kinetics.

Interestingly, the observation of various bradykinin degradation products showed that crustacean peptidases can also cleave this peptide even though it is non-naturally occurring in crustacean systems. This could be explained by the existence of non-specific peptidases, which target any peptide bond from a peptide/protein as an elimination/immune response mechanism to remove any exogenous substances. Another possibility is the presence of bradykinin peptide analogue in crustacean systems that yet to be discovered. The degradation profile was further confirmed in the *in vivo* microdialysis study where various degradation products were observed.

6.4.3 *In vivo Microdialysis MALDI Imaging*

In addition to the implementation of the *in vitro* MALDI-MS-based assay for rapid determination of NP degradation rates, a MALDI-MS imaging (MSI) platform was developed to couple with *in vivo* microdialysis experiments for 'real-time' monitoring of dynamic biological processes such as NP degradation. The MALDI-MS platform offers the capability of maintaining sample temporal resolution, which complements continuous microdialysis collection. To address the challenges of quantifying NP changes with MALDI, MSI was employed. Constructing MSI images of collected microdialysate with *m/z* distributions and signal intensity provided quantitative information in the form of ratio changes at different time points. An MSI image contains information about the identities of targeted molecules, spatial distributions and signal intensities. In this platform, microdialysis collection and matrix application were carried out simultaneously and required no additional sample preparation steps.

Microdialysis has been widely applied in various *in vivo* neuroscience studies to monitor substances of interest under different physiological conditions. Moreover, it has also been widely used as a drug delivery method as well as in drug metabolism studies. In this work, FMRFamide, FLP I, CabTRP Ia and AST-B were delivered individually with and without bradykinin in each experiment *via* retrodialysis. NPs were added into perfusion crab saline solution at different concentrations and infused for 3 hr at a flow rate of 0.5 μL/min before switching back to crab saline perfusion. Collection of microdialysate was done continuously onto customized MALDI target plate. The overall workflow is illustrated in **Figure 6-4**. As expected, results from the *in vivo* study differed from *in vitro* hemolymph incubation of peptides, revealing the involvement of more peptidases in the signaling network.

Since the physiological concentrations of these NPs are unknown, we started with 10 µM of NPs in crab saline and perfused through the microdialysis inlet while collecting samples at outlet. This concentration proved to be too low for detection via MS for the *in vivo* assay. The recovery rate of the microdialysis probe [24] would lead to loss of delivered NPs, where in general only 30% to 40% of NPs were exposed to the *in vivo* system and the same factor also applied to the collection of generated degradation products. In addition, the volume of hemolymph in male Jonah crabs is approximately 5 mL [45], which caused further dilution of delivered NPs.

The increase of NP amounts was investigated by either increased NP delivery duration or increased peptide concentration in the perfusion solution. As a result, the concentration of NPs in perfusion crab saline was chosen to be 3 mM for further investigation. The prolonged deliver duration did not show much improvement. Although total amount of NPs increased in this method, the NP concentration did not increase at every time point. Over time, the delivered amount of NPs would accumulate. However, NP degradation is a dynamic process and NPs could be rapidly processed after being introduced into the system and thus eliminated or pumped out of the circulatory system.

It took approximately 1- 1.5 hr from the start of delivered NPs reaching the probe implantation site to detect related MS signals in collected microdialysate trace as shown in **Figure 6-5**. The first trace was collected starting from 1 hr. The length of each trace was around 20-25 min. The brighter color indicates higher intensity and the black image in the first half of the traces indicates no detectable signals of *m/z* values of interest. One of the limiting factors is the MS instrument sensitivity, thus accumulation of generated *in vivo* degradation products is required in order to reach the detection limit. As shown in the

results, intact NPs along with various degradation products were detected simultaneously, such as bradykinin and its degradation product PPGFSPFR (*m/z* 904.4676). RFa (*m/z* 321.2034) is a sequence shared between FLP I and FMRFamide, whereas LRFa and FLRFa, belonging to FLP I, were also detected around the similar time period. Such results confirmed our assumption of substance accumulation in the circulatory system and diffusion across the microdialysis probe. The detection of these degradation products from continuous administration of NPs also served as evidence that physical concentration of these NPs were kept at steady levels by various peptidases *in vivo*. **Figure 6-6** illustrates the MSI results of the AST-B peptide throughout microdialysate collection. As the administration of peptide continued for 3 hr, theoretically if no proteolytic processing was occurring, the signal intensity, which was a reflection of peptide concentration, would increase over time. However, as shown in the results, the signal intensity maintained around a certain level once it became detectable. The perfusion solution was switched back to crab saline at 180 min, and the collection continued for another two hours where the signal intensity was at a similar level, possibly due to reduced degradation. This result also agreed with the slow degradation rate of this peptide determined with *in vitro* assay. The signal was slightly variable over the traces, which is most likely due to the inconsistency of trace collection and matrix application at such a slow flow rate. The homogeneity of matrix crystallization also affects the detection. The CabTRP Ia, which exhibited quite unique degradation profile as discussed in the degradation rate session, was also detected at a similar level of signal intensity throughout every trace.

In addition to providing information about the timeline of degradation product generation, this platform also gave us the opportunity to observe the dynamic, changing

patterns of NPs and their degradation products, which could potentially provide interesting insights into their functional roles. For example, after switching back to crab saline perfusion, over time the signal for the intact FLP I peptide gradually became undetectable, as shown in **Figure 6-7** where the image turned darker. Some of the degradation products of FLP I, on the other hand, had very different changes. During the 25 min collection time, the intact peptide *m/z* 1053.5588 disappeared in the last 10 min. Two of the degradation products, DRNFLRFa and RNFLRFa were present a bit longer within the trace. Signals of several shorter-chained degradation products, including NFLRFa, FLRFa and LRFa, became stronger towards the end of this trace when the intact peptide was eliminated. The MSI results suggest that the shorter-chained degradation products were generated from longer-chained peptide degradation products or from even the intact peptide itself. The difference in their generation time might result from the specific activities of multiple peptidases involved. The cleavage of peptide bonds at different residues required different enzymes.

This MALDI-MSI platform coupled with microdialysis collection offered the unique opportunity to monitor the *in vivo* degradation processes of NPs in crustaceans in an off-line, 'real-time' manner. By maintaining the temporal resolution of microdialysis collection, the spatial information contained in the MSI results allowed for visualization of dynamic changes throughout the degradation process. This platform holds great promise for future applications to study biological events.

6.5 Conclusions

In this work, a MALDI-based strategy was established to elucidate the degradation profiles of NPs from representative crustacean NP families: RFamide, AST-B, and

CabTRP. Non-endogenous NPs: FMRFamide and bradykinin were also investigated. Degradation products from all NPs were characterized, which could provide information about the presence of various peptidases in the crustacean nervous system and their action sites. A rapid and robust quantitative method to determine the degradation rates and degradation products of NPs was developed. Moreover, a MALDI-MSI coupled with microdialysis sampling platform was developed to monitor *in vivo* degradation of the studied NPs. The unique advantages of microdialysis and MSI were retained to enable visualization of 'real-time' changes to these NPs in crustacean. The findings about NP degradation may reveal some of the missing factors in signaling pathways, the fate of NPs after secretion and the functional consequence of NP degradation.

6.6 References

1. Han, K.K. and Martinage, A., *Post-translational chemical modification(s) of proteins.* Int J Biochem, 1992. **24**(1): p. 19-28.
2. Wilkinson, C.W., *Roles of acetylation and other post-translational modifications in melanocortin function and interactions with endorphins.* Peptides, 2006. **27**(2): p. 453-71.
3. Eipper, B.A., Stoffers, D.A., and Mains, R.E., *The biosynthesis of neuropeptides: peptide alpha-amidation.* Annu Rev Neurosci, 1992. **15**: p. 57-85.
4. Hook, V., Funkelstein, L., Lu, D., Bark, S., Wegrzyn, J., and Hwang, S.R., *Proteases for processing proneuropeptides into peptide neurotransmitters and hormones.* Annu Rev Pharmacol Toxicol, 2008. **48**: p. 393-423.
5. Yu, Q., Liang, Z., Ouyang, C., and Li, L., *Biologically Active Peptides in Invertebrates: Discovery and Functional Studies*. Colloquium Series on Neuropeptides. 2015: Morgan & Claypool Publishers.
6. Hoyle, C.H., *Neuropeptide families: evolutionary perspectives.* Regul Pept, 1998. **73**(1): p. 1-33.
7. Raggenbass, M., *Overview of cellular electrophysiological actions of vasopressin.* Eur J Pharmacol, 2008. **583**(2-3): p. 243-54.
8. Eigler, T. and Ben-Shlomo, A., *Somatostatin system: molecular mechanisms regulating anterior pituitary hormones.* J Mol Endocrinol, 2014. **53**(1): p. R1-19.
9. Karhunen, T., Vilim, F.S., Alexeeva, V., Weiss, K.R., and Church, P.J., *Targeting of peptidergic vesicles in cotransmitting terminals.* J Neurosci, 2001. **21**(3): p. RC127.
10. Saideman, S.R., Ma, M., Kutz-Naber, K.K., Cook, A., Torfs, P., Schoofs, L., Li, L., and Nusbaum, M.P., *Modulation of rhythmic motor activity by pyrokinin peptides.* J Neurophysiol, 2007. **97**(1): p. 579-95.
11. Zappulla, J.P., Wickham, L., Bawab, W., Yang, X.F., Storozhuk, M.V., Castellucci, V.F., and DesGroseillers, L., *Cloning and characterization of Aplysia neutral endopeptidase, a metallo-endopeptidase involved in the extracellular metabolism of neuropeptides in Aplysia californica.* J Neurosci, 1999. **19**(11): p. 4280-92.
12. Wood, D.E. and Nusbaum, M.P., *Extracellular peptidase activity tunes motor pattern modulation.* J Neurosci, 2002. **22**(10): p. 4185-95.
13. Coleman, M.J., Konstant, P.H., Rothman, B.S., and Nusbaum, M.P., *Neuropeptide degradation produces functional inactivation in the crustacean nervous system.* J Neurosci, 1994. **14**(10): p. 6205-16.
14. Albo, F., Antonangeli, R., Cavazza, A., Marini, M., Roda, L.G., and Rossi, P., *Neuropeptide degradation in naive and steroid-treated allergic saliva.* Int Immunopharmacol, 2001. **1**(9-10): p. 1777-88.

15. Ludwig, R., Lucius, R., and Mentlein, R., *A radioactive assay for the degradation of neuropeptide Y.* Biochimie, 1995. **77**(9): p. 739-43.

16. Chung, J.S. and Webster, S.G., *Angiotensin-converting enzyme-like activity in crab gills and its putative role in degradation of crustacean hyperglycemic hormone.* Arch Insect Biochem Physiol, 2008. **68**(3): p. 171-80.

17. Roosterman, D., Cottrell, G.S., Padilla, B.E., Muller, L., Eckman, C.B., Bunnett, N.W., and Steinhoff, M., *Endothelin-converting enzyme 1 degrades neuropeptides in endosomes to control receptor recycling.* Proc Natl Acad Sci U S A, 2007. **104**(28): p. 11838-43.

18. Torang, S., Bojsen-Moller, K.N., Svane, M.S., Hartmann, B., Rosenkilde, M.M., Madsbad, S., and Holst, J.J., *In vivo and in vitro degradation of peptide YY3-36 to inactive peptide YY3-34 in humans.* Am J Physiol Regul Integr Comp Physiol, 2016: p. ajpregu 00394 2015.

19. Frost, D.C., Greer, T., Xiang, F., Liang, Z., and Li, L., *Development and characterization of novel 8-plex DiLeu isobaric labels for quantitative proteomics and peptidomics.* Rapid Commun Mass Spectrom, 2015. **29**(12): p. 1115-24.

20. Frost, D.C., Greer, T., and Li, L., *High-resolution enabled 12-plex DiLeu isobaric tags for quantitative proteomics.* Anal Chem, 2015. **87**(3): p. 1646-54.

21. Goeminne, L.J., Gevaert, K., and Clement, L., *Peptide-level robust ridge regression improves estimation, sensitivity and specificity in data-dependent quantitative label-free shotgun proteomics.* Mol Cell Proteomics, 2015.

22. Kramer, G., Woolerton, Y., van Straalen, J.P., Vissers, J.P., Dekker, N., Langridge, J.I., Beynon, R.J., Speijer, D., Sturk, A., and Aerts, J.M., *Accuracy and Reproducibility in Quantification of Plasma Protein Concentrations by Mass Spectrometry without the Use of Isotopic Standards.* PLoS One, 2015. **10**(10): p. e0140097.

23. Liang, Z., Schmerberg, C.M., and Li, L., *Mass spectrometric measurement of neuropeptide secretion in the crab, Cancer borealis, by in vivo microdialysis.* Analyst, 2015. **140**(11): p. 3803-13.

24. Schmerberg, C.M. and Li, L., *Mass spectrometric detection of neuropeptides using affinity-enhanced microdialysis with antibody-coated magnetic nanoparticles.* Anal Chem, 2013. **85**(2): p. 915-22.

25. Faiman, M.D., Kaul, S., Latif, S.A., Williams, T.D., and Lunte, C.E., *S-(N, N-diethylcarbamoyl)glutathione (carbamathione), a disulfiram metabolite and its effect on nucleus accumbens and prefrontal cortex dopamine, GABA, and glutamate: a microdialysis study.* Neuropharmacology, 2013. **75**: p. 95-105.

26. Jiang, S., Liang, Z., Hao, L., and Li, L., *Investigation of signaling molecules and metabolites found in crustacean hemolymph via in vivo microdialysis using a multi-faceted mass spectrometric platform.* Electrophoresis, 2015.

27. Azeredo, F.J., Dalla Costa, T., and Derendorf, H., *Role of microdialysis in pharmacokinetics and pharmacodynamics: current status and future directions.* Clin Pharmacokinet, 2014. **53**(3): p. 205-12.

28. Scott, D.E., Willis, S.D., Gabbert, S., Johnson, D., Naylor, E., Janle, E.M., Krichevsky, J.E., Lunte, C.E., and Lunte, S.M., *Development of an on-animal separation-based sensor for monitoring drug metabolism in freely roaming sheep.* Analyst, 2015. **140**(11): p. 3820-9.

29. Perry, M., Li, Q., and Kennedy, R.T., *Review of recent advances in analytical techniques for the determination of neurotransmitters.* Anal Chim Acta, 2009. **653**(1): p. 1-22.

30. Guihen, E. and O'Connor, W.T., *Current separation and detection methods in microdialysis the drive towards sensitivity and speed.* Electrophoresis, 2009. **30**(12): p. 2062-75.

31. Kutz, K.K., Schmidt, J.J., and Li, L., *In situ tissue analysis of neuropeptides by MALDI FTMS in-cell accumulation.* Anal Chem, 2004. **76**(19): p. 5630-40.

32. Jungmann, J.H. and Heeren, R.M., *Emerging technologies in mass spectrometry imaging.* J Proteomics, 2012. **75**(16): p. 5077-92.

33. Edgar, R.S., Green, E.W., Zhao, Y., van Ooijen, G., Olmedo, M., Qin, X., Xu, Y., Pan, M., Valekunja, U.K., Feeney, K.A., Maywood, E.S., Hastings, M.H., Baliga, N.S., Merrow, M., Millar, A.J., Johnson, C.H., Kyriacou, C.P., O'Neill, J.S., and Reddy, A.B., *Peroxiredoxins are conserved markers of circadian rhythms.* Nature, 2012. **485**(7399): p. 459-64.

34. Strauss, J. and Dircksen, H., *Circadian clocks in crustaceans: identified neuronal and cellular systems.* Front Biosci (Landmark Ed), 2010. **15**: p. 1040-74.

35. Nassel, D.R., *Tachykinin-related peptides in invertebrates: a review.* Peptides, 1999. **20**(1): p. 141-58.

36. Christie, A.E., Kutz-Naber, K.K., Stemmler, E.A., Klein, A., Messinger, D.I., Goiney, C.C., Conterato, A.J., Bruns, E.A., Hsu, Y.W., Li, L., and Dickinson, P.S., *Midgut epithelial endocrine cells are a rich source of the neuropeptides APSGFLGMRamide (Cancer borealis tachykinin-related peptide Ia) and GYRKPPFNGSIFamide (Gly1-SIFamide) in the crabs Cancer borealis, Cancer magister and Cancer productus.* J Exp Biol, 2007. **210**(Pt 4): p. 699-714.

37. Brinckerhoff, L.H., Kalashnikov, V.V., Thompson, L.W., Yamshchikov, G.V., Pierce, R.A., Galavotti, H.S., Engelhard, V.H., and Slingluff, C.L., Jr., *Terminal modifications inhibit proteolytic degradation of an immunogenic MART-1(27-35) peptide: implications for peptide vaccines.* Int J Cancer, 1999. **83**(3): p. 326-34.

38. Adessi, C. and Soto, C., *Converting a peptide into a drug: strategies to improve stability and bioavailability.* Curr Med Chem, 2002. **9**(9): p. 963-78.

39. Zatylny-Gaudin, C. and Favrel, P., *Diversity of the RFamide Peptide Family in Mollusks.* Front Endocrinol (Lausanne), 2014. **5**: p. 178.

40. Cruz-Bermudez, N.D., Fu, Q., Kutz-Naber, K.K., Christie, A.E., Li, L., and Marder, E., *Mass spectrometric characterization and physiological actions of GAHKNYLRFamide, a novel FMRFamide-like peptide from crabs of the genus Cancer*. J Neurochem, 2006. **97**(3): p. 784-99.

41. Stay, B. and Tobe, S.S., *The role of allatostatins in juvenile hormone synthesis in insects and crustaceans.* Annu Rev Entomol, 2007. **52**: p. 277-99.

42. Garside, C.S., Nachman, R.J., and Tobe, S.S., *Injection of Dip-allatostatin or Dip-allatostatin pseudopeptides into mated female Diploptera punctata inhibits endogenous rates of JH biosynthesis and basal oocyte growth.* Insect Biochem Mol Biol, 2000. **30**(8-9): p. 703-10.

43. Jungmann, J.H., Smith, D.F., MacAleese, L., Klinkert, I., Visser, J., and Heeren, R.M., *Biological tissue imaging with a position and time sensitive pixelated detector*. J Am Soc Mass Spectrom, 2012. **23**(10): p. 1679-88.

44. Ottaviani, E. and Caselgrandi, E., *Neutral endopeptidase-24.11 (NEP)-like activity in molluscan hemocytes.* Peptides, 1997. **18**(8): p. 1107-10.

45. Chen, R., Ma, M., Hui, L., Zhang, J., and Li, L., *Measurement of neuropeptides in crustacean hemolymph via MALDI mass spectrometry*. J Am Soc Mass Spectrom, 2009. **20**(4): p. 708-18.

6.7 Figures and Tables

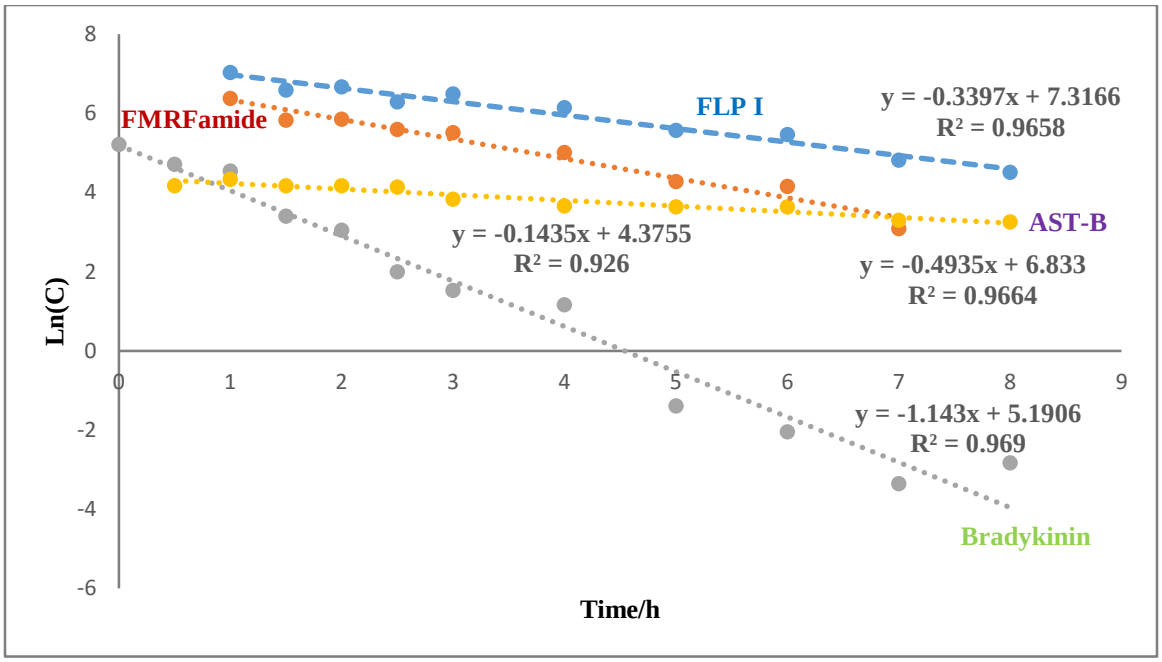

Figure 6-1. An example dataset showing how to calculate the degradation rate constant, k. The relative abundances of neuropeptides were calculated based on the ratio of the neuropeptide peak intensity to the internal standard (IS), Substance P, peak intensity over an 8 hour period. The natural log (Ln) was calculated for the relative abundance and was plotted as a function of time to obtain a trend line which correlates with the equation $Ln[NP]=cons.-k_{cat}*C_E/K_m*t$, in which $k_{cat}*C_E/K_m$ represent the degradation rate constant, k. Three spectra were taken at each time point to give an average abundance, and three biological replicates were performed to get an average k.

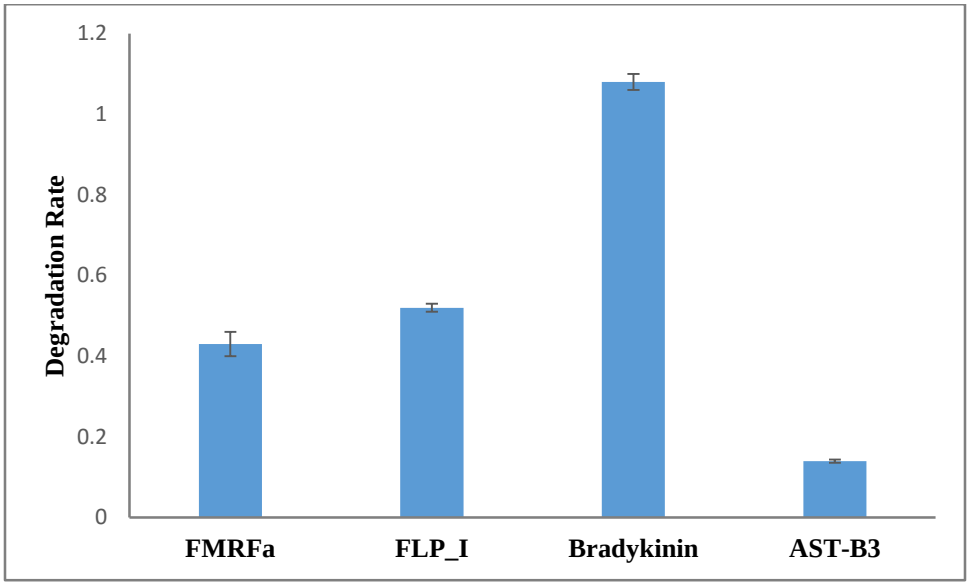

Figure 6-2. The degradation rates of different neuropeptides incubated with crude hemolymph. Every experiment was performed three times to get average data; The standard error of the mean (SEM) is indicated as error bars. FMRFamide, k=0.43, SEM=0.03; FLP I, k=0.52, SEM=0.01; Bradykinin, k=1.08, SEM=0.02; AST-B, k=0.14, SEM=0.004.

Table 6-1. Amino acid sequence and calculated monoisotopic masses of degradation products of neuropeptides using Protein Prospector (UCSF). a indicates C-terminal amidation.

Neuropeptide Sequence	Amino Acid Sequence of Degradation Product	Theoretical $[M+H]^+$	Measured $[M+H]^+$
FMRFamide	FMRFa	599.3122	599.3146
	FMR	435.2173	435.2198
	FM	279.1162	279.0864
	MRFa	452.2428	452.2455
	RFa	321.2034	321.2048
	RFa-NH_3	304.1768	304.1783
FLP I SDRNFLRFamide	SDRNFLRFa	1053.5588	1053.5625
	SDRNFLRFa-H_2O	1035.5483	1035.5539
	SDRNGLRFa-NH_3	1036.5323	1036.5380
	DRNFLRFa	966.5268	966.5302
	RNFLRFa	851.4999	851.5033
	NFLRFa	695.3988	695.4010
	FLRFa	581.3588	581.3581
	LRFa	434.2874	434.2894
	SDRNFLR	889.4639	889.4692
	SDRNFL	733.3682	733.3546
CabTRP APSGFLGMRamide	APSGFLGMRa	934.4927	934.4957
	PSGFLGMRa	863.4456	863.4586
	SGFLGMRa	766.4029	766.4057
	GFLGMRa	679.3708	679.3729
	FLGMRa	622.3494	622.3512

	FLGMRa-NH_3	605.3228	605.3257
	LGMRa	475.2809	475.2822
	LGMRa-NH_3	458.2544	458.2564
	GMRa	362.1969	362.1983
	GMRa-NH_3	345.1703	345.1720
	APSGFL	573.3031	573.2935
AST-B SGKWSNLRGAWamide	SGKWSNLRGAWa	1260.6569	1260.6650
	GKWSNLRGAWa	1173.6276	1173.6327
	KWSNLRGAWa	1116.6061	1116.6109
	WSNLRGAWa	988.5112	988.5150
	WSNLRGAWa-NH_3	971.4846	971.4877
	SNLRGAWa	802.4318	802.4346
	NLRGAWa	715.3998	715.4020
	LRGAWa	601.3569	601.3590
	RGAWa	488.2728	488.2744
	SGKWSNLRGA	1057.5538	1057.5360
	SGKWSNLRG	986.5166	986.4945
	SGKWSNLR	929.4952	929.4984
	SGKWSNL	773.3941	773.3964
	SGKWSN	660.3100	660.3082
	SGKWS	546.2671	546.2702
	SGKWS-H_2O	528.2565	528.2574
	SGKWS-NH_3	529.2405	529.2343
	SGKW	459.2350	459.2371
	SGK	273.1557	273.1564
Bradykinin RPPGFSPFR	RPPGFSPFR	1060.5687	1060.5736
	PPGFSPFR	904.4676	904.4697

	PPGFSPFR-NH_3	887.4410	887.4467
	PGFSPFR	807.4148	807.4177
	PGFSPFR-H_2O	790.3883	790.3968
	PGFSPFR-NH_3	789.4042	789.3913
	GFSPFR	710.3620	710.3631
	FSPFR	653.3402	653.3427
	SPFR	506.2722	506.2745
	PFR	419.2401	419.2423
	FR	322.1874	322.1890
	RPPGFSPF	886.4570	886.4586

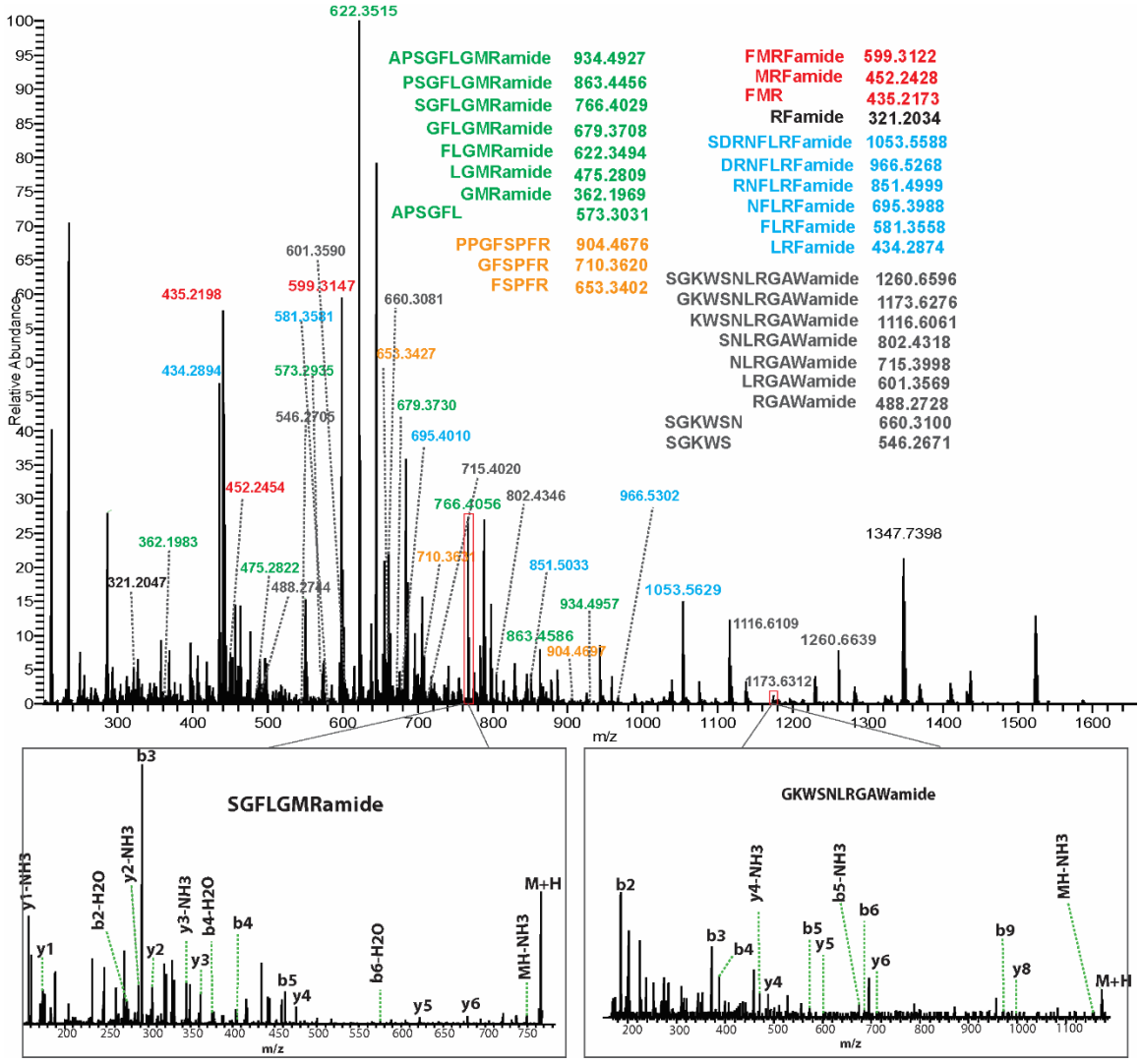

Figure 6-3. Degradation products of the neuropeptide mixture incubated with hemolymph at 12 ^{o}C for 5 hr. Degradation products of different neuropeptides were color coded. Listed *m/z* values represent theoretical values; *m/z* values annotated in spectrum were detected *m/z* values. Tandem mass spectra of two example degradation products, SGFLGMRamide and GKWSNLRGAWamide, are presented in the bottom panel with b- and y-ions annotated.

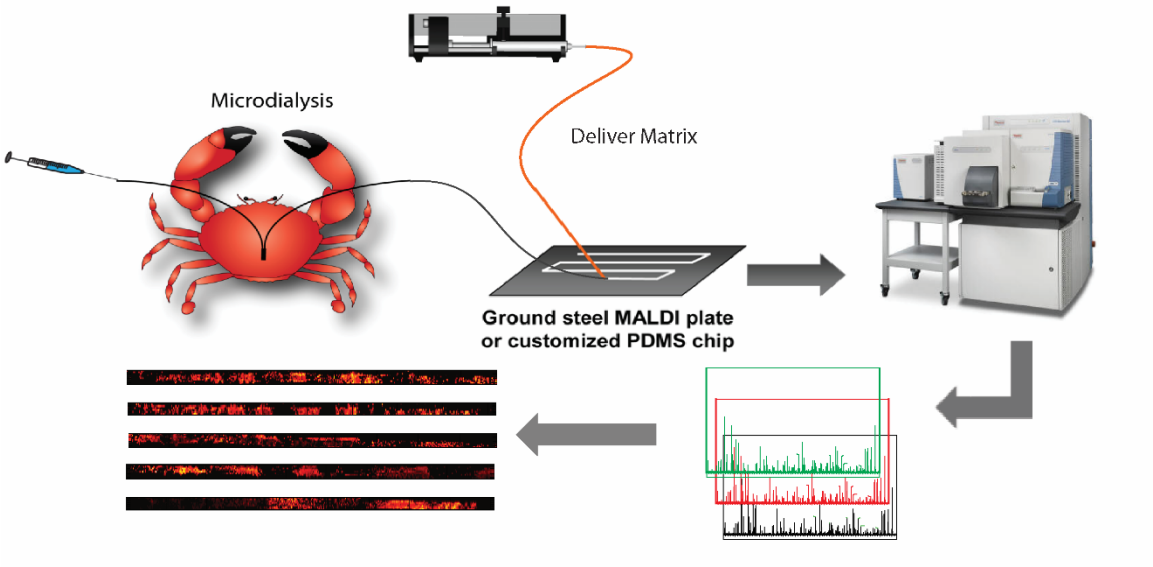

Figure 6-4. Graphic illustration of the microdialysis-MALDI-MSI workflow. Microdialysate collection and matrix application were done simultaneously onto a customized MALDI target plate.

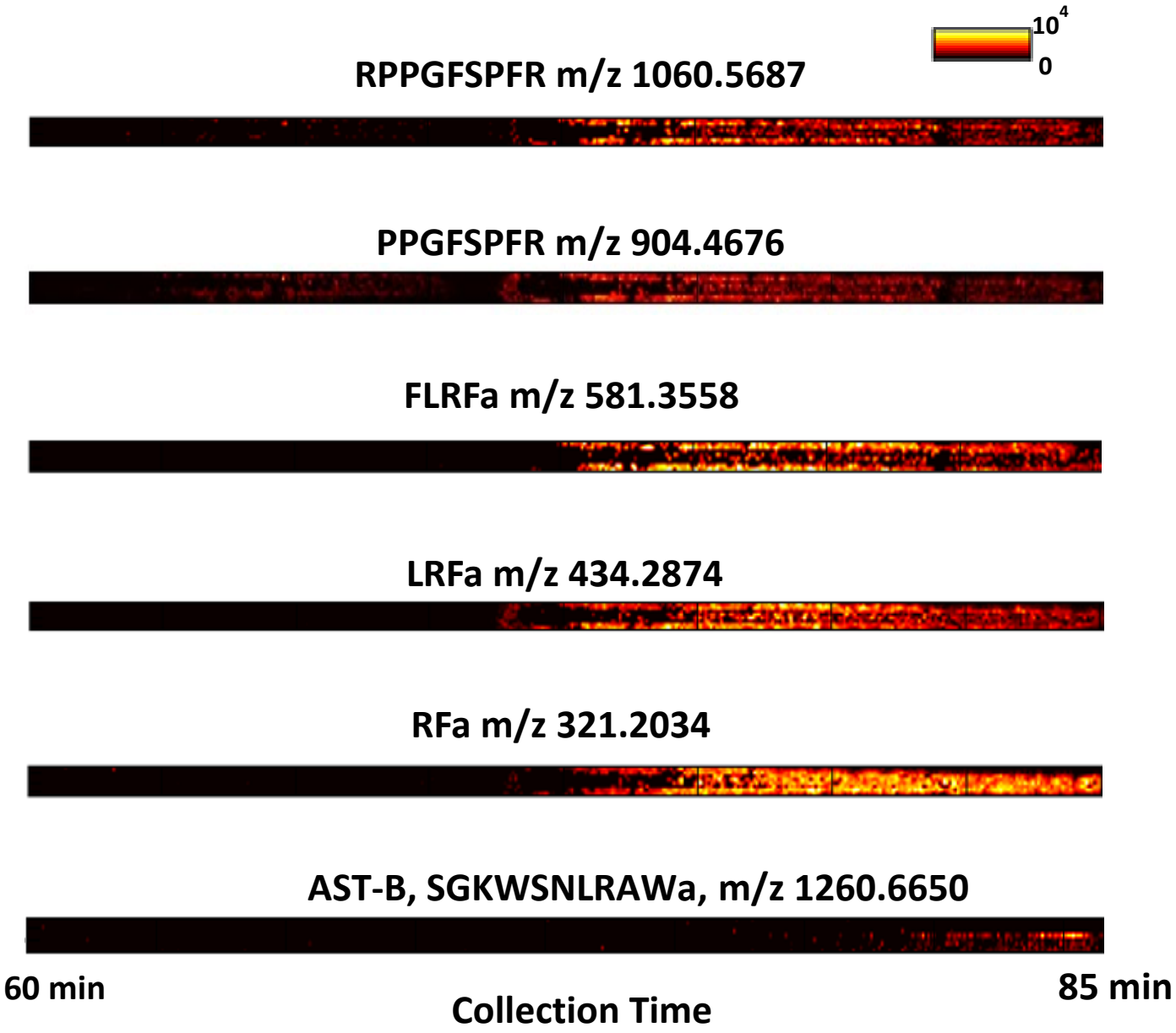

Figure 6-5. Examples of first microdialysate traces where NPs became detectable. Images of intact NPs, CabTRP Ia and bradykinin were extracted together with several degradation products.

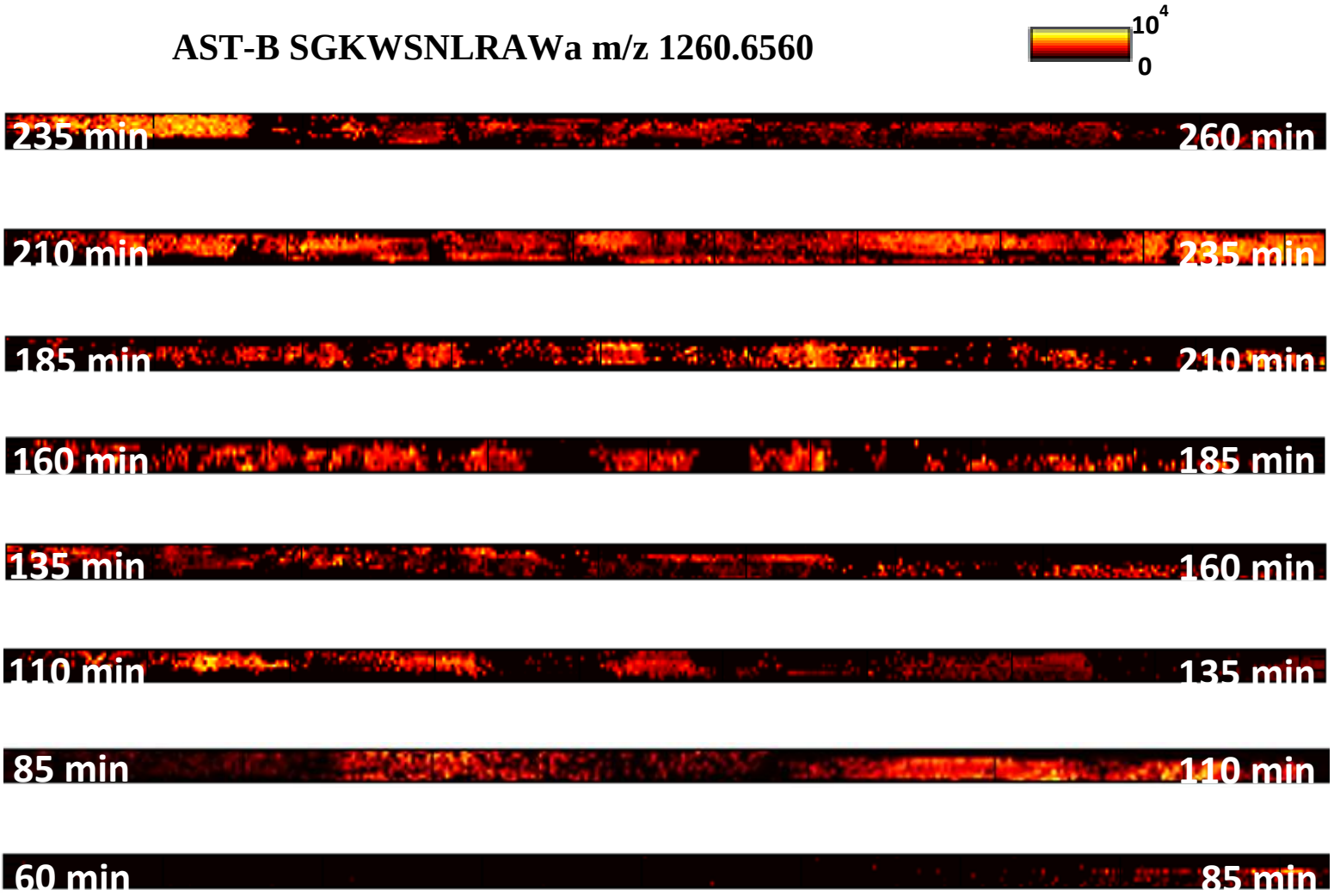

Figure 6-6. MSI results of AST-B throughout microdialysate collection. As indicated by images, it became detectable after 80 min, and maintained similar concentration levels until the end of collection.

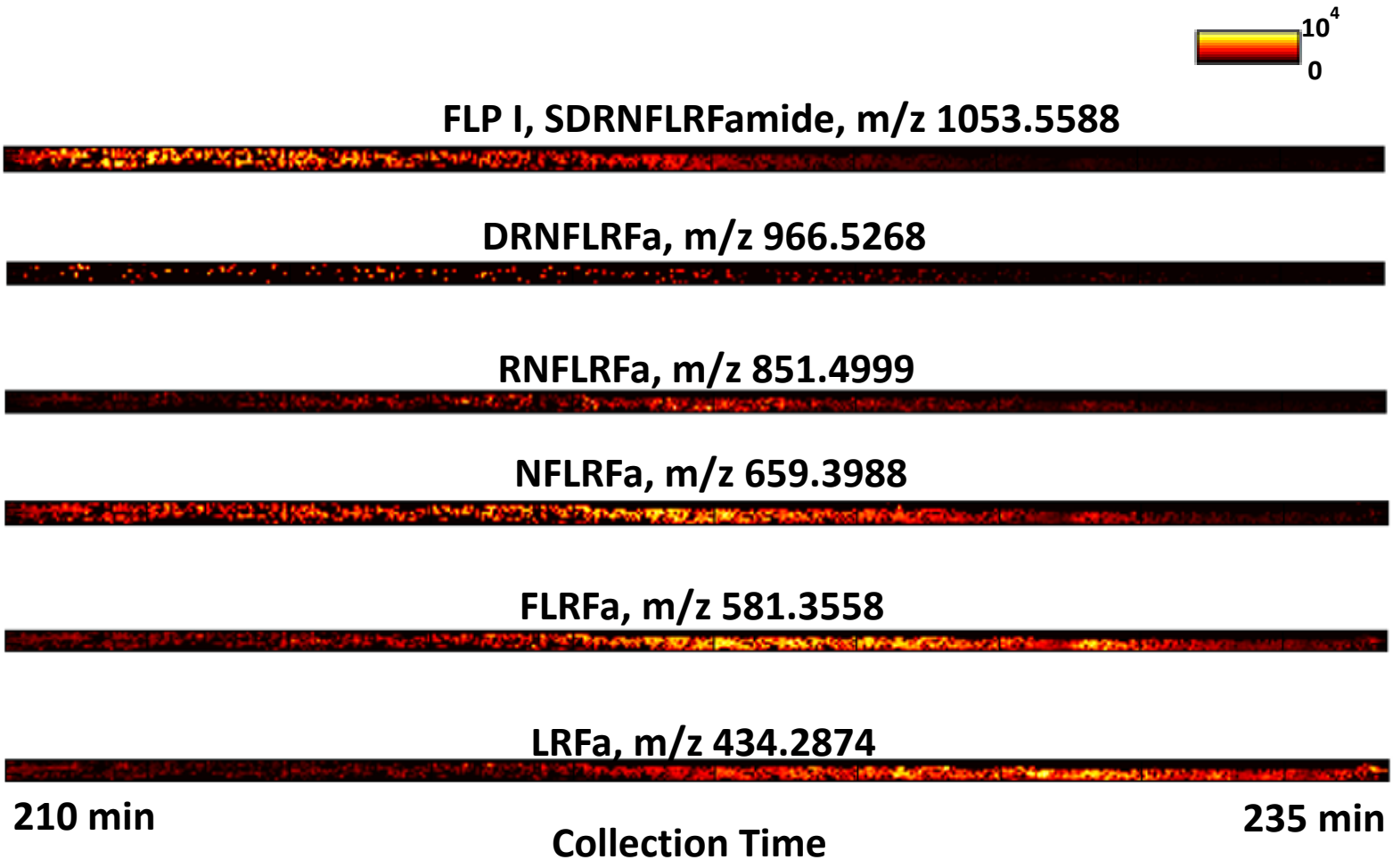

Figure 6-7. Extracted image of FLP I and several degradation products in trace collection from 210 min to 235 min.

Chapter 7

Coupling *In Vivo* Microdialysis with a Multifaceted Mass Spectrometric Platform to Investigate Signaling Molecules and Metabolites in Crustacean

Adapted from: Shan Jiang, **Zhidan Liang**, Ling Hao, Lingjun Li. **'**Investigation of signaling molecules and metabolites found in crustacean hemolymph via in vivo microdialysis using a multi-faceted mass spectrometric platform**'**. *Electrophoresis*, **2016**, *37*, 1031-1038.

Abstract

Physiological processes are regulated by intricate network of cell-cell signaling. Modes of cell-cell signaling include direct cell-cell interaction and actions of secreted signaling molecules. One of the reasons account for the multiple varieties of signaling comes from the wide varieties of secreted signaling molecules. Neurotransmitters (NTs) represent one of the extensively studied signaling molecules and have been proven to play essential roles in regulating various physiological processes in animals. Detection of these molecules is often challenging mostly due to their low concentrations and fast degradation rate. To study secreted NTs in crustacean, herein we employed *in vivo* microdialysis sampling method coupled with mass spectrometry (MS) detection. Capillary electrophoresis (CE) and ion mobility MS were utilized to aid NT detection in this work. MALDI mass spectrometric imaging (MALDI-MSI) technique was used for the identification purpose. The performance of MALDI-MS platform was compared with LC-ESI-MS regarding NT identification. This MALDI-MS-based platform requires much less sample volume benefitted from CE separation and thus enabled improved microdialysis collection temporal resolution by approximately 10 fold compared with LC-ESI-MS analysis. A total of 208 metabolite molecules were identified, of which 39 were identified as secreted signaling molecules. More importantly, this platform promises its application in studying highly dynamic biological events.

7.1 Introduction

Monitoring signaling molecules in the circulatory systems can provide important insight into functional behavior related to environmental change, drug effects, and disease states [1]. *In vivo* microdialysis (MD) is a powerful sampling technique that allows direct collection of signaling molecules from extracellular space with minimum disturbance to their physiological conditions. Usually, MD probe consists of two pieces of microporous tubings sheathed in a semi-permeable membrane that is plugged at one end. With MD probe implanted into area of interest in animals, molecules that fall below the molecular-weight cutoff threshold will passively diffuse across the membrane according to their concentration gradients. Perfusion through the membrane, typically performed at 0.1-3.0μL/min, generates a stream of dialysate that can be analyzed for compounds of interest [2, 3]. MD sampling technique has been applied into a wide variety of tissues and organs in the body including liver, heart, skin, blood, placenta, stomach and ear, with analytes of interest ranging from low molecular weight substances including amino acids and metabolites, to higher molecular substances such as neuropeptides [4-7]. The advantages and benefits of MD enables a variety of applications in neurochemical and clinical studies [8, 9].

Tremendous challenges confront the scientists attempting *in vivo* neurochemical measurements as neurotransmitters may change their concentration rapidly thus requiring high temporal resolution detection capability. The low endogenous level of these compounds presented *in vivo*, typically at nM-pM range [10] is another big hurdle in the detection of these molecules. Despite the unique advantage of *in vivo* sampling of MD, low recovery rate of molecules poses additional challenges. To solve these problems,

researchers made great advancements in both MD sampling and subsequent analysis platform. Attempt to increase MD recovery was made by various means such as affinity-enhanced MD, where affinity agents were added into perfusion fluid and could bind with analytes of interest thus reducing concentration of free analytes and driving more analytes passing through MD membrane [11-14]. High temporal resolution, defined as the shortest time duration over which a dynamic change event can be observed, is critical in MD for the functional study of targeted compounds. To be able to accurately correlate the concentration of analytes with behavior or stimuli, the analysis time must be less than the duration of measured events. As temporal resolution of MD collection is limited by the detection sensitivity, highly sensitive methods like capillary electrophoresis (CE) with laser-induced fluorescence detection have been reported to couple with MD with temporal resolution as high as a few seconds [15-19]. Such methods revealed potential and further improvements in which temporal resolution was limited by flow and diffusion of body fluid. Analysis of MD samples by CE can provide improved temporal resolution compared to LC, as smaller amount of sample is needed for CE separation due to its capability of handling sub-uL volume of samples. Dialysate were on-line or off-line collected and injected to CE system for NTs, amino acids, peptides, and biomarkers detection [20].Decoupling of sampling and detection allows the analysis platform to be extremely versatile. Thus, analytical separation method can be coupled with dialysate collection, to achieve good sensitivity and selectivity for mass spectrometric measurement.

In this work, we employed CE separation coupled to *in vivo* MD on Jonah crab (*Cancer borealis*) to study secreted neurotransmitters (NTs) in crustacean hemolymph.

Instead of analyzing CE fractions by ESI-MS, we incorporated MALDI mass spectrometric imaging (MSI) with CE separation for small molecule identification. With higher tolerance to salts and impurities using MALDI, dialysate from crab was further separated by CE-MSI without desalting and cleaning up steps which significantly reduced sample loss, in the meanwhile, remaining high temporal resolution. NTs have lower molecular mass than peptides or proteins and often makes identifying isobaric molecules challenging. Even with mass error less than 3 ppm, it is still possible to have multiple metabolic features that were unable to separate by CE. To address this issue, second dimension separation were applied and achieved by ion mobility mass spectrometry (IMS). MD-CE fractions of crustacean hemolymph were further separated based on their drift times in the gas phase. With the flexibility of integrating multi-faceted MS platforms, metabolic coverage of crustacean hemolymph was significantly improved. Additionally, multiplexed MSI, which enables full MS and tandem mass fragmentation acquired in parallel, provided more information of bio-chemical characterization compared with previous work. Sensitivity and performance of this platform were also evaluated by comparing to LC-MS approach with high-mass accuracy and high-resolution orbitrap analyzer [21-23].

7.2 Materials and Methods

7.2.1 *Chemicals and Materials*

Acetic acid, ammonium hydroxide, acetone, acetonitrile (ACN), methanol (MeOH), ammonium bicarbonate, and urea were purchased from Fisher Scientific (Pittsburgh, PA). α-Cyano-4-hydroxycinnamic acid (CHCA)and formic acid (FA) were from Sigma Aldrich (St. Louis, MO). Fused-silica capillary with 75 μm i.d. and 365 μm o.d. was purchased from Polymicro Technologies (Phoenix, AZ). A TM-Sprayer from HTX Technologies

(Carrboro, NC) was used to spray MALDI matrix (10 mg/mL CHCA in 50% ACN). Millipore C_{18} Ziptip column was used for sample cleaning, and all water used in this study was doubly distilled on a Millipore filtration system (Bedford, MA).

7.2.2 *Microdialysis Supplies and Procedure*

CMA/20 Elite probes with 4 mm membranes of polyarylethersulfone (PAES) were purchased from CMA Microdialysis (Harvard Apparatus, Holliston, MA, USA). A KD Harvard 22 (Harvard Apparatus, Holliston, MA, USA), and a Pump 11 Elite Nanomite Syringe Pump (Harvard Apparatus, Holliston, MA, USA) were used to drive perfusate through MD probes and tubing. Probes were rinsed with crab saline prior to implantation.

Jonah crabs, *Cancer borealis*, were purchased from Ocean Resources, Inc. (Sedgwick, ME, USA) and The Fresh Lobster Company (Gloucester, MA, USA). Crabs were maintained in an artificial seawater tank at 10–13 °C and were allowed to adjust to the tanks for at least one week after shipment before performing microdialysis. Details of animal housing procedures were described elsewhere [14]. Animals were housed, treated and sacrificed following the animal care protocol in accordance with the University of Wisconsin-Madison's animal care guidelines. The surgery of microdialysis was adapted from previous publications [24]. After the probe was surgically implanted in the crab, the animal was allowed to recover for at least 24 h before dialysate was collected for MS analysis. Physiological crab saline (440 mM NaCl; 11 mM KCl; 13 mM $CaCl_2$; 26 mM $MgCl_2$; 10 mM HEPES acid; pH 7.4, adjusted with NaOH) was used as perfusion solution. The flow rate was set to be 0.5 µL/min by a programmable syringe pump. Dialysate samples were collected with a refrigerated fraction collector (BASi HoneyComb, Bioanalytical Systems, Inc. Indianapolis, IN, USA). The dialysates were concentrated ~10

fold in a SpeedVac (Thermo Fisher Scientific, Waltham, MA, USA) before subsequent analysis.

7.2.3 *CE-MSI*

Interface of CE coupled to mass spectrometric imaging was modified from previous work in our group [25, 26]. Briefly, a 60 cm long with 75 μm i.d./365 μm o.d. fused-silica capillary was pretreated and used for CE separation. A fracture was made near the outlet of the capillary and coated with cellulose acetate membrane to form an ion permeable channel. The inlet end of CE column was placed 15 cm higher than outlet to maintain siphoning flow after retraction by pressure.

CE flow was collected directly on a customized MALDI plate (Thermo Scientific, San Jose, CA, USA) which is mechanically controlled by a syringe pump. After CE elution gets dried, CHCA matrix 10 mg/mL was deposited by an automated sprayer to generating a homogenous trace on the plate. The parameters were carefully adjusted and set as follows: matrix flow rate: 200 mL/min; nozzle velocity: 1200 mm/min; temperature: 85 degree Celsius; gas pressure: 13 psi; line spacing: 3mm; number of layers: 2; dry time: 1 min. The acquired CE trace was then analyzed by a MALDI LTQ Orbitrap XL (Thermo Scientific, San Jose, CA, USA) with imaging experimental set up. In order to improve multiplexing and throughput, instrument method consisting of full MS scan at m/z 100-900 as well as several tandem mass scans was set up in parallel so that more powerful information of chemical characterization is benefit with reduced sample preparation time and increased reproducibility. By setting up raster and spiral movements of MALDI laser beam, orbitrap full scans were acquired every 100 μm with 11 μJ MALDI laser energy, followed by three

targeted ion trap tandem mass scans at 50 μm with HCD collision energy ranging from 35 to 55. The imaging data was further processed by ImageQuest software.

7.2.4 *MALDI-Ion Mobility Mass Spectrometry*

Data was acquired on a MALDI-IM-MS instrument (Synapt G2 Q-TOF, Waters, Milford, MA, USA) with a YAG laser with a repetition rate of 200 Hz. External calibration was performed using Glu-1-Fibrinopeptide B (Glu-Fib) standard of 1.0 μM before each experiment. Mass spectra were acquired in sensitivity mode and over a mass range of m/z 100 to 900 for MD-CE fractions of crustacean hemolymph. Laser energy attenuation was 300 (arbitrary units). Ion mobility separation was performed at a drift gas pressure of 2.30 Torr using nitrogen gas, a wave velocity of 650 m/s, and a wave height of 40.0 V.

7.2.5 *LC-MS Analysis*

LC-MS approach was also carried out to compare the performance of MALDI platform. The automated combination of positive and negative ionization method was utilized to achieve comprehensive identification of small molecule metabolites. This extended feature of fast polarity switching in Orbitrap analyzer enables unbiased detection of metabolites in complex biological samples. For LC-MS analysis, microdialysate was collected for five hours, desalted by C_{18} Ziptip, and concentrated into 0.1% FA in H_2O. Dionex UltiMate 3000 LC system was coupled with a Q-Exactive™ Orbitrap mass spectrometer (San Jose, CA). Metabolite separation was achieved on a Phenomenex biphenyl column (75.1 μm × 150 mm, 1.7 μm, 100 Å) at a flow rate of 0.3 ml/min. Mobile phase A was 0.1% FA in H_2O and mobile phase B was 0.1% FA in MeOH. The 12 min binary gradient was set as follows: 0-5 min, 0-2% solvent B; 5-10 min, 2%-50% solvent B; 10-12min, 90% solvent B. Full MS scans were acquired from 70 to 1000 m/z for both

positive and negative ESI mode. Resolution was 70 K, automatic gain control (AGC) target was 1×10^6, and maximum injection time (IT) was 100 ms. Raw data files were processed by SIEVE^{TM} software for peak alignment and framing to generate a list of detected mass features.

7.3 Results and Discussion

7.3.1 *CE-MSI offline coupled to in vivo MD sampling technique (MD-CE-MSI) for untargeted metabolomics study*

Our group has employed MD sampling technique on crabs to study neuropeptide content in the circulating hemolymph [4, 14, 24]. But the study on NT in the system, which is an essential component of neuromodulators in the nervous system, was lacking. One of the advantages of MD sampling is that it yields cleaner samples due to the size-defined molecular weight cut off dialysis membrane which excludes large molecules such as proteins, lipids and proteases. Two-hour collection duration was selected and the resulting dialysate was concentrated ten folds before CE-MSI analysis. As an alternative ionization tool to ESI, MALDI-MS offers complementary coverage of analytes in complex sample. More importantly, coupling CE with MALDI-MS provides increased flexibility for the independent optimization of CE and MS experiments and makes the CE fractions available for reanalysis and further biochemical characterization. In MD coupled to CE MALDI imaging experiments, a syringe pump was used to drive crab saline through MD probes at a flow rate of 0.5 uL/min. Offline CE separation was performed on a homemade CE device, a fracture was made near the outlet of the CE capillary, and then coated with cellulose acetate membrane to form an ion permeable channel. In order to preserve the resolution from separation dimension, we introduced trace level mass spectrometric imaging

incorporated with CE. Instead of getting discrete spots on MALDI plate and excessive amount of MS profiles to process, CE elution was continuously collected on a horizontally moving MALDI target plate on top of a syringe pump. CHCA of 10 mg/mL delivered by a TM sprayer formed a uniform and homogenous matrix layer on the acquired CE trace. With higher tolerance to contaminations and impurities using MALDI, we omitted desalting steps prior to MALDI Orbitrap analysis, which increases the recovery rate of target analytes.

7.3.2 *Multiplex imaging of MD-CE-MSI*

MD-CE-MSI data was acquired in the small molecule range m/z 100-900 Da on a MALDI Orbitrap analyzer. Each analyte appeared as the colored image which can be extracted from background in the trace. **Figure 8-1** (D) showed the TIC of the imaging data of CE separation from 2 min to 20 min, in which signals were all over the trace since it contained both analytes of interest and matrix peaks. Unlike TIC or matrix, target analytes featured specific elution time, indicated by the colored region in the CE trace showed in **Figure 8-1** (A, B and C). A couple of representative image extracted were shown here, in which 5-HIAA, the main metabolite of serotonin through enzymatic conversion by monoamine oxidase-A, was eluted at 11 min. According to distinct CE migration time, each spatial point on ROI represents a specific mass spectrum. Also each m/z value corresponds to a unique colored image. **Figure 8-1** (B) showed MSI data of aminobenzoic acid, a substrate of enzyme anthranilate hydroxylase in benzoate degradation via hydroxylation pathway, also known as a component of tryptophan metabolism. Different small molecules also featured different image patterns. As shown in **Figure 8-1** (C), it could be either proline $[M+K]^+$, or acetamidopropanal which is an oxidatively reactive by

product under the disturbance in polyamine metabolism, and is associated with urea cycle and metabolism of arginine, proline, glutamate, aspartate and asparagine. The MALDI mass spectra of each metabolites and their corresponding structures were provided in **Figure 8-1** (E, F, G), respectively.

By setting up raster and spiral movements of MALDI laser beam, orbitrap full MS was acquired every 100 μm, followed by three targeted ion trap tandem mass scans at 50 um illustrated by **Figure 8-2** (C). Taking one of the NTs identified from MD-CE-MSI as an example, showed in **Figure 8-2** (E), the precursor and fragment ions of observed dopamine (DA) matched pretty well with DA standard. The imaging data can also be demonstrated by a three-dimensional **Figure 8-2** (B), in which we had the CE separation time as X axis, and image width as Y axis, the extra Z axis represented signal intensity of the extracted region of interest (ROI). With the ability of doing tandem mass fragmentation on MD-CE-MSI, analytes were identified with higher confidence and revealed the potential of studying neurotransmitters in a more targeted way. However, ambiguity still existed when assigning the identities of these neurotransmitters, as many small molecules shared the exact same m/z even with mass accuracy less than 3 ppm. For one identical mass, it possibly contains multiple metabolic features. In order to address this problem, we employed second dimension for separation, ion mobility, combined with MALDI MS (MALDI-IMS).

7.3.3 *MALDI-IMS for separation of isobaric molecules*

Ion mobility (IM) brings an added value to MALDI-MS by separation of different compounds families. The ion mobility cell, positioned between quadrupole and time-of-flight analyzer in Synapt G2 mass spectrometer, allows the separation of isobaric

compounds with similar m/z based on their conformations, which cannot be differentiated by single mass criterion [27-29]. Different ion conformations have different ion cross sections and result in different drift time. This particular property makes it comparable to LC separation and allows for separation and identification of chemical families such as matrix, lipids, and small molecules by their retention time inside the ion mobility cell. Here MD-CE fractions of crustacean hemolymph were further separated by ion mobility mass spectrometry. As observed in the averaged mass spectrum of one fraction eluted at 11min measured with MALDI-IM-MS in **Figure 8-3** (A), many compounds had same/z, but it is possible to discriminate between them according to their drift time. **Figure 8-3** (B) showed the driftscope corresponding to the 3D visualization of detected signals. The mass scale was y axis, the drift time was x axis, and the color scale representing signal intensity constituted the third dimension of the driftscope. Target analytes were filtered from background at a minimum intensity threshold of 1,000 counts visualized in this 3D mapping **Figure 8-3** (C). As shown in the figure, isobaric ions were successfully separated by their different conformations in the mobility cell.

The zoomed in driftscope **Figure 8-4** illustrated how the added drift time differentiated isobaric small molecules from diverse classes. Taking the metabolite of m/z 191.0468 as an example, four different small molecules showed on driftsope in the mass range of 1 Da, indicated by red dots in white circle in the enlarged driftscope visualization **Figure 8-4** (A and B). Three of them shared the same m/z of 191.0468, and were successfully separated by their mobility in gas phase. Although only one peak was observed in the mass spectrum, it actually contained three different compounds. Through HMDB search, they were 2,3-diaminosalizylic acid found in blood, sodiated adduct of

pyrroloylglycine which is the biomarker of hyperlipidemia and 1-(2-Furanyl)-1-pentanone appears to be an additive found in animal food. The other metabolite co-eluted in this MD-CE fraction was protonated ion 191.1280, which was matched as beta-damascenone belonging to lipid class. This example illustrated how ion mobility differentiates a large number of isobaric molecules by their IM retention time and gets rid of the exogenous metabolites. Approximately 20% more peaks have been detected with the addition of ion mobility separation.

7.3.4 *LC-MS approach for comprehensive investigation and comparison to MALDI platform*

Lastly, the performance of multi-staged MALDI platform was further evaluated by comparing it with LC-MS approach. We utilized the automated combination of positive and negative ionization mode mass spectra derived from fast polarity switching that has been widely used in lipidomics and drug metabolomics area [30, 31]. This extension enables the automated and unbiased detection of metabolites in complex biological samples and provided complementary identification of untargeted metabolomics [32, 33]. Owing to fast polarity switching approach, two total ion chromatograms revealed its benefit of complementary recognition gained from the integration of two ionization modes as shown in **Figure 8-5** (A and B). Resulting data was aligned by SIEVE^{TM} for peak detection and processed through HMDB, yielding 140 metabolites identified in total. Among them, 85 of those were detected exclusively using LC-ESI approach. For MALDI-MS platform integrated with CE imaging and ion mobility, 71 were uniquely found. A list of the small molecule metabolites was provided in **Table 7-1**. These findings underlined the

comparable and complementary performance in metabolite identification gained by incorporating multi-faceted separation techniques.

7.4 Concluding Remarks

In summary, we applied micro-separation approaches, CE and ion mobility, coupled with multiplexed MALDI imaging platform for small molecule NT identification. LC-MS was also used for evaluation and comprehensive investigation, yielding 211 small molecule metabolites identified in total. Among them, 33 are amino acids and amino acid pairs, 50 are fatty acids, 3 of them are nucleosides, 40 are signaling neurotransmitters while the rest are their derivatives. More importantly, the improved temporal resolution with CE-MSI platform, 5 min, comparing to 1h dialysate collection in LC-MS approach, enables more accurate monitoring of NT release and promises for more powerful function-related deduction.

7.5 References

1. Kennedy, R.T., *Emerging trends in in vivo neurochemical monitoring by microdialysis.* Current Opinion in Chemical Biology, 2013. **17**(5): p. 860-867.
2. Watson, C.J., Venton, B.J., and Kennedy, R.T., *In Vivo Measurements of Neurotransmitters by Microdialysis Sampling.* Analytical Chemistry, 2006. **78**(5): p. 1391-1399.
3. OuYang, C., Liang, Z., and Li, L., *Mass spectrometric analysis of spatio-temporal dynamics of crustacean neuropeptides.* Biochimica et Biophysica Acta (BBA) - Proteins and Proteomics, 2015. **1854**(7): p. 798-811.
4. Behrens, H.L., Chen, R., and Li, L., *Combining Microdialysis, NanoLC-MS, and MALDI-TOF/TOF To Detect Neuropeptides Secreted in the Crab,Cancer borealis.* Analytical Chemistry, 2008. **80**(18): p. 6949-6958.
5. Nandi, P. and Lunte, S.M., *Recent trends in microdialysis sampling integrated with conventional and microanalytical systems for monitoring biological events: A review.* Analytica Chimica Acta, 2009. **651**(1): p. 1-14.
6. Shippenberg, T.S. and Thompson, A.C., *Overview of Microdialysis.* 2001.
7. Cebada, J., Alvarado-Álvarez, R., Becerra, E., Neri-Bazán, L., Rocha, L., and García, U., *An improved method for long-term measuring of hemolymph fluctuations of non-essential amino acids, GABA and histamine from freely moving crayfish.* Journal of Neuroscience Methods, 2006. **153**(1): p. 1-7.
8. Timofeev, I., Carpenter, K.L.H., Nortje, J., Al-Rawi, P.G., O'Connell, M.T., Czosnyka, M., Smielewski, P., Pickard, J.D., Menon, D.K., Kirkpatrick, P.J., Gupta, A.K., and Hutchinson, P.J., *Cerebral extracellular chemistry and outcome following traumatic brain injury: a microdialysis study of 223 patients.* Brain, 2011. **134**(2): p. 484-494.
9. Bossers, S.M., de Boer, R.D.H., Boer, C., and Peerdeman, S.M., *The diagnostic accuracy of brain microdialysis during surgery: a qualitative systematic review.* Acta Neurochirurgica, 2012. **155**(2): p. 345-353.
10. Li, Q., Zubieta, J.-K., and Kennedy, R.T., *Practical Aspects of in Vivo Detection of Neuropeptides by Microdialysis Coupled Off-Line to Capillary LC with Multistage MS.* Analytical Chemistry, 2009. **81**(6): p. 2242-2250.
11. Duo, J. and Stenken, J.A., *Heparin-immobilized microspheres for the capture of cytokines.* Analytical and Bioanalytical Chemistry, 2010. **399**(2): p. 773-782.
12. Duo, J. and Stenken, J.A., *In vitro and in vivo affinity microdialysis sampling of cytokines using heparin-immobilized microspheres.* Analytical and Bioanalytical Chemistry, 2010. **399**(2): p. 783-793.
13. Pettersson, A., Amirkhani, A., Arvidsson, B., Markides, K., and Bergquist, J., *A Feasibility Study of Solid Supported Enhanced Microdialysis.* Analytical Chemistry, 2004. **76**(6): p. 1678-1682.

14. Schmerberg, C.M. and Li, L., *Mass Spectrometric Detection of Neuropeptides Using Affinity-Enhanced Microdialysis with Antibody-Coated Magnetic Nanoparticles.* Analytical Chemistry, 2013. **85**(2): p. 915-922.

15. Lada, M.W., Vickroy, T.W., and Kennedy, R.T., *High Temporal Resolution Monitoring of Glutamate and Aspartate in Vivo Using Microdialysis On-Line with Capillary Electrophoresis with Laser-Induced Fluorescence Detection.* Analytical Chemistry, 1997. **69**(22): p. 4560-4565.

16. Hogan, B.L., Lunte, S.M., Stobaugh, J.F., and Lunte, C.E., *Online Coupling of in vivo Microdialysis Sampling with Capillary Electrophoresis.* Analytical Chemistry, 1994. **66**(5): p. 596-602.

17. Zhou, Y., Mabrouk, O.S., and Kennedy, R.T., *Rapid Preconcentration for Liquid Chromatography–Mass Spectrometry Assay of Trace Level Neuropeptides.* Journal of The American Society for Mass Spectrometry, 2013. **24**(11): p. 1700-1709.

18. Wang, M., Hershey, N.D., Mabrouk, O.S., and Kennedy, R.T., *Collection, storage, and electrophoretic analysis of nanoliter microdialysis samples collected from awake animals in vivo.* Analytical and Bioanalytical Chemistry, 2011. **400**(7): p. 2013-2023.

19. Hao, L., Zhong, X., Greer, T., Ye, H., and Li, L., *Relative quantification of amine-containing metabolites using isobaric N,N-dimethyl leucine (DiLeu) reagents via LC-ESI-MS/MS and CE-ESI-MS/MS.* Analyst, 2015. **140**: p. 467-475.

20. Guihen, E. and O'Connor, W.T., *Capillary and microchip electrophoresis in microdialysis: Recent applications.* Electrophoresis, 2010. **31**(1): p. 55-64.

21. Kluger, B., Bueschl, C., Neumann, N., Stückler, R., Doppler, M., Chassy, A.W., Waterhouse, A.L., Rechthaler, J., Kampleitner, N., Thallinger, G.G., Adam, G., Krska, R., and Schuhmacher, R., *Untargeted Profiling of Tracer-Derived Metabolites Using Stable Isotopic Labeling and Fast Polarity-Switching LC–ESI-HRMS.* Analytical Chemistry, 2014. **86**(23): p. 11533-11537.

22. Yamada, M., Kita, Y., Kohira, T., Yoshida, K., Hamano, F., Tokuoka, S.M., and Shimizu, T., *A comprehensive quantification method for eicosanoids and related compounds by using liquid chromatography/mass spectrometry with high speed continuous ionization polarity switching.* Journal of Chromatography B, 2015. **995-996**: p. 74-84.

23. Oh, H.-A., Kim, D., Lee, S.H., and Jung, B.H., *Simultaneous quantitative determination of celecoxib and its two metabolites using liquid chromatography–tandem mass spectrometry in alternating polarity switching mode.* Journal of Pharmaceutical and Biomedical Analysis, 2015. **107**: p. 32-39.

24. Liang, Z., Schmerberg, C.M., and Li, L., *Mass spectrometric measurement of neuropeptide secretion in the crab, Cancer borealis, by in vivo microdialysis.* The Analyst, 2015. **140**(11): p. 3803-3813.

25. Wang, J., Ye, H., Zhang, Z., Xiang, F., Girdaukas, G., and Li, L., *Advancing Matrix-Assisted Laser Desorption/Ionization-Mass Spectrometric Imaging for*

Capillary Electrophoresis Analysis of Peptides. Analytical Chemistry, 2011. **83**(9): p. 3462-3469.

26. Zhang, Z., Ye, H., Wang, J., Hui, L., and Li, L., *Pressure-Assisted Capillary Electrophoresis Coupling with Matrix-Assisted Laser Desorption/Ionization-Mass Spectrometric Imaging for Quantitative Analysis of Complex Peptide Mixtures.* Analytical Chemistry, 2012. **84**(18): p. 7684-7691.

27. Stauber, J., MacAleese, L., Franck, J., Claude, E., Snel, M., Kaletas, B.K., Wiel, I.M.V.D., Wisztorski, M., Fournier, I., and Heeren, R.M.A., *On-tissue protein identification and imaging by MALDI-Ion mobility mass spectrometry.* Journal of the American Society for Mass Spectrometry, 2010. **21**(3): p. 338-347.

28. Xu, L., Kliman, M., Forsythe, J.G., Korade, Z., Hmelo, A.B., Porter, N.A., and McLean, J.A., *Profiling and Imaging Ion Mobility-Mass Spectrometry Analysis of Cholesterol and 7-Dehydrocholesterol in Cells Via Sputtered Silver MALDI.* Journal of the American Society for Mass Spectrometry, 2015. **26**(6): p. 924-933.

29. Cole, L.M., Mahmoud, K., Haywood-Small, S., Tozer, G.M., Smith, D.P., and Clench, M.R., *Recombinant " IMS TAG" proteins - A new method for validating bottom-up matrix-assisted laser desorption/ionisation ion mobility separation mass spectrometry imaging.* Rapid Communications in Mass Spectrometry, 2013. **27**(21): p. 2355-2362.

30. Gallart-Ayala, H., Courant, F., Severe, S., Antignac, J.P., Morio, F., Abadie, J., and Le Bizec, B., *Versatile lipid profiling by liquid chromatography–high resolution mass spectrometry using all ion fragmentation and polarity switching. Preliminary application for serum samples phenotyping related to canine mammary cancer.* Analytica Chimica Acta, 2013. **796**: p. 75-83.

31. Shin, M., Ji, D., Kang, S., Yang, W., Choi, H., and Lee, S., *Screening of multiple drugs of abuse and metabolites in urine using LC/MS/MS with polarity switching electrospray ionization.* Archives of Pharmacal Research, 2013. **37**(6): p. 760-772.

32. Guo, B., Wang, M., Liu, Y., Zhou, J., Dai, H., Huang, Z., Shen, L., Zhang, Q., and Chen, B., *Wide-Scope Screening of Illegal Adulterants in Dietary and Herbal Supplements via Rapid Polarity-Switching and Multistage Accurate Mass Confirmation Using an LC-IT/TOF Hybrid Instrument.* Journal of Agricultural and Food Chemistry, 2015. **63**(31): p. 6954-6967.

33. Braña-Magdalena, A., Leão-Martins, J.M., Glauner, T., and Gago-Martínez, A., *Intralaboratory Validation of a Fast and Sensitive UHPLC/MS/MS Method with Fast Polarity Switching for the Analysis of Lipophilic Shellfish Toxins.* Journal of AOAC International, 2014. **97**(2): p. 285-292.

7.6 Figures and Tables

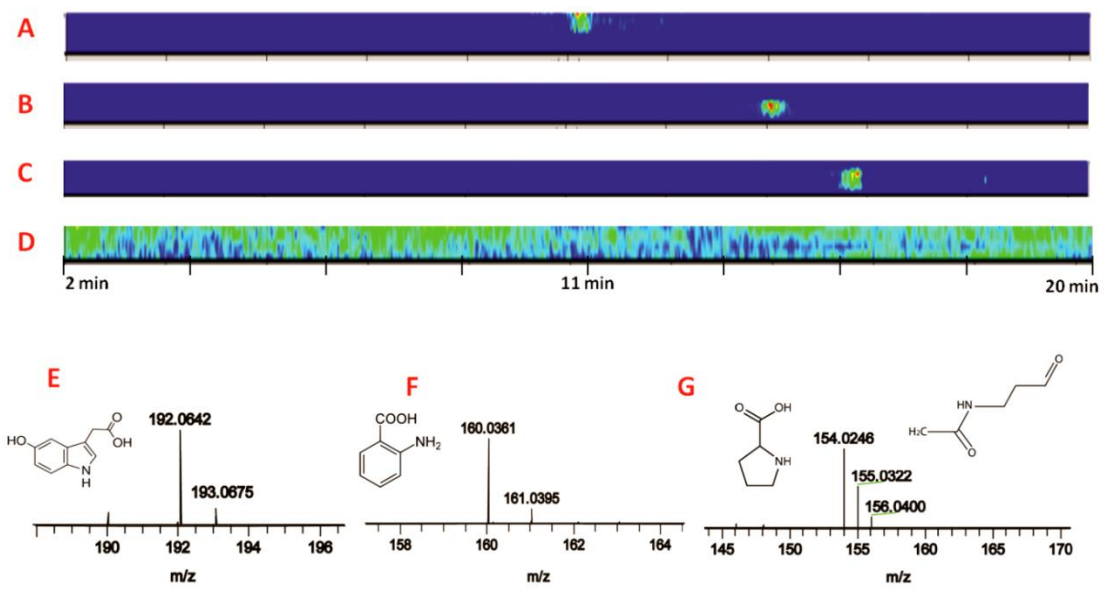

Figure 7-1. MALDI Orbitrap imaging of small molecule metabolites separated by CE.

(A, B, C) 2D image of 5-HIAA $[M+H]^+$, aminobenzoic acid and proline $[M+K]^+$/acetamidopropanal, respectively. (D) Image of total ion count (TIC) of the acquired CE-MSI. (E, F, G) Mass spectra and structures of 5-HIAA $[M+H]^+$, aminobenzoic acid and proline $[M+K]^+$/acetamidopropanal, respectively.

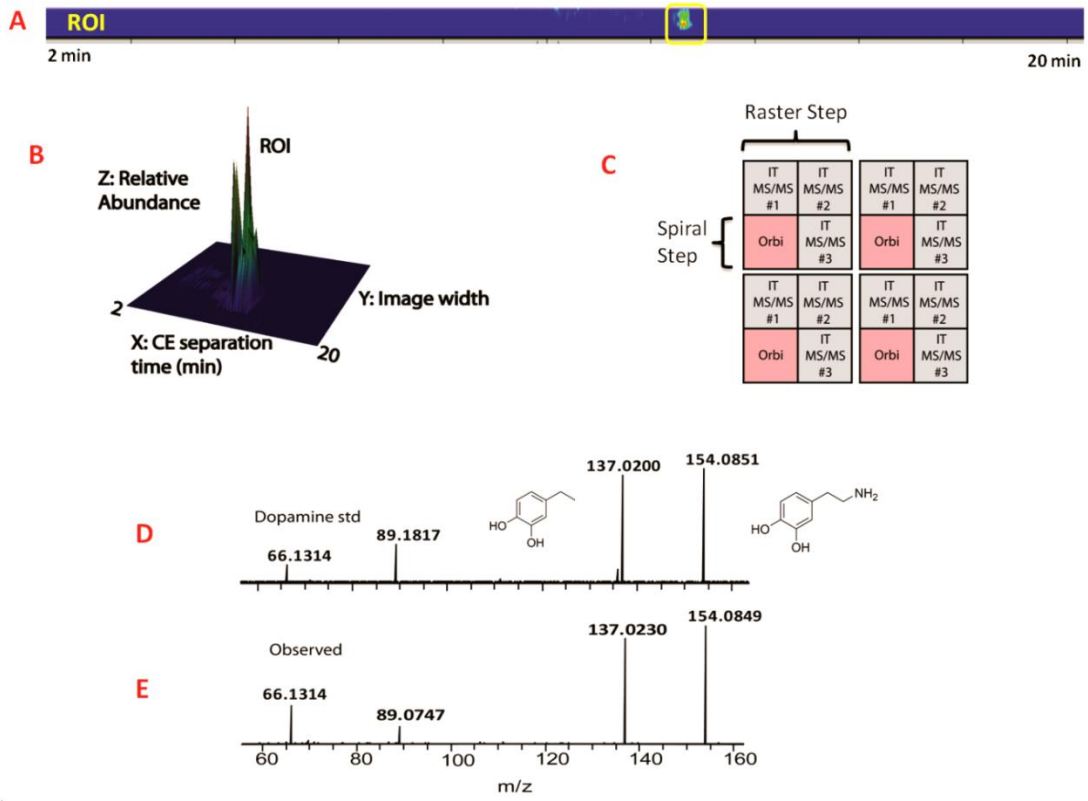

Figure 7-2. Illustration of multiplexed MD-CE-MSI on MALDI Orbitrap instrument.

(A) 2D imaging of dopamine identified in MD-CE-MSI. (B) 3D imaging of dopamine identified in MD-CE-MSI. The x axis in the 3D image represents CE separation time from 2 to 20 min. Y axis is the width of the CE image that is 0.6-1.0 mm. Z axis showed relative abundance of the extracted ion from TIC. (C) Illustration of laser movement in the multiplexed method. Orbitrap full scan was acquired every 100 µm shown in pink color, followed by three ion trap tandem mass fragmentation every 50 µm. (D) MS/MS fragmentation of dopamine standard acquired under the same experimental condition acquired on MALDI Orbitrap. (E) MS/MS spectrum of observed dopamine in MD-CE-MSI.

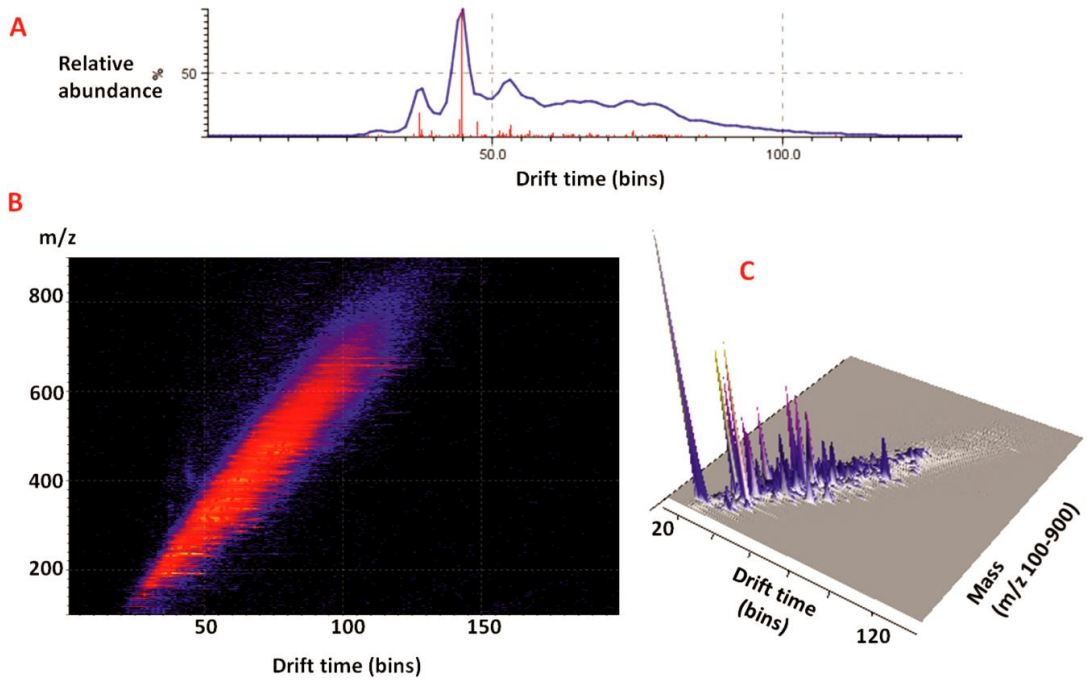

Figure 7-3. Ion mobility separation of MD-CE fractions.

(A) Total ion chromatogram of MD-CE fraction eluted at 12min which is further separated by ion mobility mass spectrometry. (B) Figure from drift scope showed drift times of small molecules from m/z 100 to 900. (C) As shown in 3D drift scope, isobaric molecules in one MD-CE fraction were successfully separated by their drift times.

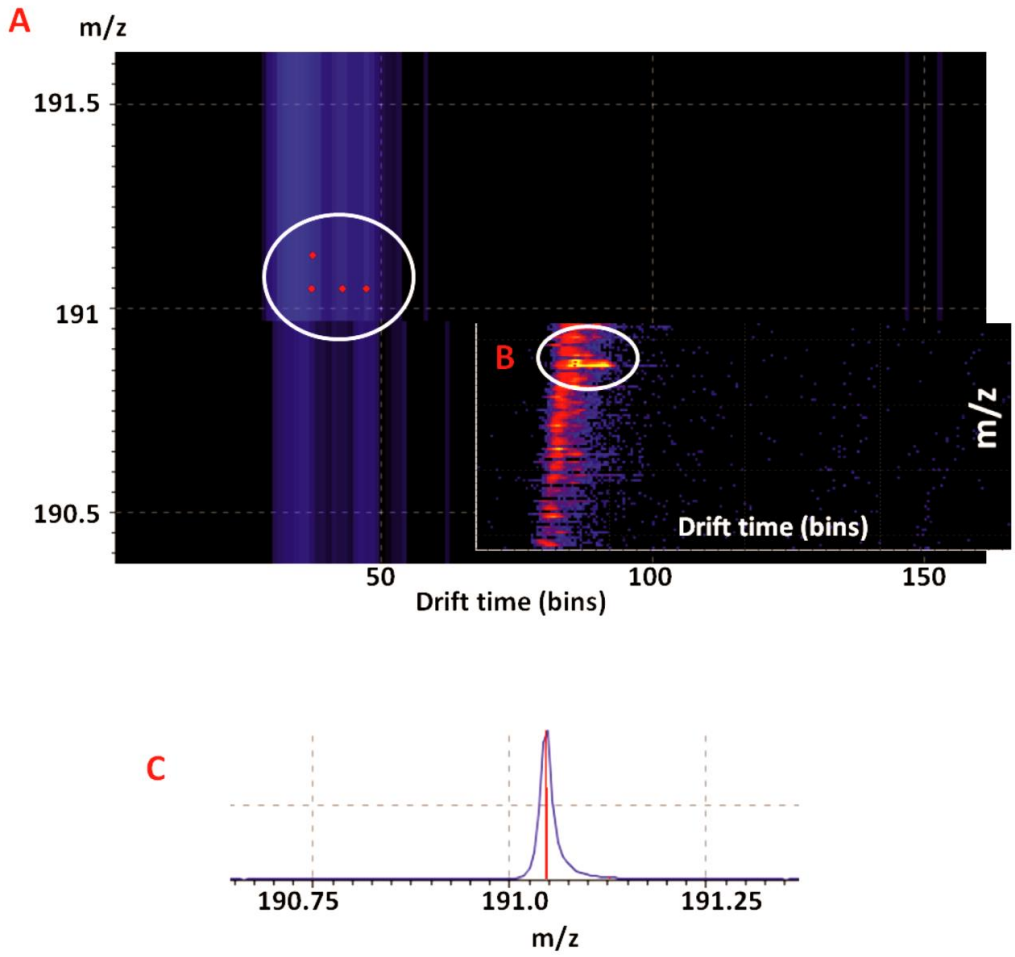

Figure 7-4. Ion mobility separation of small molecules in different classes with identical mass.

(A) Zoom in figure of four different compounds eluted in one chromatographic peak. (B) Heat map of isobaric compounds filtered from background. (C) Chromatographic peak shared by four different molecules.

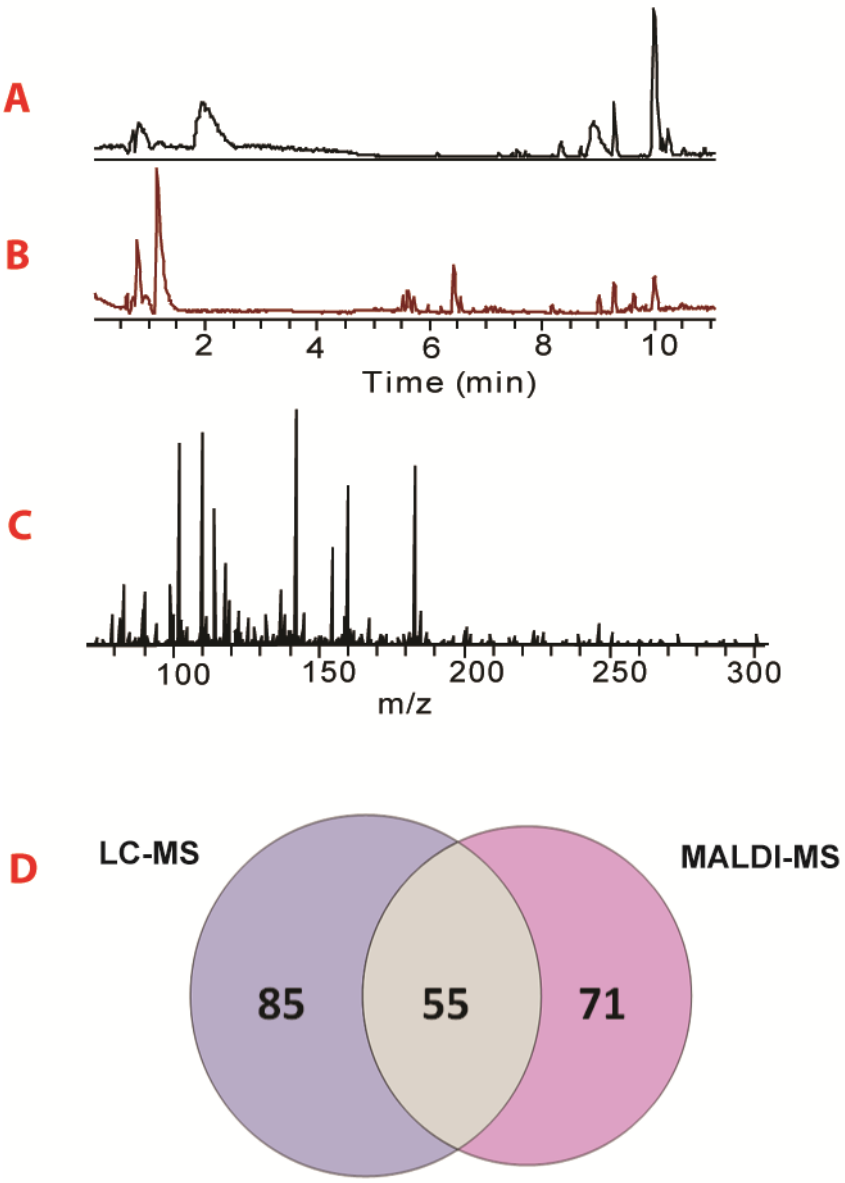

Figure 7-5. Untargeted LC-MS analysis of hemolymph metabolites.

(A) Base peak ion chromatograph acquired in negative mode. (B) Base peak chromatograph acquired in positive mode. (C) Averaged mass spectrum of detected mass features. (D) Venn diagram showed comparison of metabolomics identification of MALDI-MS and LC-MS platform. 85 metabolites were identified only by LC-MS, while 71 metabolites were exclusively found by MALDI-MSI platform.

Table 7-1. Complementary identification of metabolites by MALDI-MSI and ESI-MS*.

Compound MW	Composition	Compound ID	MALDI	ESI
92.0478	$C_3H_9O_3$	Glycerol		x
99.1052	$C_6H_{14}N$	2-Methylpiperidine		x
101.1208	$C_6H_{16}N$	Hexylamine		x
103.0633	$C_4H_9NO_2$	Dimethylglycine		x
103.0633	$C_4H_9NO_2$	N-Ethylglycine		x
103.0637	$C_4H_{10}O_2N$	Aminoisobutyric acid		x
104.059	$C_3H_9O_2N_2$	2,3-Diaminopropionic acid	x	x
105.0793	$C_4H_{12}O_2N$	Diethanolamine	x	x
115.0636	$C_5H_{10}O_2N$	Proline	x	x
116.084	$C_6H_{13}O_2$	2-Methylpropyl acetate	x	
117.0792	$C_5H_{12}O_2N$	L-Valine	x	x
117.0792	$C_5H_{12}O_2N$	Norvaline	x	
119.0583	$C_4H_{10}O_3N$	L-Threonine	x	
122.0482	$C_6H_7ON_2$	Niacinamide	x	
127.0634	$C_6H_{10}O_2N$	D-1-Piperideine-2-carboxylic acid	x	x
127.0998	$C_7H_{14}ON$	1-(1-Pyrrolidinyl)-2-propanone		x
131.0947	$C_6H_{14}O_2N$	Leucine	x	
132.0419	$C_6H_3N_4$	Dodecanedioic acid		x
134.0943	$C_6H_{15}O_3$	Polypropylene glycol		x
136.0385	$C_5H_5ON_4$	Threonic acid	x	
137.0477	$C_7H_8O_2N$	Aminobenzoic acid	x	x
137.0841	$C_8H_{12}ON$	Tyramine	x	
139.0996	$C_8H_{14}ON$	4,5-Dimethyl-2-propyloxazole		x
141.1153	$C_8H_{16}ON$	Conhydrinone	x	
143.0735	$C_{10}H_{10}N$	Quinaldine		x
143.0945	$C_7H_{14}O_2N$	Proline betaine	x	
144.1262	$C_7H_{17}ON_2$	N-Acetylcadaverine		x
145.0738	$C_6H_{12}O_3N$	Isobutyrylglycine	x	
146.0576	$C_7H_5N_4$	Trimethoprim		x
147.0684	$C_9H_{10}ON$	3-(2-Furanylmethyl)-1H-pyrrole		x
148.0524	$C_9H_9O_2$	Cinnamic acid	x	
152.0949	$C_8H_{13}ON_2$	Isopropyl-methoxypyrazine	x	
153.0173	$C_5H_9NO_2$	Acetamidopropanal	x	
153.0789	$C_8H_{11}NO_2$	Dopamine	x	
157.1102	$C_8H_{16}O_2N$	Homostachydrine		
158.0577	$C_8H_5N_4$	Vitamin B5		x

159.1259	$C_8H_{18}O_2N$	2-Aminooctanoic acid	x	x
160.0887	$C_{11}H_{13}O$	3-Phenyl-4-pentenal	x	
161.1051	$C_7H_{16}O_3N$	L-Carnitine		x
162.1255	$C_8H_{19}O_3$	(3R,7R)-1,3,7-Octanetriol		x
165.0789	$C_9H_{12}O_2N$	Phenylalanine	x	
165.0789	$C_9H_{12}O_2N$	L-Phenylalanine	x	x
170.1305	$C_{10}H_{19}O_2$	Citronellic acid		x
173.0686	$C_8H_6N_5$	Methylglutaric acid		x
176.0472	$C_{10}H_9O_3$	4-Methylumbelliferone	x	x
177.9974	$C_2H_3O_6N_4$	Arsenobetaine	x	
179.1673	$C_{12}H_{22}N$	Memantine		x
187.0844	$C_9H_8N_5$	Phthalic acid		x
187.1196	$C_9H_{16}O_3N$	3 or 9 Hydroxydecanoic acid		x
187.1207	$C_9H_{18}O_3N$	Polyethylene glycol		x
187.1207	$C_9H_{18}O_3N$	N-Heptanoylglycine		x
188.1035	$C_9H_{15}O_4$	Histidinyl-Arginine	x	x
188.1399	$C_{10}H_{19}O_3$	N-Acetyldopamine	x	
188.1524	$C_9H_{21}O_2N_2$	N6,N6,N6-Trimethyl-L-lysine	x	x
190.0395	$C_7H_8N_2O_3$	2,3-Diaminosalicylic acid	x	
190.0395	$C_7H_8N_2O_3$	2-Pyrroloylglycine	x	
190.1355	$C_{13}H_{19}O$	beta-Damascenone	x	x
191.0436	$C_6H_{10}O_6N$	gamma-Carboxyglutamic acid	x	x
191.0582	$C_{10}H_9NO_3$	5HIAA	x	
194.093	$C_{11}H_{13}O_3$	3-Oxododecanoic acid	x	
195.0882	$C_{10}H_{12}O_3N$	13E-tetranor-16-carboxy-LTE4		x
197.0674	$C_5H_8O_2N_7$	DL-Dopa/N-Hydroxy-L-tyrosine		x
198.1618	$C_{12}H_{23}O_2$	Dodec-2-enoic acid	x	
202.0452	$C_4H_7O_4N_6$	D-Glucose	x	
203.1145	$C_9H_{16}O_4N$	2 or 3 or 4-Octenedioic acid	x	
203.1156	$C_9H_{18}O_4N$	L-Acetylcarnitine		x
204.051	$C_6H_5ON_8$	Cyromazine	x	
204.0899	$C_{11}H_{13}O_2N_2$	Tryptophan	x	x
204.1148	$C_{13}H_{17}O_2$	6-(1-Hydroxyethyl)-2,2-dimethyl-2H-1-benzopyran		x
207.0387	$C_7H_6O_3N_5$	2-Amino-4-hydroxy-6-pteridinecarboxylic acid	x	
207.0884	$C_{11}H_{12}O_3N$	Inosine	x	x
207.0894	$C_{11}H_{14}O_3N$	Phenylpropionylglycine	x	x
210.1618	$C_{13}H_{23}O_2$	Citral propylene glycol acetal		x
211.0834	$C_{10}H_{12}O_4N$	2-Octenedioic acid	x	
212.0947	$C_{13}H_{13}ON_2$	Harmine		x
212.1142	$C_6H_{13}ON_8$	L-prolyl-L-proline	x	x
213.0256	$C_4H_4O_4N_7$	Carboxyglutamic acid	x	x

213.0999	$C_{10}H_{16}O_4N$	Phenazopyridine	x	x
214.1558	$C_{12}H_{21}O_3$	Olmesartan		x
215.1511	$C_{11}H_{20}O_3N$	3,4-Methylenesebacic acid	x	
215.152	$C_{11}H_{22}O_3N$	N-Nonanoylglycine	x	
216.135	$C_{11}H_{19}O_4$	Ribose-1-arsenate		x
217.1313	$C_{10}H_{20}O_4N$	Propionylcarnitine	x	x
218.1881	$C_{12}H_{27}O_3$	8,8-Dimethoxy-2,6-dimethyl-2-octanol	x	
219.1096	$C_9H_{16}O_5N$	Succinylacetone	x	
220.1098	$C_{13}H_{17}O_3$	Ethyl 2-benzylacetoacetate		x
222.089	$C_{12}H_{15}O_4$	Monoisobutyl phthalic acid		x
224.1886	$C_{13}H_{25}ON_2$	Cuscohygrine	x	x
225.0764	$C_9H_{12}O_4N_3$	Polyethylene glycol	x	x
225.944	H_3O_{14}	2,5-Dichloro-4-oxohex-2-enedioate	x	x
226.014	$C_{15}HON_2$	Phenyl vinyl sulfide		x
226.1064	$C_9H_{15}O_3N_4$	Histidinyl-Alanine	x	x
226.1195	$C_{12}H_{17}O_4$	Kynurenic acid (KYNA)	x	x
226.1203	$C_{12}H_{19}O_4$	3,4-Methylenesebacic acid	x	
226.168	$C_{12}H_{23}O_2N_2$	Gamma-Cadinene		x
226.193	$C_{14}H_{27}O_2$	Tsuzuic acid	x	
229.0206	$C_4H_4O_5N_7$	2-Amino-4-hydroxy-6-pteridinecarboxylic acid	x	x
229.1668	$C_{12}H_{22}O_3N$	Tyrosyl-Lysine	x	x
230.1508	$C_{12}H_{21}O_4$	N-Decanoylglycine		x
231.1469	$C_{11}H_{22}O_4N$	Isobutyryl-L-carnitine		x
233.1261	$C_{10}H_{20}O_5N$	Hydroxypropionylcarnitine	x	
234.085	$C_8H_{15}O_6N_2$	Threoninyl-Aspartate	x	
237.1338	$C_9H_{16}ON_7$	N-Nonanoylglycine		x
238.1178	$C_9H_{15}O_2N_6$	Undecanedioic acid		x
238.1203	$C_{13}H_{19}O_4$	2-Hexenoylcholine		x
238.156	$C_{14}H_{21}O_3$	Estriol-3 or 16 or 17-glucuronide		x
238.1567	$C_{14}H_{23}O_3$	Hydroxydodecanoic acid	x	
240.1353	$C_{13}H_{19}O_4$	Imiquimod		x
240.1698	$C_{10}H_{21}ON_6$	Spermine		x
242.0801	$C_{11}H_{15}O_6$	Elenaic acid	x	x
242.1509	$C_{13}H_{21}O_4$	3,3'-Dithiobis[2-methylfuran]	x	x
243.0853	$C_9H_{14}O_5N_3$	Cytidine	x	
243.1826	$C_{13}H_{24}O_3N$	Halobetasol propionate	x	
243.1833	$C_{13}H_{26}O_3N$	N-Undecanoylglycine	x	
245.1626	$C_{12}H_{24}O_4N$	Valerylcarnitine	x	
250.1317	$C_{13}H_{19}O_3N_2$	Isoleucyl-Proline	x	x
251.1495	$C_{10}H_{18}ON_7$	N-Decanoylglycine		x
252.1948	$C_{13}H_{25}ON_4$	Capryloylcholine	x	x

253.0948	$C_8H_{12}O_3N_7$	N-Acetylvanilalanine	x	
254.0553	$C_{11}H_7O_2N_6$	5-L-Glutamyl-taurine		x
254.1514	$C_{10}H_{19}O_2N_6$	Heptanoylcholine		x
254.1879	$C_{11}H_{23}ON_6$	Kessyl glycol		x
256.0497	$C_2H_9O_7N_8$	Hydroxyprolyl-Cysteine	x	x
257.1989	$C_{10}H_{24}ON_7$	N-Lauroylglycine		x
258.0808	$C_5H_{15}O_8N_4$	Cysteinyl-Histidine	x	x
259.1782	$C_9H_{22}O_2N_7$	Hexanoylcarnitine	x	
260.1022	$C_{10}H_{17}O_6N_2$	L-alpha-glutamyl-L-hydroxyproline		x
265.1312	$C_{10}H_{16}O_2N_7$	Tiglylcarnitine	x	x
265.1651	$C_{11}H_{20}ON_7$	N-Undecanoylglycine		x
266.1644	$C_{14}H_{23}O_3N_2$	Myristic acid	x	
267.0965	$C_{10}H_{14}O_4N_5$	Glutamyl-Valine	x	x
267.1445	$C_9H_{22}O_6N_3$	Pivaloylcarnitine		x
268.0801	$C_{10}H_{11}O_5N_4$	Carbinoxamine	x	
268.0805	$C_{10}H_{13}O_5N_4$	Inosine	x	x
271.2144	$C_{11}H_{26}ON_7$	Tridecanoylglycine	x	
272.0246	$C_4H_9O_{10}N_4$	Cysteinyl-Hydroxyproline	x	
273.9657	$C_2HO_{12}N_4$	Sebacic acid or 2-Ethylsuberic acid		x
274.0951	$C_{10}H_{11}O_2N_8$	Serinyl-Phenylalanine	x	x
274.1391	$C_9H_{19}O_4N_6$	Glutamyl-Lysine	x	
276.1294	$C_7H_{17}O_4N_8$	Saccharopine		x
278.1264	$C_{10}H_{15}O_2N_8$	Prolyl-Tyrosine	x	
278.1992	$C_{12}H_{23}N_8$	Palmitaldehyde	x	
279.1808	$C_{11}H_{26}O_5N_3$	N-Lauroylglycine		x
280.0208	$C_9HO_2N_{10}$	5-phosphonooxy-L-lysine		x
282.1828	$C_{12}H_{23}O_2N_6$	N1-Acetylspermine	x	
283.0914	$C_9H_{18}O_9N$	Guanosine		x
285.1937	$C_{11}H_{24}O_2N_7$	2-Octenoylcarnitine	x	
288.1546	$C_{10}H_{21}O_4N_6$	Arginyl-Asparagine	x	
290.0623	$C_8H_7O_3N_{10}$	Arabinosylhypoxanthine	x	
290.1182	$C_6H_{13}O_4N_{10}$	LPA		x
291.1829	$C_{17}H_{26}O_3N$	Norcapsaicin	x	x
292.0904	$C_{10}H_{17}O_8N_2$	Edetic Acid	x	x
294.1441	$C_{11}H_{23}O_7N_2$	Tocopheronic acid		x
294.1827	$C_{13}H_{23}O_2N_6$	9-Decenoylcholine	x	
298.1162	$C_9H_{15}O_4N_8$	7-Methylguanosine	x	x
299.173	$C_{11}H_{22}O_3N_7$	Diphthine		x
301.225	$C_{12}H_{28}O_2N_7$	2,6 Dimethylheptanoyl carnitine		x
304.0919	$C_{11}H_{17}O_8N_2$	N-Acetylaspartylglutamic acid	x	x
306.1805	$C_{13}H_{27}O_6N_2$	5'-Carboxy-gamma-chromanol		x

306.1939	$C_{13}H_{23}ON_8$	Retinal	x	x
309.1683	$C_{15}H_{22}O_4N_3$	Diethyl glutarate	x	
310.139	$C_{11}H_{23}O_8N_2$	Arginyl-Asparagine	x	
310.1777	$C_{13}H_{23}O_3N_6$	Valdiate		x
311.1701	$C_{12}H_{20}O_3N_7$	N-Undecanoylglycine		x
312.1061	$C_8H_{13}O_4N_{10}$	N2-(3-Hydroxysuccinoyl)arginine	x	
313.225	$C_{13}H_{28}O_2N_7$	9-Decenoylcarnitine		x
314.1154	$C_{18}H_{18}O_5$	Hydroxyenterolactone	x	x
315.2406	$C_{17}H_{34}O_4N$	Decanoylcarnitine		x
316.0485	$C_2H_9O_9N_{10}$	(o-carboxybenzamido) Glutaramic acid	x	
318.1474	$C_7H_{23}O_8N_6$	Hydroxyenterodiol	x	
320.098	$C_{11}H_{13}O_4N_8$	7-Methylguanosine		x
321.1547	$C_{12}H_{24}O_7N_3$	Diphthine	x	
321.1785	$C_{10}H_{24}O_5N_7$	Phenylalanyl-Arginine	x	x
326.1338	$C_{11}H_{23}O_9N_2$	Sakacin A		x
326.1939	$C_{14}H_{31}O_8$	Dodecylbenzenesulfonic Acid	x	
327.1501	$C_8H_{22}O_7N_7$	6-Acetylmorphine		x
332.1807	$C_{12}H_{25}O_5N_6$	Betulalbuside A or Unshuoside A		x
334.0881	$C_8H_{19}O_{12}N_2$	Rofecoxib-threo-3,4-dihydrohydroxy acid	x	
334.2144	$C_{20}H_{30}O_4$	Dehydropinifolic acid		x
336.0543	$C_8H_{15}O_{14}$	Thyrotropin releasing hormone	x	
336.2271	$C_{15}H_{33}O_6N_2$	Leukotriene B4	x	x
340.1419	$C_{19}H_{21}O_4N_2$	19-Oxotestosterone	x	
340.2064	$C_{11}H_{27}O_6N_6$	3-O-Methylrosmarinic acid		x
341.1658	$C_9H_{24}O_7N_7$	Peroxysimulenoline	x	x
341.2562	$C_{15}H_{32}O_2N_7$	trans-2-Dodecenoylcarnitine		x
341.2563	$C_{19}H_{36}O_4N$	2-Dodecenoylcarnitine		x
345.0018	$H_8O_{15}N_7$	Clopidogrel carboxylic acid derivative	x	x
358.2328	$C_{15}H_{31}O_4N_6$	Kinetensin 1-3		x
362.1698	$C_{16}H_{21}O_4N_6$	Ethyl 4-ethoxybenzoate	x	
365.2692	$C_{20}H_{36}O_3N_3$	Stearoylethanolamide	x	
374.1003	$C_8H_{17}O_{11}N_6$	2-Acetolactate	x	x
376.1889	$C_{10}H_{29}O_9N_6$	18-Oxocortisol	x	x
381.0798	$C_{11}H_{12}O_7N_9$	N-(1-Deoxy-1-fructosyl)tyrosine	x	x
381.2512	$C_{21}H_{36}O_5N$	2-Hydroxylauroylcarnitine	x	x
390.2225	$C_{15}H_{31}O_6N_6$	Lubiprostone		x
398.1703	$C_{18}H_{27}O_8N_2$	18-Oxocortisol	x	x
400.1518	$C_{11}H_{25}O_{10}N_6$	Hydroxyleptocarpin	x	x
400.2568	$C_{16}H_{33}O_4N_8$	2-Arachidonylglycerol	x	x
406.1878	$C_8H_{28}O_9N_{10}$	3-Indolebutyric acid	x	
413.1477	$C_6H_{22}O_{12}N_9$	Undecanedioic acid	x	

414.2038	$C_{21}H_{23}N_{10}$	Eplerenone		x
416.1977	$C_{11}H_{29}O_9N_8$	Bixin		x
418.1624	$C_{11}H_{27}O_{11}N_6$	(R)-Byakangelicinn 2'-(3-methylbutanoate)		x
434.2433	$C_{21}H_{39}O_7P$	LPA(18:2(9Z, 12Z)/0:0)		x
434.2441	$C_{12}H_{33}O_9N_8$	Phenylpropionylglycine	x	
445.2166	$C_{13}H_{32}O_{10}N_7$	LysoPE(0:0/14:1(9Z))		x
446.2078	$C_{24}H_{25}O_3N_6$	PA(20:4(5Z,8Z,11Z,14Z)e/2:0)		x
446.2082	$C_{24}H_{27}O_3N_6$	Heliocide B2		x
464.2038	$C_{13}H_{31}O_{12}N_6$	N-Heptanoylglycine	x	x
475.2992	$C_{21}H_{42}O_7N_5$	Netilmicin		x
484.1845	$C_9H_{27}O_{13}N_{10}$	L-Acetylcarnitine	x	x

* Metabolites were checked by x if found by MALDI or ESI platform.

Chapter 8

Protocols for Mass Spectrometric Studies of Neuropeptides and Neurotransmitters: Tissue and Hemolymph Analysis, Dissection, Extraction, Microdialysis and Instrumentation

8.1 Chemicals and Materials

1. Physiological saline: (440 mM NaCl, 11 mM KCl, 26 mM $MgCl_2$, 13 mM $CaCl_2$, 11 mM Trizma base, 5 mM maleic acid; adjust pH to ~7.45), stored at 4 ^oC
2. Acetonitrile, UPLC grade (Fisher Scientific, Fair Lawn, New Jersey)
3. Methanol: purge and trap grade (Fisher Scientific, Fair Lawn, New Jersey)
4. Ammonia (Roundy's Inc., Milwaukee, WI)
5. Ammonium bicarbonate (Acros Organics, Thermo Fisher Scientific, NJ)
6. Isopropanol (Sigma-Aldrich, St. Louis, MO)
7. Formic acid (Sigma-Aldrich, St. Louis, MO)
8. Glacial acetic acid (Fisher Scientific, Fair Lawn, New Jersey)
9. 2,5-dihydroxybenzoic acid (DHB) matrix (ICN Biomedicals, Aurora, OH)
10. α-cyano-4-hydroxycinnamic acid (CHCA) (Sigma-Aldrich, St. Louis, MO)
11. Deionized water (Millipore, Bedford, MA)
12. Formaldehyde (Sigma-Aldrich, St. Louis, MO)
13. D-formaldehyde (Sigma-Aldrich, St. Louis, MO)
14. ZipTips C_{18} (Millipore, Bedford, MA)
15. C_{18} spin column desalting step (Argos, Elgin, IL)
16. Amicon Ultra-0.5 mL10 K molecular weight cut-off (MWCO) (Millipore, Bedford, MA)

17. CMA/20 Elite probes with 4 mm membranes of polyarylether sulfone (PAES) (CMA Microdialysis (Harvard Apparatus, Holliston, MA)
18. FEP tubing (CMA), PEEK tubing (Upchurch-Scientific, Idex Health and Science, Oak Harbor, WA)
19. Flanged connectors: CMA, BASi (West Lafayette, IN)
20. 2.5 mL, 1002 LT SYR syringe and 500 μL, 1750 LT SYR syringe (Hamilton Robotics, Reno, NV)
21. KD Harvard 22 (Harvard Apparatus, Holliston, MA), and 11 Elite Nanomite Syringe Pump (Harvard Apparatus, Holliston, MA)
22. Fraction collector (BASi Honeycomb, Bioanalytical Systems, Inc. Indianapolis, IN)

8.2 *Orconectes rusticus* Protocols

Orconectes rusticus were kindly provided by Alex Laztka, a former graduate student in the laboratory of Jake Vander Zanden, in the Department of Limnology at the University of Wisconsin-Madison, and his co-workers. Lindsay Sargent from University of Notre Dame generously helped with the crayfish trapping also. Rusty crayfish were obtained from fresh water lakes in Northern Wisconsin centered around the Limnology Department's Trout Lake Research Station, on Trout Lake in Boulder Junction, WI. Animals were sampled as part of a National Science Foundation (NSF)-funded Long-Term Ecological Research (LTER) study, and were obtained and transported with the permission of the Wisconsin Department of Natural Resources. Permission for transport must be obtained due to the status of *O. rusticus* as an invasive species in Wisconsin.

8.2.1 *Dissection*

For *O. rusticus* neuropeptidome study, brain and eyestalk were dissected without the aid of a microscope. The whole process is illustrated as below with some pictures and brief remarks. Tissues were stored in acidified methanol (90:9:1 methanol: acetic acid: H_2O) at -80^{o}C until extraction.

(1). Severing the tail nerve.

(2). Removing the legs.

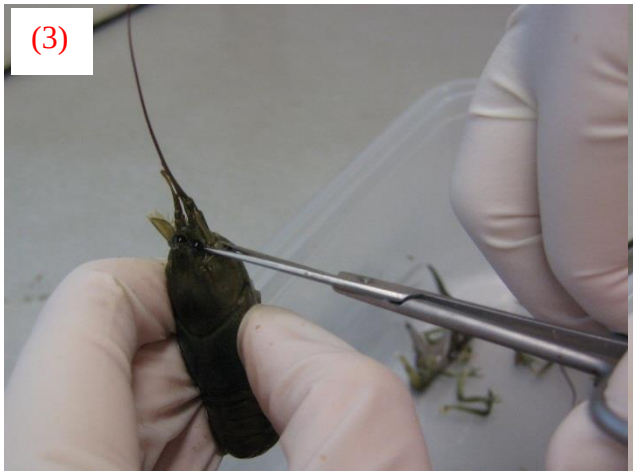

(3). Removing anntennules and antennae.

(4). Snapping off the rostrum.

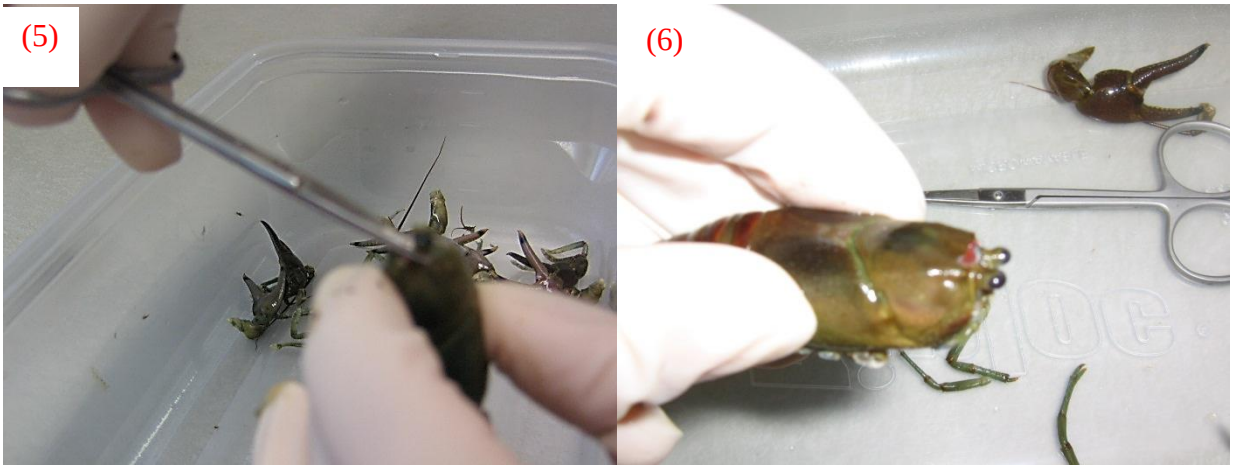

(5). Cut off the eyestalk at the base. (6). Different angel view of the exposed eyestalks.

(7). Make a cut all the way around the carapace as indicated.

(8). Separate the rostral portion of the shell.

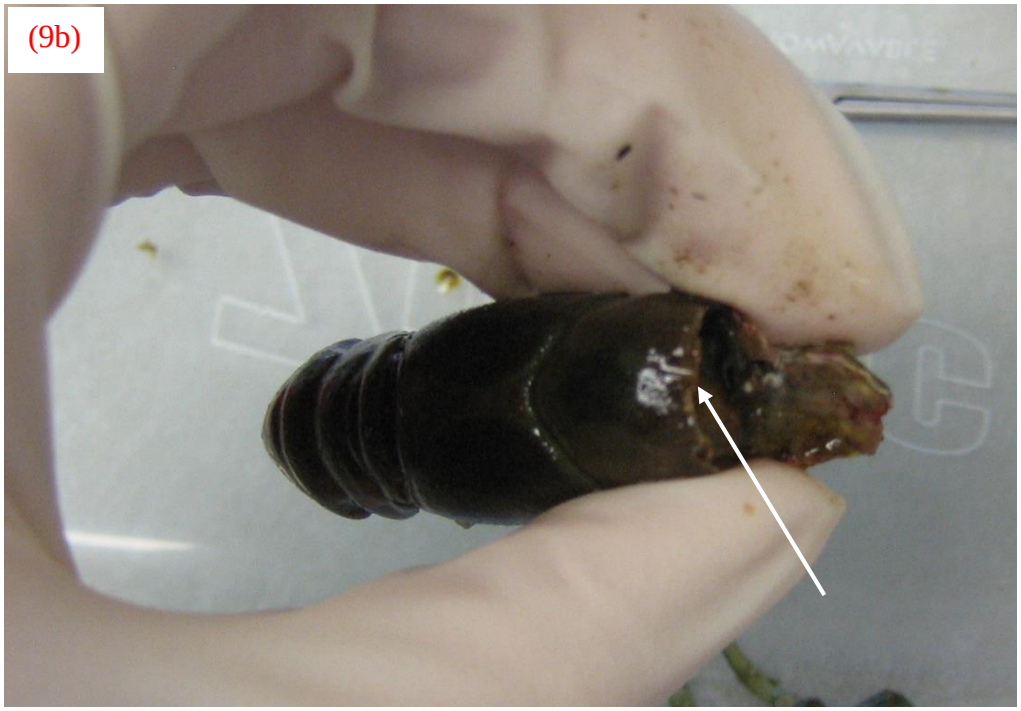

(9). Locate the brain inside the rostral portion of the shell, which is the whitish structure the arrow is pointing to.

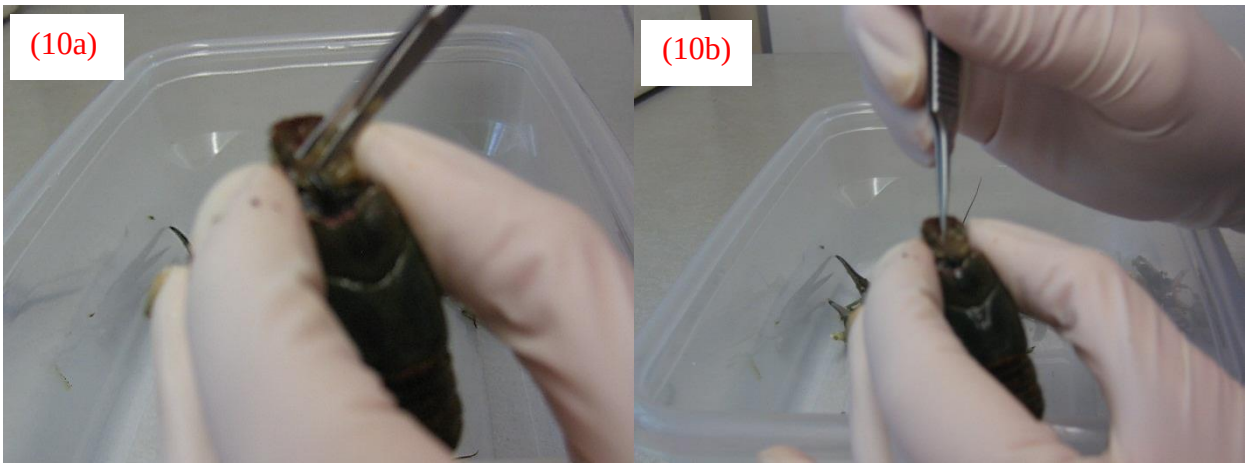

(10) Cut the nerves surrounding the brain and hold it in place. Then remove it with forceps.

8.2.2 *Tissue Extraction*

1. For brain tissues, place them in the collection tube with extraction buffer, acidified MeOH, and use a plastic pestle to grind the tissue into pieces as small as possible. For whole eyestalks, place in a glass vial and grind with pestle until as homogeneous as possible. Put the eyestalk homogenate back into a microtube with extraction buffer. Vortex the sample.
2. Sonicate the tube containing tissue and liquid for 5 min. Do not add heat.
3. Centrifuge 8 min x 16,100 g.
4. Remove supernatant and set aside in a new tube.
5. Add a volume of acidified methanol equal to the original liquid volume to the pellet.
6. Repeat steps 1-5 twice (for a total of 3 extractions) and combine the supernatants. The pelleted solids can be saved, but it has been determined that the first and second extractions of most tissues contain the most neuropeptides. Subsequent extractions contain primarily lipids and/or no compounds of interest.
7. Evaporate the solvent using the speedvac. Medium or Low heat is recommended.

8.3 *Cancer borealis* Protocol

Jonah crabs (*Cancer borealis*) were obtained from The Fresh Lobster Company (Gloucester, MA) and Ocean Resources (Sedgwick, ME). Male Jonah crabs were used in all experiments. All crabs were allowed to adjust to tank settings for at least one week before performing any experiment. Animal room has a temperature set at 18 ^{o}C, and reverse light setting of 12 h: 12 h light-dark cycle with light goes on at 10:00 pm and off at 10:00 am. The tanks are maintained at water temperature of 10-13 ^{o}C and the salinity is maintained at 32-38 ppt range. Water quality, including nitrate, nitrite, ammonia, pH and

dissolved oxygen, is checked weekly to ensure it being at optimum level for crustacean survival.

8.3.1 ***Hemolymph Preparation***

8.3.1.1 Hemolymph Withdrawal

1. Remove the animal from the tank and anesthetized on ice for 5 min. Place the crab with ventral side up in a metal dissecting pan and hold with the thumb and forefinger of the experimenter's non-dominant hand on the tail section. This hold will make most species unable to use their chelae to harm the experimenter.
2. Normally a 25-gauge needle is attached to a 1mL or 3 mL BD plastic syringe and insert at one of the soft leg joints for hemolymph withdrawal. Typically, the best location is through the junction of the thorax and abdomen into the pericardial chamber. This allows access to the central compartment of the animal, which contains more hemolymph that is in direct contact with neuroendocrine and other organs. Insert the needle into the soft tissue and withdraw the plunger on the syringe to create a vacuum. Change the orientation of the needle inside the body until hemolymph is observed to enter the syringe. Once a good location is obtained, the syringe and needle are held still until either the desired amount of hemolymph is collected or the flow of hemolymph into the syringe ceases, even with additional pressure applied via the plunger. Multiple locations may need to be used to obtain enough hemolymph.
3. Place freshly drawn hemolymph into equal volume of acidified methanol and vortex to mix well for neuropeptide extraction.
4. Extracted samples were stored at -80^{o}C until further preparation.

8.3.1.2 Hemolymph Sample Preparation

Different extraction buffer systems were evaluated by Chen *et al*. [1]. Briefly, for neuropeptide analysis, due to the presence of a wide range of interfering molecules such as lipids, large proteins *etc*, extensive sample clean up steps are necessary including 10k MWCO and desalting.

MWCO Procedure

1. Rinse MWCO device with 0.2mL 0.1M NaOH by adding solution to tube and spin 4 min x 14,000g.
2. Rinse MWCO with 0.5 mL of 50/50 H_2O/MeOH: spin 8 min x 14,000g.
3. Dissolve sample in 0.5mL 30/70 MeOH/H_2O (sonicate if necessary to re-suspend), and load into device. Spin for 15-20 min x 14,000g for substances smaller than the MWCO to run through the membrane.
4. Rinse sample tube with 0.1 mL of 30/70 MeOH/H_2O, and run through the membrane by centrifuging 5 min x 14,000g. Combine it with the flow-through in step 3.
5. Both the flow-through and concentrate were saved, but only the flow-through was used for neuropeptide analysis.
6. Dry down the flow-through using a speedvac (Low/Med heat).

Desalting Procedure

Generally, tissue and hemolymph extracts as well as concentrated microdialysate were subjected to a desalting step prior to mass spectrometric analysis. Desalting could

be achieved by using C_{18} ZipTip or C_{18} micro spin column following manufacture's protocols.

8.4 *In vivo* Microdialysis on Jonah Crab

8.4.1 *Additional Materials*

Ice, 30% bleach, ethanol, rotary tool (Dremel), 1/32" drill bit for Dremel, hot glue and hot glue gun, food coloring, Loctite super glue gel (Loctite, Westlake, OH), Mighty Putty (epoxy materials suspended in a clay-like base, Mighty Putty, North Wales, PA), plastic electrical cord protector (from hardware store). Detailed surgery procedures and figures of surgery are provided as below [2].

1. Place crab on ice for 20 min to anesthetize. Depth of anesthesia is monitored by watching for voluntary movement. It is maintained by keeping the crab on ice throughout the surgery.
2. Wash the crab's shell in the area immediately above the pericardial sinus with 30% bleach followed by 70% ethanol. Scrubbing the shell vigorously until color no longer appears to come off. This can be done while the crab is being anesthetized.
3. Score the shell in this area by making cross-hatching diagonal lines using a grinding wheel on a rotary tool.
4. Apply a small amount of hot glue to the MD probe on the shaft above the membrane area to build block and mark the deepest point to which the probe will be inserted. The tubing for the probe should already be connected and the integrity of the tubing and probe can be checked throughout surgery by gently

depressing the syringe plunger. Artificial crab saline is the perfusate. Rinse the probe with crab saline prior to implantation.

5. Drill a 1/32” hole in a location estimated to be immediately above the heart. Do not apply pressure to the drill bit while drilling, and stop once the shell has been drilled through. If hemolymph does not come out of the hole, the epidermis has not been punctured. Use the needle that comes with the probe to gently puncture the epidermis. Dry off the shell.
6. Carefully insert the probe. This should stop hemolymph from leaking out of the hole.
7. Apply Loctite super glue gel in a small circle around the probe.
8. Mix the Mighty Putty and apply on top of this glue circle and form a log of approximately 2” in length with the diameter of a pen. This can then be placed on the shell and molded into a cone shape around the exposed part of the probe.
9. Fill any remaining voids with super glue gel.
10. Insert the probe tubing into a 1’ section of plastic tubing for protecting electrical cords.
11. Attach this tubing to the putty cone on the crab’s shell with hot glue.
12. Keep the crab on ice until the putty is no longer pliable, and then place the crab in the tank. The surgery should not take more than 45 min, and a typical surgery is around 25 min. The crab may not wake up if it is kept on ice for longer than 45 min.
13. Start the syringe pump and refrigerated fraction collector as desired.

14. When starting an experiment, determine the dead volume from the probe tip to collection vial as follows and incorporate this information to collect the proper samples. Tubing volume: 1.8 µL/10cm, probe tip to outlet: 3.0 µL, fraction collector needle: 7.1 µL
15. After the experiment is concluded, which be no more than 7 days after surgery, sacrifice the crab. The crab can be kept for other experiments if desired.
16. Follow the normal dissection protocol with the following changes.
17. While the crab is on ice, cut the MD tubing and protective tubing short and connect a syringe with 0.1mL of diluted food coloring (dilute 1:1 v: v) to the inlet tube.
18. Manually push the dye through the tubing and through the outlet tube. Make sure at least a few drops go all the way through.
19. When dissecting, be careful not to disturb the probe inside the shell.
20. At the point when you remove the shell over the pericardial region, take additional care. Note the location of the probe and/or dye spot. There should be a spot of dye on the crab's heart.

Figure 8-2. Illustration of *in vivo* microdialysis on Jonah Crab.

8.4 Instrumentation

8.4.1 *HPLC Fractionation*

Mobile phase: neutral pH solvents (7.4, solvent A: 25mM NH_4HCO_2, solvent B: 9:1 ACN: 25mM NH_4HCO_2). Reversed-phase Inertsil ODS-4 column, 3µm, 2.1 x 150 mm (GL Sciences, Tokyo, Japan), Alliance HPLC with UV detection (Waters, Milford, MA), Rainin Dynamax Model FC-4 fraction collector, tubes, and speedvac.

1. Inject sample on a 120 min RP separation that will run 95%A to 5%A and back.
2. Collect fractions every 3 min after the first 5 min have elapsed.
3. Dry samples down with speedvac.
4. Combine early eluting fractions with late eluting fractions to reduce the total number of samples while maintaining separation.

8.4.2 ***UPLC-MS and MS/MS Analysis***

8.4.2.1 ESI-QTOF

Waters nanoAcquity UPLC system (Waters Corp, Milford, MA, USA) is coupled at the front end of our ESI QTOF instrument, Synapt G2 (Waters). Zorbax 300SB-C18, 300 µm x 5 mm trap column (Agilent Technologies Inc., Santa Clara, CA), holder for 5 mm trap cartridges (Agilent), stainless steel nano-tee (IDEX Health & Science LLC, Oak Harbor, WA), conductive filter capsule with 2 µm filter and holding bracket (IDEX), home packed column, C18 reverse-phase column (BEH130 C18, 1.7 µm, 75 µm x 100 mm, Waters), trap column (Waters), home-pulled ESI tips, 0.1% FA in ACN (Optima or LC-MS grade), 0.1% FA in H_2O (Optima or LC-MS grade).

Typically, an acidic reversed phase gradient with 0.1% FA in water and 0.1% in ACN as mobile phase was employed with run time ranging from 25 min to 120 min depending on the application. The change in gradient ranged from 5%B to 95%B or 10%B to 45%B (for highly hydrophilic peptides). A trapping step is employed, ranging in length from 1 min for clean samples to 5 min for very salty samples. A commercial column is used with a column heater and a separate home-pulled capillary emitter tip. For DIA MS/MS mode, use a high energy scan having a voltage ramp from 25 to 65 V. For

DDA, use a basic file that selects 3 precursors at a time. Use Glu-fibrinopeptide for lockspray calibration.

8.4.2.2 Q-Exactive Orbitrap

A Waters nanoAcquity UPLC system (Waters Corp, Milford, MA, USA) is coupled to a quadrupole-Orbitrap™ Q-Exactive mass spectrometer (Thermo Scientific, Bremen, Germany). Chromatographic separations were performed on a home-packed C_{18} reversed phase capillary column (360 µm OD, 75 µm ID × 15 cm length, 1.7 µm particle size, 150 Å pore size, (BEH C18 material obtained from Waters UPLC column, part no. 186004661). The mobile phases used were: 0.1% FA in water (A) and 0.1% FA in acetonitrile (B). Sample dissolved in 0.1% FA in water was injected and loaded onto the column without trapping. A 108 min gradient was employed with 0-0.5 min, 0-10% B; 0.5-70 min, 10-35% B; 70-80 min, 35-75% B; 80-82 min, 75-95% B; 82-92 min, 95% B; 92-93 min, 95-0% B; 93-108 min, 100% A. Data was collected under positive electrospray ionization data dependent acquisition (DDA) mode with the top 10 most abundant precursor ions selected for HCD fragmentation. The MS scan range was from *m/z* 300 to 2000 at 70,000 resolution, and the MS/MS scan was at 17,500 resolution from *m/z* 120 to 6000 with an isolation width of 2 Da, collision energy 30.

8.4.2.3 MALDI-LTQ-Orbitrap

MALDI-LTQ-Orbitrap XL mass spectrometer (Thermo Scientific, Bremen, Germany) equipped with 60 Hz 337 nm N_2 laser detection performed in positive ion mode. Neuropeptide is analyzed using a mass range of *m/z* 500-2000, a mass resolution of 60,000 (at *m/z* 400), and a mass error of ≤ 5 ppm. MS/MS were performed in HCD mode with normalized collision energies of 45 and isolation window of 3 *m/z*. MALDI

imaging acquisition could also be performed on the same instrument. For peptides, full MS scan was set up for selected traces from m/z 100 -2000 at a raster step size of 150 µm with 8µJ laser energy. The acquired imaging data was further processed through MSiReader and all images were normalized by internal standard.

For small molecule metabolites imaging analysis, instrument method consisting of full MS scan at m/z 100-900 as well as several tandem mass scans was set up in parallel so that more powerful information of chemical characterization is benefit with reduced sample preparation time and increased reproducibility. By setting up raster and spiral movements of MALDI laser beam, orbitrap full scans were acquired every 100 µm with 11 µJ MALDI laser energy, followed by three targeted ion trap tandem mass scans at 50 µm with HCD collision energy ranging from 35 to 55.

8.4.2.4 MALDI-Ion Mobility (IM) Mass Spectrometry

Data was acquired on a MALDI-IM-MS instrument (Synapt G2 Q-TOF, Waters, Milford, MA, USA) with a YAG laser with a repetition rate of 200 Hz. External calibration was performed using Glu-1-Fibrinopeptide B (Glu-Fib) standard of 1.0 µM before each experiment. Mass spectra were acquired in sensitivity mode and over a mass range of m/z 100 to 900 for small molecules analysis. Laser energy attenuation was 300 (arbitrary units). Ion mobility separation was performed at a drift gas pressure of 2.30 Torr using nitrogen gas, a wave velocity of 650 m/s, and a wave height of 40.0 V.

8.5 Data Processing

8.5.1 *DIA Quantitation via Skyline* [2, 3]

1. If desired, generate a .pkl file using the correct preprocessing file. This can be searched in Mascot but cannot be used in PEAKS.
2. More typically, quantitation will be conducted. Generate the appropriate quantitation file in Skyline software [4] (https://skyline.gs.washington.edu/labkey/project/home/software/Skyline/begin.view).
3. The following files has been created by a former lab member: 475 crab NPs labeled with H and D formaldehyde, 475 crab NPs unlabeled, 475+CPRPs and other long NPs unlabeled, NPs from Chen's feeding paper [5] and myoglobin tryptic digest, sets of neuropeptide standards,.
4. Upload data files into Skyline.
5. Manually check integrations for alignment with predicted retention time, retention time alignment across replicates, choice of the correct peak, uniqueness of the peak for that peptide, etc.
6. Export desired results. Analyze in Excel and/or JMP. Make sure to sort peptides by name and sum all transitions from the same peptide.

Additional Skyline settings: Modifications were added to peptides manually. A non-specific enzyme type was used, with cleavage at every amino acid, and 9 missed cleavages permitted, the most allowed. Skyline does not have a "no enzyme" option built in and this is the closest approximation possible. Most NPs are shorter than 9 amino acids, this should be acceptable. In addition, Skyline will quantify peptides that do not meet its filter criteria if they are input manually and the exception to the filters is noted by the user. The iRT function with retention time predictor was used, calibrated off of

results from Mascot identifications of (Matrix Science, London, UK) equine myoglobin tryptic peptides in a previous LC run of the myoglobin digest alone under the same conditions. The 2^+ and 3^+ precursors were monitored to the 4 most abundant 1^+ and 2^+ b and y ions, and in some cases (CCAP, somatostatin-14) the precursor ion itself was also monitored. MS/MS filtering parameters were set to DIA with MSe isolation, and 10,000 resolving power.

8.5.2 *Database Searching for DDA Data*

Mascot and PEAKS Studio 7.0 were both used for database MS matching and PEAKS could also perform *de novo* sequencing of neuropeptides. A customized database containing all known crustacean neuropeptides was constructed in our lab and used in this work for more confident identification. Post translational modifications used are C-terminal amidation, pyroglutamic acid, methionine oxidation. No enzyme cleavage specified. For QTOF data, the mass tolerance was set to 0.5 Da for precursors and 0.25 Da for fragments. For orbitrap data, the mass tolerance was set to 20 ppm for precursors and 0.01 Da for fragments. Peptide spectrum matches with a -10logP value of 15 in PEAKS and 10 in Mascot were considered for further validation.

8.5.3 *MALDI-MS Data Analysis*

Neuropeptide profiling was done by accurate mass matching with less than 5 ppm error using in house constructed crustacean neuropeptide database. For MALDI-based peptide quantitation, the abundance of each peptide was normalized based on the abundance ratio of the neuropeptide versus the spiked peptide standard, and then ratios of different replicates were averaged. In formaldehyde labeling experiments, locate peptide light and heavy labeled ion pairs, which bear a 28 Da or 32 Da mass shift. After

normalization, the ratio was get by comparing the abundance of heavy labeled peptides versus light labeled peptide.

8.6 References

1. Chen, R., Ma, M., Hui, L., Zhang, J., and Li, L., *Measurement of neuropeptides in crustacean hemolymph via MALDI mass spectrometry.* J Am Soc Mass Spectrom, 2009. **20**(4): p. 708-18.
2. Schmerberg, C.M., *Functional neuropeptidomics in the decapod crustacean: method development and application to behavioral neuroscience research*, in *School of Pharmacy*. 2012, University of Wisconsin-Madison. p. 485.
3. Schmerberg, C.M., Liang, Z., and Li, L., *Data-independent MS/MS quantification of neuropeptides for determination of putative feeding-related neurohormones in microdialysate.* ACS Chem Neurosci, 2015. **6**(1): p. 174-80.
4. MacLean, B., Tomazela, D.M., Shulman, N., Chambers, M., Finney, G.L., Frewen, B., Kern, R., Tabb, D.L., Liebler, D.C., and MacCoss, M.J., *Skyline: an open source document editor for creating and analyzing targeted proteomics experiments.* Bioinformatics, 2010. **26**(7): p. 966-8.
5. Chen, R., Hui, L., Cape, S.S., Wang, J., and Li, L., *Comparative Neuropeptidomic Analysis of Food Intake via a Multi-faceted Mass Spectrometric Approach.* ACS Chem Neurosci, 2010. **1**(3): p. 204-214.

Chapter 9

Conclusions and Future Directions

Conclusions

In this dissertation, advanced mass spectrometric analytical methods were developed for analysis of neuropeptides and small molecule neurotransmitters in the decapod crustacean nervous system, with special emphasis on the circulating content using a fluid-based sample preparation. The application of mass spectrometry-based techniques has facilitated the characterization of these compounds, and provided valuable insights into their potential physiological function. The methods developed in the course of this work have a great potential to be applied to other, more complicated biological systems.

Mass Spectrometric Characterization of the Neuropeptidome of the Crayfish *Orconectes rusticus*

In this study, multiple neuronal tissues were used for more comprehensive neuropeptide content identification from crayfish, *Orconectes rusticus*. It represents the first comprehensive characterization of neuropeptidme study in this species. A customized database containing all known crustacean neuropeptides was constructed in our lab and used for more confident identification in this work. Two-dimensional separation was employed to reduce sample complexity and minimize signal interference. The performances of two data processing approaches, database searching from Mascot and PEAKS and *de novo* sequencing using PEAKS were compared. In total, 262 high-quality peptide-spectrum matches (PSMs) were made to MS/MS spectra, with 215 out of which could be mapped to peptides previously observed in decapod crustaceans using mass spectrometry, from 10 different neuropeptide families. The additional spectra mapped to 47 putative neuropeptides from 12 families. This species is of particular

interest to neuroscience study and the identification of neuropeptides will aid further studies into this organism.

Mass Spectrometric Characterization of Circulating Neuropeptides in Jonah Crab, *Cancer borealis*

Crude hemolymph extract and microdialysis sampling from Jonah crab, *Cancer borealis* were used to couple with mass spectrometry detection to characterize circulating neuropeptides. *In vivo* microdialysis was proven to be a better sampling option over direct hemolymph withdrawal in this study. More than 50 neuropeptides from 9 different peptide families were identified from microdialysate, and 22 neuropeptides from 7 families were detected from a direct hemolymph preparation. In addition, an important feature of microdialysis, temporal resolution, was evaluated to yield the best neuropeptide coverage. The comparison between tissue-based neuropeptide identification and such fluid-based study provided interesting insights into their potential functions. The fact that these neuropeptides were present in both neuronal tissues and the circulatory system may suggest that they could be functioning as neuromodulators and hormones.

Data-Independent MS/MS Quantification for Profiling of Temporal Dynamics of Neuropeptides in Microdialysate

In vivo microdialysis enables sample collection while the animal is alert thus allowing the correlation of neurochemical content with physiological process. Characterization of neurochemical dynamics within microdialysate under different behavioral stages could offer important function-related information. An untargeted quantification method using data-independent acquisition (DIA) MS/MS was developed by performing post-acquisition filtering with Skyline software. The *Cancer borealis*

neuropeptidome was monitored and by coupling with microdialysis collection, the relative concentration changes of neuropeptides during feeding and light-dark phases were characterized in a timely resolved manner. This method had shown great potential in correlating global neuropeptide changes with behavior thus could be applied in function-related studies in different biological systems.

Coupling *in vivo* Microdialysis with a Multifaceted Mass Spectrometric Platform to Investigate Signaling Molecules and Metabolites in Crustacean

In addition to neuropeptides, circulating small molecule metabolites were also characterized in Jonah crab, *Cancer borealis*. Capillary electrophoresis (CE) and ion mobility MALDI imaging platform was developed for neurotransmitter and metabolite identification. Its performance was also compared with LC-MS detection for more comprehensive coverage. A total of 209 compounds from 11 families including nucleosides, amino acids, peptides and analogues, and amines were identified. Benefit from the nature of sub-µL sample consumption of CE separation, microdialysis temporal resolution (~ 5 min) was greatly improved over LC-MS (~ 1 h) analysis. The improved temporal resolution promises more accurate monitoring of neurotransmitter release and dynamic changes, thus this platform exhibit great potential for future functional studies.

Capture of *in vivo* Neuropeptide Degradation Using MALDI-Mass Spectrometry

In vivo microdialysis was coupled with MALDI-MS imaging technique for direct analysis of neuropeptide *in vivo* degradation profile. MALDI imaging maintained the temporal resolution of microdialysis collection. Dialysate was continuously deposited onto customized MALDI target plate thus enabled the characterization of '*in vivo*' secretion in an off-line 'real-time' manner. Relative concentration changes could be

directly visualized from MS images, which potentially detoured the limitation of MALDI-MS quantitation. An *in vitro* assay, where neuropeptides were incubated with freshly collected hemolymph, was used to rapidly and accurately assess the degradation rate of different neuropeptides. The results from this study provided useful information to improve our understanding of *in vivo* peptidergic signaling pathway. Moreover, this analytical platform should be readily transferable to the study of other biological event in a highly dynamic fashion.

Ongoing Projects and Future Directions

Neuropeptide Co-modulation during Feeding Behavior in *Cancer borealis*

Likely in all nervous systems, neural networks are co-modulated by various inputs [1]. However, the functional consequences of co-modulation and the underlying mechanism remain rather elusive in many systems. To date, a majority of studies on modulation of neural network activity has focused on individual modulator. The crab stomatogastric nervous system has been extensively studied in terms of neurons, neuronal networks and neuromodulators. As an example, the gastric mill central pattern generator (CPG) in the isolated stomatogastric nervous system is well-defined at the cellular level. Its modulation has been studied by individual modulatory neuron stimulation and neuropeptide application [2-4]. To elucidate the effect of co-modulation, we use mass spectrometry to identify the co-circulating peptide modulator candidates during feeding behavior by performing quantitative analysis. This biochemical assay is coupled with electrophysiological experiments to determine the influence of crude hemolymph as well as a subset of potential peptide regulators on the rhythmic activity of the gastric mill CPG and its muscle targets.

Preliminary feeding experiments were performed with Jonah crab *Cancer borealis* and samples were collected through direct hemolymph extract and *in vivo* microdialysis. Neuropeptide changes during feeding behavior were measured by Orbitrap mass spectrometer *via* isotopic labeling (hemolymph extract) and label-free (microdialysate) methods. Preliminary results indicated a general increasing trend in abundance for most identified neuropeptides, including RFamides, and RYamides among others. To best characterize the neuropeptides changes during this dynamic process, temporal resolution study was also conducted by collecting microdialysate continuously for 1 h, 2 h and 6 h before and after feeding. Peptide changes were characterized by normalizing to internal standard and then comparing the peptide abundances in post-feeding and pre-feeding dialysates collected with the same temporal resolution. For most neuropeptides, higher collection temporal resolution gave bigger changes. As shown in **Figure 9-1**, a truncated crustacean hyperglycemic hormone precursor-related peptide (CPRP) exhibited the most dramatic change when collected with 1 h temporal resolution.

Several future directions about this project are proposed here. First, more biological replicates need to be analyzed for both hemolymph extract and microdialysis experiment. The highly dynamic open circulatory system and *in vivo* digestion along with various factors would cause variability which is a main issue at this stage. Also, correlation between results from these two sampling methods will be performed to better understand the neurochemical players involved in dynamic regulation of feeding process. Second, time course study needs to be carried out. Hemolymph extraction experiment has been performed at 1 h post-feeding time point. In the future different time points will be investigated both with direct hemolymph withdrawal and microdialysis to provide a more

detailed description of the involvement of neuropeptides during different feeding stages, thus providing better guidance for electrophysiological study. Third, collaboration with electrophysiologists will help to test the co-modulation effect of selected peptide candidates from our quantitative studies on the neural circuits.

Study the Interplay between Neurotransmitters and Neuropeptides in *Cancer borealis*

Many different kinds of signaling molecules, such as neurotransmitters, and peptide hormones or neuropeptides, are present in living organisms to transmit information between cells [5]. Mass spectrometry has greatly advanced the research on neuropeptidomics and metabolomics. In this dissertation, we have characterized the secreted neuropeptide and metabolite content in *Cancer borealis*. However, many physiological processes such as feeding [6] are known to be regulated by a wide range of signaling molecules including neuropeptides, neurotransmitters, and proteins. The interactions between different kinds of signaling molecules are essential for the characterization of signaling pathways. By investigating neurotransmitter induced neuropeptide release in crustacean nervous system, we hope to provide more insights into their interactions thus reveal more signal networking information.

In this project, we use *in vivo* microdialysis to deliver neurotransmitters into Jonah crab *Cancer borealis*. Dialysate is collected and mass spectrometry is used for neuropeptide content analysis. Preliminary results showed that administration of serotonin induced the release of one B-type allatostatin (AST-B) member, SGKWSNLRGAWamide and one crab tachykinin-related peptide (Cb-TRP) APSGFLGMRamide. Dopamine administration caused the release of one RFamide

peptide, TNRNFLRFamide. **Figure 9-2** showed the MS/MS identification of AST-B peptide SGKWSNLRGAWamide in microdialysate with serotonin administration and Cb-TRP peptide APSGFLGMRamide with mixture of serotonin and dopamine administration.

The results are still very preliminary and need to be validated by additional biological replicates. Furthermore, in addition to serotonin and dopamine, other neurotransmitters such as acetylcholine and also mixture of different neurotransmitters will be studied to gain a more comprehensive understanding of potential interactions between neurotransmitters and neuropeptides. Finally, we will collaborate with electrophysiologists to characterize and quantify the physiological response of animals. Our preliminary experiment demonstrated that the administration of serotonin induced very distinct behavioral response in a very reproducible manner while no obvious response was observed with dopamine. Hopefully through collaborative investigation of neurochemical-induced behavioral pattern changes, more function related information could be obtained.

References

1. Bargmann, C.I., *Beyond the connectome: how neuromodulators shape neural circuits.* Bioessays, 2012. **34**(6): p. 458-65.
2. Marder, E. and Bucher, D., *Understanding circuit dynamics using the stomatogastric nervous system of lobsters and crabs.* Annu Rev Physiol, 2007. **69**: p. 291-316.
3. Blitz, D.M. and Nusbaum, M.P., *Modulation of circuit feedback specifies motor circuit output.* J Neurosci, 2012. **32**(27): p. 9182-93.
4. Rodriguez, J.C., Blitz, D.M., and Nusbaum, M.P., *Convergent rhythm generation from divergent cellular mechanisms.* J Neurosci, 2013. **33**(46): p. 18047-64.
5. Cooper, G.M., *The Cell: A Molecular Approach.*, in *Signaling Molecules and Their Receptors.* 2000, Sinauer Associates.
6. Schwartz, M.W., Woods, S.C., Porte, D., Jr., Seeley, R.J., and Baskin, D.G., *Central nervous system control of food intake.* Nature, 2000. **404**(6778): p. 661-71.

Figures

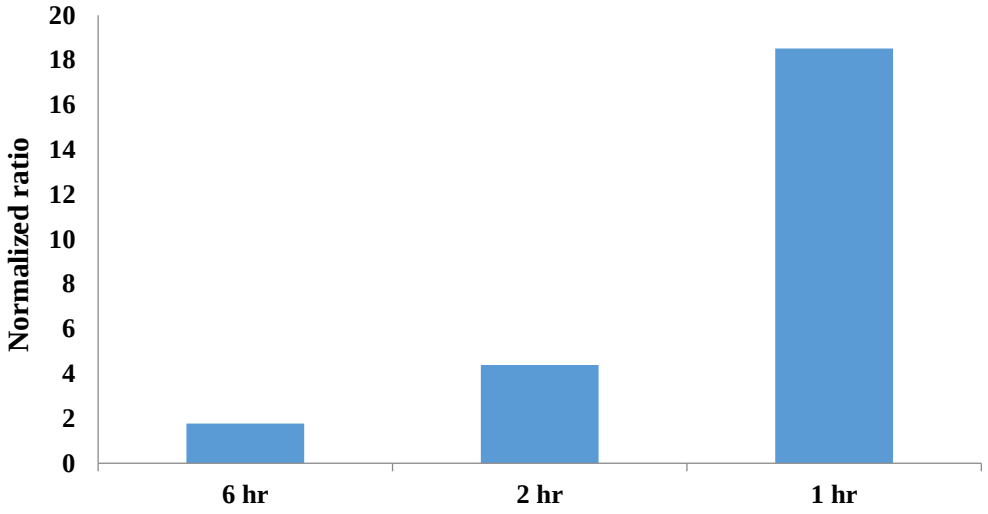

Figure 9-1. Intensity changes of one truncated CPRP peptide, GSLGHPV, after feeding. Peptide signal was normalized by adding internal peptide standard, and then compared to it in pre-feeding microdialysate collected at the same correlating temporal resolution.

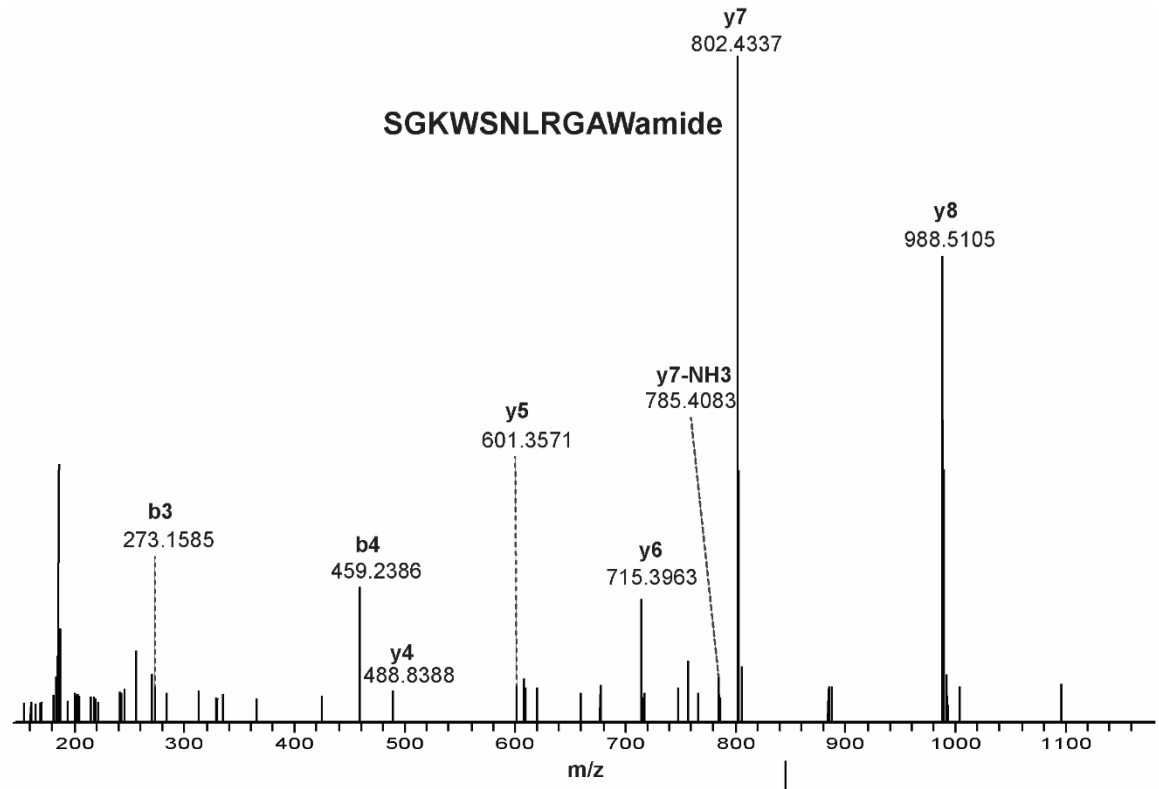
SGKWSNLRGAWamide
y7
802.4337
y8
988.5105
y7-NH3
785.4083
y5
601.3571
b3
273.1585
b4
459.2386
y6
715.3963
y4
488.8388
200
300
400
500
600
700
800
900
1000
1100
m/z

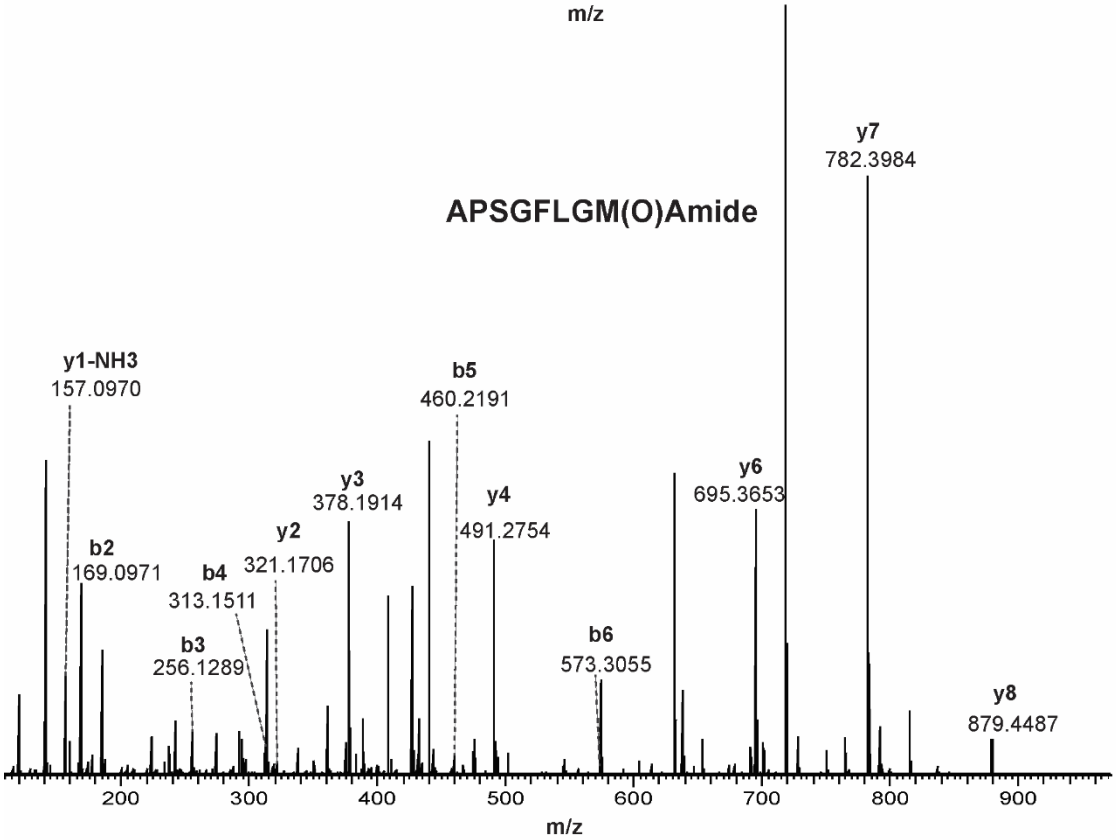
APSGFLGM(O)Amide
y7
782.3984
y1-NH3
157.0970
b5
460.2191
y3
378.1914
y6
695.3653
y4
491.2754
y2
321.1706
b2
169.0971
b4
313.1511
b3
256.1289
b6
573.3055
y8
879.4487
200
300
400
500
600
700
800
900
m/z

Figure 9-2. MS/MS identification of AST-B peptide SGKWSNLRGAWamide in microdialysate with serotonin administration and Cb-TRP peptide APSGFLGMRamide with mixture of serotonin and dopamine administration.

Appendix I

List of Publications and Presentations

Publications:

1. Mass spectrometric measurement of neuropeptide secretion in the crab, *Cancer borealis*, by *in vivo* microdialysis. **Liang Z**, Schmerberg CM, Li L. *Analyst*. **2015**, *140*, 3803-3813.
2. Mass Spectrometric Characterization of the Neuropeptidome of the Crayfish *Orconectes rusticus*. **Liang Z**, Schmerberg CM, Li L. *J. Proteome. To be submitted*.
3. Enzymatic Degradation of Neuropeptides Probed by *in vivo* microdialysis coupled with MALDI Mass Spectrometry. **Liang Z**, Jiang S, Li L. *Analyst, to be submitted*.
4. Investigation of signaling molecules and metabolites found in crustacean hemolymph via in vivo microdialysis using a multi-faceted mass spectrometric platform. Jiang S, **Liang Z**, Li L. *Electrophoresis*, 2016, *37*, 1031-1038.
5. Data-Independent MS/MS Quantification of Neuropeptides for Determination of Putative Feeding-Related Neurohormones in Microdialysate. Schmerberg CM, **Liang Z**, Li L. *ACS Chem Neurosci*. **2015**, *6*, 174-180.
6. Mass spectrometric analysis of spatio-temporal dynamics of crustacean neuropeptides. **Liang Z**, Ouyang C, Li L. *Biochim Biophys Acta*. **2015**, *1854*, 798-811.
7. Biologically active peptides in invertebrates: *Discovery and Functional Studies*. Yu Q, **Liang Z**, Ouyang C, Li L. *Morgan & Claypool Life Sciences, Colloquium series on neuropeptides* # 5.
8. Development and characterization of novel 8-plex DiLeu isobaric labels for quantitative proteomics and peptidomics. Frost DC, Greer T, Xiang F, **Liang Z**, Li L. *Rapid Commun Mass Spectrom*. **2015**, *29*, 1115-1124.
9. Mass Spectrometric Characterization of the Crustacean Neuropeptidome. Yu Q, Ouyang C, **Liang Z**, Li L. *EuPA Open Proteomics*, **2014**, *3*, 152-170.
10. *In vivo* neurochemical monitoring of the crab *cancer borealis* via microdialysis and mass spectrometry. **Liang Z**, Li L. Book Chapter, *Acceptance pending minor revision.*
11. Gas-phase ion isomer analysis reveals the mechanism of peptide sequence scrambling. Jia C, Wu Z, Lietz CB, **Liang Z**, Cui Q, Li L. *Anal Chem*, **2014**, *86*, 2917-2924.
12. Mass spectrometric characterization of the neuropeptidome of the ghost crab Ocypode ceratophthalma (Brachyura, Ocypodidae). Hui L, D'Andrea BT, Jia C, **Liang Z**, Christie AE, Li L. *Gen Comp Endocrinol.* **2013**, *184*, 22-34.

Selected Presentations:

1. **Liang Z** and Li L. **'**Mass spectral measurement of feeding-related neuropeptide secretion in crustacean via *in vivo* microdialysis', Poster presentation, 63rd ASMS Conference on Mass Spectrometry and Allied Topics, St Louis, MO, 2015.
2. **Liang Z** and Li L. **'**Mass spectral measurement of feeding-related neuropeptide secretion in crustacean via *in vivo* microdialysis', Poster presentation, Wisconsin Human Proteomics Symposium 2015, Madison, WI, 2015.
3. **Liang Z**, Schmerberg CM, and Li L. 'Mass Spectral Investigation of Circadian Rhythm-related Neuropeptides Secretion in Crustacean via *in vivo* Microdialysis', Oral presentation, 62nd ASMS Conference on Mass Spectrometry and Allied Topics, Baltimore, MD, 2014.
4. **Liang Z**, Schmerberg CM, and Li L. 'Towards Correlating Circadian Rhythm and Neuropeptide Release during Light-Dark Cycle in Crustacean via *In Vivo* Microdialysis Coupled with Mass Spectrometry', Oral presentation**,** Society for Neuroscience Annual Meeting, San Diego, CA, 2013.
5. **Liang Z**, Schmerberg CM, and Li L. 'Mass spectral characterization of the neuropeptidome of the crayfish *Orconectes rusticus',* Poster presentation, 61st ASMS Conference on Mass Spectrometry and Allied Topics, Minneapolis, MN, 2013.
6. **Liang Z**, Schmerberg CM, and Li L. 'Mass spectral characterization of the neuropeptidome of the crayfish *Orconectes rusticus',* Poster presentation, Wisconsin Human Proteomics Symposium 2013, Madison, WI, 2013.
7. Jiang S, **Liang Z**, and Li L. 'Identification of metabolites in crustacean hemolymph via *in vivo* microdialysis by capillary electrophoresis-matrix-assisted laser desorption ionization mass spectrometric imaging platform', Oral presentation, 63rd ASMS Conference on Mass Spectrometry and Allied Topics, St Louis, MO, 2015.
8. Yarger AM, **Liang Z**, Li L, and Stein W. 'Electrophysiological and mass spectral investigation of long-term *in vivo* motor activity and neuropeptide release in the crab *Cancer borealis*', Society for Neuroscience Annual Meeting, Washington, DC, 2014.